Mercury cycling in a remote boreal drainage basin

by

Gretchen Lynne Lescord

A thesis submitted in partial fulfilment of the requirements for the degree of Doctor of Philosophy (PhD) in Boreal Ecology

The Faculty of Graduate Studies
Laurentian University
Sudbury, Ontario, Canada

THESIS DEFENCE COMMITTEE/COMITÉ DE SOUTENANCE DE THÈSE
Laurentian Université/Université Laurentienne
Faculty of Graduate Studies/Faculté des études supérieures

Title of Thesis
Titre de la thèse — Mercury cycling in a remote boreal drainage basin

Name of Candidate
Nom du candidat — Lescord, Gretchen Lynne

Degree
Diplôme — Doctor of Philosophy

Department/Program
Département/Programme — Boreal Ecology

Date of Defence
Date de la soutenance December 14, 2018

APPROVED/APPROUVÉ

Thesis Examiners/Examinateurs de thèse:

Dr. Tom Johnston
(Co-Supervisor/Co-directeur de thèse)

Dr. John Gunn
(Co-Supervisor/Co-directeur de thèse)

Dr. Marc Amyot
(Committee member/Membre du comité)

Dr. Nelson Belzile
(Committee member/Membre du comité)

Dr. Igor Lehnherr
(Committee member/Membre du comité)

Dr. Richard Andrew Bodaly
(External Examiner/Examinateur externe)

Dr. François Caron
(Internal Examiner/Examinateur interne)

Approved for the Faculty of Graduate Studies
Approuvé pour la Faculté des études supérieures
Dr. David Lesbarrères
Monsieur David Lesbarrères
Dean, Faculty of Graduate Studies
Doyen, Faculté des études supérieures

ACCESSIBILITY CLAUSE AND PERMISSION TO USE

I, **Gretchen Lynne Lescord**, hereby grant to Laurentian University and/or its agents the non-exclusive license to archive and make accessible my thesis, dissertation, or project report in whole or in part in all forms of media, now or for the duration of my copyright ownership. I retain all other ownership rights to the copyright of the thesis, dissertation or project report. I also reserve the right to use in future works (such as articles or books) all or part of this thesis, dissertation, or project report. I further agree that permission for copying of this thesis in any manner, in whole or in part, for scholarly purposes may be granted by the professor or professors who supervised my thesis work or, in their absence, by the Head of the Department in which my thesis work was done. It is understood that any copying or publication or use of this thesis or parts thereof for financial gain shall not be allowed without my written permission. It is also understood that this copy is being made available in this form by the authority of the copyright owner solely for the purpose of private study and research and may not be copied or reproduced except as permitted by the copyright laws without written authority from the copyright owner.

Abstract

The consumption of freshwater fish and seafood is the main source of mercury (Hg), a widespread neurotoxic pollutant, in humans, a fact which has sparked decades of research on Hg cycling in aquatic systems. More specifically, the formation and bioaccumulation of methylmercury (MeHg) is of particular importance because it biomagnifies through aquatic food webs, resulting in relatively high levels in predatory fish despite typically low concentrations in the surrounding water.

The main goal of this thesis was to assess how various watershed-level processes affect Hg bioaccumulation and biomagnification through freshwater food webs across the relatively pristine Attawapiskat Drainage Basin (ADB) in the remote Far North of Ontario. This watershed overlaps with the mineral-rich region known as the "Ring of Fire" which is expected to be heavily developed in the coming decades, likely altering the physico-chemical environments of surrounding lakes and rivers. In total, 58 lakes and river sites across the ADB were sampled for surface water quality, aquatic macroinvertebrates, and fish from 2014 to 2016. Water samples were analyzed for 39 chemical parameters including total Hg (THg; the sum of all Hg species) and MeHg concentrations ([MeHg]). Biotic samples were analyzed for [THg] and/or [MeHg], as well as carbon and nitrogen stable isotope ratios, which are indicative of an animal's food web position.

In Chapter 1 of this thesis, I provide an overview of our current knowledge on Hg cycling in aquatic systems of the boreal region. In Chapter 2, I present an extensive assessment of the chemical, physical, and ecological gradients across the ADB, and an analysis of the relationships between Hg and these environmental gradients. I determined that less productive systems with higher concentrations of dissolved organic matter (DOM) had higher aqueous and biotic [Hg]. In Chapter 3, I examined how changes in the quality of DOM across the ADB relate to [Hg] in water and biota. Findings from this study suggest that more labile DOM complexes enhance MeHg bioaccumulation into food webs, while systems with more humic and aromatic DOM had higher aqueous total [Hg]. The fourth chapter critically examined the speciation of Hg in fish from across the ADB and showed substantially lower percentages of MeHg (relative to total Hg) in

muscle of smaller-sized fish, particularly those which feed on littoral-based food webs and had higher lipid content in their tissue. These novel findings challenge the general assumption, used in many biomagnification studies and consumption guidelines, that all fish muscle tissue has > 95% MeHg. Finally, in Chapter 5, I discuss the implications of my research for subsistence fishers, specifically those from remote communities, where freshwater fish are important for both culture and sustenance. Here I developed some preliminary approaches to better communicating the risks and benefits of consuming fish when presenting fish tissue contaminant results in remote northern communities, including those in and around the ADB.

Understanding the major influences on MeHg cycling is vital to properly monitoring the effects of industrial development (e.g., the Ring of Fire development) and climate change, which can greatly alter the physico-chemical environment of surrounding lakes and rivers. The results from my thesis indicate significant physical and chemical differences between waters in the two ecozones (i.e., the Boreal Shield and Hudson Bay Lowlands) across the ADB, presumably due to changes in bedrock geology and riparian characteristics. No other study, to my knowledge, has explored the effects of landscape position and the associated changes in physico-chemical characteristics on Hg bioaccumulation, speciation, and biomagnification on such a large scale. My findings demonstrate that monitoring programs will need to effectively track changing nutrient concentrations, DOM characteristics, and Hg bioaccumulation patterns that vary across large spatial gradients.

Keywords: mercury, methylmercury, bioaccumulation, biomagnification, boreal, food web, environmental monitoring, subsistence fish, nutrients, dissolved organic matter (DOM), drainage basin

Acknowledgements

There are countless people I wish to thank for their guidance and support over the course of my Ph.D. First and foremost I sincerely thank my supervisors, Drs. John Gunn and Tom Johnston who together provided an ideal and supportive learning environment that enabled me to perform in-depth, applicable, and collaborative science. I am fortunate to have had the opportunity to work closely with you both and I hope to emulate your scientific integrity and dedication as my career develops. I also thank Dr. Brian Branfireun who refined my analytical skills and provided invaluable input to the papers which constitute the bulk of this thesis. I sincerely thank my committee members: Drs. Nelson Belzile, Marc Amyot, and Igor Lehnherr who provided much needed expertise and guidance throughout the development and execution of this thesis.

My research was made possible through the funding support of the Natural Sciences and Engineering Research Council (NSERC) through the Canadian Network for Aquatic Ecosystem Services (CNAES) and Discovery Grant programs, by the Ontario Ministry of Natural Resources and Forestry (OMNRF), and the W. Garfield Weston Fellowship Program through the Wildlife Conservation Society of Canada (WCSC). In-kind support of field logistics was provided by DeBeers Canada. I also thank the NSERC EcoLac (Pierre-Olivier Benoit and Marie-Andrée Fallu) and CNAES (Jennifer Robinson and Don Jackson) networks for supporting my studies and participation in conferences, workshops, and short courses. I thank the OMNRF Biodiversity and Monitoring Section for providing samples and data from the BsM program, and for performing fish age determinations at the NW Ageing Lab. Similarly, I thank the Ontario Ministry of Environment and Climate Change (OMOECC) for providing water chemistry and historic fish mercury data.

I would also like to sincerely thank many people associated with the Vale Living with Lakes Centre (VLWLC): Karen Oman and Liz Bamberger for their help with the day-to-day details and logistical support which truly enabled the research presented herein; Emily Smenderovac and Michelle Gillespie for their managerial help in organizing field and lab work, assistance with data analysis, and their supportive friendships; Caroline Emilson and Amy Boudreau for their hard work in the field and lab; Dr. Erik Emilson for

sharing his expertise and supportive humor; past and present staff/students with the OMNRF (Kristen Patterson, Lee Haslam, Andrew Corston, Mike MacKenzie, Matt Heerschap, Jamie Montgomery, Kelsey Bender, Alexandra Sumner, Christina Mozzon, and Michelle Quesnel) without whom the extensive field work for this project would not have been possible; past and present staff with the OMOECC (Jocelyne Heneberry, Nicole Novodvorsky, Vanessa Bourne, and Dr. John Bailey) who kindly shared data and collected valuable samples from northern rivers for this thesis; Chantal Sarrazin-Delay and Dr. David Pearson for sharing their expertise in science communication which enabled me to effectively communicate my research to remote First Nation communities; and other students and staff for their help and friendship.

I thank Jeff Wagner and other staff at the Biotron Laboratory (Western University) for their time and analytical expertise during the lab work for this thesis. I especially thank Jasmine Louste-Fillion for spending long hours in the lab with me to generate these data; your friendship and positive attitude turned the tiring days into happy memories. I also thank Dr. Karen Kidd, who has continued to guide my research and provided much appreciated support throughout my graduate studies.

I thank my extraordinary family and friends for the unconditional love and support throughout my years as a student: Nancy Gray, Bryan Lescord, Meaghan Allen, Elizabeth Gray, Amanda Bain, Heather McMahon, Varun Gupta, Pascale Savage, Emily Smenderovac, Michael Carson, Kurt Yakimovich, Rory Woods, Michelle Gillespie, Michael Matson, and many others. Their support enabled me to complete this thesis despite the challenges that arose over the past 4 years.

Lastly, I thank and lovingly dedicate this thesis to my dad, Gregory Tyler Gray (1953-2017). He taught me to exploit the hardships in my life for the lessons they could teach me and that a genuine curiosity about the world around us is more valuable than any degree. Both Greg and Dr. Gunn taught me to keep asking questions; the worst thing anyone will ever say is no. And “after the final no, there comes a yes. And on that yes, the future world depends.” -Wallace Stevens

Co-Authorship and Publication Statement

While this thesis was written with me as the primary author, co-authors were involved in varying aspects of this work. Individual contributions to research chapters are outlined below, though any oversights or errors throughout the thesis are my own.

Chapter 1: An overview of mercury cycling in Canadian boreal freshwater systems
This chapter was based on a draft of a review paper intended for publication. Several co-authors have therefore contributed: **Gretchen L. Lescord**[1], Thomas A. Johnston[1 2], Brian A. Branfireun[3], Amanda E. Poste [4], Karen A. Kidd[5], Hans Fredrik Veiteberg Braaten[4], Heidi K. Swanson[6], John M. Gunn[1]
[1]Vale Living with Lakes Center, Laurentian University, Sudbury ON, Canada; [2]Ontario Ministry of Natural Resources and Forestry, Sudbury ON, Canada; [3]The University of Western Ontario, London ON Canada; [4]Norwegian Institute for Water Research, Oslo, Norway; [5]University of New Brunswick and the Canadian Rivers Institute, Saint John NB, Canada; [6]University of Waterloo, Waterloo ON, Canada

Chapter 2: Mercury bioaccumulation in relation to changing physicochemical and ecological factors across a large and undisturbed boreal watershed
This chapter has been submitted to *The Canadian Journal of Fisheries and Aquatic Sciences,* in November 2018, under the following citation: **Gretchen L. Lescord [1],** Thomas A. Johnston [1,2], Brian A. Branfireun[3], John M. Gunn [1] Gradients of physicochemical and ecological factors across an undisturbed boreal drainage basin and their effects on mercury bioaccumulation. cjfas-2018-0465
[1]Vale Living with Lakes Center, Laurentian University, Sudbury ON, Canada; [2]Ontario Ministry of Natural Resources and Forestry, Sudbury ON, Canada; [3]The University of Western Ontario, London ON, Canada
G.L. Lescord collected the majority of field samples, performed most lab and data analyses, and wrote the first draft of the chapter/manuscript; T.A. Johnston provided funding, field and laboratory support, input on study design and statistical analysis, and edited the draft; B.A. Branfireun provided laboratory support, and provided feedback on the manuscript; J.M. Gunn provided funding and field support, input on study design, and edited the draft.

Chapter 3: The optical properties of dissolved organic matter and their relation to mercury concentrations in water and biota across a remote freshwater drainage basin
This chapter is presented as published in *Environmental Science and Technology* under the following citation: **Gretchen L. Lescord[1]**, Erik J.S. Emilson[2], Thomas A. Johnston[1,3], Brian A. Branfireun[4], and John M. Gunn[1]. Optical properties of dissolved organic matter and their relation to mercury concentrations in water and biota across a remote freshwater drainage basin. *Environmental Science and Technology*, 52: 3344−3353. DOI: 10.1021/acs.est.7b05348
[1]Vale Living with Lakes Center, Laurentian University, Sudbury ON, Canada; [2]Natural Resources Canada, Great Lakes Forestry Centre, Sault Ste. Marie ON, Canada; [3]Ontario

Ministry of Natural Resources and Forestry, Sudbury ON, Canada; [4]The University of Western Ontario, London ON, Canada

G.L. Lescord collected the majority of field samples, performed most lab and data analyses, and wrote the first draft of the chapter/manuscript. E.J.S. Emilson assisted with fluorescence and spectroscopy analyses of water samples, performed the PARAFAC modeling, assisted in data interpretation, and wrote part of the Methods section. T.A. Johnston provided funding, field and laboratory support, input on study design and statistical analysis, and edited the draft; B.A. Branfireun provided laboratory support, and provided feedback on the manuscript; J.M. Gunn provided funding and field support, input on study design, and edited the draft.

Chapter 4: Percent methylmercury in the muscle tissue of freshwater fish varies with body size, age, and among species

This chapter is presented as published in *Environmental Toxicology and Chemistry* under the following citation: **Gretchen L. Lescord**[1], Thomas A. Johnston[1,2], Brian A. Branfireun[3], and John M. Gun [1]. Percent methylmercury in the muscle tissue of freshwater fish varies with body size, age, and among species. *Environmental Toxicology and Chemistry.* DOI: 10.1002/etc.4233

[1] Vale Living with Lakes Center, Laurentian University, Sudbury ON, Canada; [2] Ontario Ministry of Natural Resources and Forestry, Sudbury ON, Canada; [3] The University of Western Ontario, London ON, Canada

G.L. Lescord collected the majority of field samples, performed most lab and data analyses, and wrote the first draft of the chapter/manuscript; T.A. Johnston provided funding, field and laboratory support, input on study design and statistical analysis, and edited the draft; B.A. Branfireun provided laboratory support, and provided feedback on the manuscript; J.M. Gunn provided funding and field support, input on study design, and edited the draft.

Chapter 5: Thesis conclusions and their implications for the Ring of Fire Development and subsistence fishers

Parts of this chapter will be submitted to *Environmental Health Perspectives* after the compilation of complimentary survey data (expected in November 2018) under the following citation: **Gretchen L Lescord[1]**, Chantal Sarrazin-Delay[1], Thomas A. Johnston[1,2], John M. Gunn[1], and David Pearson[1]. Food for thoughts: on communicating fish consumption recommendations and contaminant science to subsistence fishers in remote northern communities across Ontario.

[1]Vale Living with Lakes Center, Laurentian University, Sudbury ON, Canada; [2]Ontario Ministry of Natural Resources and Forestry, Sudbury ON, Canada

G.L.Lescord wrote the main draft of this review, helped design various communications materials, and participated in community visits. C. Sarrazin-Delay and D. Pearson led community visits and helped design various communications materials. All co-authors reviewed this draft and provided feedback and interpretation.

Acronyms

Absorbance	Abs
Alkalinity	Alk
Aluminum	Al
Ammonia + Ammonium	NH_3+NH_4
Arsenic	As
Calcium	Ca
Chloride	Cl
Concentration	[ ]
Condition Factor	Con.
Conductivity	Cond
Copper	Cu
Dissolved inorganic carbon	DIC
Dissolved organic carbon	DOC
Dissolved oxygen	DO
Dissolved organic matter	DOM
DOM Abs Ratio	E2:E3
DOM Component 1	C1
DOM Component 2	C2
DOM Component 3	C3
DOM Component 4	C4
DOM Component 5	C5
DOM Component 6	C6
DOM Component 7	C7
DOM Fluorescence Index	FI
DOM Freshness Index	β:α
DOM Humification Index	mHIX
DOM Specific abs coefficient	SAC
DOM Specific UV abs	SUVA
Drainage area	DA
Iron	Fe
Lake surface area	SA
Latitude	Lat
Lifetime growth rate	LGR
Longitude	Long
Magnesium	Mg
Manganese	Mn
Mean drainage basin slope	Slope
Methylmercury	MeHg
Nitrate + Nitrite	NO_2+NO_3
Potassium	K
Selenium	Se

Silicon	Si
Sodium	Na
Sulfate	SO_4
Surface temperature	Temp
Titanium	Ti
Total Nitrogen	TN
Total Phosphorus	TP
Total mercury	THg
True Colour	Colour
Ultra-Violet	UV
Wetlands area	Wetlands

Table of Contents

List of Figures

List of Tables

Chapter 1 : An overview of mercury cycling in Canadian boreal freshwater systems

1.1 Introduction

Fish is one of the healthiest sources of protein available, abundant with omega-3 fatty acids that are good for cardiovascular health and adolescent development (Daviglus et al. 1997; Domingo et al. 2007). The consumption of locally-caught freshwater fish is a dietary staple in remote northern communities across Canada and fishing practices are of great cultural importance. However, fish is also the main pathway for the uptake of contaminants, including mercury (Hg), one of the most ubiquitous contaminants detected in freshwater systems around the world. In its organic form, Hg is a neurotoxic and bioaccumulative metal that has adverse effects on the development of fetuses and young children and has been linked to various diseases in adults (Clarkson and Clarkson 1997, Poręba et al. 2012). Depending on their trophic ecology and habitat conditions, freshwater fish can have elevated Hg concentrations ([Hg]), sometimes exceeding recommended limits (e.g., 0.2, 0.3, 0.5, and 1.0 ppm Hg w.w.; WHO 2008, U.S. EPA, Health Canada 2007, U.S. FDA 2011, respectively) and posing considerable risk to subsistence consumers.

The ubiquitous nature of Hg in northern aquatic systems is due, in large part, to the atmospheric transport of gaseous and particulate Hg species that are deposited onto landscapes distant from any point source (Demers et al. 2007; Steffen et al. 2008; Amos et al. 2012). Although it is a naturally occurring element, the majority of Hg actively cycling in the environment today was anthropogenically released *via* industrial processes

(UNEP 2013; Pacyna et al. 2010, 2016). Atmospherically-transported Hg is readily deposited into aquatic systems where it can be converted into methylmercury (MeHg), the toxic and bioaccumulative form that constitutes the majority of total Hg (THg, the sum of all Hg species present in a sample) found in large-bodied and adult fish (Bloom 1992; Schaefer et al. 2014; Lescord et al. 2018b). This is because MeHg is readily bioconcentrated at the base of aquatic food webs and, given its strong binding within biotic tissues, is bioaccumulated and biomagnified up food chains to top predatory fish. As a result, fish populations that are distant from any anthropogenic activity can have elevated Hg levels and pose risks to human consumers (Marien and Patrick 2001; Johnsson et al. 2005; Mahaffey et al. 2011).

Substantial variability in [Hg] in water and biota can exist among freshwater systems, even those in close proximity to one another, for reasons that are not yet fully understood. Aquatic cycling of Hg species is complex and various physical (e.g., lake size, depth, stream order) and chemical (e.g., pH) characteristics of freshwater systems may alter Hg transportation, methylation/demethylation, and bioaccumulation. Understanding the effects of these characteristics is vital because many variables that alter Hg speciation and bioavailability in water and organisms at the base of food webs ultimately influence [Hg] in top predators, the most sought-after fish by both sport and subsistence fishers.

Several extensive syntheses detailing the mechanistic effects of various physicochemical variables on Hg cycling have been published in the last 20 years (e.g., Ullrich et al. 2001; Lehnherr 2014; Paranjape and Hall 2017). However, the dominant physicochemical factors that have a strong influence on Hg cycling may change

regionally based on local conditions (Ahonen et al. 2018). Furthermore, because many of these physicochemical factors are themselves subject to climate- and development-induced changes (e.g., temperature, pH, and concentrations of dissolved organic carbon, DOC), a thorough understanding of the local drivers of Hg speciation, bioaccumulation, and biomagnification is required to accurately monitor changes in aquatic [Hg] in a given region.

A considerable amount of research on how physicochemical factors affect Hg cycling has been conducted in remote northern regions (i.e., boreal or Arctic, above 45° N) around the world. While several reviews have been published highlighting such findings in Arctic systems (e.g., Riget et al. 2000, Lehnherr 2014, Chételat et al. 2015), syntheses on Hg cycling in the boreal are more limited. In this chapter, I review the current state of knowledge on Hg cycling in boreal freshwater systems, and briefly synthesize the key factors known to affect MeHg bioavailability, bioaccumulation, and biomagnification. I highlight recent findings and discuss their implications in the context of anticipated industrial development and climate change, both of which could alter the physicochemical characteristics of boreal lakes and rivers (Keller 2007; Webster et al. 2015). Finally, I present the research goals of my thesis and explain how the following chapters address some of the current gaps in knowledge and contribute to the broader understanding of Hg cycling in remote boreal watersheds.

1.2 The boreal ecozone and freshwater mercury cycling

The boreal ecozone is a circum-global belt in the northern hemisphere that is bounded by temperate forest to the south and subarctic tundra to the north. Definitions of

the boreal are based on climatic (e.g. mean annual temperatures between 3 and 6 ºC; Wieder et al. 2006) and, to a lesser extent, ecological variables (e.g. relatively species poor in vegetation and dominated by old-growth conifer trees; Hare and Ritchie 1972; Brandt 2009; Brandt et al. 2013). The boreal covers approximately 1.6 billion hectares distributed across 15 countries (Shvidenko and Apps 2006; Wieder et al. 2006). Given its size, this ecozone greatly influences various global processes; regulating year-round temperatures (Bonan et al. 1992), carbon storage (Luyssaert et al. 2008), and freshwater cycling (Young-Robertson et al. 2016).

Overall, approximately 30% of the boreal ecozone is located in Canada, which contains some of the boreal's most intact stretches of forest and 25% of its freshwater reserves, stored in vast peatlands and massive freshwater watersheds (Wells et al. 2010; Brandt et al. 2013). These watersheds provide key resources to remote indigenous communities scattered across northern Canada. For example, freshwater fish from boreal lakes and rivers are harvested through both commercial and sport fisheries (e.g., Kinnunen 2003), but also through vital subsistence fisheries, providing an affordable and nutritious food source (Loring et al. 2010; Fang et al. 2012). Healthy boreal ecosystems are therefore essential to the livelihoods, culture, and economies of many boreal communities, as well as global processes and broader planetary health.

1.2.1 Sources of mercury to boreal freshwater systems

Three main Hg species are involved in global transport and bioaccumulation: (1) elemental Hg (Hg^0), which is carried long distances through the atmosphere, (2) inorganic Hg (Hg(II)), which is deposited into aquatic systems, and (3) MeHg, the

bioaccumulative form of Hg (O'Driscoll et al. 2005; Steffen et al. 2008). Globally, it is widely accepted that the industrial and residential combustion of coal, as well as small-scale artisanal gold-mining are the dominant contributors of primary Hg^0 emissions (UNEP 2013; Pacyna et al. 2010, 2016). However, despite successful efforts to reduce industrial coal emissions in North America (Pacyna et al. 2010, 2016), fish [THg] does not appear to be decreasing in accordance; in fact, [THg] in some fish populations in the Canadian boreal region have increased since the 1970's (Tang et al. 2013; Gandhi et al. 2014). This may be due to the re-release of legacy Hg, originally emitted prior to the 1950's, from aquatic and terrestrial Hg reservoirs, by various processes (Amos et al. 2013; Pacyna et al. 2016).

Deposition of atmospherically-transported Hg on the boreal landscape is ubiquitous, including not only direct input into freshwater systems, but also onto forest cover and soils (Blackwell and Driscoll 2015), as well as peatlands (Enrico et al. 2016). As such, snow-melt or precipitation generated surface run-off from forested or peatland catchments contribute substantial amounts of Hg to boreal freshwater systems, largely through co-transport with dissolved organic matter (DOM) complexes (Kraus 2011; Schelker et al. 2011; Eklöf et al. 2012). Direct input of falling leaf-litter from foliage is also a significant source of both Hg (Rea et al. 1996; Graydon et al. 2009) and DOM (France et al. 1996; Hanson et al. 2011) to boreal freshwaters. Indeed, correlations between riparian conifer densities, the dominant trees in boreal forests (Brandt 2009), and piscine Hg concentrations have been reported (Eagles-Smith et al. 2016).

While direct atmospheric deposition of MeHg is possible (Lehnherr et al. 2012; Kirk et al. 2014), most mercury is deposited in boreal systems as Hg(II) and converted to

MeHg during the oxidation of organic matter by certain strains of anaerobic bacteria (mainly sulfate- and iron-reducing bacteria; SRBs and FeRBs, respectively; Gilmour et al. 2013; Hsu-Kim et al. 2013; Parks et al. 2013). Such bacterial methylation has been shown to occur in anoxic sediments or waters and, to a lesser extent, littoral or riparian regions of lakes (Watras et al. 2005; Eckley and Hintelmann 2006; Hamelin et al. 2011; Vidon et al. 2014). Peatlands are generally anoxic environments with bacterial communities that are abundant with SRB and FeRB, providing ideal conditions for Hg(II) methylation (St. Louis et al. 1994). Provided there is hydrological connectivity, peatlands can therefore be a major source of MeHg to nearby freshwater systems (St. Louis et al. 1994; Branfireun and Roulet 2002). Arctic snowpack can also have significant concentrations of both MeHg and THg, which enter polar lakes and rivers during the annual spring melt (Larose et al. 2013; Kirk et al. 2014). However, Hg dynamics in Arctic snow are largely influenced by photochemical reactions (Mann et al. 2014), and it is unclear how these processes might differ in the boreal region.

1.2.2 The physico-chemical and ecological drivers of mercury cycling

High variation in the concentrations of aqueous and biotic Hg among boreal freshwater systems is likely due, in part, to differences in physical, chemical, and ecological factors among these systems. In general, conditions that promote anaerobic bacterial growth and activity, such as low dissolved oxygen (DO), high sulfate concentrations, availability of labile DOM, and warmer waters, tend to increase methylation rates and subsequent aqueous and biotic [MeHg]. Similarly, factors that facilitate transport of Hg into freshwater systems, such as high concentrations of aromatic

DOM, tend to increase [THg]. Ecologically, an aquatic organism's carbon sources, trophic position, and growth rates all affect the amount of Hg bioaccumulated from their diet.

While extensive reviews of these factors' effects on Hg cycling have been provided previously by Ullrich et al. (2001), Lehnherr (2014), and Paranjape and Hall (2017), some examples of these factors relevant to this thesis are briefly discussed below.

Dissolved organic matter (DOM)

Dissolved organic matter (DOM) is well known to have both stimulating and inhibiting effects on MeHg production; it can serve as a substrate for bacterial activity and thus increase MeHg production (Wolf et al. 2009; Graham et al. 2013; Herrero Ortega et al. 2017; Bravo et al. 2017) or bind with Hg(II) and limit bacterial uptake, therefore hindering methylation (Hammerschmidt et al. 2008). Once formed, MeHg can also bind with DOM, facilitating its transport throughout watersheds (Wallschlager et al. 1996; Braaten et al. 2014) while simultaneously limiting its uptake into biota (French et al. 2014). High concentrations of DOM (generally measured as concentrations of dissolved organic carbon, [DOC]) tend to limit UV penetration in water, thus substantially lowering rates of photo-demethylation (Klapstein et al. 2017; Klapstein and O'Driscoll 2018).

Several recent studies have shown that [MeHg] in water and biota have a concentration-dependent relationship with aqueous [DOC]. French et al. (2014) reported that below concentrations of ~11 mg/L, DOC in Arctic lakes was comprised largely of fulvic acids, a more bioavailable form that stimulates methylation. In lakes with [DOC] > 11 mg/L DOC, amphipods had lower [MeHg], presumably due to the presence of more

humic acids that limited methylation and/or bioaccumulation (French et al. 2014). Braaten et al. (2018) also reported a parabolic relationship between [THg] in Eurasian perch (*Perca fluviatilis*) and aqueous [DOC] in Norwegian lakes, though no structural measurements of DOM were examined. Despite these findings, very few studies have considered the quality of DOM in relation to Hg cycling.

pH and ions

pH controls many aspects of Hg cycling, particularly those related to redox-mediated reactions (Scudder et al. 2010 and references therein). In general, more acidic waters have higher aqueous and biotic [Hg], though some discrepancies have been reported (e.g., Moore et al. 2009). More specifically, pH has been shown to mediate Hg uptake by methylating bacteria (Kelly et al. 2003), sorption in soils and sediments (Yin et al. 1997; Zhu et al. 2010), and binding strength with sulfur- and oxygen-based compounds in DOM complexes (Haitzer et al. 2003). Other ions can compete with Hg(II) for strong binding sites to DOM complexes, potentially lessening DOM-bound transportation of Hg (O'Driscoll and Evans 2000). Furthermore, in order for Hg(II) to be methylated, it must cross the membrane of anaerobic bacteria (passively or actively); cations tend to bind with polysaccharides along these membranes, stabilizing it and making it less permeable to Hg(II), limiting methylation (Daguené et al. 2012).

Sulfate and sulfides

Sulfate-reducing bacteria are generally recognized as the dominant methylators of Hg in boreal aquatic systems (Gilmour et al. 2013). As such, additions of sulfate tend to increase methylation and [MeHg] in surrounding waters (Compeau and Bartha 1985; Jeremiason et al. 2006; Kucharzyk et al. 2015). However, when rates of sulfate-reduction

are high, Hg(II) can also bind with the abundant, charged sulfide species that are produced. These complexes are not able to cross bacterial membranes and therefore, are not bioavailable for methylation or biotic uptake (Benoit et al. 2003; Hammerschmidt et al. 2008). Therefore, similar to DOC, sulfate has a concentration-dependent relationship with MeHg production when levels vary broadly (i.e., < 0.5 to ~12 mg/L). More recently, non-linear relationships have been reported between fish [THg] and aqueous sulfate concentrations. More specifically, piscine [THg] shows a positive relationship with sulfate concentrations up to 12 mg/L, but a negative relationship thereafter (Gabriel et al. 2014; Sumner 2016).

Growth rate and size

As an organism feeds, it ingests differing amounts of dietary MeHg depending on the food source and location (Karimi et al. 2016). Due to its strong binding with sulfhydryl groups within proteins and overall low excretion rates, MeHg is bioaccumulated over time (Peng et al. 2016; Bradley et al. 2017). As such, a fish's [Hg] is generally positively correlated with its length, weight, and age; larger and older fish tend to have higher [Hg] than smaller and younger fish of the same species. However, if a fish has a faster growth rate (i.e., more mass added per unit of time) or efficiency (i.e., more mass added per unit of energy consumed), its overall body concentration will likely be lower than that of a similar-sized fish with slower growth. This effect, known as bio-dilution, arises because flesh anabolism tends to increase at a more rapid rate than Hg absorption with increasing growth rate (Pickhardt et al. 2006; Karimi et al. 2007).

1.2.3 Anticipated impacts of climate change and industrial development on boreal ecosystems

The myriad effects of various physico-chemical and ecological parameters on Hg cycling are further complicated by the effects of climate change. While the type and magnitude of effects will vary regionally, an increasing number of studies suggest that boreal freshwater systems will experience higher DOC inputs and more extreme weather events (i.e., more severe droughts followed by intensified flooding periods) as the climate continues to warm (Stewart et al. 1998; Keller 2007; Adrian et al. 2009; Clark et al. 2010). Both of these factors may result in higher amounts of Hg in boreal freshwater lakes and rivers: changes to precipitation and weather patterns may directly alter atmospheric deposition of Hg onto boreal landscapes (Harris et al. 2007; Megaritis et al. 2014), while higher inputs of DOC may increase the amount of Hg transported in from riparian areas (Selvendiran et al. 2008; Bushey et al. 2008). Repeated and drastic alterations to water tables and hydrological patterns in peatlands can change the redox states of various parameters, including sulfate, stimulating bacterial reduction and, by extension, Hg methylation (Reiche et al. 2009; Wasik et al. 2015). Furthermore, the Hg species present in peatlands may be more mobile under future hydrological regimes and shifting vegetation communities (Szkokan-Emilson et al. 2013; Haynes et al. 2016).

Additional effects of climate change on boreal lacustrine environments have been reported, including warmer temperatures and shorter seasonal ice-cover which, paired with the brownification of waters, can cause changes to algal community structure and thermal- or oxic-structure of lakes (Keller 2007; Adrian et al. 2009; Edlund et al. 2017). However, the extent of these effects are dependent on regional conditions and system

morphology; larger, shallower lakes at higher latitudes are exhibiting stronger responses to thermal changes than smaller and more southerly systems (Pachauri et al. 2014; Magee and Wu 2017). Increasing temperatures are also expected to increase productivity of boreal freshwater systems and have been linked to enhanced growth of benthic primary producers (Baulch et al. 2005). Such an increase in productivity can result in an increased mass of primary producers and a subsequent bio-dilution of Hg within the plant material (Pickhardt et al. 2002).Warming temperatures may also result in longer growing periods, increasing fish growth rates and reducing [Hg], though recent lab-based studies examining the effects of temperature on Hg bio-dilution have reported unexpected increases in piscine [Hg] in warmer waters, possibly due to metabolic costs of thermal stress (Dijkstra et al. 2013; Thomas et al. 2018).

In addition to alterations due to a changing climate, many boreal habitats are stressed by industrial development that can directly or indirectly alter Hg cycling, including its bioavailability and bioaccumulation (Kreutzweiser et al. 2013; Webster et al. 2015). While the effects of some industrial activities have been well studied and their influence over Hg cycling are well understood (e.g., acid rain deposition, chlor-alkali production), other types require further investigation. Given the linkages between boreal forests and freshwater lakes and rivers (see section 1.2.1 above), it is not surprising that many studies have examined the effects of forestry on Hg cycling (Porvari et al. 2003; Bishop et al. 2009; Wu et al. 2018). Unlike forestry, however, the effects of various types of mining on Hg cycling have not been well studied. Given the strong relationships between Hg and various metallic ions (particularly Au, Fe, and Mn; Hylander et al. 2000; Albanese et al. 2007), mining has the potential to significantly affect Hg cycling. For

example, mining operations in the boreal often drain large areas of peatlands, a process which can have many secondary effects on surrounding systems (Landry and Rochefort 2012). The discharge from mining operations can also greatly alter the water chemistry of receiving waterbodies, affecting pH, sulfate and various other ions, all factors which can alter Hg dynamics (Johnson et al. 2016; Wellen et al. 2018).

1.3 Thesis overview

1.3.1 Research objectives

The overarching goal of my thesis was to assess patterns of Hg bioaccumulation and biomagnification in freshwater systems across a large, and relatively pristine boreal drainage basin. In the subsequent chapters, I determined the key drivers of Hg concentrations and speciation in biota from lakes and river sites spanning broad physical, chemical, and ecological conditions. Specifically, I studied systems across the Attawapiskat drainage basin (ADB) in the Far North of Ontario (Figure 1-1); a vast watershed (50,000 ha) beginning as headwater lakes in the Boreal Shield Ecozone and transitioning into shallow lakes, small tributaries, and the mainstem Attawapiskat River that passes through the Hudson Bay Lowlands (aka Hudson Plains) Ecozone, one of the world's largest wetlands (Gorham 1991; Glooschenko et al. 1994). Lakes located on the shield landscape are deeper, clearer, have higher ion concentrations, and a more verdant riparian zone compared to lakes on the lowlands (MacLeod et al. 2017). I therefore utilized the diverse nature of this remote watershed to better understand how physico-chemical and ecological factors affect [Hg] in water, sediments, invertebrates, and fish on a relatively large scale (i.e., across a watershed of ~50,000 km^2) but within a relatively

narrow climatic range. Furthermore, this watershed, which is a key resource for several First Nations communities, crosses the newly discovered mineral-rich area known as the "Ring of Fire." The Ontario Ministry of Northern Development and Mines reports significant discoveries of chromite, nickel, copper and platinum-group metals in this area, and 21 companies have proposed plans for mining developments in this area. Only one mine is currently active within the ADB; the Victor diamond mine (DeBeers Canada) on the lower Attawapiskat River, where operations are beginning to slow and remediation efforts will begin shortly.

As discussed in sections 1.2.2 above, the mechanistic interactions between Hg and various physical, chemical, and biological characteristics of aquatic systems have been well established in laboratory settings, and within individual aquatic systems. This thesis builds upon this earlier knowledge to understand Hg cycling on a broader, landscape scale. In particular, I will investigate the role and influence of various factors believed to influence MeHg bioavailability and bioaccumulation throughout the drainage basin. The three main goals of my dissertation are to:

(1) Model Hg cycling, bioaccumulation, and speciation in relation to large-scale environmental gradients across the ADB;

(2) Measure and report [Hg] in subsistence fish and the food webs that support them; and

(3) Provide a summary of findings and baseline data to environmental monitoring programs for the Ring of Fire

1.3.2 Thesis structure and research significance

This thesis is divided into 5 chapters, including this literature review and introduction (Chapter 1); the content and significance of each subsequent chapter are briefly discussed below.

i. Chapter 1: An overview of mercury cycling in Canadian boreal freshwater systems.

ii. Chapter 2: Mercury bioaccumulation in relation to changing physicochemical and ecological factors across a large and undisturbed boreal watershed.

While many studies have examined how latitudinal gradients effect Hg cycling and bioaccumulation in freshwater systems (e.g., Ahonen et al. 2018), this chapter was the first study, to the best of my knowledge, to examine how a system's landscape position within a drainage basin affects its physico-chemical conditions and Hg accumulation. The natural gradients of physical, chemical, and ecological factors across the watershed were reported and key drivers of Hg concentrations and biomagnification rates were determined. This chapter also provides the baseline data (largely provided in the supplemental information (SI) file herein) that will be valuable for future monitoring programs assessing the effects of climate change and industrial development, particularly in and around the Ring of Fire mineral exploration and development zone. This chapter was recently submitted for publication in the *Canadian Journal of Fisheries and Aquatic Sciences* and is currently under review.

iii. Chapter 3: The optical properties of dissolved organic matter and their relation to mercury concentrations in water and biota across a remote freshwater drainage basin.

In this chapter, I utilized fluorescence and absorbance spectroscopy to identify key structural components of DOM and assessed the changing structure moving from headwater lakes to outlet streams. The effects of these structural characteristics on the bioaccumulation of Hg were also examined. The data from this study were highly novel, showing not only the changes in DOM structure across such a large-scale watershed for the first time, but also the utility in fluorescence spectroscopy (a relatively easy and inexpensive analysis) in understanding Hg dynamics in boreal systems. This chapter has been published in *Environmental Science and Technology* (DOI:10.1021/acs.est.7b05348).

iv. Chapter 4: Percent methylmercury in the muscle tissue of freshwater fish varies with body size, age, and among species.

Most modern studies examining Hg in fish muscle tissue assume that the vast majority of the THg present is in the methylated form. This assumption, however, is based largely on studies examining Hg speciation in the muscle of large-bodied piscovores. This study, now published in *Environmental Toxicology and Chemistry* (DOI: 10.1002/etc.4233), assessed the percent of MeHg (%MeHg = 100 x [MeHg] / [THg]) in the muscle tissue of individual fish from five species across wide ranges of body sizes (35 to 800 mm total length) and ages (YOY to 20 years old). Results hold major

implications for the current practice of analyzing [THg] as a proxy for [MeHg] in muscle tissue from fish species regardless of size and trophic ecology.

v. Chapter 5: General conclusions and considerations for communicating fish consumption guidelines in the Far North of Ontario.

In the final thesis chapter, I review the major conclusions of each chapter and discuss their overall importance to the broader Hg literature. I also briefly discuss my experiences working in remote northern communities and synthesize techniques my colleagues and I employ to effectively communicate Hg science, our research, and consumption recommendations set by the Ontario provincial government. I also highlight key considerations for future researchers and communicators in the Far North of Ontario and identify research gaps that will help inform government guidelines and, by extension, the consumers. This work is intended for a publication in *Environmental Health Perspectives* once associated survey data has been collected.

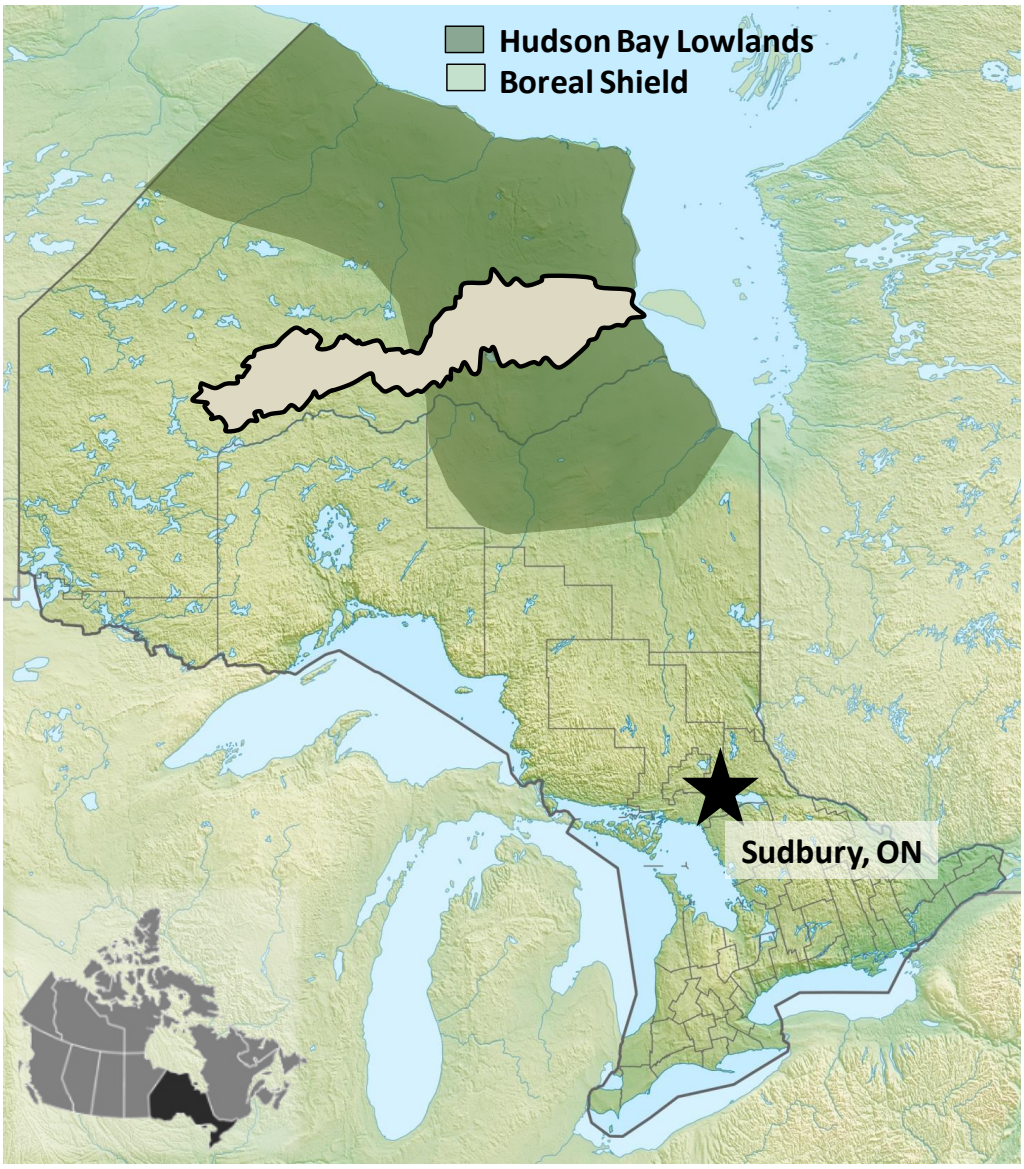

Figure 1-1: The Attawapiskat Drainage Basin (ADB) in the Far North of Ontario

Chapter 2 : Mercury bioaccumulation in relation to changing physicochemical and ecological factors across a large and undisturbed boreal watershed

2.1 Abstract

1. Within a drainage basin, the position of a lake or river site can greatly affect its limnological and ecological characteristics, including system size, nutrient loadings, and biotic community structure. These factors may also affect the cycling of mercury (Hg), a neurotoxic metal that has been detected in remote northern watersheds around the world.

2. In this study, we examined how 43 physical, chemical and ecological end-points change across 58 lake and river sites within a remote and undisturbed boreal watershed in northern Ontario, Canada, and assessed their influence on aqueous and biotic total and/or methyl Hg concentrations ([Hg]). We sampled in and around the mineral-rich region known as the “Ring of Fire,” which is expected to be heavily developed in the coming years to facilitate decades of resource extraction.

3. We found several physico-chemical parameters, but few ecological factors, that varied in systematic patterns across the watershed. Overall, [Hg] in water and, to a lesser extent, fish increased in systems with decreasing landscape position (i.e., a lower elevation). In particular, fish [Hg] increased moving downstream in the Attawapiskat River across the Hudson Bay Lowlands.

4. Aqueous and biotic [Hg] were most strongly related to DOC and nutrient concentrations across the watershed. In biota, [Hg] was lower in more productive systems, indicating a possible bio-dilution effect. Interestingly, concentrations of nitrates and nitrites were a consistent positive predictor of biotic [Hg], suggesting an indirect relationship between Hg and N cycling that warrants further study.

5. Results and baseline data from this study will be valuable for future research and monitoring programs to assess the effects of climate change and industrial development, particularly in and around the Ring of Fire region.

Key words: mercury, landscape position, water chemistry, drainage basin, food webs

2.2 Introduction

The Canadian boreal ecozone contains some of the largest relatively undisturbed watersheds in the world, which support a diverse array of aquatic life and provide vital ecosystem services for surrounding communities (Urquizo et al. 2000; Browne 2007; Bogdanski 2008; Wells et al. 2010; USEPA 2012). Freshwater lakes and rivers are subjected to natural physical and chemical gradients across such watersheds, which influence their limnology, fish habitat and other important ecological characteristics (Kratz et al. 1997; Ellis and Jones 2013). For example, the position of a system within a drainage basin (also known as its "landscape position") can strongly influence its physical attributes (Martin and Soranno 2006), water chemistry (Johnson et al. 2000), and biological community structure (Smith and Kraft 2005). In general, headwater lakes with a higher landscape position are expected to be smaller, have lower concentrations of

dissolved organic carbon (DOC) and silica, receive a higher proportion of water from precipitation than groundwater, and have lower species richness in their fish communities when compared to systems at a lower landscape position (Kratz et al. 1997). Similar effects are observed along a river continuum with organic matter becoming increasingly finer and invertebrate communities becoming functionally less diverse moving downstream (Vannote et al. 1980).

Shifts in physicochemical and biological characteristics of aquatic systems across watersheds can alter other important limnological and ecological processes, including the cycling of mercury (Hg), a bioaccumulative metal of concern in boreal freshwater systems. Much of the Hg found in boreal lakes and rivers originates from distant industrial sources, entering remote systems *via* atmospheric-transport and deposition. Once deposited in the inorganic form, Hg(II), it can be methylated by sulfate-reducing and other anaerobic bacteria (Gilmour et al. 2013). The neurotoxic methylmercury (MeHg) produced can bioaccumulate and biomagnify through aquatic food webs, resulting in relatively high concentrations in predatory fish that pose a potential health risk to residents of northern communities who consume these fish regularly for subsistence. However, aquatic Hg transport, methylation, and bioaccumulation are all strongly influenced by the surrounding physico-chemical environment (Lehnherr 2014; Paranjape and Hall 2017). While several studies have examined how physico-chemical or biological traits of aquatic systems affect Hg cycling (Gantner et al. 2010; Lescord et al. 2015; Sumner 2016; Ahonen et al. 2018; Chételat et al. 2018), none, to our knowledge, have explored the effects of landscape position within a drainage basin, and the associated changes in physico-chemical characteristics, on Hg bioaccumulation.

Our objectives were to assess how mercury concentrations in water and biota varied across a large, northern drainage basin, and to determine the key landscape and limnological drivers of this variation. We sampled 58 lake and river sites across the Attawapiskat Drainage Basin (ADB), a vast (>50,000 km^2), unregulated, boreal watershed located in northern Ontario, Canada (Figure 2-1). We assessed 38 physicochemical variables across sites and analyzed a subset of invertebrates and fish for various ecological endpoints (e.g., food web position, growth rates) as well as [Hg] to determine: (1) spatial gradients of physical features, water chemistry, ecological factors, and Hg cycling across the ADB, and (2) the key drivers of Hg bioaccumulation and biomagnification among its lakes and rivers. We hypothesized that DOC concentrations, water hardness, and lake depth would show the largest degrees of change across the ADB and, consequently, have the strongest influence over Hg concentrations in water and biota throughout the watershed.

The ADB is one of the largest relatively undisturbed boreal freshwater watersheds in the world, making it an ideal study location for understanding how landscape position of a system affects its limnology and Hg bioaccumulation. Furthermore, while only one mine is currently active in the ADB (DeBeers Victor diamond mine on the lower Attawapiskat River), the watershed contains a large portion of the Ring of Fire mineral deposit (Figure 2-1), where extensive development to support resource extraction is expected (MNDM 2018). A baseline understanding of how a system's landscape position affects its physico-chemistry, aquatic ecology, and Hg dynamics will be a vital to monitoring environmental impacts of both future land-use and further changes to the climate in the ADB as well as in other boreal watersheds.

2.3 Methods

2.3.1 Study area

The ADB spans two distinct northern ecozones, the Boreal Shield (hereafter referred to as the Shield) and the Hudson Bay Lowlands (also known as the Hudson Plains, hereafter referred to as the Lowlands), the lakes and rivers of which differ considerably in their physical and chemical characteristics (MacLeod et al. 2017). The western portion of the ADB (~ 200 – 410 m elevation) is on the Shield and is composed of a vast lake-river network with thin soils over igneous Precambrian Shield rock. The eastern portion (~ 0 – 200 m elevation), on the Lowlands, is composed of glaciofluvial deposits underlain by sedimentary limestones and dolostones and is dominated by rivers flowing into lower James Bay (Figure 2-1). Lakes located on the Shield are generally larger, deeper (> 5 m maximum depth), clearer, and have densely forested riparian areas. In contrast, Lowland lakes tend to be shallower (≤ 3 m maximum depth), more turbid, surrounded by vast peatlands, and have less historical data when compared to Shield lakes (MacLeod et al. 2017; Lescord et al. 2018a). To date, the ADB has experienced minimal anthropogenic disturbance (see SI section for further details).

In total, 31 lakes (20 on the Shield and 11 on the Lowlands) and 27 river sites (10 on the mainstem Attawapiskat River and 17 tributaries) were sampled for this study (Figure 2-1). Only 2 river sites (both mainstem) were on the Shield, the remaining 25 were on the Lowlands. Many Lowland lakes in the ADB were too shallow for float plane access, and to increase our sample size in this ecozone, we sampled four of the Lowland lakes

immediately south of the ADB: three in the Albany River drainage basin, and one in the Kapiskau River drainage basin (Figure 2-1). Overall, the 58 sites sampled in this study spanned a large geographic area (~ 575 km^2 and 400 m of elevation) including parts of the Ring of Fire mineral deposit (Figure 2-1).

2.3.2 Sample collection

Sampling methods were similar to those described in Lescord et al. (2018a, b). Water samples were collected from 28 lakes (9 Lowland and 19 Shield) and 19 of the river sites in late July or early August of 2015. All sites were sampled using ultra-clean methods for [THg] (unfiltered), [MeHg] (unfiltered), and 26 other water chemistry parameters including concentrations of DOC, total phosphorus (TP), total nitrogen (TN), sulfate, and base cations (e.g., total unfiltered calcium, Ca, or sodium, Na), as well as pH, conductivity, and true colour. A full list of all parameters measured and their abbreviations can be found in the Supplemental Information (SI) file (Table SI-1). Additional data from water collections on two Lowland lakes and five river sites in 2013 were obtained from the Ontario Ministry of the Environment and Climate Change (MOECC), though not all parameters were measured in these analyses (n = 3-36 parameters depending on the site; see Tables SI-2 through SI-7). Water samples were taken at the surface of all lakes and river sites approximately 1 m below surface by hand or with a Van Dorn sampler. Temperature and dissolved oxygen (DO) readings were taken at the surface of all sites. A full water column temperature and DO profile was taken at the deepest location of each lake to assess summer stratification (data not shown); only four Shield lakes showed marked stratification, with decreases in

temperature and DO at depth (> 12 m). Secchi depths were also determined at the deepest location of each lake.

Four landscape features were obtained for each lake and river site using the Ontario Flow Assessment Tool (OFAT; OMNRF 2017) or NRCAN Toporama (Natural Resources Canada 2017): elevation, mean drainage basin slope (herein referred to as slope), total drainage basin area, and area of wetlands in the basin (herein referred to as wetlands). Surface areas and maximum depths of lakes were obtained from the Ontario Ministry of Natural Resources and Forestry's (MNRF) Aquatic Habitat Inventory database. Measurements of all physico-chemical parameters are provided in the SI section, Table SI-2 through SI-7.

Benthic macroinvertebrates were collected at 1-3 nearshore sites in each of 10 Shield and six Lowland lakes, as well as at single reaches in each of six river sites by kick sweeping during July-August of 2014 or 2015. Collected invertebrates were pooled by order (Amphipoda, Ephemeroptera, and Trichoptera, as well as Plecoptera from river sites only; herein referred to as amphipods, mayflies, caddisflies, and stoneflies, respectively) to ensure adequate biomass for all laboratory analyses. Unionid clams were collected from nearshore areas of lakes and from riffle zones of mainstem river sites. Crayfish (Decapoda) were collected in the nearshore by kick and sweep and electrofishing, and snails (Gastropoda) were gathered by hand from the nearshore zone. Bulk zooplankton was collected in lakes by towing a Wisconsin net (25 cm diameter, 100 cm long, 80 μm mesh) horizontally at ~ 0.5 m depth behind a boat for approximately 3 to 5 minutes in the offshore zone. This process was repeated 3 times and each tow was considered 1 composite zooplankton sample (n = 3 / lake). All invertebrate samples were

frozen until further analysis. Table SI-8 shows the sample sizes of each invertebrate group caught at each lake or river site. In subsequent tissue analysis the foot muscle, tail muscle, and whole viscera (body minus shell) were removed from individual clams, crayfish, and snails, respectively; composite samples of whole bodies were used for all other invertebrate groups.

Large-bodied fishes were collected using multimesh, monofilament, benthic gill nets in both nearshore and offshore areas on 17 Shield and 10 Lowland lakes, and in low-current locations at each of the 10 mainstem river sites from 2009 to 2015. Up to 20 individual white sucker (*Catostomus commersonii*; herein referred to as sucker), lake whitefish (*Coregonus clupeaformis*, herein referred to as whitefish), northern pike (*Esox Lucius*, herein referred to as pike), and walleye (*Sander vitreus*) were collected at each site, though not all species were captured at all sites (see Table SI-9 for collection years, and sample sizes of each species at each site). Spottail and emerald shiners (*Notropis* sp.; herein referred to as shiners), common small-bodied forage fishes consumed by walleye and pike, were also sampled in nearshore zones of lakes with small-mesh gill nets, and by electrofishing. All fish were weighed and measured for total and fork lengths, and dorsal muscle was removed and frozen until later analysis. Ageing structures were collected from large-bodied species; these included sagittal otoliths for whitefish and walleye, cleithra for pike, and pectoral fin rays for sucker (see SI section for aging methods). Attribute data from each large-bodied fish were used to calculate lifetime growth rate (LGR; body weight divided by age, in g/year) and body condition (the residual loge mass from a pooled species-specific loge mass vs loge total length relationship; Kaufman et al. 2007).

2.3.3 Laboratory analysis

All water samples were analyzed for [THg] and [MeHg] at the ISO 17025 accredited Biotron trace-metal laboratory at the University of Western Ontario (London, ON). A full description of Hg analytical procedures is presented in Lescord et al. (2018a). Analyses were conducted as per the United States Environmental Protection Agency (USEPA) methods 1631 and 1630 on Tekran instruments. All results were blank-corrected using the mean method blank concentrations of a given batch. While no samples were below the method detection limits (MDLs) for THg (0.05 ng/L), two samples were below the 0.006 ng/L MDL for MeHg; these samples was assigned a random value less than half of the limit. Percent recoveries of all standard checks and spikes were high (93.8 to 106%, n = 9-22) and within accredited standards. Relative percent differences of duplicates were low, 1.8-3.0% (n = 15, see Table SI-10 for all QA/QC results). All other water chemistry analyses were performed at MOECC laboratories (Dorset and Etobicoke, ON, Canada) following standard procedures (OMOECC 1983).

Tissue samples of all invertebrates and small-bodied fishes, and muscle sub-samples of large-bodied fishes were freeze-dried using a LABCONCO FreeZone Bulk Tray Dryer, and homogenized using a Retsch MM400 ball mill at Laurentian University (Sudbury, ON). Invertebrate and shiner samples were analyzed for MeHg using a hot-block and potassium hydroxide (KOH) digestion (Bloom and Fitzgerald 1988); detection was performed using the same methods as for water (USEPA 1630). A total of 2,212 large-bodied fish muscle samples were analyzed for total [Hg] (the sum of all Hg forms) using one of two methods: (1) by Thermal Decomposition and Amalgamation Atomic

Absorption Spectroscopy (TDA-AAS) on a Milestone direct mercury analyzer (DMA-80) following USEPA method 7473 at the Biotron Laboratory (n = 614; ppm dry mass); or (2) by cold vapor-flameless atomic absorption spectroscopy (CV-FAAS) at the MOECC Laboratory Services Division, following protocol HGBIO-WS057 (n = 1,598; ppm wet mass). Using a broader dataset of 302 suckers, 104 whitefish, 189 pike, and 863 walleye from Ontario lakes that had been analyzed using both methods we developed species-specific linear relationships between methods (see SI section for equations) to convert all CV-FAAS wet mass [THg] estimates to TDA-AAS dry mass [THg] estimates. It was assumed that the majority of [THg] (>80%) was the methylated form, though it is important to note that some smaller fish may have lower proportions of MeHg in their muscle tissue (Lescord et al. 2018b).

Freeze-dried and ground tissue samples were analyzed for carbon and nitrogen stable isotope ratios at the University of New Brunswick's Stable Isotopes in Nature Laboratory using methods described by Jardine et al. (2003). Carbon and nitrogen stable isotope (SI) values are used to infer an animal's food web position in terms of primary production sources and trophic elevation, respectively (Post 2002). Ratios of heavy to light SIs were expressed in parts per thousand (‰) as standard delta (δ) notation relative to International Reference Standards using the formula: $\delta X = [(R_{sample} / R_{standard}) - 1] \times 1000$, where X is ^{13}C or ^{15}N, and R is the corresponding ratio, $^{13}C/^{12}C$ or $^{15}N/^{14}N$ (Peterson and Fry 1987; Fry 2006). Certified standards and duplicates were similar to target values (i.e., relative percent differences <0.01±0.01 to 0.2±7.5%); all QAQC results for isotope analyses are presented in Table SI-11.

2.3.4 Data handling and statistics

All statistical analyses were performed using R (v. 3.4.3; R Core Team, 2017) and alpha was set at 0.05 in all tests. Graphics were produced using the R package *ggplot2* (v.2.2.1; Wickham and Chang, 2016).

In analyses across lake and river sites, within-site means of each biotic variable were used to represent the populations. For large-bodied fish, means of [THg], isotope ratios, and body condition were adjusted for body size covariation; least-square means of these variables were estimated for each population at 500 g (the approximate median weight of fish herein) from an ANCOVA model (y ~ weight + site + weight*site). LGR was standardized to 1000g using the same method. Prior to some statistical analyses, fish isotopic data were also adjusted for baseline variation among sites. Within-site mean $\delta^{13}C$ and $\delta^{15}N$ of clam foot muscle were subtracted from that of the fish population, resulting in baseline-corrected values (i.e., $\delta^{13}C_{cor}$ and $\delta^{15}N_{cor}$). Clam data were available in 21 lakes; an additional 8 lakes had other invertebrate data which were used to estimate clam values based on linear relationships developed across ADB sites where both taxa were present (see SI section and Table SI-12 for details). Raw isotope measurements were used for invertebrates in all tests. System mean values for all ecological end-points are presented in Tables SI-13 through SI-18.

Spatial patterns in water chemistry and physical variables

A total of 25 physical and chemical characteristics of lakes and river sites were entered into a Principal Components Analysis (PCA) to assess environmental gradients across the ADB using the *prcomp* R package (Sigg, 2014). The loadings of each variable on all resulting rotated Principal Components (PCs) with eigenvalues > 1 are presented in

Table SI-19. Using only lake data, a second PCA was performed with the same 25 variables, plus three additional variables unique to lakes: surface area, maximum depth, and Secchi depth. Parameter loadings for this analysis are presented in Table SI-20. Additionally, all 28 physico-chemical variables were compared among the three groups of aquatic systems (i.e., Shield lakes, Lowland lakes, river sites) using Kruskal Wallis H-tests; post-hoc comparisons were performed using Convers test from the *PMCMR* package (Pohlert 2016) and are presented in the SI section (Table SI-21).

Ten phyisco-chemical variables (surface DO, slope, sulfate, pH, Ca, NO_2+NO_3, Na, DOC, TP, and TN) were chosen for further modeling throughout this study; based on PC loadings, these variables accounted for relatively unique variation in the overall dataset. Furthermore, they are relevant to Hg biogeochemistry and are anticipated to change with climate change and future industrial development. To further assess spatial patterns in these variables, each measure (n = 1/lake or river site) was examined with respect to system elevation, an index of landscape position within the ADB (Kratz et al., 1997; Table SI-22).

Spatial patterns in biotic mercury concentrations and ecological end points

Similar to physico-chemical variables, [THg] and/or [MeHg] in water (n = 1/site) and biota (variable n/site) were first examined with respect to system elevation. Because fish from this study were collected over a 9-year period, the relationships between predicted mean [THg] at 500 g and system elevation were assessed using linear mixed effects (LME) models that included collection year as a random variable. Similarly, benthic invertebrates were sampled over a 2-year period (2014 and 2015) and the relationships between mean [MeHg] and system elevation for each taxon were also assessed with a

LME model that included sampling year as a random factor. In addition to LME models across the drainage basin, [MeHg] and [THg] in water and biota (standardized to 500 g in large-bodied fish) were compared among the three groups of aquatic systems (Shield lakes, Lowland lakes, river sites) using Kruskal Wallis H-tests; post-hoc comparisons were performed using Convers test from the PMCMR package (Pohlert 2016; Table SI-22 and SI-23). A similar approach was used to analyze patterns in other ecological variables across the ADB including $\delta^{13}C$ and $\delta^{15}N$ in invertebrates, and $\delta^{13}C_{cor}$, $\delta^{15}N_{cor}$, body condition (all standardized to 500 g), and LGR (standardized to 1000 g) in large-bodied fish (post-hoc results shown in Tables SI-24).

Spatial patterns in biomagnification

To assess the rate of Hg biomagnification within each lake or river site, trophic magnification slopes (TMSs) were calculated by regressing $\log_{10}$[Hg] (MeHg in invertebrates and forage fish and THg in large-bodied fish) against raw $\delta^{15}N$ for all sampled biota, as per Lavoie et al. (2013). The intercepts of these relationships, often referred to as the trophic magnification intercept (TMI), are used as an index of [Hg] at the base of the food web. We calculated TMSs and TMIs in systems with at least three composite samples of benthic invertebrates (caddisflies, mayflies, stoneflies, and/or amphipods) as well as data from four fishes (shiners, suckers, pike, and walleye). In total, 8 Shield lakes, 6 Lowland lakes, and 4 river food webs were modeled in this way. Table SI-25 shows the TMS, TMI, and other regression results, as well as the taxa included in each food web model. Resulting TMSs and TMIs were plotted against system elevation to assess changes in rates of Hg biomagnification and Hg inputs, respectively, across the drainage basin; these relationships were assessed as simple linear regressions. Similar to

water and biotic [Hg], TMSs and TMIs were compared among groups (i.e., river sites, Lowland lakes, and Shield lakes) using Kruskal Wallis H-tests and Convers test, as described previously (Table SI-23).

Modeling drivers of mercury concentrations and biomagnification

To determine which physico-chemical factors were most strongly linked to Hg bioaccumulation and biomagnification, AIC model averaging was performed using the R-package *AICmodavg* (Mazerolle 2017) as per Sumner (2016) and Grueber et al. (2011). In total, modeling exercises were performed using lake as the replicate for 11 dependent variables: mean [THg] in surface water, mean [MeHg] in surface water, mean [MeHg] in each of four invertebrate groups (amphipod, caddisfly, mayfly, and zooplankton), predicted mean muscle [THg] at 500 g in each of three large-bodied fish species (sucker, pike, and walleye), and biomagnification metrics (TMSs and TMIs). Stonefly, shiner, and whitefish sample sizes were deemed too low for modelling. Due to missing water chemistry data from river sites with biotic data, these 11 models were run using lake data only. Additional water models were run across all lakes and river sites (results shown in SI section).

For all water models, 10 standardized predictor variables (DO, sulfate, TP, TN, NO2+NO3, DOC, slope, Na, Ca, and pH) were entered into a global model. All models containing combinations of up to 2 predictor variables (plus an intercept) were fitted and ranked using AICc, a form of AIC used when sample sizes are <100 (Burnham and Anderson 2002). Coefficients of each of the 10 predictors were then averaged across all models with a delta AICc value (ΔAICc, the difference between a model's AICc value and the overall lowest AICc value in the full model ranking) less than 4 (Burnham and

Anderson 2002; Burnham et al. 2011). When a parameter was not included in a model, a 0 was included for coefficient averaging (Grueber et al. 2011). For modeling invertebrate [MeHg] these same 10 predictor variables were used, plus mean $\delta^{13}C$ and $\delta^{15}N$, and the same model selection and coefficient averaging methods were applied. Similarly, for modeling large-bodied fish [THg] at 500 g, the same 10 predictor variables were used plus $\delta^{13}C_{cor}$, $\delta^{15}N_{cor}$, and body condition (standardized to 500 g). Variance Inflation Factors (VIFs) were monitored for issues with multicollinearity in all tests. Results of each modeling exercise are listed in Tables SI-26 through SI-39.

2.4 Results

2.4.1 Physical and chemical gradients across the watershed

As expected, systems across the ADB showed particularly broad ranges in [DOC] (5.4 – 29.1 mg/L), water clarity (colour = 12 – 282 TCU, Secchi depth = 0.5 – 3.1 m), cation concentrations (e.g., [Ca] = 2.7 – 31.9 mg/L), and DO (5.6 – 9.7 mg/L; Table 2-1). Concentrations of various nutrients also ranged broadly (e.g., [TN] = 0.03 – 0.56 mg/L, $[NO_2+NO_3]$ = <1 – 30 µg/L) across the ADB (Table 1). Furthermore, the mean slope and area of wetlands in each drainage basin varied considerably (0.9 – 4.0% and 0 – 28,528 km^2, respectively; Table 2-1). Within lakes, the maximum depths ranged from 1.3 – 23.4 m and surface areas ranged from 44 – 28,100 ha (see Table 2-1). The river site immediately downstream of the active diamond mine showed markedly elevated concentrations of sulfate (9.45 mg/L) and other ions (e.g., [Na], 12.9 mg/L) and was removed as an outlier in all PCA analyses and regional comparisons.

Results showed a general decrease in DO, pH, mean drainage basin slope, and concentrations of sulfate and NH_3+NH_4 with decreasing landscape position (Figure 2-2a). Conversely, concentrations of nutrients (i.e., TN, NO_2+NO_3, TP), as well as DOC and water colour tended to increase toward the outflow (Figure 2-2a). Indeed, all of these measures were found to be significantly different among the groups (i.e., Shield lakes, Lowland lakes, and river sites; p = <0.001 - 0.045). Sulfate and Al concentrations, water colour, and DO were significantly different among all regions (Table 2-1; p = <0.001 – 0.038). Concentrations of Cl and K, as well as mean drainage basin slope were only significantly different between Shield and Lowland lakes (p <0.001 to 0.003), and between Shield lakes and river sites (p <0.001 to 0.011), but not between Lowland lakes and river sites (p = 0.110 to 0.999), implying substantial regional effects on these parameters (Table 2-1). DOC and As concentrations, on the other hand, showed significant differences between each of the lake types (i.e., Shield and Lowland) and river sites (p <0.001 to 0.015), but not between the lake types themselves (p = 0.181 and 0.167 for DOC and As, respectively), implying an effect of system type on both parameters (Table 2-1).

2.4.2 Spatial patterns of ecological characteristics across the watershed

Delta ^{13}C values were not significantly related to system elevation in any invertebrate group (p = 0.22-0.72, r^2 = 0.007-0.094; Table 2-2), indicating no consistent change in invertebrate diets throughout the watershed. This agrees with the lack of significant differences found in any invertebrate $\delta^{13}C$ values among regions (i.e., Shield vs. Lowland vs. River; p = 0.219-0.591). However, $\delta^{15}N$ in zooplankton was positively

related to system elevation, suggesting higher trophic elevation of pelagic invertebrates in headwater systems ($p = 0.006$, $r^2 = 0.385$; Table 2-2). Indeed, $\delta^{15}N$ of zooplankton was significantly higher in Shield lakes (5.11±0.97 ‰) than Lowland lakes (3.16±1.21 ‰; $p = 0.006$). No other significant relationships were found between invertebrate $\delta^{15}N$ and system elevation ($p = 0.10$-0.87; $r^2 = 0.002$-0.147; Table 2-2) nor differences in invertebrate $\delta^{15}N$ among regions ($p = 0.054$-0.558).

Mean $\delta^{13}C_{cor}$ at 500 g was significantly and negatively related to system elevation in whitefish, but not in any other fish species examined (Table 2-2; $p = 0.002$, $r^2 = 0.650$). Indeed, whitefish had significantly different $\delta^{13}C_{cor}$ among regions ($p = 0.027$), with riverine fish having lower signatures (2.32±2.99 ‰) when compared to those from Lowland (8.62±1.15 ‰) and Shield lakes (4.33±1.90 ‰). However, $\delta^{15}N_{cor}$ values at 500 g were significantly and positively related to system elevation in suckers only ($p = 0.016$, $r^2 = 0.209$; Table 2-2). Among-region comparisons showed significant differences in $\delta^{15}N_{cor}$ of suckers ($p = 0.006$) as well as pike ($p = 0.010$). In both cases, $\delta^{15}N_{cor}$ values were significantly higher in riverine sites when compared to lakes.

Neither condition nor size-standardized LGR were significantly related to system elevation, except condition in pike, which increased moving downstream in the ADB (Table 2-2). Indeed, pike had a significantly lower condition in lakes (mean = -0.03 and -0.02 in Lowland and Shield lakes, respectively) when compared to river sites (mean = 0.07; $p = 0.001$). LGR in pike was also significantly different among regions ($p = 0.042$) but the mean differences were small (i.e., 200 vs. 166 vs. 201 g/year in river sites, Lowland lakes, and Shield lakes, respectively). No significant among-region differences were found in condition or LGR for the other fish species tested.

2.4.3 Mercury concentrations and rates of biomagnification across the watershed

Overall, aqueous [MeHg] and [THg] were generally low but variable across the ADB, ranging from <0.001 to 0.116 and 0.32 to 7.35 ng/L UF, respectively. Both [MeHg] and [THg] increased significantly with decreasing system elevation (Figure 2-3a), with river sites having significantly higher concentrations of both when compared to Lowland and Shield lakes ($p < 0.001$-0.023).

Invertebrate [MeHg] was low across the ADB, ranging from 6 - 53, 7 - 107, 17 - 76, and 4 - 32 ng/g (dry wt.) in amphipods, mayflies, caddisflies, and zooplankton, respectively. Unlike concentrations in water, invertebrate [MeHg] showed no clear relationship with system elevation across the ADB (Figure 2-3c). Furthermore, benthic invertebrate [MeHg] was not significantly different among regions ($p = 0.063$-0.464). Similar to $\delta^{15}N$, however, zooplankton [MeHg] was significantly higher in Shield lakes when compared to Lowland lakes ($p = 0.032$).

Size-standardized [THg] was significantly different among large-bodied fish species ($p < 0.001$). Not surprisingly, [THg] at 500 g was highest in piscivores, ranging from 0.33 - 2.42 µg/g dry in walleye, and 0.32 - 1.54 µg/g dry in pike. Insectivores had lower [THg], ranging from 0.09 - 0.56 µg/g dry in suckers, and 0.12 - 1.32 µg/g (dry, at 500g) in whitefish. Across the watershed, the strongest trends in size-standardized [THg] were seen in whitefish, significantly increasing with decreasing landscape position (Figure 2-3d). Furthermore, whitefish [THg] at 500 g was significant different among the 3 groups (i.e., river sites, Lowland lakes, and Shield lakes; $p = 0.024$). Although no linear

relationship was found between sucker [THg] and system elevation (Figure 2-3d), significant group differences were also found ($p = 0.011$). In both cases, post-hoc results showed significant differences in [THg] between river sites and each of the lake types ($p = 0.005$-0.039), but not between the lake types themselves ($p = 0.152$-0.928). No such group differences were seen in either pike or walleye [THg]. However, a notable and consistent increase was seen in [THg] of all large-bodied species moving downstream in the mainstem Attawapiskat River (Figure 2-3d).

Across the ADB, TMSs and TMIs ranged from 0.158 to 0.292 and -2.68 to -1.63, respectively, and Figure 4 shows examples of biomagnification models from a Shield lake, Lowland lake, and river site. Across all systems modeled, the TMIs represented a wide range of predicted [MeHg] (2 to 23 ng/g dry) entering at the bases of these food webs (i.e., at $\delta^{15}N = 0$). No relationship was found between TMI and system elevation (Figure 2-3b) and TMIs were similar in lakes (-2.24, n = 20) and river sites (-2.25, n = 6). Mean TMSs were slightly higher in riverine food webs (0.236) when compared to lacustrine ones (0.223). However, there were no significant differences among river sites, Lowland lakes, and Shield lakes in either TMSs ($p = 0.710$) or TMIs ($p = 0.968$).

2.4.4 Drivers of mercury concentrations in water and biota

Across the ADB, measures of [Hg] in surface waters were strongly related to various physico-chemical variables ($r^2 = 0.55$-0.73; Table 2-3). Specifically, [TP], [NO_2+NO_3], and [DOC] were strong predictors (i.e., had large standardized coefficients) of [MeHg] in surface waters, with [TP] having a negative effect and the latter two predictors having positive effects (Table 2-3). Total [Hg] in surface waters was also

strongly and positively related to [DOC] and [NO_2+NO_3]. TP concentration was a positive predictor of aqueous [THg], while the mean drainage basin slope was a negative predictor (Table 2-3).

Across benthic invertebrate models, nutrients (e.g., [TN], [NO_2 + NO_3]) were the most consistent predictors of [MeHg], with lower concentrations in lakes with higher nutrient content (Table 2-3). All other predictors had differing effects on [MeHg] among taxa (Table 2-3). Drainage basin slope, for example, was a relatively strong positive predictor of amphipod [MeHg], but a negative predictor of caddisfly [MeHg]. Similarly, sulfate, which was a positive predictor of amphipod and mayfly [MeHg], was a negative predictor of caddisfly [MeHg] (Table 2-3). Sodium concentration was a negative predictor of caddisfly and zooplankton [MeHg], which was also strongly and negatively related to DO (Table 2-3). Across invertebrate models, [MeHg] in amphipods and mayflies was positively related to $\delta^{15}N$, but only caddisfly [MeHg] was related to $\delta^{13}C$ (Table 2-3).

Similar to invertebrates, fish [THg] at 500 g was generally negatively related to various measures of total nutrients (i.e., TN, TP), though standardized coefficients were not large in any model (Table 2-3). The strongest and most consistent physico-chemical predictor of piscine [THg] was [NO_2+NO_3], similar to aqueous [Hg] models (Table 2-3). Fish condition was also included in all fish models, though its effect varied among species and the coefficients were generally small (Table 2-3). Similarly, C and N isotopes had a small effect (i.e., their coefficients were generally small; Table 2-3) on fish [THg], though $\delta^{15}N_{cor}$ was, not surprisingly, a consistently positive predictor (Table 2-3).

In contrast to water and most biotic models, TMS and TMIs were not as strongly related to physico-chemical variables (r^2 = 0.01-0.26; Table 2-3). Similar to benthic invertebrates, TMIs were most strongly and negatively related to [TN] and [DOC], though the relationships were not statistically significant (Table 2-3). All predictors in TMS models had relatively small coefficients with statistically insignificant effects (<0.1; Table 2-3).

2.5 Discussion

2.5.1 Spatial patterns in physical, chemical, and ecological traits across the ADB

Across the ADB, physical features and water chemistry varied with declining landscape position moving from the headwaters to the lower river sites (e.g., drainage basin slopes and [SO4] decreased, [DOC] increased). Similar to previous studies in northern Ontario watersheds, some physico-chemical variables differed by region more so than linearly across the watershed, likely due to the influence of bedrock geology and riparian characteristics (MacLeod et al. 2017). Such regional differences in physical and chemical characteristics are important considerations for future studies and monitoring programs in the area; systems in both regions should be monitored to thoroughly assess the impacts of future stressors in the Far North of Ontario.

Although we did not assess species richness, an ecological variable known to shift with landscape position (Kratz et al. 1997), there were some differences in other ecological parameters among taxa across the ADB. For example, bulk zooplankton had significantly higher trophic positions in headwater Shield lakes when compared to

Lowland systems. This is likely due to regional differences in zooplankton communities (MacLeod et al. 2018) and, potentially, the presence of *Chaoborus* sp., a predatory pelagic invertebrate that was observed in samples from the deeper Shield systems.

Overall, trophic levels, dietary carbon signatures, body condition, and LGR in the various fish species showed few spatial trends across the ADB. Whitefish were the only taxon which showed marked decreases in their $\delta^{13}C$ with increasing system elevation, suggesting more nearshore feeding in Lowland lakes and river sites when compared to Shield lakes. This is likely an effect of: (1) the shallower nature of Lowland lakes limiting profundal habitat and, therefore, differentiation of offshore and nearshore carbon isotopes and (2) anadromous behaviour of riverine whitefish at downstream sites (i.e., closer to the outflow; Dejong 2017). Some northern pike were also found to be anadromous in the rivers of northern Ontario (Dejong 2017) and while this study did not find any significant differences in pike $\delta^{13}C$ across the ADB, it did detect a significant increase in condition factors with decreasing landscape position. Higher fish condition closer to the outlet may be due to the influence of marine inputs to the food webs, given that the transition between freshwater and marine environments has been shown to affect fish growth and morphology (Eldøy et al. 2015; Kipanyula et al. 2016).

2.5.2 Variation in Hg concentrations with system landscape position

Overall, concentrations of Hg in water and biota varied widely in systems across the ADB. Aqueous concentrations of both THg and MeHg increased with decreasing landscape position, a likely consequence of the mirrored increase of [DOC] across the ADB (i.e., by 23.7 mg/L from Shield to riverine systems). Many studies have shown

strong linkages between aqueous Hg and DOC concentrations (Lescord et al., 2018a), which is thought to bind and mobilize Hg species from riparian regions and throughout watersheds (Wallschlager et al. 1996; Eklöf et al. 2016) and alter microbial methylation rates (Hammerschmidt et al. 2008).

Despite high variability in concentrations, benthic invertebrate [MeHg] showed no consistent trend with system landscape position across the ADB. Similarly, no clear differences were seen in TMIs, which are used as a measure of basal MeHg inputs into food webs. In pelagic zooplankton, however, both [MeHg] and $\delta^{15}N$ were significantly higher in Shield Lakes when compared to Lowland systems, again suggestive of the presence of *Chaoborus* sp., the predatory behaviour of which could increase overall [MeHg] of a pooled sample.

Similar to water, [THg] in whitefish showed a significant increase with decreasing elevation across the ADB. Similar to shifts in diet, spatial variability in whitefish [THg] may be related to differences in lake morphology across the ADB. It is unlikely that the known anadromous behaviour of riverine whitefish would explain the higher [THg] in riverine whitefish; marine inputs to freshwater food webs are generally thought to lower Hg burdens (Schartup et al. 2015b, 2015a). Furthermore, notable increases in [THg] moving downstream were also evident in the other, less-anadromous fish species (sucker, pike, and walleye; Figure 2-3d). While river sites were not included in the predictive modeling due to missing data, they had higher [NO_2+NO_3], the strongest positive predictor of piscine [THg] in this study. It is therefore possible that an unmeasured physico-chemical effect (e.g., [NO_2+NO_3]) account for the higher [THg] in fish with decreasing landscape position of river sites.

2.5.3 Drivers of Hg bioaccumulation and biomagnification

Overall, concentrations of total nutrients (P and N) were included as negative predictors of aqueous and some biotic [MeHg] across the ADB. Taken together, these negative relationships indicate that biota generally have lower [MeHg] accumulation in more nutrient-rich and productive waters. Other studies have shown that increases in nutrients and productivity can cause a reduction of individual MeHg body-burdens across a larger biomass, a process known as bio-dilution (Pickhardt et al. 2002; Walters et al. 2015). However, some biotic models included TN and/or TP as weak positive predictors and some recent studies have reported positive effect of nutrients and other measures lake productivity on biotic [MeHg] (Ahonen et al. 2018; Emmerton et al. 2018). It is possible that particulate N species associated with colloids increase Hg transport into lakes and have been correlated with rough proxies of methylation (i.e. %MeHg in water; Emmerton et al. 2018).

Another consistently influential variable over [Hg] across the ADB was [NO_2+NO_3], a positive predictor of aqueous, piscine, and invertebrate [Hg]. In general, NO_2^- and NO_3^- are products of the nitrification of NH_3+NH_4 (the product of N fixation) and are a frequent concern in agricultural run-off; no large-scale agricultural activities exist in the ADB and the concentrations were generally low but variable (<1 to 30 µg/L). While not frequently reported as an influential parameter in Hg cycling, some studies suggest that additions of NO_3 enhance denitrification, a process that is bio-energetically favoured over sulfate reduction but does not produce MeHg as a by-product, therefore lowering overall [MeHg] (Compeau and Bartha 1985; Palmer-Young et al. 2008;

Todorova et al. 2009). It is possible that the relationships between [MeHg] and [NO_2+NO_3], which was somewhat correlated with [DOC], water colour, and [Fe], are an indirect collinear effect. Nevertheless, taken together, the relatively strong effects of [TN] and [NO_2+NO_3] found herein suggest strong links (whether direct or indirect) between Hg and N cycling that warrant further investigation.

Despite the links between sulfur and Hg cycling (Clayden et al. 2017), sulfate had surprisingly inconsistent relationships with [MeHg] in water and biota across the ADB. It is possible that the concentration range of sulfate in this study was too narrow to detect an effect (0.02 -0.9 mg/L), unlike other studies which report significant parabolic relationships (Sumner 2016; <0.5 to ~9 mg/L). Furthermore, methylation may be occurring in riparian regions (Despault 2016), therefore limiting the effect of sulfate concentrations measured in this study. Concentrations of DOC, on the other hand, varied widely across the ADB, yet modeling showed minimal effect on biotic Hg concentrations. Previous studies have reported parabolic relationships between biotic [Hg] and [DOC] due to structural changes in organic matter complexes (French et al. 2014; Braaten et al. 2018). Indeed, our previous work revealed significant effects of various structural characteristics of organic matter, potentially explaining the lack of a linear effect of DOC on our multivariate models herein (Lescord et al. 2018a).

2.5.4 Implications of results in the context of industrial development and climate change

The predicted effects of climate change and industrial development have important implications for Hg cycling and bioaccumulation in boreal watersheds. Overall,

the effects of climate change will likely be directly or indirectly related to the predicted increased to water temperatures, which is anticipated throughout the boreal ecozone (Keller 2007). For example, studies have shown that TP, a positive predictor in some aqueous and biotic [Hg] across the ADB, is rapidly declining in boreal lakes in some regions (Huser et al. 2018) with warming linked to high productivity and rapid P uptake by plants (Findlay et al. 2001; Keller 2007). Droughts and subsequent floods anticipated in the boreal region from climate change or industrial-related activities may flush these nutrients out of peatlands and also alter the timing of nutrient loadings to systems, changing the overall C, N, and P cycles (Keller 2007; Elser et al. 2009; Landry and Rochefort 2012). Climatic effects may also impact [NO_2+NO_3]; recent work has shown that nitrate concentrations are strongly correlated with the duration of ice-cover on lakes (Powers et al. 2017). Warmer temperatures may, therefore, result in less nitrification and lower [NO_2+NO_3] which, according to our findings, may lower [Hg] bioaccumulation.

The anticipated increase in [DOC] expected in boreal waters will also limit UV penetration and photochemistry (Clark et al. 2010; Ritson et al. 2014; Poste et al. 2015). However, [DOC] was not a consistent predictor of biotic [Hg] across the ADB at present. It is possible that an increase in more humic and structurally-complex DOM, a likely effect of both climate- and industrial-related droughts and other land-use practices, will have a bigger effect (Wilson and Xenopoulos 2009; Szkokan-Emilson et al. 2013; French et al. 2014).

2.6 Conclusions

In conclusion, this extensive study showed significant variation in physical, chemical and biological conditions of aquatic systems across the ADB, though the patterns of variation with respect to landscape position were highly variable. Clear trends along the basin elevational gradient were evident in some physical and chemical parameters, and in [Hg] of water, but were less evident in biotic [Hg] and ecological variables. Our results indicate that nutrient cycling, particularly N cycling, is related to Hg bioaccumulation throughout the ADB. Monitoring programs and studies should therefore consider the spatial differences in physico-chemical parameters (especially concentrations of total nutrients, various N species, and DOC) reported herein and examine a range of systems to capture the unique aspects of boreal Shield and Hudson Bay Lowlands when assessing future trends in Hg cycling.

2.7 Tables and Figures

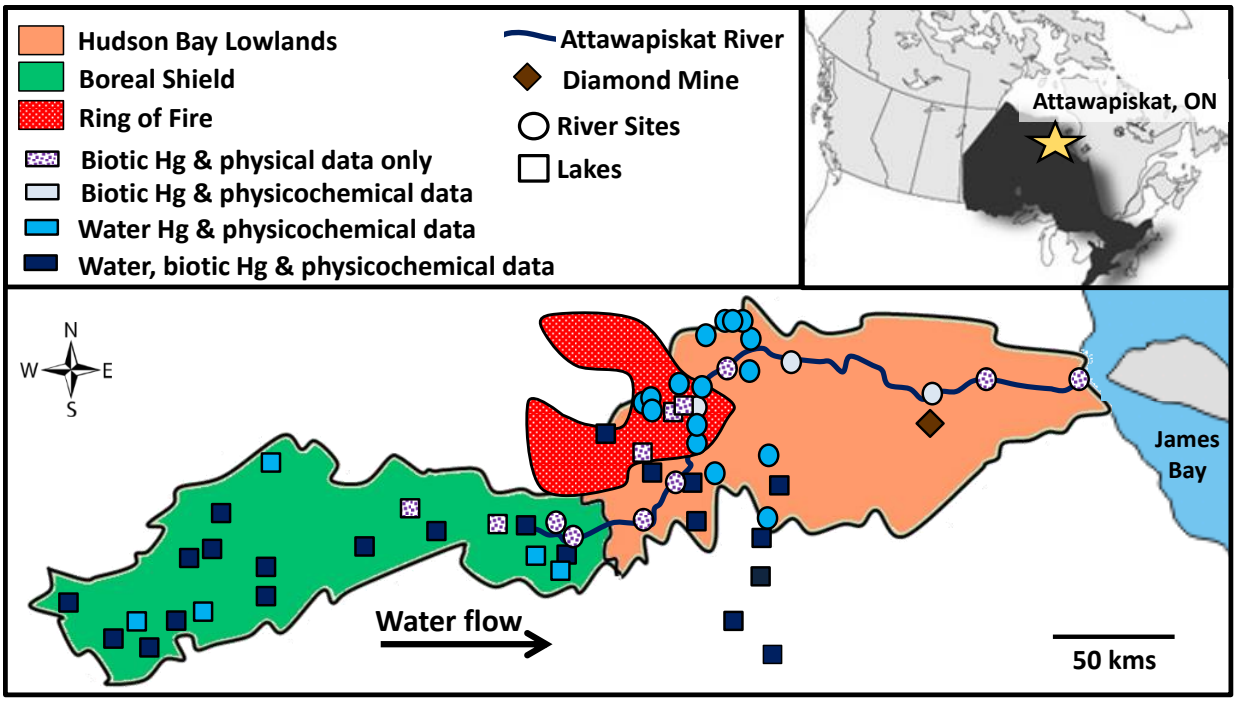

Figure 2-1: The locations of sampled lakes and river sites, as well as the Ring of Fire mineral deposit in the Attawapiskat Drainage Basin (ADB) in the Far North of Ontario, Canada. Locations are approximated.

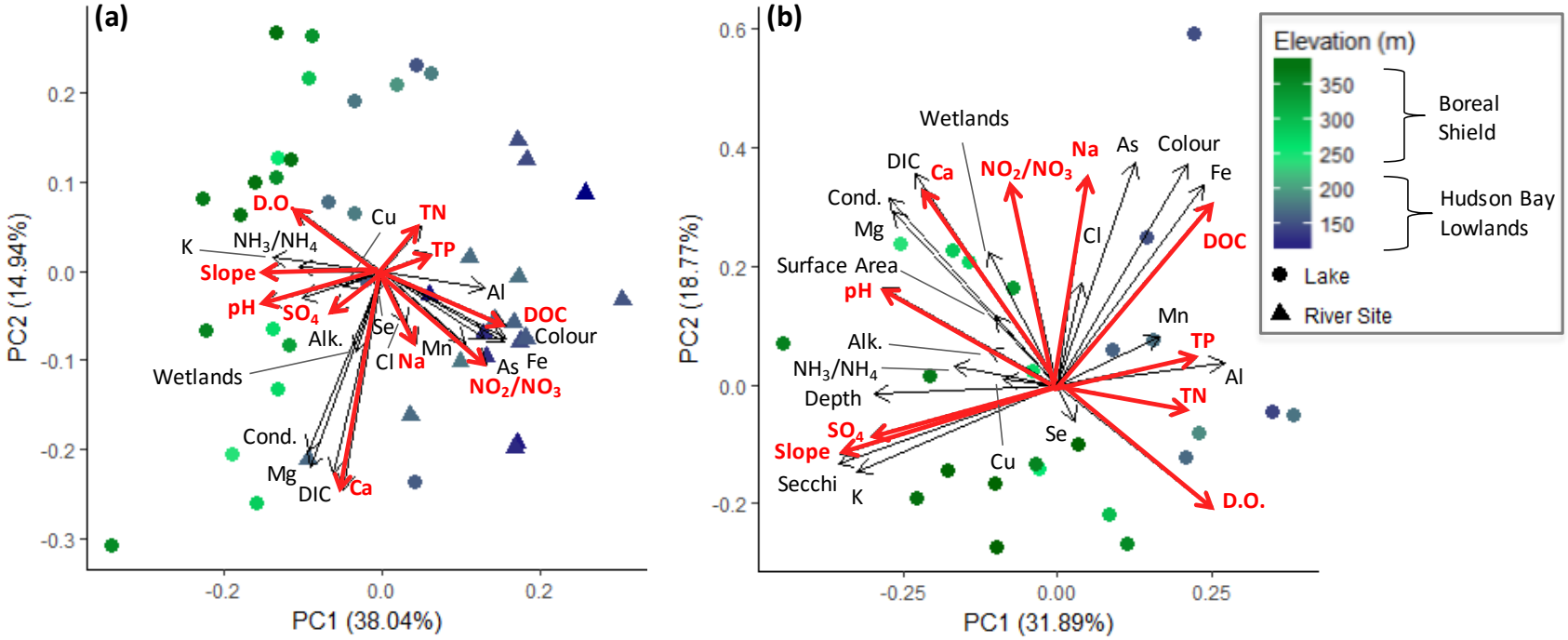

Figure 2-2: Bi-plot of the first 2 Principal Components (PCs) resulting from a Principal Components Analysis (PCA) on 24-26 water chemistry variables and physical attributes of lakes and rivers across the Attawapiskat Drainage Basin. Panel (A) shows the results of a PCA using all lake and river sites; panel (B) shows results of a PCA using only data from lakes. Red vectors and labels are the parameters chosen as potential predictors of Hg concentrations in AIC-modeling. Variable loadings on PCs are shown in Table SI- 19 and Table SI- 20. Note: Al = aluminum, Alk = alkalinity, As = arsenic, cond = conductivity, Ca = calcium, Cl = chloride, Cu = copper, DOC = dissolved organic carbon, Fe = iron, K = potassium, Mg = magnesium, Na = sodium, NH_3/NH_4 = ammonia and ammonium, NO_2+NO_3 = nitrate and nitrite, Se = selenium, slope = average riparian slope, SO_4 = sulfate, TP = total phosphorus, TN = total nitrogen, Wetlands = area of wetlands in the catchment.

1

Table 2-1: Means ± SD (n) and ranges for various physico-chemical parameters across the Attawapiskat Drainage Basin. All measurement shown were taken from surface waters (n = 1/site). DIC = dissolved inorganic carbon; DOC = dissolved organic carbon; nitrate + nitrite = NO_2+NO_3; ammonia + ammonium = NH_3+NH_4; Slope = mean drainage basin slope.

		(Headwaters → *Outlet)*					
Parameter	**Units**	**Boreal Shield Lakes**		**Hudson Bay Lowland Lakes**		**River sites**	
		Mean ± SD	*Range*	*Mean ± SD*	*Range*	*Mean ± SD*	*Range*
Aluminum (Al)*[1,2,3]	µg/L	17.5±9.6 (18)	1.6 - 32.2	47.0±35.9 (11)	25.4 - 148.0	68.5±37.2 (20)	5.3 - 163.0
Alkalinity (Alk)*[1]	mg/L	73.0±67.1 (18)	23.5 - 219.0	29.0±13.3 (11)	6.0 - 57.2	34.9±10.9 (24)	17.2 - 60.4
Arsenic (As)*[2,3]	µg/L	0.3±0.4 (18)	0.01 - 1.3	0.6±0.3 (11)	0.01 - 1.3	1.0±0.3 (20)	0.01 - 1.7
Calcium (Ca)	mg/L	12.3±5.8 (18)	5.4 - 31.9	10.1±4.1 (11)	2.7 - 18.1	12.3±3.0 (24)	7.6 - 21.2
Chloride (Cl)*[1,2]	µg/L	101±94 (18)	19 - 420	206±81 (11)	110 - 390	1224±4582 (22)	16 - 21700
Colour*[1,2,3]	TCU	58±22 (18)	12 - 90	93±36 (11)	38 - 168	162±63 (24)	63 - 282
Conductivity (Cond)	uS/cm	78.1±35.8 (18)	34.7 - 200.0	61.0±24.9 (11)	17.8 - 113.0	75.9±36.8 (24)	39.8 - 227.0
Copper (Cu)	µg/L	0.20±0.23 (18)	0.02 - 0.90	2.31±5.98 (11)	0.01 - 20.20	0.20±0.29 (20)	0.01 - 1.30
Dissolved Oxygen*[1,2,3]	%	8.4±0.3 (17)	8.0 - 9.0	8.8±0.5 (9)	8.2 - 9.7	7.0±0.8 (20)	5.6 - 8.1
DIC*[1]	mg/L	8.6±5.3 (18)	0.3 - 26.3	6.6±3.4 (11)	1.5 - 14.1	7.7±2.3 (21)	4.9 - 14.3
DOC*[2,3]	mg/L	12.8±2.8 (18)	5.4 - 16.2	15.7±3.3 (11)	10.5 - 21.1	20.8±4.2 (22)	11.9 - 29.1
Drainage Area^	km^2	3,183±6,416 (21)	5 – 21,361	372±266 (10)	79 - 683	9,610±16,571 (28)	2 – 49,631
Iron (Fe)*[1,2,3]	mg/L	0.08±0.03 (18)	0.03 - 0.14	0.22±0.15 (11)	0.06 - 0.61	0.51±0.19 (20)	0.10 - 0.90
Potassium (K)*[1,2]	mg/L	0.34±0.17 (18)	0.15 - 0.86	0.15±0.03 (11)	0.11 - 0.21	0.18±0.18 (24)	0.03 - 0.68
Max depth*[1]	m	11.0±7.8 (21)	1.4 - 23.5	3.7±2.9 (10)	1.3 - 10.4	NA	NA
Magnesium (Mg)	mg/L	2.39±1.14 (18)	1.19 - 6.37	1.71±0.66 (11)	0.43 - 2.95	2.19±1.00 (24)	1.06 - 6.09
Manganese (Mn)	µg/L	18.0±4.5 (18)	9.6 - 24.1	22.5±9.8 (11)	5.5 - 35.8	32.0±15.9 (20)	8.1 - 59.7
Sodium (Na)*[2]	mg/L	0.43±0.15 (18)	0.24 - 0.89	0.56±0.17 (11)	0.32 - 0.82	1.18±2.52 (24)	0.25 - 12.90
NH_3+NH_4*[2]	µg/L	19.2±8.6 (18)	0.9 - 40.0	12.0±12.2 (11)	0.2 - 32.0	9.0±13.6 (24)	0.0 - 62.0
NO_2+NO_3*[3]	µg/L	7.1±5.4 (18)	0 - 18	5.6±4.4 (11)	0 - 14	18.8±9.8 (24)	2 - 30
pH*[2]	---	7.65±0.22 (18)	7.23 - 8.25	7.49±0.30 (11)	6.71 - 7.97	7.34±0.31 (24)	6.81 - 7.87
Selenium (Se)	µg/L	0.12±0.07 (18)	0.02 - 0.24	0.13±0.07 (11)	0.02 - 0.24	0.14±0.07 (20)	0.01 - 0.30
Secchi*[1]	m	2.0±0.5 (21)	1.0 - 3.1	1.0±0.4 (10)	0.5 - 1.6	NA	NA
Slope*[1,2]	%	3.0±0.5 (21)	2.2 - 4.0	1.4±0.2 (10)	0.9 - 1.7	1.6±0.6 (28)	0.9 - 3.0
Sulfate*[1,2,3]	mg/L	0.35±0.29 (18)	0.02 - 0.90	0.06±0.04 (11)	0.03 - 0.16	0.59±1.98 (22)	0.02 - 9.45
Surface Area	ha	3,353±6,123 (21)	199 – 28,100	3,219±5,479 (11)	44 – 19,212	NA	NA
Total nitrogen (TN)	mg/L	0.39±0.07 (18)	0.28 - 0.52	0.42±0.07 (11)	0.35 - 0.56	0.39±0.09 (24)	0.03 - 0.50
Total phosphorus (TP)*[1]	mg/L	0.01±0.001 (18)	0.008 - 0.023	0.02±0.01 (11)	0.010 - 0.042	0.01±0.01 (21)	0.003 - 0.025
Wetland Area	km^2	1,037±2,108 (21)	0 – 6,835	284±219 (10)	49 - 584	4,903±8,712 (28)	2 – 28,528

*Indicates a significant difference among regions according to Kruskal-Wallis H Tests; [1]Indicates a significant post hoc difference between shield lakes and lowland lakes; [2]Indicates a significant post hoc difference between shield lakes and river sites; [3]Indicates a significant post hoc difference between lowland lakes and river sites. ^Highly correlated with area of wetlands in the drainage basin; excluded from PCA analysis.

Table 2-2: Relationships between biotic variables and system elevation in the ADB. Biotic variables include fish condition (residual $\log_e$ mass), lifetime growth rate (LGR), and mean stable isotope compositions. Sampling year was included as a random variable in all models. Stable isotope values were baseline-corrected within-systems for all fish models. LGR and isotope values were also size-standardized in all fish models. Cond. = Conditional.

Dependent variable	Taxon	Equation	n*	p-value	Marginal r^2	Cond. r^2
Condition	Sucker	y = 0.001x -0.027	30	0.317	0.034	0.034
	Whitefish	y = <0.001x -0.039	17	0.734	0.007	0.325
	Pike	**y = -0.002x + 0.052**	**34**	**0.039**	**0.123**	**0.123**
	Walleye	y = <0.001x -0.019	32	0.080	0.093	0.287
LGR at 1 kg	Sucker	y = 0.014x + 127.350	30	0.837	0.001	0.001
	Whitefish	y = -0.079x + 135.806	17	0.311	0.064	0.064
	Pike	y = 0.080x + 170.454	34	0.263	0.038	0.038
	Walleye	y = 0.022x + 78.068	32	0.587	0.009	0.229
$\delta^{13}C$	Caddisflies	y = -0.003x – 29.360	18	0.724	0.007	0.007
	Mayflies	y = 0.008x – 29.628	17	0.276	0.073	0.073
	Amphipods	y = 0.007x – 28.081	17	0.216	0.094	0.094
	Zooplankton*	y = -0.008x – 28.847	17	0.393	0.046	0.046
$\delta^{13}C_{cor}$ at 500 g	Sucker	y = 0.005x + 2.388	26	0.088	0.112	0.112
	Whitefish	**y = -0.020x + 9.851**	**15**	**0.002**	**0.529**	**0.650**
	Pike	y = -0.001x + 4.514	27	0.642	0.008	0.008
	Walleye	y = -0.003x + 4.981	27	0.150	0.078	0.078
$\delta^{15}N$	Caddisflies	y = 0.004x + 2.733	18	0.104	0.147	0.147
	Mayflies	y = -0.0009x + 3.410	17	0.564	0.021	0.021
	Amphipods	y = -0.004x + 2.917	17	0.870	0.002	0.002
	Zooplankton*	**y = 0.010x + 1.752**	**17**	**0.006**	**0.385**	**0.385**
$\delta^{15}N_{cor}$ at 500 g	**Sucker**	**y = 0.003x + 2.398**	**26**	**0.016**	**0.209**	**0.209**
	Whitefish	y = 0.003x + 3.932	15	0.269	0.096	0.376
	Pike	y = 0.002x + 5.306	27	0.094	0.104	0.104
	Walleye	y = <0.001 +6.157	27	0.722	0.005	0.005

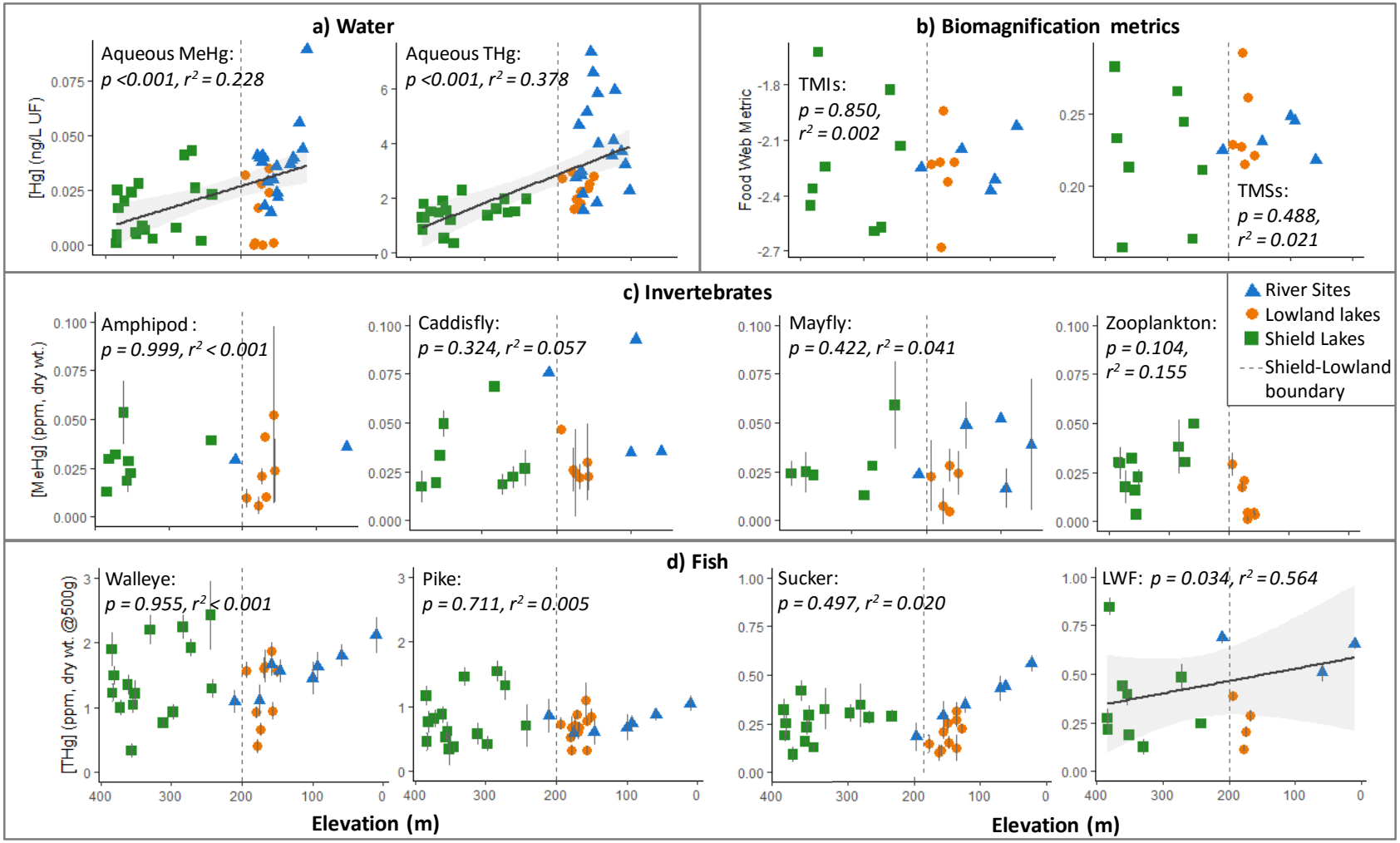

Figure 2-3: Linear relationships between various Hg measurements in water, biota, and food webs with inverted system elevation, indicative of landscape position across the ADB. For biotic models (panels c and d), the p-values and r^2 shown were produced by linear mixed effects models between Hg measures and elevation, including sampling year as a random variable.

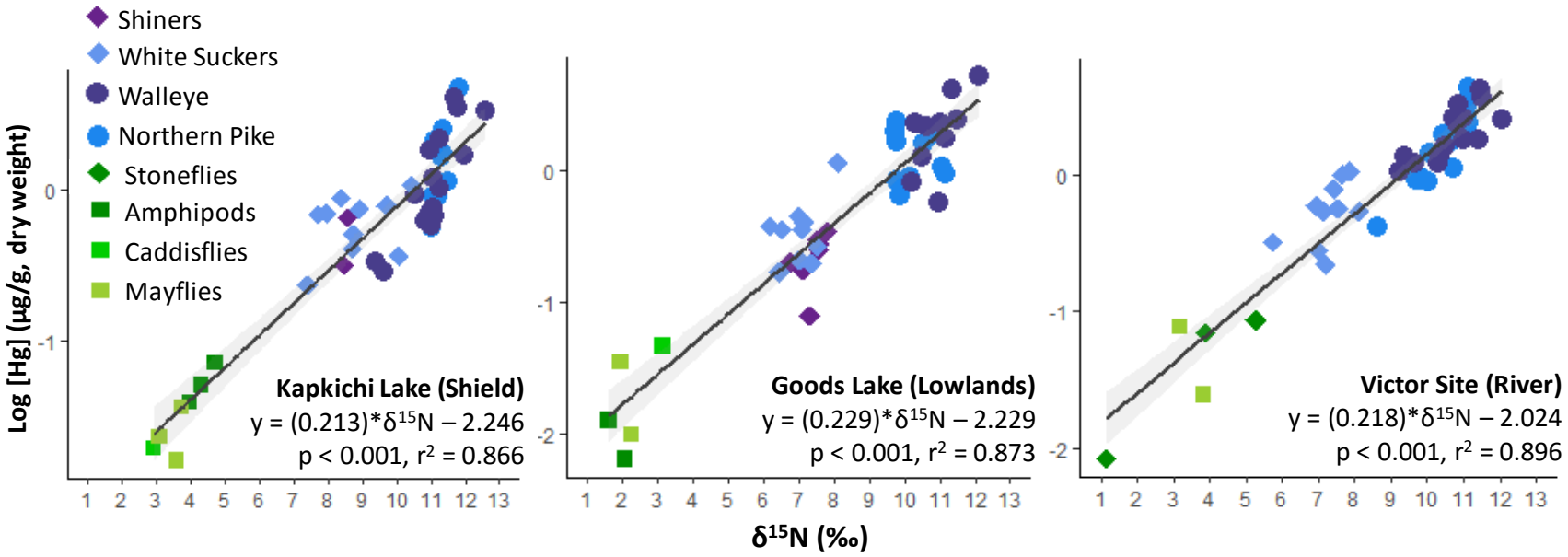

Figure 2-4: Mercury biomagnification plots (log [Hg] (MeHg in invertebrates and forage fish; THg in large-bodied fish) vs. raw $\delta^{15}N$ values) for the food webs of a shield lake (Kapkichi), lowlands lake (Goods), and a river site (Attawapiskat River at Victor Mine). Gray shaded area around each line represents the 95% confidence interval.

1

Table 2-3: Physicochemical predictors of [THg] and [MeHg] in biota and food web metrics from lakes across the ADB (chemical parameters were not available for all river sites). Results shown are the ranges of model strength (i.e., r^2 and Akaike weights) and the averaged coefficients of each predictor across all linear models with a ΔAIC_c value < 4, for each subset of data. Statistically significant predictors ($p < 0.05$ based on constrained coefficients) are bolded.

Group (n)	**Model strength** r^2	*Weight*	**Equation** (standardized full coefficients)
Surface water, all sites (43)	0.55-0.56	0.35-0.65	[MeHg] = **(0.28*DOC) - (0.82*TP) + (0.52*NO_2+NO_3)** -1.864
	0.72-0.73	0.39-0.61	[THg] **= (-0.09*Slope) + (0.23*DOC) + (0.10*TP) + (0.10*NO_2+NO_3)** + 0.359
Amphipods (14)	0.36-0.63	0.04-0.25	[MeHg] = **(0.09*Slope) + (0.07*SO_4) - (0.11*TN) + (0.04*NO_2+NO_3) - (0.29*$\delta^{13}C$) + (0.04*$\delta^{15}N$)** – 1.644
Caddisflies (13)*	0.27-0.55	0.03-0.19	[MeHg] = (-0.10*Slope) - (0.02*Ca) - (0.02*Na) - (0.03*pH) - **(0.07*SO_4)** - (0.03±0.07*TP) - (0.01*NO_2+NO_3) + (0.01*DO) + **(0.18*$\delta^{13}C$)** -1.559
Mayflies (13)*	0.61-0.71	0.04-0.29	[MeHg] = (-0.01*Slope) + (0.01*Na) - (0.03*pH) + (0.04*SO_4) + (0.01*TP) - **(0.52*TN)** + (0.05*NO2+NO3) - (0.02*DO) + (0.01*$\delta^{15}N$) -1.621
Zooplankton (16)	0.66-0.76	0.26-0.74	[MeHg] = **(-0.68±0.14*Na) - (0.23±0.17*DO)** – 1.843
Sucker (19)	0.20-0.46	0.04-0.29	[THg] = **(0.09*Slope)** + (0.01*Ca) **+ (0.08*DOC)** - (0.02*TP) + (<0.01*TN) **+ (0.10*NO_2+NO_3)** + (<0.01*DO) + (0.03*$\delta^{15}N$) - (0.01*Cond) + 0.660
Pike (18)	0.33-0.43	0.04-0.23	[THg] = (<0.01*Slope) + (<0.01*Ca) + (<0.01*Na) + (<0.01*pH) + (<0.01*DOC) + (<0.01*SO_4) - (<0.01*TP) + (<0.01*TN) **+ (0.19*NO_2+NO_3)** + (<0.01*DO) + (<0.01*$\delta^{13}C$) + (<0.01±*$\delta^{15}N$) + (-0.02*Cond) - 0.124
Walleye (19)	0.17-0.36	0.03-0.18	[THg] = (0.01*Slope) + (0.01*Ca) - (0.02*Na) + (<0.01*pH) + (<0.01*DOC) + (<0.01*SO_4) + (<0.01±0.02*TP) - (*0.01**TN) **+ (0.16*NO_2+NO_3)** + (<0.01*DO) - (0.02*$\delta^{13}C$) + (0.01*$\delta^{15}N$) + (<0.01*Cond) + 0.098
TMS (14)	0.01-0.25	0.03-0.18	TMS = (<0.001*Slope) + (<0.001*Ca) + (0.01*Na) + (<0.001*pH) + (<0.001*DOC) + (<0.001*SO_4) + (<0.001*TP) + (0.01*TN) + (<0.001*NO2+NO3) + (<0.001*D.O.)
TMI (14)	0.02-0.26	0.04-0.23	TMI = (<0.001*Slope) - (0.02*Ca) - (0.02*Na) - (0.02*pH) - (0.04*DOC) + (<0.001*SO_4) + (<0.001*TP) - (0.03*TN) + (<0.001*NO2+NO3) + (0.02*D.O.)

*DOC removed due to a high VIF value and strong correlations (Pearson's r >0.7) with numerous parameters. Slope = mean drainage basin slope; DO = dissolved oxygen, SO_4 = sulfate, total phosphorus = TP, total nitrogen = TN, nitrate + nitrite = NO_2+NO_3, dissolved organic carbon = DOC, sodium = Na, calcium = Ca.

Chapter 3 : The optical properties of dissolved organic matter and their relation to mercury concentrations in water and biota across a remote freshwater drainage basin

3.1 Abstract

Dissolved organic matter (DOM) includes an array of carbon-based compounds that vary in size and structure and have complex interactions with mercury (Hg) cycling in aquatic systems. While many studies have examined the relationship between dissolved organic carbon concentrations ([DOC]) and methyl Hg bioaccumulation, few studies have considered the effects of DOM composition (e.g., protein-content, aromaticity). The goal of this study was to explore the relationships between total and methyl [Hg] in water, invertebrates, and fish, and optically-derived measures of DOM composition from 47 lake and river sites across a boreal watershed. Results showed higher aqueous total [Hg] in systems with more aromatic DOM and higher [DOC], potentially due to enhanced transport from upstream or riparian areas. Methyl [Hg] in biota were all positively related to the amount of microbial-based DOM and, in some cases, to the proportions of labile and protein-like DOM. These results suggest that increased Hg bioaccumulation is related to the availability of labile DOM, potentially due to enhanced methylation. DOM composition explained 68% and 54% more variability in [Hg] in surface waters and large-bodied fish, respectively, than [DOC] alone. These results show that optical measures of DOM characteristics are a valuable tool for understanding DOM-Hg biogeochemistry.

3.2 Introduction

Mercury (Hg) is found in freshwater systems around the world, including those in the Canadian boreal region, largely due to long-range atmospheric transport of emissions from a range of natural and anthropogenic sources. Deposited divalent inorganic Hg (Hg(II)) can be converted into methyl Hg (MeHg), the toxic and bioaccumulative form of Hg, during the oxidation of dissolved organic matter (DOM) by sulfate-reducing (SRBs) and other anaerobic bacteria (Gilmour et al. 2013). Once produced, MeHg can enter the base of aquatic food webs and is subsequently biomagnified, sometimes resulting in top predatory fish with total Hg concentrations ([THg]) in excess of consumption guidelines or commercial sales limits (e.g., 0.5 – 1 μg/g wet weight (United States EPA and FDA 2017; Health Canada 2014)).

Understanding factors that affect methylation and MeHg bioaccumulation is essential. While many physicochemical factors interact with Hg, DOM has particularly complex effects, and can both stimulate and inhibit MeHg production (Herrero Ortega et al. 2017; Bravo et al. 2017), transport (Eklöf et al. 2013), bioaccumulation (French et al. 2014), and photodemethylation (Lehnherr and St. Louis 2009; Klapstein et al. 2017) in freshwater systems. These interactions between [DOC] and [Hg] are regulated by varying sulfur (thiol) geochemistry (Paranjape and Hall 2017) and DOM structure (Haitzer et al. 2002; French et al. 2014). Although the term DOM encompasses all dissolved (< 0.45 μm) carbon-containing compounds, it is well known that these vary widely in origin, composition, and degree of humification which in turn affects molecular weight, protein content, aromaticity, and lability (Ravichandran 2004; French et al. 2014). In general, higher molecular weight and more humic compounds have been related to lower MeHg

bioaccumulation into food webs, but enhanced Hg transport from upstream and riparian areas (e.g., peatlands; Diéguez et al. 2013; French et al. 2014). On the other hand, smaller and more labile (and therefore accessible for bacterial oxidation) DOM compounds are related to higher [MeHg] at the base of food webs (Tsui and Finlay 2011; Eklöf et al. 2012; Chen et al. 2014; French et al. 2014). While hundreds of environmental studies have examined the relationship between [THg] or [MeHg] in water, sediments, or biota and [DOC] (Ravichandran 2004; Paranjape and Hall 2017), fewer studies consider how structural characteristics of DOM affect Hg cycling. To the best of our knowledge, no large-scale environmental study has yet examined the relationships between the composition of DOM in freshwater and [THg] and [MeHg] in water and biota. Such investigations are especially important in remote northern watersheds, which are experiencing major changes from industrial development (Webster et al. 2015) and climate change (Keller 2007), both of which have been shown to alter freshwater DOM composition (Wilson and Xenopoulos 2009; Szkokan-Emilson et al. 2013; Herzsprung et al. 2017).

Our goal was to assess how [THg] and [MeHg] in water, aquatic invertebrates, and fish from northern freshwater lakes and rivers were related to the DOM composition, as inferred from its optical properties. Specifically, we studied the Attawapiskat Drainage Basin (ADB), a pristine watershed located in the northern boreal zone in Ontario, Canada, where intensive industrial development by mining companies is expected in the coming decades (in the "Ring of Fire," Figurer 3-1). Northern communities rely on the lakes and rivers in this watershed for subsistence fishing. Therefore, a sound understanding of Hg dynamics in this region has significant implications for

environmental monitoring, food security, and public health. Furthermore, this region is abundant with peatlands, a type of wetland that are often important sources of both DOM (Olefeldt et al. 2014) and Hg (Mitchell et al. 2008) to downstream freshwater systems. We used fluorescence and absorbance spectrophotometry to measure the optical properties of the DOM in surface waters from systems across the ADB and addressed two key questions:

(1) How do the various characteristics of DOM (e.g., molecular weight, aromaticity, and protein-content) relate to [THg] and [MeHg] in water, invertebrates, or fish, and does this differ between lakes and rivers?

(2) Does assessing the optical characteristics of DOM in addition to [DOC] better inform our understanding of OM-Hg interactions in boreal lakes and rivers?

3.3Methods

3.3.1 Study Site

The ADB is a large and remote watershed that spans two distinct ecozones in northern Ontario; the watershed begins with deep headwater lakes on the thinly-soiled, igneous, Precambrian Shield and transitions into shallower lakes and the main-stem Attawapiskat River on the peatland-dominated Hudson Bay Lowlands that are underlain by glaciofluvial deposits and sedimentary limestones and dolostones. Lakes on the Shield have distinctly forested riparian areas and notably different water chemistry (e.g., higher total phosphorus and alkalinity) when compared to Lowland lakes and river sites, where riparian areas are wetland-dominated (MacLeod et al. 2017). A total of 27 lakes (18 in the Boreal Shield, 9 in the Lowlands) and 20 river sites were sampled; all of these sites were in the ADB, with the exception of four Lowland lakes that were in the Albany

drainage basin, on the south side of the ADB (Figure 3-1). River sites were selected and sampled by the Ontario Ministry of the Environment and Climate Change (OMOECC) as part of their Far North monitoring program. Physical and chemical characteristics of these waters were obtained from the Ontario Ministry of Natural Resources and Forestry (OMNRF) or measured during water collection and are summarized in the supporting information (SI, Table SI- 40 to Table SI- 42). To examine DOM composition across the ADB, lake and river sites were divided into 3 groups for analysis and discussion of results: lakes on the Precambrian Shield (henceforth referred to as Shield lakes); lakes on the Hudson Bay Lowlands (henceforth referred to as Lowland lakes), and; river sites on the Hudson Bay Lowlands.

3.3.2 Field Sampling

Water samples for [THg] and [MeHg] determinations were collected, using clean methods, during late July or early August of 2015 (n = 1 sample/site). Lake water was collected from 18 Shield and 9 Lowland lakes 1-2 m below surface over the deepest point using a Van Dorn sampler. Samples were stored in 240 mL acid-washed glass bottles and acidified to 0.5% v/v with ultra-trace grade HCl (Certified ACS Plus, Fisher Chemical) immediately after collection. River water samples were collected by hand, below the surface flow in the mid-stream reach of 20 sites, stored in glass bottles and acidified, as described above. For DOM and total dissolved organic carbon (DOC) analyses, additional water samples were taken at the same time and location as Hg samples, filtered at 0.22 µm in the field and stored at 4°C in acid-washed amber glass vials until analyses. We chose to filter at 0.22 µm because this filter size reduces bacterial counts compared to

0.45 µm (and thus sample shelf-life) with minimal effect on optical properties of DOM (Nimptsch et al. 2014).

Between 2014 and 2015, 12 Shield lakes, 9 lowland lakes, and 4 main-stem river sites were sampled for biota between early July and mid-August in each year. For each of these sites, benthic invertebrates were collected at 3 locations in the nearshore zone by the kick-and-sweep technique, and hand-picked and sorted by order (Ephemeroptera, Trichoptera, and Amphipoda) to ensure adequate biomass for Hg analysis (~0.5 g fresh weight). In lakes, bulk zooplankton samples were collected near the deepest point; three horizontal tows (3-5 min each, ~0.5 m depth, net = 25 cm dia. and 80 µm mesh) were performed during daytime and nighttime (total n = 6 tows/lake). Zooplankton were not collected at river sites. Small-bodied fish (spottail and emerald shiners, *Notropis* spp.) and large-bodied fish (white sucker, *Catostomus commersonii*, northern pike, *Esox lucius*, and walleye, *Sander vitreus*) were collected by electrofishing and gill netting, respectively (target n = 10/species/lake or river site). All fish were measured for length and weight, and axial muscle tissue was removed for Hg analyses. All biotic samples were frozen until analyzed. For the 4 river sites and 6 of the Shield lakes, historical fish [THg] data (collected 2011-2013) were obtained from the OMOECC and large-bodied fish were not resampled at these locations.

3.3.3 Analytical techniques

Water: DOC concentrations were determined at Ontario Ministry of the Environment and Climate Change (OMOECC) laboratories (Etobicoke, ON, Canada) following standard procedures (i.e., UV Digestion and Automated Colorimetry; OMOECC 1983).

DOM fluorescence was measured on an Agilent Cary Eclipse Fluorescence Spectrophotometer at the Vale Living with Lakes Centre (VLWLC; Laurentian University, Sudbury, ON, Canada). Three-dimensional scans were performed at 5 nm excitation steps from 250 to 450 nm, reading emissions at 2 nm steps from 300 to 600 nm (5 nm slit widths), generating excitation-emission matrices (EEMs) for each water sample. Absorbance measures, analyzed from 250 to 600 nm on a Varian Cary 60 UV-Vis spectrophotometer, were used to correct for inner-filter effects, and to calculate DOM absorbance indices (see section 2.4). Rayleigh and Raman scatter areas were cut and interpolated according to Bahram et al. (2006) and all spectral corrections were done using a combination of in-house R-scripts and the drEEMMatlab toolbox (Murphy et al. 2014).

All analyses of Hg in water samples were conducted at the ISO 17025 accredited Biotron Laboratory (Western University, London, ON, Canada) following the United States Environmental Protection Agency (EPA) methods 1631 and 1630 for THg and MeHg, respectively, on Tekran© instruments (see SI section for a more detailed methods summary). Briefly, aqueous THg samples were oxidized with BrCl, reduced with $SnCl_2$ and the evolved gaseous Hg was detected by cold vapour atomic fluorescence spectroscopy (CVAFS) on a Tekran© 2600 automated system. Aqueous MeHg samples were distilled, ethylated with tetraethylborate ($NaBEt_4$), speciated by gas chromatography, and detected by CVAFS on a Tekran© 2700 automated MeHg Analysis System. Percent recoveries of standards, duplicates, method spikes, and precision replicates were acceptable, and within accredited quality standards (see SI section for all

quality assurance and control (QA/QC) results). All results were blank-corrected using the mean method blank concentrations.

Biota: All biological samples were freeze-dried using a LABCONCO® FreeZone Bulk Tray Dryer and homogenized using a Retsch® MM400 ball mill. Due to biomass constraints, all samples of benthic invertebrates collected within a lake or river site were pooled within orders, and zooplankton was dried and ground as bulk samples (1 sample /tow). Fish muscle samples were freeze-dried and homogenized individually. Benthic and pelagic invertebrates, as well as shiners were analyzed for MeHg using a KOH hot block digestion and then detection using the same methods as water samples (EPA 1630; Bloom and Fitzgerald 1988) All [MeHg] in biotic samples were blank-corrected using the mean method blank concentrations within their corresponding batch. Large-bodied fish muscle samples were analyzed for [THg] (which comprised 80.7-90.9% MeHg across species; Lescord et al. unpublished data) using a Milestone® DMA-80 Hg analyzer following EPA method 7473. All [Hg] are reported as ppm on a dry weight basis. For historical fish data, samples were analyzed on a wet weight basis and converted to dry weight estimates by assuming a 75% moisture content (Lavoie et al. 2013).

3.3.4 Statistical analysis

Spatial patterns of DOM composition and mercury concentrations

Using the absorbance and EEM data, we calculated 6 optical indices of DOM quality: humification index (mHIX), fluorescence index (FI), freshness index (β:α), specific absorbance coefficient at 340 nm (SAC), specific ultraviolet absorbance (SUVA), and the absorbance ratio (E2:E3, Table 3-1) in R (v.3.4.0). Additionally, we used parallel factor

analysis (PARAFAC) of DOM EEMs, performed with Matlab R2015b according to the methods outlined in Murphy et al. (2013) to further quantify the optical composition of DOM. The seven resulting components were validated by a split-half method, explaining 99.2% of the variation in the EEMs (Figure SI- 2). Each component was identified by the closest match to known (i.e., published) components in the OpenFluor database (Table 3-1; Murphy et al. 2014)

To compare DOM composition among the 3 regions, Kruskal Wallis H tests were run on the 6 indices, 7 PARAFAC components, and [DOC]. Post-hoc pairwise comparisons were done using Conover's-test for multiple comparisons of independent samples with a Bonferroni correction using the *PMCMR* package in R (Pohlert 2016; results of these pairwise comparisons are shown in Table SI- 45). Additionally, a Principal Components Analysis (PCA) was run on all measures of DOM composition (Table 3-1) and [DOC] measured from 45 sites across the ADB (2 outliers were removed as per Cook's distance test) using the *prcomp* (Sigg 2014) package in R. A biplot was created with the first 2 principal components (PCs) and parameter loadings are presented in Table SI- **46**. Two additional PCAs were run using data from lakes only (i.e., river sites excluded) and data from rivers only (i.e., lakes excluded); the results loadings and bi-plots are presented in the SI section.

Relationships between mercury concentrations and optical properties of DOM

To assess the relationship between the optical characteristics of DOM and [THg] and [MeHg] in water and biota, least absolute shrinkage and selection operator (LASSO) regressions were utilized through the R package *lars* (Hastie and Efron 2013). LASSO is

a form of Least Angle Regression that includes a penalty parameter (lambda, λ) which forces predictors with less effect on the dependent variable out of the model (i.e., their coefficients are reduced to 0). It uses forward selection of predictors by reducing this penalty parameter, allowing more variables to enter the model with increasing degrees of freedom. LASSO was used in this study because several measures of DOM composition were significantly correlated (Pearson $r > 0.7$) with each other and [DOC]; when assessing the effect of correlated predictors on a given dependent variable, LASSO has been shown to produce more accurate models than other linear techniques (Hastie et al. 2009; Dormann et al. 2013; Hebiri and Lederer 2013). Nevertheless, LASSO models were run using only 7 predictor variables (FI, SAC, C1, C5, C6, C7, and [DOC]) that were less correlated ($r = 0.039 - 0.840$) but still represented a wide array of DOM characteristics (a full Pearson's correlation table is presented in the SI section). Final model coefficients were chosen based on Mallow's C*p*, an information theory method used when sample sizes are low (i.e., $n < 100$; James et al. 2013). The model with the lowest *Cp* value (> 2, to prevent over-fitting models) was chosen (James et al. 2013). The significance of each predictor variable was determined using the R package *selectiveInference* (Tibshirani et al. 2017), which estimates the p-values for each predictor included in a given model at the corresponding level of λ.

A total of 10 LASSO models were fit, one using each of [THg] in water, [MeHg] in water, system mean [MeHg] in each of the 4 invertebrate taxa (bulk zooplankton, mayflies, caddisflies, and amphipods), and system mean [THg] in each of the 4 fish groups (walleye, northern pike, white sucker, and shiners) as dependent variables (all log-transformed except for aqueous [MeHg] which was not normal when logged), and all

using the 7 DOM characteristics as predictor variables. All proportion variables were logit-transformed before analysis using the *car* package in R (Fox et al. 2017). Data were scaled and pooled across the 3 regions for all models. Fish [THg] data were adjusted to a standard length (mean length across all populations) for each species using ANCOVA models (LogTHg = site + length + site*length) and the *lsmeans* package in R (Lenth and Love 2017). The resulting estimated marginal means for each system were then entered into LASSO models by species. Because biotic catches differed between groups/species, the sample size of each LASSO model also differed (Table 3-2).

Assessing the relative importance of DOM composition and DOC concentration

To estimate the variance explained by DOM composition, [DOC], and the combined effects of the two, variance was partitioned through redundancy analysis (RDA) and partial redundancy analysis (pRDA) using the *vegan* package in R (Oksanen et al. 2017). Due to biomass constraints and patchiness in invertebrate data, only water and fish data were used in RDA and pRDA analyses. Total and methyl [Hg] in surface waters (n = 18 river sites, 9 Lowland lakes, and 17 Shield Lakes after outlier removal *via* Cook's distance test) were entered as dependent variables in a pRDA model with 6 of the DOM characteristics (FI, SAC, C1, C5, C6, C7) as explanatory variables and [DOC] as a condition (i.e., its effect was partialled-out). Two additional models were run using the same dependent variables: one pRDA model using [DOC] as a single explanatory factor while adjusting for the 6 DOM optical indices, and one full RDA model keeping [DOC] and the 6 DOM optical indices as explanatory variables. By comparing the variability explained by each of the pRDAs to the total variability explained by the full RDA model,

the variability explained by [DOC], DOM composition, and the combined collinear effect of the two was estimated similar to the approach of Valois et al. (2010) and Gugger (2012). The same process was then repeated for length-standardized mean [THg] in large-bodied fish (n = 2 river sites, 8 Lowland lakes, and 8 Shield lakes). Variance inflation factors (VIF) were below 20, suggesting no issues with multicollinearity (Valois et al. 2010). PARAFAC components were logit-transformed and all explanatory variables were scaled before RDA or pRDA analysis.

3.4 Results and Discussion

3.4.1 Measures of DOM composition

Table 3-1 describes the 6 indices calculated as well as the 7 components resulting from the PARAFAC model. The components detected represented a wide range of DOM qualities, including low molecular weight (LMW) and microbially-altered humic acids (HA's) (C1, C2), high molecular weight (HMW) HA's (C3), reduced HA's (C5), fulvic acids (C4), and protein-like compounds (C6, C7). On average, the humic acid components (C1-C3, C5) constituted 88, 87, and 89% of the FDOM (fluorescent DOM) in river sites, Lowland lakes, and Shield lakes, respectively. Fulvic acids (C4) and protein-like components only accounted for 2 to 9 % of the FDOM in surface waters across the ADB (see Table SI- **44**).

All the DOM indices, PARAFAC components, and [DOC] differed significantly across the ADB sampling sites ($p < 0.002$) except for proportions of tyrosine-like DOM (C7, $p = 0.550$, see Table SI- **45** for pairwise comparisons). The largest differences in DOM composition of surface waters were found between river sites and both Lowland

and Shield lakes (i.e., post-hoc $p < 0.001$ to 0.004 for all DOM measures except C7, $p = 0.520$), while little to no variation was detected between the 2 lake types themselves (post-hoc $p = 0.046$ to 0.999 for all DOM measures; Table SI- **45**). Our results indicate that downstream lotic waters have higher [DOC] and more aromatic (↑SAC, SUVA) and humic (↑mHIX) DOM, as well as higher proportions of HMW and reduced HA's (C3, C5) and fluvic acids (C4, see PCA plot, Figure 3-2A). DOC concentrations were indeed higher at river sites (mean ± SD, 22.1 ± 3.0 mg/L) when compared to both Lowland (15.7 ± 3.1 mg/L) and Shield (13.1 ± 2.9 mg/L) lakes (all concentrations are shown in Table SI- **44**). Though retention time and season has been shown to affect DOM quality in the Attawapiskat River (Despault 2016), the higher humic content of riverine DOM may be due to the influence of surrounding peatlands, which have been shown to more greatly impact lotic OM dynamics than lentic (e.g., Lowland lakes; Austnes et al. 2010; Gergel et al. 2010; Orlova and Branfireun 2014). Additionally, runoff and shallow groundwater derived from the surrounding peatland landscape contains both humic and protein-like DOM (Tareq et al. 2013; Tye and Lapworth 2016), and is likely a significant source of water to these systems during periods of hydrological connectivity, influencing riverine DOM composition (Orlova and Branfireun 2014; Despault 2016).

While differences in the DOM composition of lake water across regions was minimal, considerable variation was seen within each region, particularly in the extent of humification (mHIX) and protein-like DOM (i.e., C7), as seen along the PC2 axis in Figure 3-2A. When the Secchi and maximum depths of each site were considered, deeper and clearer lakes (6 -16 m max. depth, 3-4 m secchi depth) in both the Shield and Lowlands had lower [DOC], more microbial-derived DOM (↑FI) and more labile LMW

HA's (↑C1 and C2; Figure 3-2B and 3-2C), indicating more DOM from autochthonous production as opposed to allochthonous inputs in these systems. Water from shallower, darker lakes (1 - 4 m max. depth, 0.4 - 2 m Secchi depth), on the other hand, had fresher (↑β:α) and more protein-like DOM (↑C6, C7; Figure 3-2B, Figure 3-2C). While less is known overall about DOM composition in lentic systems when compared to lotic, it is possible that other physical lake characteristics also affect DOM quality across a watershed, warranting further investigation by future studies.

3.4.2 Relationships between mercury concentrations and measures of DOM composition

Across all 10 LASSO models, the Mallow's *Cp* values were low and close to the number of parameters, indicating relatively precise models (Table 3-2). Furthermore, r^2 values were moderate to high across models (range: 0.36 – 0.78, except for amphipod model, $r^2 = 0.18$; Table 3-2), indicating strong relationships between [Hg] and DOM composition in this dataset. Table 3-2 also shows the coefficients of the DOM parameters included in the final LASSO models for each biotic or abiotic measure of Hg and the fixed inference p-values of each parameter at the given level of the penalty parameter (λ). LASSO path plots for each of these models are shown in the SI section.

Water

Mercury concentrations in surface waters from across the ADB were low but variable, ranging from 0.32 to 7.4 ng/L UF for [THg] and from <0.004 to 0.09 ng/L UF for [MeHg]. These values are similar to [Hg] measured in water from boreal rivers (e.g., [THg] = 3.6 - 3.9 and [MeHg] = 0.06 - 0.07 ng/L UF; Braaten et al. 2013) and lakes (e.g.,

[THg] = 2.5 - 8.0 and [MeHg] = 0.05 - 0.21 ng/L UF; Poste et al. 2015) Total [Hg] increased moving from headwater Shield lakes (mean ± SD, 1.49 ± 0.43 ng/L UF, n = 18) to Lowland lakes (2.33 ± 0.47, n = 9) and were highest in river water (3.92 ± 1.70, n = 18). Mean [MeHg] was also higher in river water (0.038 ± 0.016 ng/L) when compared to both Shield and Lowland lakes (0.017 ± 0.013 and 0.015 ± 0.015 ng/L, respectively; see Table SI- **44**).

DOC concentrations and aromaticity (SAC) were two of the strongest predictors (i.e., had large coefficients) of aqueous [THg] (Table 3-2), with increasing concentrations in surface waters across the ADB as OM content and aromaticity increased. Numerous studies across the boreal region of North America and Scandinavia report positive relationships between [DOC] and [THg] in freshwater lakes (e.g., Braaten et al. 2014), rivers (e.g., Jeremiason et al. 2016), streams (e.g., de Wit et al. 2014), and reservoirs (e.g., Hall et al. 2009). Furthermore, many other studies have reported a positive relationship between aqueous [THg] and OM aromaticity, (Skyllberg et al. 2009; Schelker et al. 2011; Burns et al. 2012; Eklöf et al. 2012) presumably due to strong complexation of Hg by these DOM complexes (Haitzer et al. 2002). Higher molecular weight and more aromatic DOM has strong reduced sulfur binding sites for Hg (Tsui and Finlay 2011) than simpler, fresher, and short-chain DOM molecules (Waples et al. 2005; Paranjape and Hall 2017).

FI was another positive predictor of aqueous [THg], indicating higher concentrations with more microbial-based DOM (as opposed to terrestrial-based; Table 3-2). This result was unexpected given that many studies have found high [Hg] entering systems through riparian run off, presumably transported by terrestrially-derived DOM (Eklöf et al. 2012,

2014). Other more direct measures of terrestrial OM in this study (e.g., C3) were strongly and positively correlated with aqueous [THg] ($r = 0.728$; Table SI-47 though 49).

Similar to [THg] in water, DOC was the strongest predictor of aqueous [MeHg] (Table 3-2). However, the LASSO model also showed that aqueous [MeHg] was unexpectedly higher in surface waters with less LMW terrestrial HAs (C1), as well as lower proportions of protein-like DOM (C6, C7; Table 3-2), all of which are labile forms of DOM. These results were unexpected given that labile DOM has been shown to stimulate bacterial Hg methylation and increase aqueous [MeHg] (Schartup et al. 2015b; Herrero Ortega et al. 2017). Furthermore, sulfate reducing bacteria have been shown to alter the composition of DOM and Luek et al. (2017) report an increase in detection of LMW HA's (C1) components with more SRB activity. It is therefore not surprising that, in the aqueous MeHg LASSO model, the effect of these labile components was not statistically significant ($p = 0.436$-0.676; Table 3-2).

While DOM has been shown to be a key ligand for both total and methyl Hg in surface waters (Haitzer et al. 2002), [DOC] and DOM optical measures had stronger relationships with aqueous [THg] than [MeHg] (i.e., $r^2 = 0.72$ vs. 0.47, respectively; Table 3-2). Other studies similarly report strong relationships between [DOC] and [THg] but little to no relationship between [DOC] and [MeHg] in water (e.g., Chen et al. 2014). It is important to note that all aqueous [THg] and [MeHg] data in this study were derived from unfiltered samples, representing the total (dissolved + particulate) Hg pool in surface water samples. Tsui and Finlay (2011) report a positive relationship between [DOC] and DOM aromaticity (*via* SUVA measurements) and dissolved [MeHg] (as well as dissolved [THg]) in stream waters. Future studies should consider comparing the effect

these DOM characteristics have on different fractions of Hg in water (i.e., dissolved, particulate, and total). Furthermore, the relationship between DOM and Hg is influenced by surrounding water chemistry, such as the availability of sulfur compounds, to which Hg has preferential binding (Paranjape and Hall 2017), or the concentrations of other dissolved cations, which compete with Hg for binding site on DOM complexes (O'Driscoll and Evans 2000).

Invertebrates

Invertebrate catches at river sites were limited and no data were available for zooplankton or amphipods. However, similar to water, caddisflies and mayflies from river sites had higher [MeHg] (0.084 and 0.042 μg/g d.w., respectively) when compared to Lowland (0.026 and 0.037 μg/g d.w., respectively) and Shield lakes (0.032 and 0.018 μg/g d.w., respectively; see Table SI- **44**). All riverine invertebrates were only sampled at sites on the main-stem Attawapiskat River and not on any tributaries.

Across the benthic invertebrate groups, [MeHg] in caddisflies and amphipods were significantly and positively related to higher proportions of microbial-based DOM (FI); all other components/indices had varying relationships among the invertebrate groups (Table 3-2). This positive relationship indicates higher invertebrate [MeHg] concentrations in systems with more bacterial activity, potentially due to enhanced Hg methylation. However, while previous studies have shown that aqueous [MeHg] (as well as rates of Hg methylation) are higher with influx of labile humic substances and algal-derived DOM (Herrero Ortega et al. 2017), the labile DOM components in our study (i.e., C1, C6, C7) had mixed relationships with [MeHg] across invertebrate orders. For example, LMW HA's (C1) was a negative predictor of caddisfly [MeHg], while

tryptophan-like DOM (C6) was positively related to [MeHg] in mayflies. However, despite this positive relationship with C6, mayfly [MeHg] was not related to the other protein-like DOM component, C7. In fact, C7 was not included in any benthic invertebrate LASSO model (Table 3-2). While both protein-like components are thought to be derived from bioavailable autochthonous DOM sources, tryptophan-like DOM (C6) is commonly found in areas of high productivity and is more closely associated with bacterial activity when compared to the more widely distributed tyrosine-like component, C7 (Hudson et al. 2007 and references therein).

Mayfly [MeHg] were also positively related to DOM aromaticity (SAC) which has been shown to enhance bacterial uptake of Hg(II) (Graham et al. 2013), likely by increasing the number of preferential binding sites and therefore Hg transport and, subsequently, methylation (Waples et al. 2005; Paranjape and Hall 2017). Methyl [Hg] in amphipods were similarly positively related to DOM aromaticity (SAC), while caddisflies [MeHg] were negatively related, though neither relationship was statistically significant. The proportion of reduced HAs (C5) was the strongest predictor of mayfly [MeHg], with higher [MeHg] when less reduced DOM was present. The oxidation state of the DOM is affected by source (e.g., anoxic peatlands produce highly reduced HA) and redox condition of the system, and reduced HAs are more proton-reactive, having a higher binding affinity for metal cations (e.g., MeHg) than less reduced substances (Maurer et al. 2012). Furthermore, these reduced DOM complexes have been shown to enhance photochemical degradation of MeHg 3 times faster than oxidized DOM, potentially explaining the negative relationship between mayfly [MeHg] and C5 (Qian et al. 2014).

The mixed relationships between measures of DOM composition and [MeHg] among benthic invertebrate groups may be partly due to the level of taxonomic resolution; the orders examined included multiple genera with differing trophic levels and life histories. Future studies with more invertebrate biomass should consider classifying to a lower level to examine the effect DOM composition has on [MeHg] in different functional feeding groups. Furthermore, while all invertebrate samples were collected in the summer months (i.e., July-August), studies have shown that [Hg] in invertebrates change over the growing season and some temporal variability may exist in our dataset (Zhang et al. 2012).

Similar to benthic invertebrates, the amount of microbial-based (as opposed to terrestrial-based) DOM (↑FI) was a strong positive predictor of [MeHg] in bulk zooplankton. Schartup et al. (2015) also reported a negative relationship between marine zooplankton [MeHg] and the percent of terrestrial-based DOM (i.e., ↓FI). The second strongest predictor of zooplankton [MeHg] was [DOC], with a positive effect (Table 3-2), similar to aqueous [THg]. In fact, the overall zooplankton LASSO path was similar to the aqueous [THg] model in that both DOC and FI entered the model early and retained large positive coefficients throughout the test (see corresponding LASSO plots in Figure SI- 5 and Figure SI- 7). Previous studies have shown that organic matter is a key source of Hg to pelagic primary produces and, subsequently, zooplankton due to direct ingestion of Hg-OM complexes or the passive diffusion of Hg transport *via* DOM (Plourde et al. 1997; Tremblay et al. 1998; Kainz and Mazumder 2005; Diéguez et al. 2013; Le Faucheur et al. 2014), potentially explaining the link between [Hg] in pelagic waters and invertebrates found herein.

Fish

While no shiners were caught at river sites, riverine walleye and white sucker had higher length-standardized [THg] (1.32 ± 0.50 and 0.42 ± 1.24 μg/g d.w., respectively) than fish caught in Lowland (1.16 ± 1.58 and 0.24 ± 1.33 μg/g d.w., respectively) and Shield (1.12 ± 1.81 and 0.31 ± 1.48 μg/g d.w., respectively) lakes (concentrations presented in Table SI- **44**). Conversely, northern pike had higher length-standardized [THg] in Lowland (1.16 ± 1.58 μg/g d.w.) and Shield (1.12 ± 1.81 μg/g d.w.) lakes when compared to river sites (0.98 ± 1.10 μg/g d.w.; SI section). Similar to invertebrates, riverine fish were only sampled on the mainstem Attawapiskat River not on any smaller tributaries. All piscine [THg] in our studies were within the range of concentrations measured in fish from other parts of boreal Canada (Depew et al. 2013).

Similar to the benthic invertebrates, results from LASSO models of fish [THg] varied among taxa except for the effect of the amount of microbial DOM (FI), which was a positive predictor of [THg] in all fish species, though the relationship was not statistically significant in the northern pike model (Table 3-2). In fact, it is notable that FI was a strong positive predictor in all biotic [MeHg] LASSO models (with the exception of mayflies, Table 3-2). Shiners in particular had different model results when compared to other fish species. Similar to mayflies, shiner [THg] was positively related to DOM aromaticity (SAC), as well as the protein-like DOM (C7; Table 3-2). Contrary to mayflies however, the amount of reduced HAs was a significant positive predictor of both shiner and northern pike [THg], Table 3-2). Overall, the northern pike LASSO model also had notably different results compared to other fish models but none of the coefficients were statistically significant, similar to aqueous [MeHg]. Results from the

white sucker and walleye LASSO models, on the other hand, were comparable; FI and [DOC] were the strongest predictors of [THg] in both species (a positive relationship; Table 3-2), similar to both aqueous [THg] and zooplankton [MeHg] (see Figure SI- **5** to Figure SI- **7**). Both walleye and white suckers were caught off-shore during field sampling for this project, where water and zooplankton samples were also collected. Conversely, northern pike are more restricted to nearshore and littoral environments and their Hg-DOM models may be more reflective of nearshore processes than walleye or white sucker results. Overall, these results suggest that DOM composition affect Hg bioaccumulation in open-water (i.e., zooplankton, white suckers, and walleye) and nearshore (i.e., mayflies, shiner, and northern pike) dwelling organisms differently.

It is unclear why DOM composition may affect [Hg] accumulation in fish species differently, but it may be related to differences in MeHg bioavailability among habitats and fish diet. Given that the vast majority of a fish's Hg burden comes from its diet (Hall et al. 1997), it follows that the varying relationships between DOM composition and invertebrate [MeHg] will indirectly alter fish Hg burdens as well. Furthermore, small amounts of Hg are also bioconcentrated from the surrounding water, the degree to which changes based on fish size and ecology (Pickhardt et al. 2002; Wang and Wong 2003). It is therefore possible that water chemistry, including DOM composition, could affect the bioavailability of dissolved MeHg differently among species (Zhang et al. 2013).

3.4.3 Contribution of DOM composition and quantity to variability in mercury concentrations

Redundancy analyses showed that the matrix of 6 optical properties of DOM (i.e., FI, SAC, C1, C5, C6, and C7) significantly affect [Hg] in surface water (ANVOA, p = 0.006) and large-bodied fish (ANVOA p = 0.049) across the ADB regardless of variation in [DOC] (Table SI- **50**). According to our variance partitioning results, the 6 indices of DOM composition explained 84% of the variability in [THg] and [MeHg] in surface waters independent of [DOC], which on its own only explained 16% of variability in aqueous Hg concentrations (p = 0.041, Table SI- **50**). Similarly, DOM composition accounted for 77% of the variability in large-bodied fish (i.e., white sucker, northern pike, and walleye) [THg], while [DOC] only accounted for 23%, and the relationship was not statistically significant (p = 0.152, Table SI- **50**). These results indicate that DOM composition independently explains more variability in aquatic and piscine [Hg] than [DOC] alone. However, given the strong correlations between [DOC] and various DOM characteristics across the lakes and river sites in this dataset and the small but significant independent effect of [DOC] on [Hg] in water, both DOM quality and quantity should be considered when assessing the effect of DOC on [Hg] in biota in boreal systems (Jaffé et al. 2008).

3.6 Conclusions and future considerations

While many different factors affect Hg cycling in boreal aquatic ecosystems, our results indicate that DOM fluorescence spectroscopic data which is relatively inexpensive and easy to generate, is a valuable addition to routine water chemistry analysis in future Hg research and monitoring. In particular, our study showed that biotic [MeHg] are related to the amount of microbial-based OM, and, in some cases to the proportion of labile protein-like DOM and reduced HAs. These results are important to consider when

assessing potential effects of future land-use practices and predicted effects of climate change. For example, Wilson and Xenopoulos (2009) report higher proportions of microbial-based DOM that is less structurally complex in streams surrounded by agricultural land-use when compared to wetland-dominated streams in the same region. Furthermore, it has been shown that re-wetting of drought-affected peatlands can increase DOM aromaticity and DOC concentrations in runoff (Herzsprung et al. 2017), both factors which were found to be positively associated with aqueous [THg] across the ADB.

3.7 Tables and Figures

Table 3-1: Six indices and seven PARAFAC components calculated from UV absorption and/or fluorescence spectroscopy and used to characterize DOM composition. Note: em = emission spectra; ex = excitation; abs = absorbance; HA = humic acid, FA = fulvic acid.

Index/Component	Description	Method/Calculation
Optical Indices		
Humification Index (mHIX)	Extent of humification	Peak area under em 435 - 480 nm/300-345 nm at ex 254 nm (Ohno 2002)
Fluorescence Index (FI)	Source of DOM; 1.8 indicates microbial; 1.2 indicates terrestrial	Ratio of peak areas at em 470 nm and 520 nm at ex 370 nm (Cory and Mcknight 2005)
Freshness Index (β:α)	Ratio of recently derived (β) to older (α) DOM	Ratio of peak areas at em 380 nm (β) and 420-435nm (α) at ex 310 nm (Parlanti et al. 2000)
Abs Ratio (E2:E3)	Measure of molecular weight and aromaticity	Abs at 250 nm / absorbance at 365nm (Helms et al. 2008)
Specific UV abs (SUVA)	Estimate of aromaticity of DOM	Abs. at 254 nm/ [DOC] (Weishaar et al. 2003)
Specific abs coefficient (SAC)	Amount of aromatic DOM	= (2.303 * Abs_{340nm})*pathlength (cm^{-1})*1000 cm^3/[DOC] (Curtis and Schindler 1997)
Components (Murphy et al. 2014)		
Component 1 (C1)	Proportion of water sample as terrestrial-based LMW-HA's	Peak area under em 474 nm at ex 255-305 nm
Component 2 (C2)	Proportion of water sample as microbially-altered HMW-HA's	Peak area under em 414 nm at ex 250-305 nm
Component 3 (C3)	Proportion of water sample as terrestrial-based HMW-HA's	Peak area under em 484 nm at ex 250-345nm
Component 4 (C4)	Proportion of water sample as fulvic acids (FA's)	Peak area under em 562 nm at ex 255nm
Component 5 (C5)	Proportion of water sample as Reduced HA's	Peak area under em 342 nm at ex 250-280nm
Component 6 (C6)	Proportion of water sample as Tryptophan-like DOM	Peak area under em 306 nm at ex 275 nm
Component 7 (C7)	Proportion of water sample as Tyrosine-like DOM	Peak area under em 474 nm at ex 255-305 nm

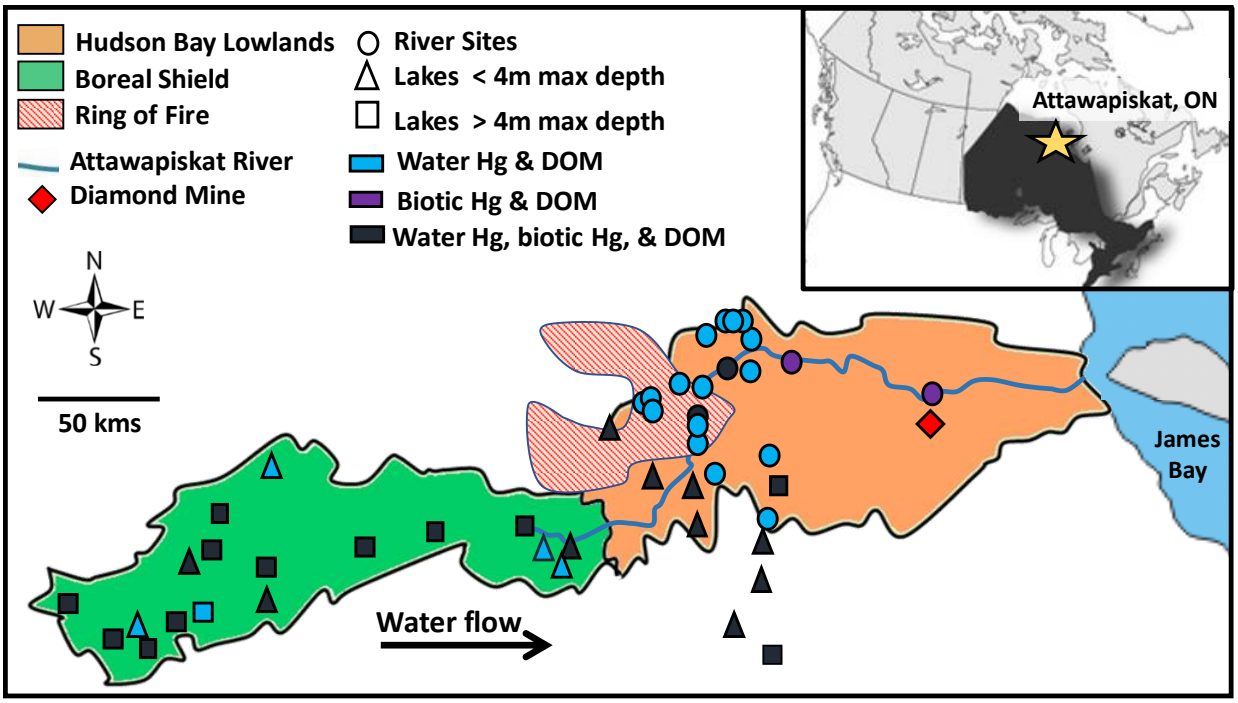

Figure 3-1: A map of the Attawapiskat Drainage Basin (ADB), showing the 18 Shield lakes, 9 Lowland lakes, and 20 river sites sampled for this study. Locations are approximated.

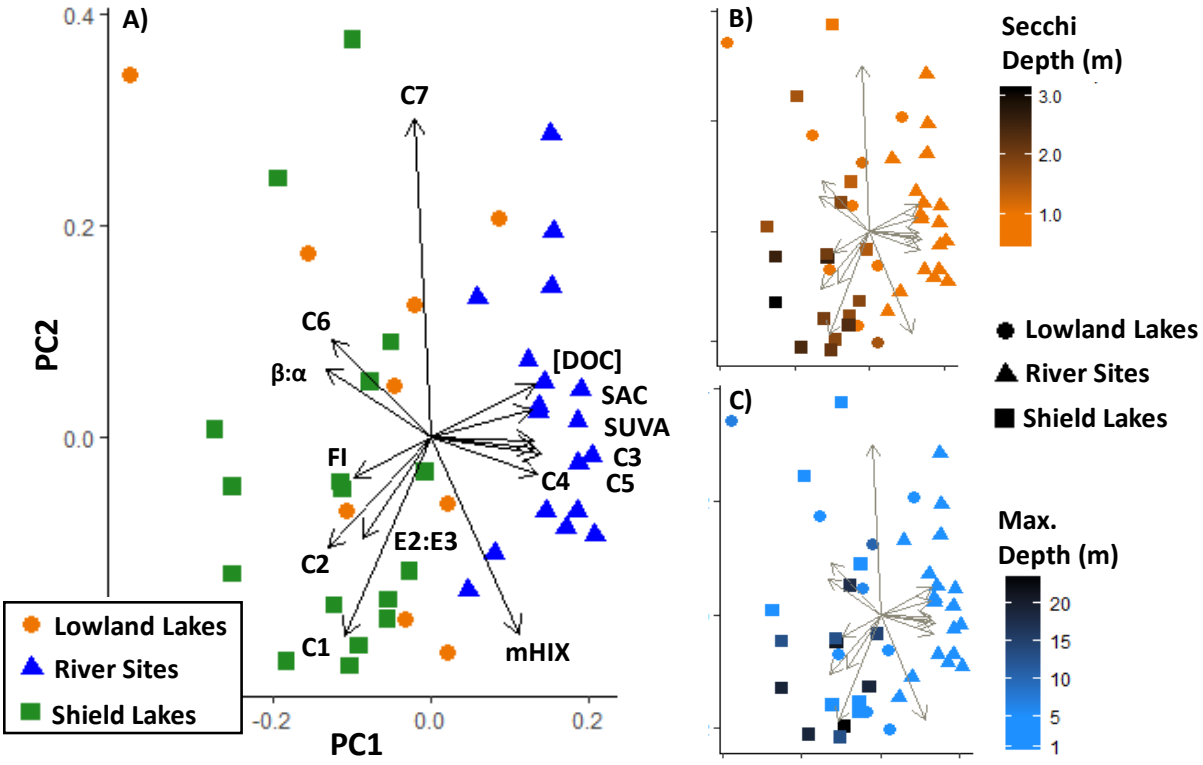

Figure 3-2: A) Scatter plot of first two principal components (PC1, PC2) of a PCA on all DOM indices, PARAFAC components and [DOC] measured in Shield lakes (green squares, n = 17), Lowland lakes (orange circles, n = 8), and river sites (blue triangles, n = 18) from across the ADB. PC1 and PC2 explained 69.5 and 13.7% of the variability in these data, respectively. Vectors show the influence of the various measures of DOM composition and [DOC] across the watershed. B) The same scatter plot as in A but with sites colour-coded by Secchi depth (darker colour indicates deeper Secchi reading). C) The same scatter plot as in A but with sites colour-coded by maximum depth (darker colour indicates greater depth). Note that maximum and Secchi depths were not measured directly at river sites; all sites were therefore assigned maximum and Secchi depths of 1 in graphs B and C.

Table 3-2: The final LASSO model coefficients for 6 optical parameters of DOM composition and [DOC] selected as per model Mallow's Cp values. LASSO path plots are shown in the SI section. P-values were calculated using inference testing and are given for each predictor below their final model coefficient. Note that β = parameters, FI = fluorescence index, SAC = specific absorbance coefficient, C = component. ^Components were logit-transformed. *Aqueous MeHg concentrations were not log-transformed.

Dependent Variable:		**n**	**λ**	**R^2**	**Mallow's Cp**	**Standardized LASSO Coefficients:**						
Group	Analyte					*FI*	*SAC*	*C1^*	*C5^*	*C6^*	*C7^*	*[DOC]*
Water	THg	43	0.15	0.72	4.88	**0.094**	**0.089**	0	0.074	0	0.032	**0.107**
p-value						**0.047**	**0.025**	---	0.195	---	0.143	**0.049**
Water	MeHg*	43	0.02	0.47	2.85	0	0	-0.002	0	-0.004	-0.002	0.007
p-value						---	---	0.725	---	0.295	0.598	0.119
Zooplankton	MeHg	18	0.24	0.48	3.23	**0.371**	0	0	0	-0.099	0.028	0.215
p-value						**0.039**	---	---	---	0.543	0.689	0.172
Caddisflies	MeHg	19	0.20	0.64	5.38	**0.115**	-0.042	-0.087	0.051	0	0	0.075
p-value						**0.028**	0.353	0.155	0.387	---	---	0.355
Amphipods	MeHg	16	0.44	0.18	2.91	0.097	0.044	0	0	0	0	0
p-value						0.138	0.472	---	---	---	---	---
Mayflies	MeHg	15	0.09	0.52	4.59	0	**0.118**	-0.002	**-0.293**	**0.063**	0	**0.223**
p-value						---	**0.018**	0.930	**0.012**	**0.023**	---	**0.010**
Shiners[1]	MeHg	13	0.02	0.78	4.25	**0.294**	**0.165**	0	**0.303**	0.054	**0.177**	0
p-value						**0.008**	**0.004**	---	**0.002**	0.421	**0.026**	---
W. Sucker[2]	THg	23	0.03	0.45	3.98	**0.079**	0	0	0	-0.022	-0.006	**0.087**
p-value						0.009	---	---	---	0.790	0.457	**0.014**
N. Pike[3]	THg	20	0.06	0.55	4.84	0.063	-0.050	0	0.062	-0.012	-0.049	0
p-value						0.159	0.315	---	0.131	0.739	0.162	---
Walleye[4]	THg	19	0.19	0.36	2.98	**0.112**	0	0.029	0	-0.028	0	0.135
p-value						**0.038**	---	0.920	---	0.174	---	0.833

1

Chapter 4 : Percent methylmercury in the muscle tissue of freshwater fish varies with body size, age, and among species

4.1 Abstract

It is commonly assumed that the majority (>95%) of mercury (Hg) found in fish muscle is the toxic form, methylmercury (MeHg), due to its efficient assimilation and retention in biotic tissue. However, this assumption is based on studies examining the percent MeHg (%MeHg, the fraction of total Hg as MeHg) in muscle from mostly large-bodied predatory fish; less is known about the %MeHg in smaller-bodied individuals or those of different trophic guilds. This study analyzed MeHg and total Hg concentrations in the muscle of two large-bodied piscivores (walleye, northern pike), one large-bodied benthivore (white sucker), and two small-bodied forage fish (sculpins, shiners) across a broad size range. We found substantially lower %MeHg than the commonly assumed 95% in several fish (e.g., 17 individuals had <70% MeHg). Muscle %MeHg significantly increased with size and age in all species except walleye, which had significantly higher %MeHg than pike or suckers, particularly in smaller and younger fish (e.g., 18-21% higher at 10g; 5-11% higher at 500g). Results of predictive modeling suggest that muscle %MeHg is higher in pelagic-feeding fish and those with lower lipid-content, though model results varied significantly among species. According to our findings, total Hg measurement in muscle is not an appropriate proxy for MeHg in smaller fish from all species, an important consideration for future piscine Hg studies and monitoring.

4.2 Introduction

Methylmercury (MeHg), a widespread neurotoxic pollutant, can be found in fish at concentrations that exceed consumption guidelines (i.e., 0.5 – 1 μg/g wet weight; EPA and FDA, 2017; Health Canada, 2014), posing public health concerns for consumers (Rice et al. 2014). Although concentrations of MeHg ([MeHg]) are generally low in fresh waters, it is readily bioaccumulated at the base of aquatic food webs and subsequently biomagnified, resulting in elevated concentrations in top predatory fish. The bioaccumulative properties of MeHg are largely due to its strong binding in biological tissues and low excretion rates (Trudel and Rasmussen 2006; Peng et al. 2016). Once accumulated, MeHg can be transported effectively throughout a fish's body, with the majority eventually depositing in muscle tissue, the most commonly consumed fish tissue (Peng et al. 2016). The less toxic inorganic Hg (Hg(II)), the dominant form detected in fresh waters (Watras et al. 1996, 2005), is more readily excreted from a fish's body with the remainder depositing more in intestinal or liver tissue than in muscle (Ribeiro et al. 2002; Pickhardt et al. 2006; Peng et al. 2016). As a result, it is commonly assumed that the vast majority of the total Hg (THg; the sum of all Hg species and the most commonly reported measure of Hg in fish) detected in fish muscle is MeHg (Bloom 1992; Harris et al. 2003).

It is common for modern studies to cite Bloom (1992), who reported that, on average, 95% of the THg detected in muscle tissue from 12 fish species (8 marine, 4 freshwater) was MeHg, to support the use of THg as a proxy for MeHg in fish muscle; THg is less costly and labour intensive to measure than MeHg, which requires considerably more sample preparation and specialized instrumentation to analyze. However, while it is clear

that the majority of Hg in muscle tissue is MeHg in many large-bodied adult fish, substantial variation does exist (Lasorsa and Allen-Gil 1995). The variability in muscle %MeHg reported by Bloom (1992) (± 20% MeHg) was attributed to incomplete tissue homogenization and analytical error. Modern homogenization techniques (e.g., ball milling) and advances in analytical precision would presumably have reduced error from these sources, yet variation is still reported for reasons that are not fully understood (Lasorsa and Allen-Gil 1995; Liang et al. 2017).

Given that diet is the main source of Hg for fish (Hall et al. 1997), it is possible that variation in the %MeHg of food sources may contribute to similar variation in fish. Invertebrate prey have particularly variable but usually lower %MeHg (e.g., 10-85%) when compared to fish (Becker and Bigham 1995; Tremblay et al. 1995; Økelsrud et al. 2016) and invertebrate consumers may therefore be exposed to lower dietary %MeHg than piscivores. To the best of our knowledge, however, no study has yet considered the effect of diet or trophic ecology on the %MeHg in fish muscle tissue.

Furthermore, while several studies have estimated %MeHg in tissues of large-bodied fishes (Latif et al. 2001; Mieiro et al. 2009; Braaten et al. 2017), far less is known about Hg speciation in smaller-bodied species. Smaller-bodied fish are subjected to different bioenergetic processes when compared to their larger counterparts and the biokinetics of Hg(II) and MeHg uptake, assimilation, and elimination can change with fish size (Dang and Wang 2012; Jørgensen et al. 2016). It is therefore possible that fish size also explains some of the variation seen in the %MeHg both within and between species.

In this study, we expanded on the findings of Bloom (Bloom 1992) by analyzing both [MeHg] and [THg] in fish tissues to assess the effects of body size and trophic ecology

on individual fish %MeHg in muscle. Samples included a wide size range of individuals across five species, including two large-bodied piscivores, one large-bodied benthivore, and two small-bodied forage fishes. These fish were sampled from relatively pristine lakes in the Canadian boreal region, without any known anthropogenic point sources of Hg contamination. Specifically, we asked three key questions using these data:

1. Does the %MeHg in muscle vary with fish size or age within species?
2. Does the %MeHg in muscle differ among species?
3. Are within- or among-species differences in muscle %MeHg related to diet (inferred from carbon stable isotope signatures, $\delta^{13}C$), trophic position (inferred from nitrogen stable isotope signatures, $\delta^{15}N$), or tissue quality (e.g., lipid or protein content)?

We also report on the %MeHg in additional tissues (i.e., liver, gonads, and soma, defined as whole body minus liver and gonads) from a subset of fish to compare among species.

4.3 Methods

4.3.1 Field methods

A total of 144 fish across five species were collected from Ontario lakes. Eight of these lakes were located in the remote Attawapiskat River drainage basin in Ontario's Far North; one additional lake, Lake Nipissing, was located on the southern Boreal Shield. Fishes sampled included two large-bodied piscivores (walleye, *Sander vitreus*, and northern pike, *Esox lucius*, herein referred to as pike), one large-bodied benthivore (white sucker, *Catostomus commersoni*, herein referred to as sucker), and two forage fish species groups: sculpins (slimy sculpin, *Cottus cognatus* and mottled sculpin, *C. bairdii*),

and shiners (spottail shiner, *Notropis hudsonius*, and emerald shiner, *N. atherinoides*). Fish collection for this work was reviewed and approved by the MNRF Aquatic Research and Monitoring Section Animal Care Committee under Animal Use Protocol ARMS-ACC-97. Table SI-51 in the Supplemental Information (SI) section provides the geographic coordinates and attributes of all study lakes, including samples sizes for each species.

To ensure the capture of a wide size range of individuals, fish were sampled through both electrofishing and multi-mesh gill netting. All sampling was conducted between 2011 and 2015 during mid-summer (July and August). Large-bodied fish (> 50 g in weight, caught *via* gill netting) were processed in the field; each was measured for total length (TL, mm) and round weight (g), and a dorsal muscle sample was removed. Ageing structures were also removed from all large-bodied fish >150 mm TL (otoliths for walleye, cleithra for pike, and pectoral fin rays for sucker; Mann, 2017). In addition, liver, gonads, and soma were retained from a subset of the walleye and sucker caught from Lake Nipissing (n = 5/species for all tissues except gonads, n = 2-3/species). Small-bodied fish (< 50 g in weight, caught *via* electrofishing) were sorted and bagged by species in the field. These small-bodied fish and all tissue samples were frozen until further processing.

4.3.2 Laboratory methods

Sample preparation. Ages of large-bodied species were determined by counting annuli on bony structures (see SI for detailed methodology). Small-bodied fish were thawed, measured for TL and weight, and dissected for dorsal muscle. To ensure

adequate biomass for all required analyses, some small fish (all < 90 mm TL) were combined into composite samples by species; muscle from 3-5 individuals of a similar size (i.e., within 5 mm TL) within a lake were pooled and the mean sizes and ages of these fish were used for statistical analyses. A total of 17 composite samples were made in this manner; all other muscle samples represented individual fish. Soma was homogenized using a meat grinder and a 50 g subsample was retained. All tissue samples were freeze-dried using a LABCONCO® FreeZone Bulk Tray Dryer and homogenized to a powder using a Retsch® MM400 ball mill at the Vale Living with Lakes Centre at Laurentian University. The resulting dried and ground tissue was used in all subsequent analyses described below.

Mercury analysis. All Hg analyses were conducted at the ISO 17025 accredited Biotron Laboratory (The University of Western Ontario). Total [Hg] was determined on approximately 15-30 mg of tissue by Thermal Decomposition and Amalgamation Atomic Absorption Spectroscopy (TDA-AAS) on a Milestone© Direct Mercury Analyzer-80 (DMA-80) following EPA method 7473. The method detection limit (MDL) was 2.50 ng/g (based on a 20 mg dry sample). The relative percent differences (RPD) from expected concentrations of certified reference material (1.2 ± 4.6%, n = 54, DORM-4; NRC Canada, 2012) and duplicates (0.48±6.6%, n = 61) were low and within accredited limits. Method blanks were consistently low (0.09±0.08 ng/g, n = 77, assuming a 20 mg dry sample) and no blank-corrections were applied. To determine [MeHg] in fish tissues, a potassium hydroxide (KOH) solution was added to 50-100 mg of sample prior to hot block digestion (Bloom and Fitzgerald 1988). Resulting extracts were speciated by gas chromatography and detected using Cold Vapour Atomic Fluorescence Spectroscopy

(CVAFS) on a Tekran© 2700 automated MeHg Analysis System following EPA method 1630. No MeHg determinations fell below the MDL of 0.12 ng/g (based on a 50 mg dry sample). Relative percent differences (RPDs) of reference materials and duplicates were low and within accredited limits (4.7 ± 10.7%, n = 50, and 6.5±5.5%, n = 21, respectively). Method blanks were low (6.6 ± 35.1% ng/g, n = 95, assuming a sample dry weight of 0.05 g) and all MeHg values were blank-corrected using the mean method blank concentrations within their corresponding batch. All quality assurance and control (QAQC) results are presented in Table SI-52 in the SI section. Samples from this study were analyzed with additional samples constituting a larger data set on which these reported QAQC results are based (see Lescord et al. 2018a).

Isotope and elemental composition. Dried and ground muscle samples were also analyzed for carbon (C) and nitrogen (N) content, and stable isotope composition at the Stable Isotopes in Nature Laboratory (University of New Brunswick) using Continuous Flow-Isotope Ratio Mass Spectrometry (CF-IRMS). Carbon-to-nitrogen mass ratios (C:N) were calculated from the elemental composition of each sample (i.e., %C/%N). Ratios of heavy to light isotopes were expressed in standard delta (δ) notation as parts per thousand (‰) relative to International Reference Standards using the formula: $\delta X = [(R_{sample} / R_{standard}) - 1] \times 1000$, where X is ^{13}C or ^{15}N, and R is the corresponding ratio, $^{13}C / ^{12}C$ or $^{15}N / ^{14}N$. (Peterson and Fry 1987; Fry 2006). RPDs of reference standards and duplicates were low (i.e., <0.01±0.01 to 0.2±7.5%); all QAQC results for isotope analyses are presented in Table SI- **52**. Delta-13C values were used to infer a fish's diet, with more positive values indicating more benthic carbon sources and more negative values indicating pelagic carbon sources (Post 2002). Delta-15N, on the other hand, was

used as an indicator of fish trophic level, with more positive signatures indicating a higher food web position (Post 2002). Carbon-to-nitrogen ratios were used as a proxy for the lipid content in a fish's muscle tissue, with a C:N < 3 indicating minimal lipids present (Kahilainen et al. 2016), and %N represented a rough proxy of protein-content in fish muscle.

4.3.3 Data handling and statistical analyses

All statistical analyses were performed in R (v. 3.4.3; R Core Team, 2017) or SAS (v. 9.4; SAS Institute Inc, 2013) and alpha was set at 0.05. Graphics were produced using the R package *ggplot2* (v.2.2.1; Wickham & Chang 2016). The primary dependent variable in all analyses was %MeHg, calculated as: 100*[MeHg]/[THg]. Prior to statistical analyses, eight samples with %MeHg < 30% were removed as outliers based on preliminary residuals plots. The normality of residuals from all analyses was tested using Shapiro Wilks tests. To account for baseline differences in isotopic signatures among lakes, residual errors were extracted from models $\delta X \sim$ lake, where X is ^{13}C or ^{15}N (residual values herein referred to as $\delta^{13}C_{adj}$ or $\delta^{15}N_{adj}$).

Tissue differences. While muscle was used as the primary tissue for most analyses, we also compared muscle, liver, and soma %MeHg in a small subset of fish (5 walleye, 5 suckers). Differences between tissues within each species were tested with paired-comparisons tests, and differences between species within each tissue were tested with two-sample t-tests. Note that %MeHg in gonads was not included in any statistical test due to low sample sizes (n = 2-3/species).

Within species, among individuals. Relationships between %MeHg in muscle and fish size (TL, weight) and age were assessed using linear mixed-effects models (LMEs) with lake included as a random effect to account for spatial variability in %MeHg (model: %MeHg = size/age + lake). Models were fitted separately for each species, and the significance of each predictor was assessed using partial (Type III) sums of squares. To linearize the observed relationships between %MeHg and fish TL, weight, and age, all three predictor variables were log-transformed. Similar models were also run within species using [THg] as a predictor variable; while these latter models may be spurious (Pollman and Axelrad 2014) they also offer insight into potential effects of high background [Hg(II)] in the environment, which can result in a lower %MeHg (Bloom 1992; Mieiro et al. 2009).

Among species. To assess differences in muscle %MeHg across species while accounting for fish size, LME models were used including species, weight (log-transformed), and their interaction as fixed effects and lake as a random effect (model: %MeHg = log-weight + species + log-weight*species + lake). Models were fit to three sets of data: model 1 used data from large-bodied species only (white sucker, northern pike, walleye), model 2 used data from forage fish species only (sculpins, shiners), and model 3 used data from all five species. Least squares means (LSMs) of %MeHg were estimated for each species at 10, 100, 500, and 1000 g with model 1, at 2, 4 and 8 g with model 2; and at 8 g with model 3. These LSMs were used for all interspecific comparisons. Similar models were fitted between %MeHg and age using large-bodied fish data (forage fish were not aged), again including lake as a random variable (model:

%MeHg = log-age + species + log-age*species + lake); these results are presented in the SI section.

Effects of diet and tissue quality. Finally, to assess the effects of diet and tissue quality on muscle %MeHg, linear models were constructed using fish weight (log-transformed), $\delta^{13}C_{adj}$, $\delta^{15}N_{adj}$, C:N, and %N as fixed effects. Models were run using various combinations of the data: one within each species, one across large-bodied species, one across forage fish species, and one across all species combined. In each case, all possible combinations of 3 or less predictor variables were compared using Akaike's Information Criterion corrected for small sample size (AICc) using the *AICcmodavg* package in R (Mazerolle 2017). Coefficient results from the top models (defined as any model with a delta AICc value < 4; Burnham & Anderson 2002; Burnham et al. 2011) were averaged as per Grueber et al. (2011). Variance inflation factors (VIF) were low (< 9) in all models except the within-species model for sculpin (VIF = 14-74); sculpin results were therefore not presented. Linear relationships between the %MeHg in muscle and each predictor variable ($\delta^{13}C_{adj}$, $\delta^{15}N_{adj}$, C:N, %N) were also assessed independently within and across species; these results are presented in the SI section. These models were run with lake as a random effect using the *lme4* package in R (Bates et al. 2018) and assessed with partial-F tests (type III SS) and marginal r^2 as described previously.

4.4 Results

4.4.1 The %MeHg in fish tissues

Muscle. The fish in this study spanned a broad range of sizes, ages, [THg], diets ($\delta^{13}C$), and tissue quality (i.e., C:N and %N; Table 4-1). The average %MeHg in muscle tissue from all fish across species and sizes was 83.5±19.7%. Individually however, the %MeHg in fish muscle varied widely, ranging from 39 to >100% across the five species (Table 4-1). Approximately 10% of our samples (15 out of 144) had %MeHg estimates above 100%, almost certainly due to small but cumulative errors in the analytical processes. Individual fish with estimated %MeHg > 100% were generally larger in size, and not restricted to any particular lake (see Table SI-53 in the SI section). Within species, the range of %MeHg estimates was broadest in sucker (39 to >100%), and narrowest in sculpins (71 to >100%), the species with the smallest sample size (n = 8) and range of body sizes in this study (Table 4-1). Across species, several samples had %MeHg substantially lower than the commonly assumed 95% (e.g., 42 samples < 80%, 17 samples < 70%).

Other tissues. In sucker, the %MeHg in liver was significantly lower than in both muscle and soma (paired-comparisons t-test, p = 0.012 and 0.008, respectively; Figure 4-1), while in walleye %MeHg in liver was significantly lower than in soma (p <0.001) but not in muscle (p = 0.078; Figure 4-1). Between the two species, walleye had higher %MeHg than sucker in all three tissues but these differences were only statistically significant in liver and soma (Figure 4-1). Differences in muscle %MeHg are more thoroughly assessed with a larger dataset in sections 4.4.2 and 4.4.3 below.

4.4.2 Relationships between muscle %MeHg and body size and age

Percent MeHg in fish muscle was consistently and positively related to measures of body size and age but the strength and significance of these relationships varied among species. Relationships were significant for shiners, sucker, and pike, with weight generally being the strongest predictor of %MeHg within these species (Table 4-2). Sculpins also exhibited a clear positive relationship between %MeHg and body size, but we were unable to detect a significant effect due to a low sample size (Table 4-2). In contrast, walleye muscle %MeHg showed no significant relationship with size or age (Table 4-2) and slopes between muscle %MeHg and weight were significantly lower in walleye compared to other species (Figure 4-2; ANCOVA interaction term, $p = 0.044$). A similar difference in slopes among species was found when %MeHg was regressed against age (ANCOVA interaction term, $p = 0.006$).

Relationships between the %MeHg and [THg] within-species were similarly significant for sculpins, suckers, and pike, but not walleye or shiners. Based on model strength (i.e., r^2 values), [THg] did not explain more variability in muscle %MeHg than fish size or age (Table 4-2).

4.4.3 Among species differences in muscle %MeHg

Among large-bodied species, walleye had consistently higher %MeHg than sucker and pike when standardized to the same weight (Figure 4-2) or age (Figure SI-9). Differences in muscle %MeHg between walleye and the other large-bodied species were greatest in small fish and diminished with increasing weight (Figure 4-3). Walleye had significantly higher %MeHg than sucker at all body sizes tested and significantly higher

%MeHg than northern pike up to 100 g (Figure 4-3). Pike and sucker did not differ significantly from each other at any of the standard body sizes tested (Figure 4-3).

Unlike large-bodied fish, muscle %MeHg in forage fish was not significantly different between species when standardized to 2 g (Tukey's HSD $p = 0.69$), 4 g ($p = 0.72$), or 8 g ($p = 0.85$; Figure 4-4). Furthermore, the linear relationships between %MeHg and weight had similar slopes among these small-bodied species (ANCOVA interaction term, $p = 0.96$). When compared to juveniles of large-bodied species at 8 g, shiners and sculpins had muscle %MeHg similar to that of walleye (Tukey's HSD, $p = 0.816$ and 0.979), but 20-27% higher than that of pike or sucker ($p = 0.042$-0.048; Figure 4-4).

4.4.4 The effect of diet, tissue quality, and trophic level on %MeHg in muscle

Model averaging tests showed that combinations of fish weight and measures of diet, trophic level, and/or tissue quality were significantly related to muscle %MeHg in all species (Table 4-3). Not surprisingly, weight was a significant predictor of %MeHg in fish muscle across all models except within walleye and suckers (Table 4-3). Interestingly, $\delta^{15}N_{adj}$ was only included in large-bodied fish models and in the model including data from all species, but its effect was not statistically significant and the direction of these relationships varied (Table 4-3). Linear relationships between %MeHg and $\delta^{15}N_{adj}$, independent of size or any other predictor, were also not significant in any model tested ($p = 0.183$-0.658), except among forage fish species ($p = 0.034$, $r^2 = 0.574$; shown in SI section). Similar to $\delta^{15}N_{adj}$, $\delta^{13}C_{adj}$ was included in large-bodied fish models but not forage fish models (Table 4-3). However, $\delta^{13}C_{adj}$ was the strongest predictor of

%MeHg in suckers and walleye, though the direction of these relationships were opposite in the two models (Table 4-3). In pike and across all large-bodied fish, $\delta^{13}C_{adj}$ was negatively related to muscle %MeHg, similar to the results from the walleye model (Table 4-3).

Unlike the isotope ratios, measures of tissue quality were included in all models, both within- and among-species (Table 4-3). C:N (an increase of which indicates greater tissue lipid content) was a consistent negative predictor of %MeHg in fish muscle, though the effect was only statistically significant in forage fish ($p = 0.002$-0.004; Table 4-3). However, %N, a rough proxy for protein-content in fish muscle, was also included as a weak negative predictor of %MeHg across models, but again the effect was only significant in forage fish ($p = 0.005$-0.015; Table 4-3). When assessed independently, the effect of %N on %MeHg among species was significant and positive ($r^2 = 0.109$, $p = 0.016$, shown in SI section), indicating higher %MeHg in fish as protein content increases.

4.5 Discussion

4.5.1 Potential drivers of %MeHg variation in fish tissues

Overall, many of the fish studied herein had substantially lower %MeHg in their muscle tissue than the commonly expected 95% as reported by Bloom (Bloom 1992). While Bloom's estimate is an average across muscle samples (many from marine and predatory species), it is commonly applied to fish on an individual basis regardless of species, size, age, or trophic ecology. More recent studies have also reported lower-than-expected %MeHg in muscle from various fish species, particularly those occupying lower

trophic levels (Stefansson et al. 2013), such as forage fishes (e.g., 5-100% in Common galaxias; Arcagni et al. 2018) juveniles of large-bodied species (e.g., 45-100% in rainbow trout; Arcagni et al. 2018), or herbivorous fish (e.g., 66.5% in rabbit fish; (Peng et al. 2016). These fish generally have relatively low [THg] and it is important to note that %MeHg is more sensitive to analytical or other measurement errors when values are low; the same absolute deviation in the data will affect low concentrations more than high concentrations.

In general, MeHg is believed to be the dominant form in fish muscle for three key reasons: (1) high assimilation rates after ingestion or absorption, (2) efficient transport to and strong binding in muscle tissue, and (3) low excretion from the body (Trudel and rasmussen 1997; Wang et al. 2010; Peng et al. 2016). However, several studies have shown that Hg(II) may also be assimilated into a fish's body, albeit at lower rates than MeHg (Pickhardt et al. 2006; Peng et al. 2016). Furthermore, numerous lab-based studies have shown that the rates of these bioenergetic processes are highly variable among species. For example, a review by Bradley et al. (2017) reported assimilation efficiencies ranging from 10-100% and 2-51% for MeHg and Hg(II), respectively, across 25 studies and various fish species. Once assimilated, however, both MeHg and Hg(II) are transferred into blood and transported throughout a fish's body (Bradley et al. 2017 and references therein). While the majority of Hg(II) retained is stored in intestines and liver tissue, varying amounts are also transported to muscle, though the mechanisms for this are not well understood and the internal transport of Hg(II) differs among species and with overall Hg body burden (Ribeiro et al. 2002; Cizdziel et al. 2003; Havelková et al. 2008; Peng et al. 2016). The significant differences in the %MeHg of liver and soma

tissues between walleye and sucker found herein similarly suggests varying rates and patterns of internal Hg movement among-species (Figure 4-1). Lastly, while Hg(II) is eliminated 3-7 times faster than MeHg in fish (Trudel and Rasmussen1997; Wang and Wang 2010), excretion rates are variable between species and affected by water temperature (Trudel and Rasmussen1997) and chemistry (e.g., dissolved organic carbon concentrations; Pickhardt et al. (2006). The species differences in muscle %MeHg observed in our study could therefore be due to differences in MeHg and Hg(II) uptake, assimilation, inter-organ transport, and excretion. To the best of our knowledge, however, no studies have compared the rates of these Hg bioenergetic processes in our study species.

4.5.2 Size-related differences in muscle %MeHg

Results from our study indicate that muscle %MeHg has an ontogenetic pattern, increasing as fish age and grow, but at different rates among species. While both [MeHg] and [Hg(II)] are known to increase with fish size and age, bioenergetic differences in small fish may alter the relative accumulation, distribution, and excretion of each. For example, several laboratory studies have shown that smaller fish (including forage fish and juveniles of large-bodied species) more readily absorb aqueous Hg which is generally composed of 70-95% Hg(II) (Pickhardt et al. 2006; Dang and Wang 2012). These smaller fish also excrete more MeHg when compared to larger fish of the same species (Trudel and Rasmussen 1997). Smaller fish also grow at relatively faster rates, and somatic growth dilution has been shown to lower whole-body [MeHg] more so than [Hg(II)] (Wang and Wang 2012; Sandheinrich and Drevnick 2016), which could result in lower

overall %MeHg. A recent study by Wang and Wang (Wang and Wang 2018) found that diet-elevated growth rates in freshwater tilapia (*Oreochromis niloticus*) significantly lowered MeHg accumulation but not Hg(II), which was controlled by assimilation efficiencies independent of growth rate.

In addition to size and age, we examined relationships between muscle %MeHg and muscle [THg] in all species. In most northern environments with no point sources of mercury pollution, as in this study, a positive correlation between %MeHg and [THg] would be expected because MeHg bioaccumulates and biomagnifies faster than Hg(II) (Lavoie et al. 2013). Fish from Hg-contaminated sites will bioconcentrate more Hg(II) relative to fish in pristine environments (Dutton and Fisher 2014), and consequently, will also have lower %MeHg at a given body size (Mieiro et al. 2009). However, we found that [THg] did not explain greater amounts of variation in %MeHg than did size or age for most species, with the exception of sculpins (Table 4-2). This suggests that our observed %MeHg and size/age relationships were not simply artefacts of relationships between %MeHg and [THg].

4.5.3 The influence of diet and trophic ecology on muscle %MeHg

Because diet is the main source of Hg in fish, it is possible that the size-related changes in muscle %MeHg found herein may be due to ontogenetic changes in diet. Mason et al. (Mason et al. 2000) suggested that lower %MeHg (approximately 60-80%) in juvenile brown trout when compared to adults (80-110% MeHg) was due to consumption of invertebrates, which are known to have highly variable and often low (i.e., < 50%) %MeHg (Becker and Bigham 1995; Tremblay et al. 1995; Økelsrud et al.

2016). We found relatively weak relationships between $\delta^{13}C_{adj}$ values and muscle %MeHg within and among fish species, with the exception of walleye and suckers (Table 4-3). In most models, $\delta^{13}C_{adj}$ was a negative predictor, suggesting higher muscle %MeHg in fish with pelagic-based diets. However, if shifts in diet were the primary determinant of the %MeHg and size/age relationships, then we would expect them to be stronger in species that exhibit more pronounced ontogenetic dietary shifts. Walleye are known to be primarily piscivorous over their lifespan, and this may explain the high and stable %MeHg we observed at all walleye sizes and ages. But, we found that muscle %MeHg increased with size and age in shiners and sucker, which are both believed to consume invertebrates throughout their lives.

It is well known that both [THg] and [MeHg] in fish are higher in species at higher trophic positions and it is possible that among-species differences in %MeHg may also be related to trophic position. In this study, however, $\delta^{15}N_{adj}$ did not have a strong influence on %MeHg in fish muscle after accounting for the effect of body size. Furthermore, piscivorous pike did not have significantly different muscle %MeHg from benthivorous suckers, despite drastic differences in their diets. Even when consuming the same prey items, mosquitofish and sunfish were found to have significantly different assimilation rates of dietary Hg(II) (42-51% and 9-10%, respectively; Pickhardt et al. 2006), suggesting that diet is not solely responsible for interspecific variation in muscle %MeHg. Other studies have also found that gut passage time has an effect on Hg assimilation and excretion (Zhang and Wang 2006; Dang and Wang 2012), which could alter %MeHg in tissue regardless of diet quality. It is important to note that data from multiple lakes were used for these analyses, and while we baseline-adjusted all isotope

values and statistically accounted for site-related variability, it is possible that differences in food web structure among the study lakes had an effect in our dataset.

4.5.4 The effect of tissue quality on muscle %MeHg

Given that the majority of MeHg is bound to the protein-fraction of muscle tissue (Amlund et al. 2007; Peng et al. 2016), it was expected that a higher lipid content (i.e., higher C:N ratio) and lower protein content (lower %N) would be associated with a lower %MeHg in muscle tissue. However, we found surprisingly weak relationships between %MeHg and measures of tissue quality in large-bodied fish muscle. In fact, protein content was a negative predictor of %MeHg in several models. Recent studies suggest that the utility of %N as a proxy for protein content is largely dependent on the type of nitrogenous substances present (Fagan et al. 2011) and more direct measures of protein content (e.g., amino acid measurements; Thera 2017) should be considered by future studies.

Unlike large-bodied fish, however, forage fish models showed strong significant relationships between muscle %MeHg and both C:N and %N. Inorganic Hg has been shown to bind with various lipid membranes under certain conditions, particularly when bound with chlorine (Girault et al. 1995; Hassanin et al. 2016; Kerek et al. 2017). It is unclear why muscle %MeHg would be more affected by measures of tissue quality in small-bodied than large-bodied fish but it may be due to the slightly broader range in predictor values (e.g., %N ranged from 9-15% in forage fish vs. 12-16% in large-bodied fish; Table 4-1). Overall, ranges of C:N and %N values were narrow across species from this study. For example, C:N values measured in all fish were close to 3, indicating very

low lipid-content among species (Kahilainen et al. 2016). Bloom (Bloom 1992) also assessed the relationship between %MeHg and lipid content of fish muscle and found no relationship, despite having a 25-fold difference in lipid estimates across samples. Nevertheless, further studies could consider higher lipid content fish (i.e., C:N >5), as well as other factors that affect Hg speciation in fish muscle such as selenium (Bjerregaard et al. 2011) or vitamin E content (Moniruzzaman et al. 2017).

4.6 Conclusions

Overall, this study showed that more variability in the %MeHg of fish muscle exists than is currently being considered by modern studies. Specifically, our results indicate that assuming > 95% of THg is MeHg is not appropriate for younger and smaller fish in some species. It is, however, likely still an appropriate assumption for walleye of all sizes and for larger pike. The inclusion of $\delta^{13}C_{adj}$, C:N, and %N in various models suggests that diet and tissue quality account for some variability in %MeHg in fish muscle, but further research is needed to determine the cause and strength of this effect. Indeed, a larger study is warranted to examine %MeHg for wide size and age ranges of fish species with varying trophic ecologies and tissue qualities, and across a broader range of habitats (e.g., water contaminated with Hg(II) vs. remote systems).

Results of this study have potentially major implications for future research, particularly those studying Hg biomagnification, where [THg] in fish are compared to direct measures of [MeHg] in lower trophic levels. Furthermore, because these small-bodied fish are vital prey items for larger fish, our results fill an important gap in our understanding of MeHg bioaccumulation and biomagnification through aquatic food

webs. The direct measurement of MeHg in fish muscle would also benefit monitoring programs, particularly for a subset of smaller and younger fish.

4.7 Tables and Figures

Table 4-1: Ranges of Hg concentrations, measures of tissue quality, and stable isotopes signatures measured in muscle tissue for each study species. Note: TL = total length; age 0 fish are young-of-the-year (born during sampling year, <1-year-old); ages were not determined for sculpins and shiners

Species	n	[THg] (µg/g dry)	[MeHg] (µg/g dry)	%MeHg	TL (mm)	Weight (g wet)	Age (years)	$\delta^{13}C$* (‰)	C:N	%N
Sculpins	8	0.13 - 0.74	0.10 - 0.78	71 - 106	43.8 - 92.0	1.4 - 8.9	ND	-30.1 - -24.2	3.2 - 3.7	13 - 15
Shiners	22	0.18 - 0.73	0.11 - 0.76	49 - 102	35.5 - 91.0	0.2 - 7.2	ND	-33.5 - -19.6	3.3 - 4.5	9 - 14
Sucker	42	0.08 - 1.59	0.05 - 1.57	39 - 124	51.8 - 556	1.1 - 1940	0 - 17	-31.2 - -20.7	2.8 - 4.3	12 - 16
Pike	24	0.10 - 6.41	0.05 - 7.83	46 - 122	55.5 - 800	1.0 - 3150	0 - 11	-30.2 - -17.3	3.1 - 3.4	13 - 15
Walleye	48	0.17 - 5.96	0.18 - 5.72	68 - 112	89.0 - 770	4.7 - 4748	0 - 20	-31.1 - -22.1	2.8 - 3.4	12 - 16

*Isotope values are unadjusted.

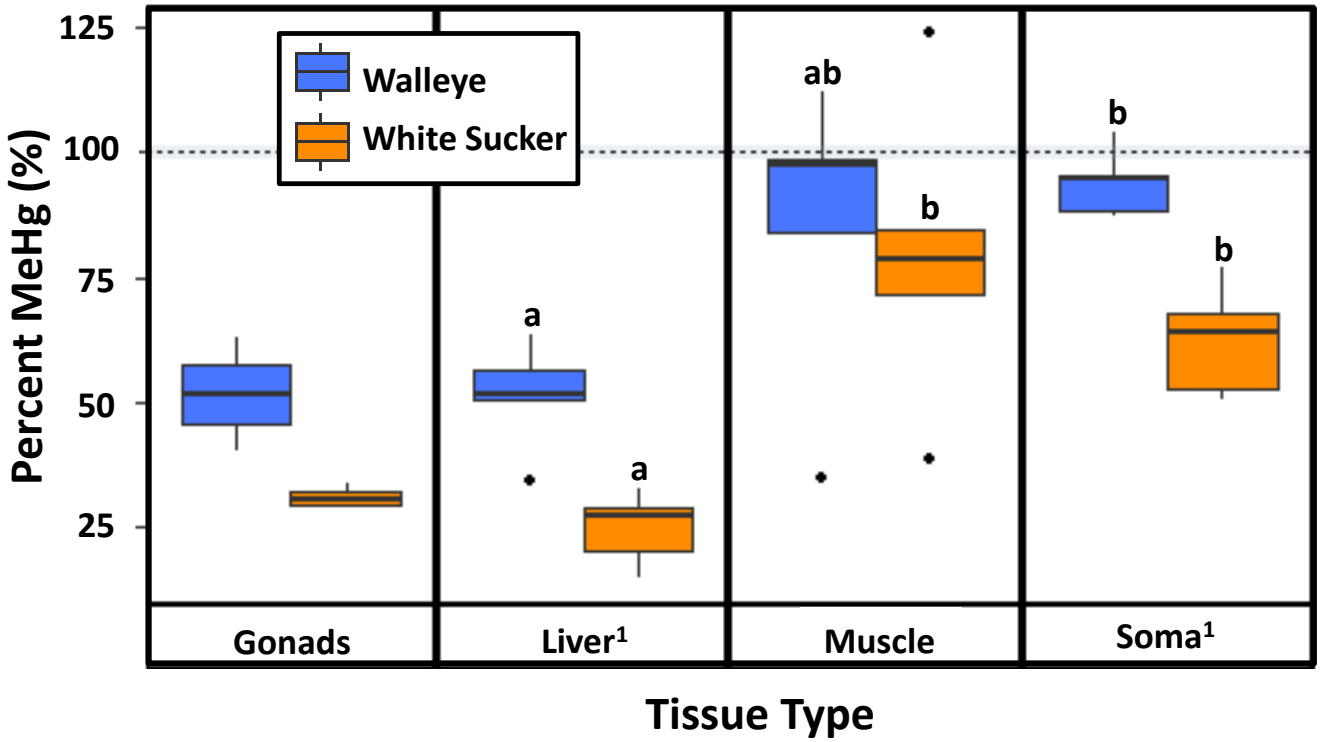

Figure 4-1: The percentage of total Hg as MeHg (%MeHg) in four tissue types from walleye and white sucker from Lake Nipissing (n = 5/species for each tissue except gonads, n = 2-3/species). Boxes represent the spread of data within each species and tissue, with the median %MeHg shown as a line within. [1]Indicates a significant difference between species within a given tissue (see Table SI-54 for statistical comparisons). Post-hoc differences within species and among tissues are indicated by differing letters (see Table SI-55 for p-values). Note that gonads were not included in any statistical comparisons due to small sample sizes.

Table 4-2: Model results for the percentage of total Hg as MeHg (%MeHg) in muscle as a function of fish size, age, or [THg]. Total length and weight were transformed as $\log_{10}$ (X), and age and [THg] were transformed as $\log_{10}$ (X+1). Lake was included as a random effect in all models. Significant results are bolded.

			Model parameters		Predictor effect		Full model
Predictor variable	Species/Group	*n*	*Intercept*	*Slope*	*F*	*p-value*	R^2
Total Length	Sculpins	8	-45.5	74.2	0.40	0.560	0.26
	Shiners	**22**	**-67.0**	**83.7**	**7.79**	**0.014**	**0.57**
	White sucker	**42**	**32.8**	**23.1**	**7.17**	**0.012**	**0.21**
	Northern pike	**24**	**-16.3**	**38.4**	**24.15**	**<0.001**	**0.63**
	Walleye	49	87.6	4.1	0.42	0.520	0.13
Weight	Sculpins	8	78.5	15.6	0.10	0.770	0.20
	Shiners	**22**	**76.6**	**24.3**	**8.36**	**0.011**	**0.58**
	White sucker	**42**	**72.1**	**7.2**	**6.92**	**0.013**	**0.21**
	Northern pike	**24**	**50.7**	**13.1**	**24.83**	**< 0.001**	**0.63**
	Walleye	49	94.2	1.5	0.54	0.470	0.14
Age	Sculpins	---	---	---	---	---	---
	Shiners	---	---	---	---	---	---
	White sucker	**42**	**65.6**	**18.6**	**6.78**	**0.014**	**0.23**
	Northern pike	**24**	**67.4**	**32.3**	**13.32**	**0.002**	**0.50**
	Walleye	49	96.5	1.6	0.15	0.700	0.13
[THg]	**Sculpins**	**8**	**65.8**	**164**	**18.90**	**0.010**	**0.86**
	Shiners	22	52.1	183	2.91	0.109	0.45
	White sucker	**42**	**75.6**	**97.4**	**10.82**	**0.002**	**0.28**
	Northern pike	**24**	**63.9**	**46.6**	**11.81**	**0.003**	**0.48**
	Walleye	49	96.9	1.7	0.06	0.810	0.13

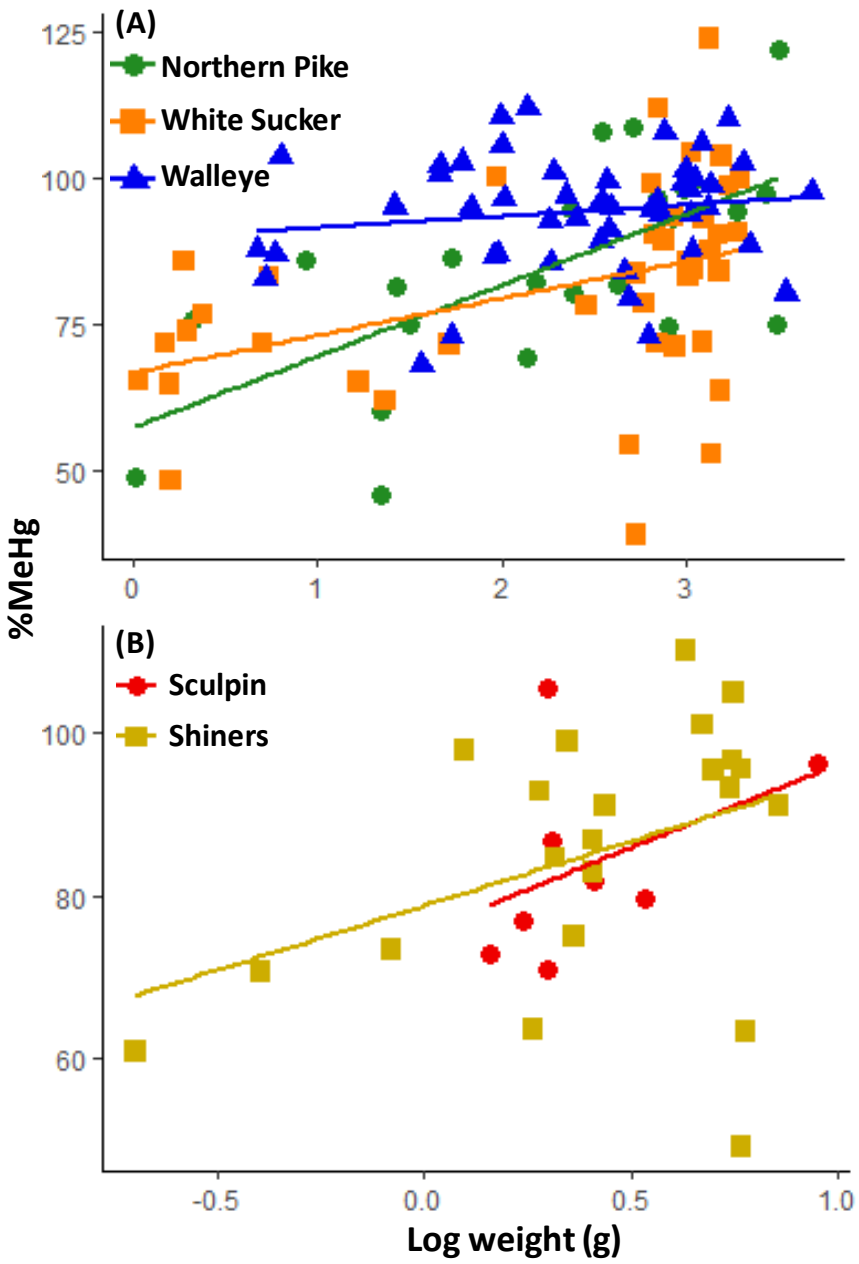

Figure 4-2: Linear relationships between the percent of MeHg (%MeHg) in fish muscle and round weight (log10 transformed) within (A) large-bodied fish species, and (B) forage fish species. The slopes of these relationships were significantly different among species (ANCOVA, interaction term, p = 0.006; see Table SI-61).

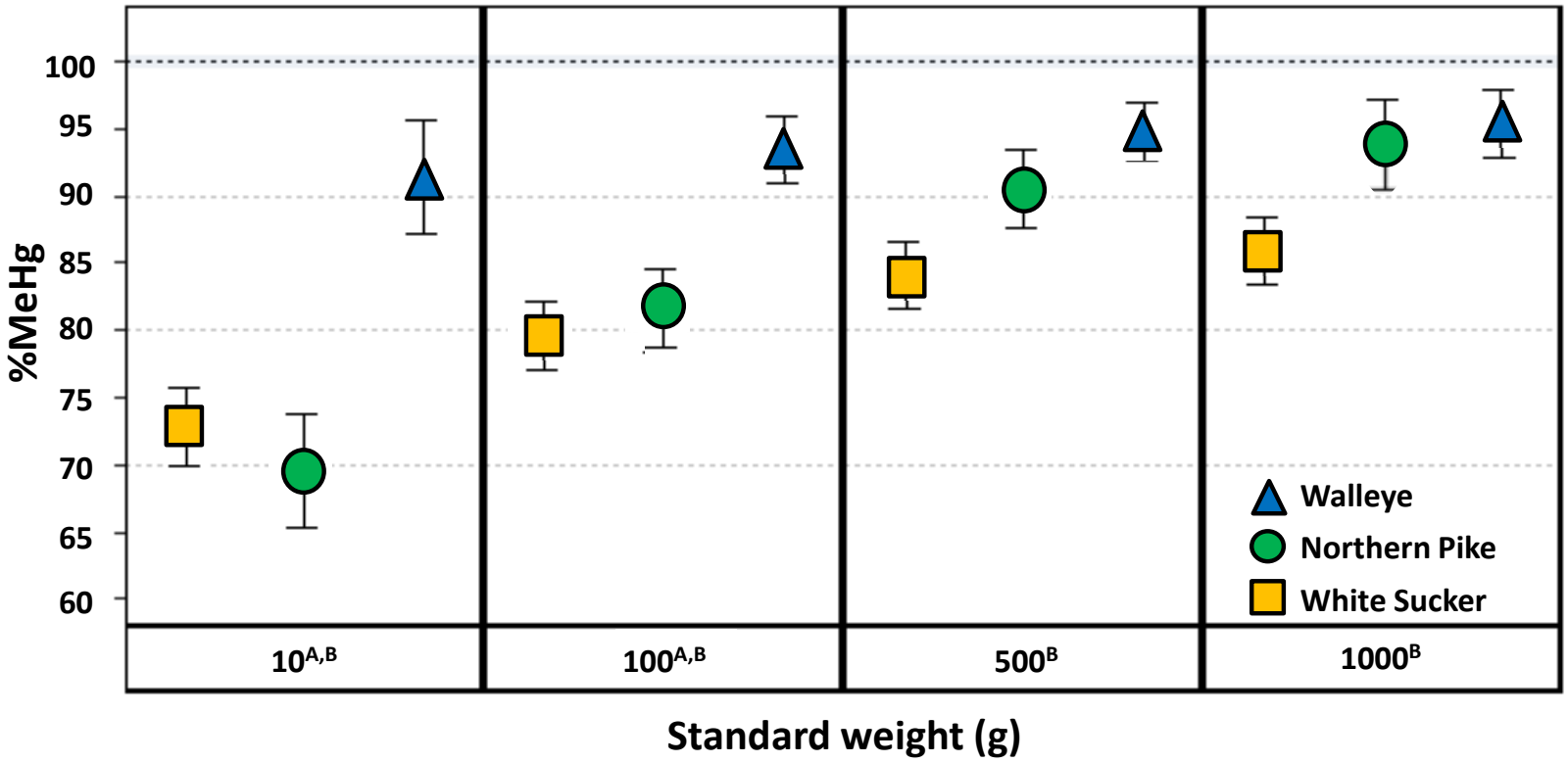

Figure 4-3: Least squares means of the percent MeHg (%MeHg, ±SE) in muscle, standardized to various body weights, in large-bodied fish: white sucker (n = 42), northern pike (n = 24), and walleye (n = 48). [A]Indicates a significant difference (Tukey's HSD, $p < 0.05$) between walleye and northern pike; [B] Indicates a significant difference (Tukey's HSD, $p < 0.05$) between walleye and white sucker. No differences were found between northern pike and white sucker at any standard weight (see Table SI-58 for post-hoc results).

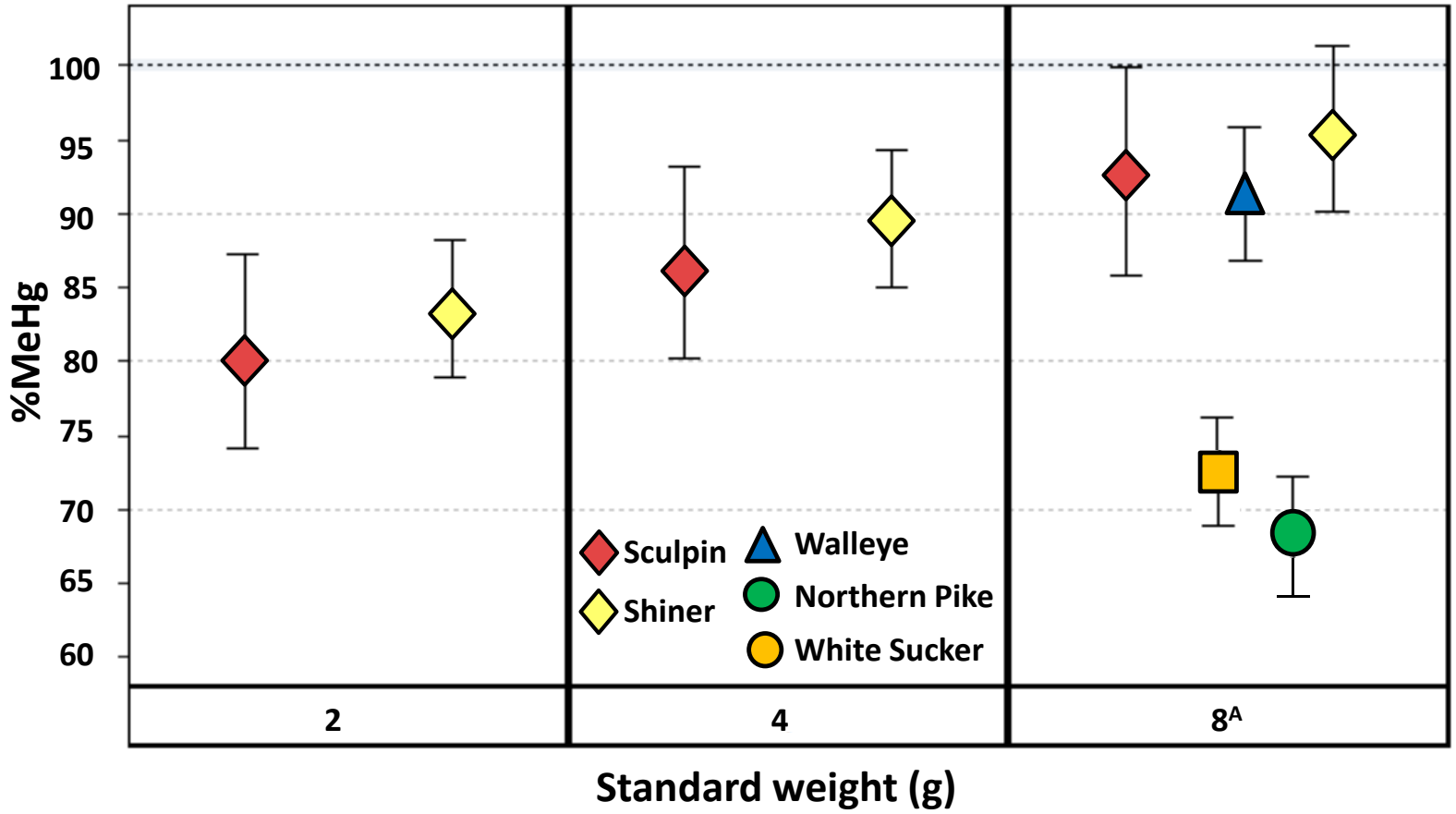

Figure 4-4: Least squares means of the percent MeHg (%MeHg, ±SE) in muscle estimated at various weights in small-bodied species (sculpins, shiners; n = 8 and 22, respectively) and the juveniles of large-bodied species (walleye, northern pike, white sucker; n = 48, 24, and 42, respectively). [A]Significant differences were detected at 8 g between shiners and pike, between shiners and sucker, between walleye and sucker, and between walleye and pike (Tukey's HSD, $p < 0.05$). No differences were found between the forage fish species at any standard weight (Tukey's HSD, $p > 0.05$; see Table SI-61 and Table SI-61 for all post hoc results).

1

Table 4-3: Results from modeling the percent MeHg (%MeHg) in muscle as a function of indices of diet, trophic level, and tissue quality. Values presented are standardized model coefficients (±SE) averaged across top-ranking models (delta AICc <4). Corresponding p-values are listed below each coefficient. Weight was log-transformed in all models. Significant values are bolded. ND = no data because parameter was not included in any of the top models. Large-bodied = 3 large-bodied fish species.

Group	Intercept	Weight	$\delta^{13}C_{adj}$	$\delta^{15}N_{adj}$	%N	C:N
All fish	**87.58 ± 1.34**	**13.25 ± 2.91**	-1.25 ± 2.34	-0.03 ± 1.17	0.15 ± 1.72	-0.64 ± 1.88
(p-value)	***(<0.001)***	***(<0.001)***	*(0.596)*	*(-0.979)*	*(-0.930)*	*(-0.734)*
Large-bodied	**87.02 ± 1.22**	**10.93 ± 2.75**	-1.12 ± 2.13	0.05 ± 1.00	-0.22 ± 1.82	-0.35 ± 1.64
(p-value)	***(<0.001)***	***(<0.001)***	*(0.601)*	*(0.961)*	*(0.905)*	*(0.834)*
Suckers	**81.50 ± 2.26**	-8.92 ± 5.48	**15.19 ± 4.92**	0.63 ± 2.47	0.13 ± 2.14	-0.06 ± 1.63
(p-value)	***(<0.001)***	*(0.112)*	***(0.003)***	*(0.802)*	*(0.953)*	*(0.971)*
Pike	**84.81 ± 2.84**	**25.77 ± 6.76**	-1.91 ± 4.83	-2.04 ± 4.52	-0.29 ± 2.62	1.28 ± 3.85
(p-value)	***(<0.001)***	***(<0.001)***	*(0.702)*	*(0.661)*	*(0.917)*	*(0.749)*
Walleye	**93.93 ± 1.39**	0.81 ± 2.06	**-6.96 ± 2.86**	-0.25 ± 1.43	-0.14 ± 1.31	-0.02 ± 0.96
(p-value)	***(<0.001)***	*(0.699)*	***(0.018)***	*(0.866)*	*(0.917)*	*(0.981)*
Forage fish	**85.08**	**13.72**	ND	ND	**-22.52**	**-27.67**
(p-value)	***(<0.001)***	***(0.006)***	---	---	***(0.015)***	***(0.004)***
Shiners	**85.49**	**15.88**	ND	ND	**-31.48**	**-35.23**
(p-value)	***(0.001)***	***(0.009)***	---	---	***(0.005)***	***(0.002)***

Chapter 5 : Thesis conclusions and implications for the Ring of Fire Development and subsistence fishers

5.1 Summary of thesis

In the Far North of Ontario, Canada, some of the largest and most intact freshwater watersheds in the world are facing changes due to planned resource extraction (e.g., the Ring of Fire mineral deposit), as well as the continued effects of rapid climate change. However, these watersheds are also relied upon to provide subsistence fish to the 31 remote communities established across northern Ontario. As such, it is vital to establish a baseline of Hg concentrations in water and biota of these systems and determine the key drivers of Hg bioaccumulation in the Attawapiskat Drainage Basin (ADB), which houses a large portion of the Ring of Fire deposit.

The overall goals of this thesis were to (1) model Hg cycling, accumulation, and speciation in relation to large-scale environmental and chemical gradients; (2) measure and report [Hg] in subsistence fish and the food webs that support them; and (3) provide a summary of findings and baseline data to environmental monitoring programs for the Ring of Fire. These goals were largely met in the previous chapters, the conclusions from which are summarized below.

While my thesis focused on the ADB, results presented herein have implications both locally, for residents of the Far North of Ontario and the Ring of Fire development, as well as for the broader global boreal region. Overall, aqueous and biotic Hg concentrations reported were variable and levels in fish sometimes exceeded consumption limits set by the federal government (i.e., 0.5 ppm, Health Canada 2007).

Not surprisingly, these exceedances were generally in larger piscivores at the top of their respective food webs (e.g., walleye and pike). Other key conclusions and outcomes from this thesis are discussed as they pertain to each thesis goal:

Goal (1): Model Hg cycling, accumulation, and speciation in relation to large-scale environmental and chemical gradients

This thesis was the first study, to the best of my knowledge, to consider the effect of watershed-level environmental gradients on Hg bioaccumulation. It was also the first to assess the quality of DOM on such a large environmental scale. Overall, gradients of physical, chemical (including DOM quality), and ecological parameters were detected across the ADB, indicating that a system's landscape position does indeed affect its environmental conditions and biological processes. However, many parameters including aqueous and biotic Hg concentrations showed substantial differences between the two ecozones of the ADB (i.e., the Boreal Shield and Hudson Bay Lowlands) rather than a linear relationship with decreasing landscape position. These regional differences are likely influenced by bedrock geology as well as riparian characteristics (i.e., forested vs. peatland-based). Regional differences are also an important consideration for future monitoring programs; systems in the boreal shield and lowlands may be affected differently by future land-use practices and climate-related changes. Continued monitoring of systems in both regions should be considered to thoroughly assess the impacts of future stressors in the Far North of Ontario.

Goal (2): Measure and report [Hg] in subsistence fish and the food webs that support them

This thesis project generated [THg] and/or [MeHg] data in over 2500 fish across 30 lakes and river sites from 2014 to 2016, while also utilizing additional historical data throughout. The new samples collected were analyzed in partnership with the Ontario Ministry of the Environment and Climate Change (MOECC), the agency responsible for monitoring fish contaminant levels and setting fish consumption guidelines across the province. These data therefore added vital new information to the updated 2018-2019 "Guide to Eating Ontario Fish," refining consumption guidelines in these remote systems important to several First Nation communities. Results from these studies and the consumption recommendations have been reported to northern Tribal Councils and environmental stewards at various conferences and land-use planning meetings, as well as through outreach documents (see section 5.3 below).

Goal (3): Provide a summary of findings and baseline data to environmental monitoring programs for the Ring of Fire

Much of the data from the studies presented herein are included in the Supplemental Information (SI) section of this thesis. As such, it is readily available for use by government agencies, First Nations community organization, and future scientists to assist in monitoring the effects of the Ring of Fire development and/or the effects of climate change on the limnology and Hg cycling across the ADB. My findings clearly identify key factors to focus on as these systems respond to change. For example results from Chapter 2 suggest that monitoring programs should consider the effects of nutrients and DOC inputs to freshwater systems, both of which were consistent and strong predictors of [Hg] in water and/or biota.

This thesis also provides particularly valuable data from the uniquely shallow lacustrine systems on the Hudson Bay Lowlands, which are logistically difficult to sample at present; future development in the Far North may provide easier access to these systems, which should be further studied to better understand seasonal changes to their limnology and ecological communities and the potentially related effects of both climate- and industry-related changes. These programs should also consider measuring [MeHg] directly in smaller and less predatory fish in which [THg] is not a suitable proxy.

5.3 Future research

Given the importance of boreal freshwater watersheds on a global-scale, studies conducted across drainage basins such as the ADB will prove important for preserving the future health and environmental services provided by boreal systems. Because of the regional differences observed between systems located on the shield and lowlands, continuous landscape gradients across the ADB were not as strongly pronounced as expected. Other watersheds with more homogenous landscapes may show a stronger linear effect of system landscape position on physico-chemistry, ecology, and Hg accumulation. From these results, I would suggest that future studies on Hg cycling should continue to address the effects of [DOC], which was found to be a strong predictor of [Hg] in water and various biotic groups. Furthermore, greater attention should be given to the quality of DOM; fluorescence and absorbance spectroscopy is a cost-effective and timely method which adds novel information to the highly complex relationships between Hg and DOC concentrations. Future studies should also consider the size and trophic

ecology of a fish before measuring THg as a proxy for MeHg concentrations in muscle tissue; the latter should be directly analyzed in small-bodied fish and lower-trophic-level, large-bodied species (e.g., white sucker), if possible. However, a larger study examining a broader range of species is strongly recommended to fully understand individual-level variability in the %MeHg of fish muscle tissue. More direct measures of protein and lipid-content should also be explored as potential predictors of this variability.

5.4 Communication needs

The results and conclusions of contaminants studies such as those presented herein need to be carefully and effectively communicated to all interested peoples. Information on contaminant concentrations in freshwater fish and the food webs that support them are a great concern for residents of remote northern communities, particularly indigenous communities for whom fishing holds strong cultural value. Furthermore, because the transportation costs of fresh and nutritional foods to remote regions is often high, many residents rely on locally-caught freshwater fish for a healthy diet (i.e., high in protein and omega-3 fatty acids). As a result, people living in remote northern regions often consume larger amounts of wild fish in comparison to more southerly residents, exposing the former to potentially higher health risks due to contaminants. While these risks must not be under-stated, moderate fish consumption has considerable health benefits (Seabert et al. 2014) and the affordable alternative food options available in northern stores are limited mostly to non-perishable food items that can be unhealthy in other ways (i.e., high sugar, saturated fats, etc.; Gates et al. 2016; Natcher et al. 2016; Jones et al. 2018). It is, therefore, important that researchers and monitors who communicate contaminant

science and consumption recommendations to subsistence fishers do so without unduly discouraging all consumption of fish (Loring et al. 2010). Instead, communicators should strive to inform consumers of fish about the risks from contaminants in parallel with its health benefits, enabling individuals to make their own informed dietary choices.

Effective and accurate communication of the risks and benefits of fish consumption can, however, be challenging. Below, I have summarized seven points which researchers and communicators should consider before discussing the risks of fish consumption with subsistence fishers. These points were developed over the course of my thesis work, in close collaboration with members of the Science Communication program at Laurentian University, MOECC scientists, and other academic researchers.

(1) It is important to differentiate the population that is highly sensitive to the effects of contaminants from the general public. Because it can cross the blood-brain barrier, Hg can be transferred from a mother to the developing fetus in her womb (Clarkson and Magos 2006). As a neurotoxin, MeHg affects early brain development in the fetus and in children; therefore, the message should be that women of child-bearing age and children should especially limit their consumption of some fish known to carry high [Hg] (e.g., large walleye; Strandberg et al. 2018).

(2) The health benefits of eating fish should be emphasized whenever possible. If available, any data on omega-3 fatty acids or other healthy end-points should be provided. Encouragement to consume lower-trophic-level species (e.g., lake whitefish) and smaller individuals of higher-trophic-level species (e.g., northern

pike) may be warranted, particularly for the non-sensitive population (i.e., adult men and women not of child-bearing age).

(3) A clear, adequate amount of background information on Hg (and/or other contaminants of concern) cycling should be provided to enable consumers to make informed decisions about their own fish consumption. In particular, the process of MeHg production, bioaccumulation, and biomagnification should be explained so consumers understand why larger, older, and more piscivorous fish species tend to have higher [Hg]. The processes of atmospheric-transport and methylation should also be discussed; this enables consumers to understand how distant sources of Hg can affect concentrations of MeHg in their local fish. Furthermore, data from other regions should be shown to emphasize that Hg is ubiquitous in similar environments (e.g., other boreal or arctic lakes).

(4) Language and other communication barriers should be diminished through the use of outreach documents translated to local dialects and avoidance of unnecessary jargon or excessive detail. Word choices should be selected with care; risks and benefits should be described as accurately as possible and all inflammatory and ambiguous statements should be avoided. Whenever possible and appropriate, pictures and diagrams should be used in place of words and tables.

(5) Outreach materials should be catered to specific communities. Lakes and river sites important to and used by a given community should be used in all examples, whenever possible. Furthermore, relevant events of industrial operations near a given community should be discussed; any concerns (or lack thereof) should also be discussed, whenever possible. When applicable, explain why extreme

examples are often the exception and largely irrelevant to the local risks (e.g., mercury contamination of the Wabigoon River; Kinghorn et al. 2007).

(6) Be honest about the limitations of current scientific knowledge. For example, consumption advisories do not consider or convey any cumulative effects of multiple contaminants in fish tissue, a topic which has not been thoroughly explored by researchers to date. In general, consumption restrictions are based on any contaminant that exceeds a set threshold based on reference doses, which are typically set by federal governments (e.g., Health Canada or the U.S. Environmental Protection Agency).

(7) Engage in a dialogue: ask questions and allow community members to voice their thoughts and concerns. Communities may have an understanding of the general risks from Hg and other contaminants in their fish but also have relevant and important questions about concentrations in specific fish species, harvesting locations, tissues types (e.g., liver or brain), or about various deformities observed (e.g., cysts on fish). Relevant information from the people that are most closely and intimately associated with their main source of food and the surrounding landscape can help guide future research and improve outreach information regarding consumption advisories.

(8) Be mindful of other social and economic issues faced by northern First Nation communities, the effects of which may be considerable at times (e.g., Skinner et al. 2013; Jaglal et al. 2013; Marquina-Márquez et al. 2016).

Guided by many of these principles, we have designed informative handouts based on the 2017-2018 “Guide to Eating Ontario Fish” published by the Ontario MOECC (https://www.ontario.ca/page/eating-ontario-fish-2017-18). This guide is a product of one of the most extensive freshwater fish contaminant monitoring programs in North America, conveying a considerable amount of valuable information to consumers; namely the maximum number of meals per month that can be consumed without concern from Hg (or other contaminants) concentrations based on Health Canada contaminant intake guidelines. The numbers are calculated based on data from a given waterbody, for various fish species and at different body sizes (see the example from Eabamet Lake in Figure 5-1). In total, recommendations are made for over 2,000 waterbodies across Ontario, including several in the Far North of Ontario which are fished by various First Nation communities. The tables in this guide can, however, be confusing to consumers (Figure 5-1). An example of a more graphical handout depicting the recommendations made by the MOECC guide, including some background information and essential facts (e.g., meal size and sensitive populations), is provided in Figure 5-2. We are currently in the process of collecting information on fish consumption (e.g., what species and tissue types are commonly consumed), Hg concerns, and the use of the MOECC guide, as well as feedback on our handouts (i.e., Figure 5-2 and other ideas), in the form of surveys distributed to communities across the Far North. The results of this survey will be submitted for publication (along with the above communication recommendations) when complete.

Overall, considerably more research into the benefits of freshwater fish consumption is needed to properly inform consumers of both the risks and benefits of local fish

consumption. Similar to contaminants, the healthy end points (i.e., omega-3 fatty acids) in fish tissue vary among species and locations, though some recent studies suggest that anadromous fish may have lower contaminants burden and higher levels of omega-3 fatty acids when compared to resident fish in the same systems or locations (Heerschap 2018; Strandberg et al. 2018). Nevertheless, continued collaboration between researchers and monitoring programs to update and expand contaminant databases and refine fish consumption guidelines will enable people across northern Ontario to make informed decisions about their dietary choices.

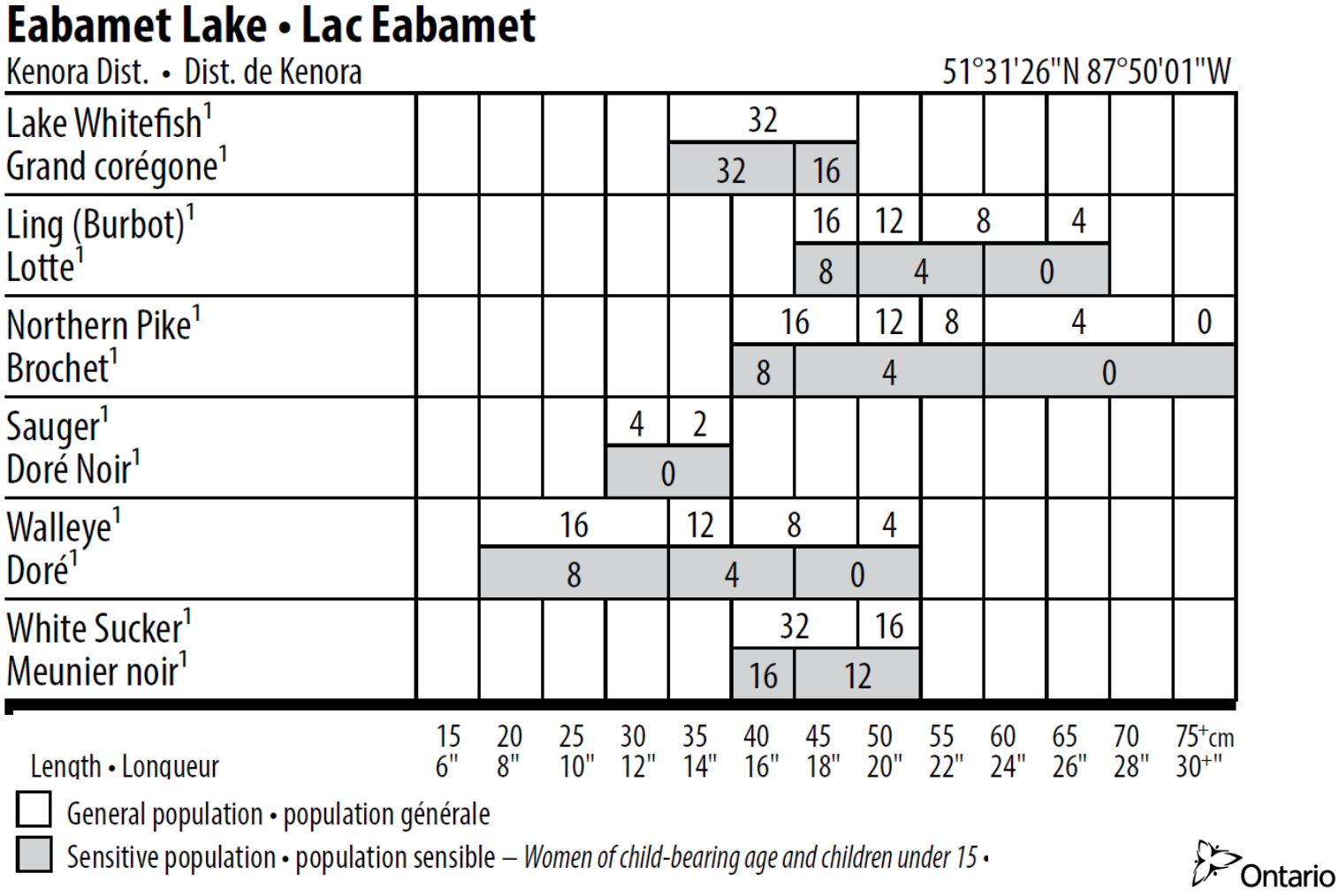

Figure 5-1: Example of a consumption recommendation table taken from the Ontario Ministry of the Environment and Climate Change (MOECC)'s 2017-2018 "Guide to Eating Ontario Fish". Each number represents the meals of fish muscle tissue that can be safely eaten for a given species across a size range from Eabamet Lake fish, a vital resource to the Eabametoong First Nation community (formerly known as Fort Hope).

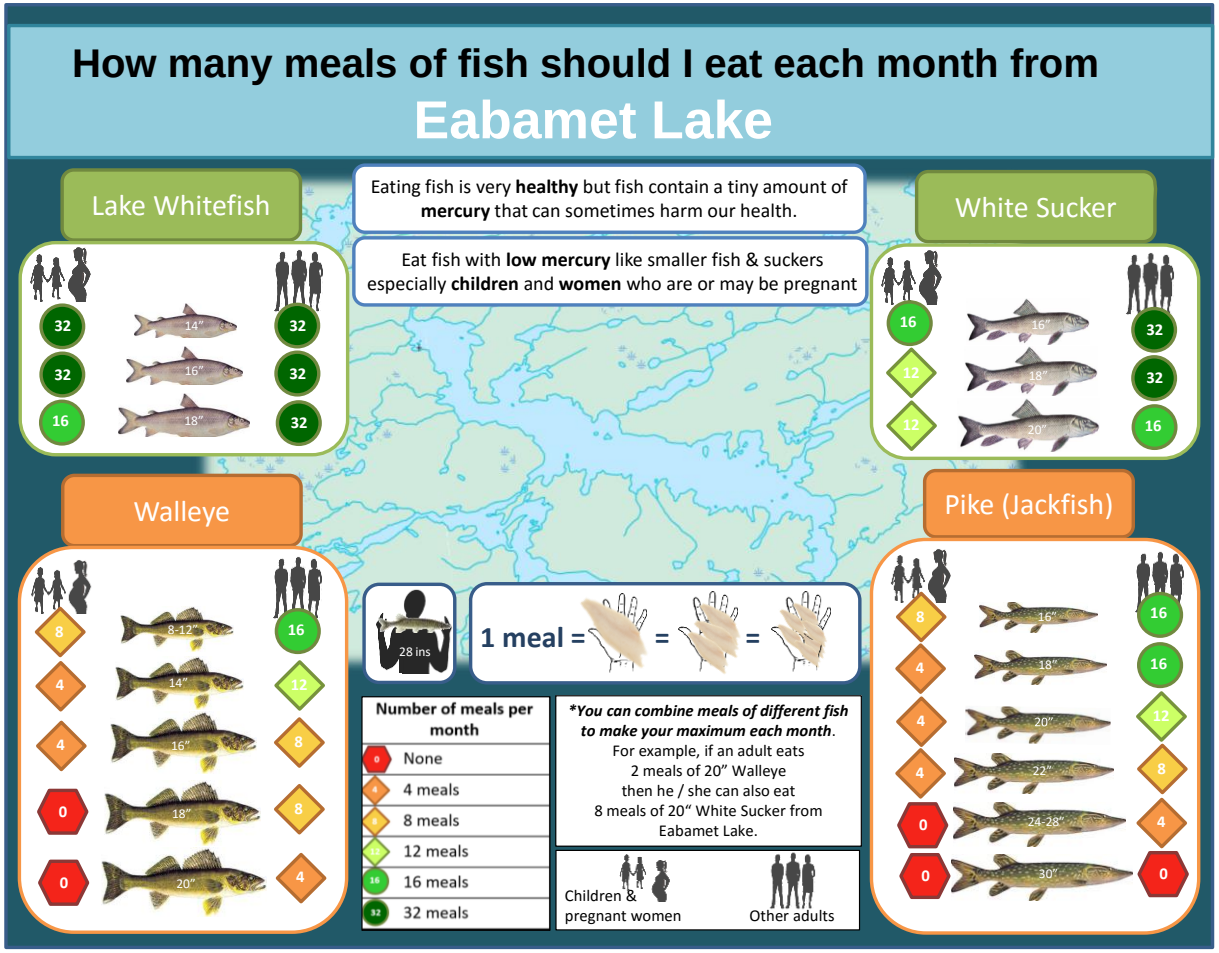

Figure 5-2: A graphic conveying the consumption recommendations made by the Ontario MOECC in 2017-2018 "Guide to Eating Ontario Fish" for Eabamet Lake fish, a vital resource to the Eabametoong First Nation community (formerly known as Fort Hope). Additional background information on meal size, sensitive populations, and other background information are also included; much of this information is described in text at the beginning of the MOECC guide book.

Literature Cited

Adrian, R., O'Reilly, C.M., Zagarese, H., Baines, S.B., Hessen, D.O., Keller, W., Livingstone, D.M., Sommaruga, R., Straile, D., Van Donk, E., Weyhenmeyer, G.A., and Winder, M. 2009. Lakes as sentinels of climate change. Limnol. Oceanogr. 54: 2283–2297. doi: 10.4319/lo.2009.54.6_part_2.2283

Ahonen, S.A., Hayden, B., Leppänen, J.J., and Kahilainen, K.K. 2018. Climate and productivity affect total mercury concentration and bioaccumulation rate of fish along a spatial gradient of subarctic lakes. Sci. Total Environ. 637–638: 1586–1596. doi:10.1016/j.scitotenv.2018.04.436.

Albanese, S., De Vivo, B., Lima, A., and Cicchella, D. 2007. Geochemical background and baseline values of toxic elements in stream sediments of Campania region (Italy). J. Geochem. Explor. 93: 21–34. doi:10.1016/J.GEXPLO.2006.07.006.

Amlund, H., Lundebye, A.K., and Berntssen, M.H.G. 2007. Accumulation and elimination of methylmercury in Atlantic cod (*Gadus morhua* L.) following dietary exposure. Aquat. Toxicol. 83: 323–330. doi:10.1016/j.aquatox.2007.05.008.

Amos, H.M., Jacob, D.J., Holmes, C.D., Fisher, J.A., Wang, Q., Yantosca, R.M., Corbitt, E.S., Galarneau, E., Rutter, A.P., Gustin, M.S., Steffen, A., Schauer, J.J., Graydon, J.A., St Louis, V.L., Talbot, R.W., Edgerton, E.S., Zhang, Y., and Sunderland, E.M. 2012. Gas-particle partitioning of atmospheric Hg(II) and its effect on global mercury deposition. Atmos. Chem. Phys. 12: 591–603. doi:10.5194/acp-12-591-2012.

Arcagni, M., Juncos, R., Rizzo, A., Pavlin, M., Fajon, V., Arribére, M.A., Horvat, M., and Ribeiro Guevara, S. 2018. Species- and habitat-specific bioaccumulation of total mercury and methylmercury in the food web of a deep oligotrophic lake. Sci. Total Environ. 612: 1311–1319. doi:10.1016/j.scitotenv.2017.08.260.

Austnes, K., Evans, C.D., Eliot-Laize, C., Naden, P.S., and Old, G.H. 2010. Effects of storm events on mobilisation and in-stream processing of dissolved organic matter (DOM) in a Welsh peatland catchment. Biogeochemistry 99: 157–173. doi:10.1007/s10533-009-9399-4.

Bahram, M., Bro, R., Stedmon, C., and Afkhami, A. 2006. Handling of Rayleigh and Raman scatter for PARAFAC modeling of fluorescence data using interpolation. J. Chemom. 20: 99–105. doi:10.1002/cem.978.

Bates, D., Maechler, M., Bolker, B., Walker, S., Christensen, R.H.B., Singmann, H., Dai, B., Scheipl, F., Grothendieck, G., and Green, P. 2018. Linear Mixed-Effects Models using "Eigen" and S4. Comprehensive R Archive Network (CRAN). Available at: https://cran.r-project.org/web/packages/lme4/lme4.pdf.

Baulch, H.M., Schindler, D.W., Turner, M.A., Findlay, D.L., Paterson, M.J., and Vinebrooke, R.D. 2005. Effects of warming on benthic communities in a boreal lake: Implications of climate change. Limnol. Oceanogr. 50: 1377–1392. doi:10.4319/lo.2005.50.5.1377.

Becker, D.S., and Bigham, G.N. 1995. Distribution of mercury in the aquatic food web of Onondaga Lake, New York. Water Air Soil Pollut. 80: 563–571. doi:10.1007/bf01189706.

Benoit, J.M.J., Gilmour, C.C.C., Heyes, A., Mason, R., and Miller, C. 2003. Geochemical and biological controls over methylmercury production and degradation in aquatic ecosystems. ACS Symp. 835: 1–33. doi:10.1021/bk-2003-0835.ch019.

Bishop, K., Allan, C., Bringmark, L., Garcia, E., Hellsten, S., Högbom, L., Johansson, K., Lomander, A., Meili, M., Munthe, J., Nilsson, M., Porvari, P., Skyllberg, U., Sørensen, R., Zetterberg, T., and Åkerblom, S. 2009. The effects of forestry on Hg bioaccumulation in nemoral/boreal waters and recommendations for good silvicultural practice. Ambio 38: 373–380. doi:10.1579/0044-7447-38.7.373.

Bjerregaard, P., Fjordside, S., Hansen, M.G., and Petrova, M.B. 2011. Dietary selenium reduces retention of methyl mercury in freshwater fish. Environ. Sci. Technol. 45: 9793–9798. doi:10.1021/es202565g.

Blackwell, B.D., and Driscoll, C.T. 2015. Using foliar and forest floor mercury concentrations to assess spatial patterns of mercury deposition. Environ. Pollut. 202: 126–134. doi:10.1016/J.ENVPOL.2015.02.036.

Bloom, N.S. 1992. On the chemical form of mercury in edible fish and marine invertebrate tissue. Can. J. Fish. Aquat. Sci. 49: 1010–1017. doi:10.1139/f92-113.

Bloom, N.S., and Fitzgerald, W. 1988. Determination of volatile mercury species at the picogram level by low-temperature gas chromatography with cold-vapour atomic fluorescence detection. Anal. Chim. Acta 208: 151–161.

Bogdanski, B.E.C. 2008. Canada's boreal forest economy: economic and socioeconomic issues and research opportunities. Natural Resources Canada. Victoria, British Columbia. Available at: http://cfs.nrcan.gc.ca/pubwarehouse/pdfs/28200.pdf.

Bonan, G.B., Pollard, D., and Thompson, S.L. 1992. Effects of boreal forest vegetation on global climate. Nature 359: 716–718. doi:10.1038/359716a0.

Braaten, H.F. V., de Wit, H.A., Larssen, T., and Poste, A.E. 2018. Mercury in fish from Norwegian lakes: The complex influence of aqueous organic carbon. Sci. Total Environ. 627: 341–348. doi:10.1016/j.scitotenv.2018.01.252.

Braaten, H.F. V, de Wit, H.A., Fjeld, E., Rognerud, S., Lydersen, E., and Larssen, T. 2014. Environmental factors influencing mercury speciation in Subarctic and Boreal lakes. Sci. Total Environ. 476: 336–345. doi:10.1016/j.scitotenv.2014.01.030.

Braaten, H.F.V., Åkerblom, S., de Wit, H.A., Skotte, G., Rask, M., Vuorenmaa, J., Kahilainen, K.K., Malinen, T., Rognerud, S., Lydersen, E., Amundsen, P.-A., Kashulin, N., Kashulina, T., Terentyev, P., Christensen, G., Jackson-Blake, L., Lund, E., and Rosseland, B.O. 2017. Spatial and temporal trends of mercury in freshwater fish in Fennoscandia (1965-2015), ICP Waters.

Braaten, H.F.V., de Wit, H.A., Harman, C., Hageström, U., Larssen, T.T., Hagestrom, U., and Larssen, T.T. 2013. Effects of sample preservation and storage on mercury

speciation in natural stream water. Int. J. Environ. Anal. Chem. 94: 381–384. doi:10.1080/03067319.2013.823489.

Bradley, M.A., Barst, B.D., and Basu, N. 2017. A review of mercury bioavailability in humans and fish. Int. J. Environ. Res. Public Health 14. doi:10.3390/ijerph14020169.

Brandt, J.P. 2009. The extent of the North American boreal zone. Environ. Rev. 17: 101–161. doi:10.1139/A09-004.

Brandt, J.P., Flannigan, M.D., Maynard, D.G., Thompson, I.D., and Volney, W.J.A. 2013. An introduction to Canada's boreal zone: ecosystem processes, health, sustainability, and environmental issues. Environ. Rev. 21: 207–226. doi:10.1139/er-2013-0040.

Branfireun, B.A., and Roulet, N.T. 2002. Controls on the fate and transport of methylmercury in a boreal headwater catchment, northwestern Ontario, Canada. Hydrol. Earth Syst. Sci. 6: 783–794.

Bravo, A.G., Bouchet, S., Tolu, J., Björn, E., Mateos-Rivera, A., and Bertilsson, S. 2017. Molecular composition of organic matter controls methylmercury formation in boreal lakes. Nat. Commun. 8: 14255. doi:10.1038/ncomms14255.

Browne, D.R. 2007. Freshwater fish in Ontario's Boreal: Status, conservation and potential impacts of development. Wildlife Conservation Society.

Burnham, K.P., and Anderson, D.R. 2002. Model Selection and Multimodel Inference: A Practical Information-Theoretic Approach (2nd ed). Ecological Modelling. Springer-Verlag New York, New York. doi:10.1016/j.ecolmodel.2003.11.004.

Burnham, K.P., Anderson, D.R., and Huyvaert, K.P. 2011. AIC model selection and multimodel inference in behavioral ecology: Some background, observations, and comparisons. Behav. Ecol. Sociobiol. 65: 23–35. doi:10.1007/s00265-010-1029-6.

Burns, D.A., Riva-Murray, K., Bradley, P.M., Aiken, G.R., and Brigham, M.E. 2012. Landscape controls on total and methyl Hg in the upper Hudson River basin, New York, USA. J. Geophys. Res. 117. doi:10.1029/2011JG001812.

Bushey, J.T., Driscoll, C.T., Mitchell, M.J., Selvendiran, P., and Montesdeoca, M.R. 2008. Mercury transport in response to storm events from a northern forest landscape. Hydrol. Process. 22: 4813–4826. doi:10.1002/hyp.7091.

Chen, C.Y., Borsuk, M.E., Bugge, D.M., Hollweg, T., Balcom, P.H., Ward, D.M., Williams, J., and Mason, R.P. 2014. Benthic and pelagic pathways of methylmercury bioaccumulation in estuarine food webs of the Northeast United States. PLoS One 9: 1–11. doi:10.1371/journal.pone.0089305.

Chételat, J., Amyot, M., Arp, P., Blais, J.M., Depew, D., Emmerton, C.A., Evans, M., Gamberg, M., Gantner, N., Girard, C., Graydon, J., Kirk, J., Lean, D., Lehnherr, I., Muir, D., Nasr, M., Poulain, A.J., Power, M., Roach, P., Stern, G., Swanson, H., and van der Velden, S. 2015. Mercury in freshwater ecosystems of the Canadian Arctic: Recent advances on its cycling and fate. Sci. Total Environ. 509–510: 41–66. doi:10.1016/j.scitotenv.2014.05.151.

Chételat, J., Richardson, M.C., MacMillan, G.A., Amyot, M., and Poulain, A.J. 2018. Ratio of methylmercury to dissolved organic carbon in water explains methylmercury bioaccumulation across a latitudinal gradient from north-temperate to Arctic lakes. Environ. Sci. Technol. 52: 79–88. American Chemical Society. doi:10.1021/acs.est.7b04180.

Cizdziel, J., Hinners, T., Cross, C., and Pollard, J. 2003. Distribution of mercury in the tissues of five species of freshwater fish from Lake Mead, USA. J. Environ. Monit. 5: 802. doi:10.1039/b307641p.

Clark, J.M., Bottrell, S.H., Evans, C.D., Monteith, D.T., Bartlett, R., Rose, R., Newton, R.J., and Chapman, P.J. 2010. The importance of the relationship between scale and process in understanding long-term DOC dynamics. Sci. Total Environ. 408: 2768–2775. doi:10.1016/J.SCITOTENV.2010.02.046.

Clarkson, T.W. 1997. The toxicology of mercury. Crit. Rev. Clin. Lab. Sci. 34: 369–403. doi:10.3109/10408369708998098.

Clarkson, T.W., and Magos, L. 2006. The toxicology of mercury and its chemical compounds. Crit. Rev. Toxicol. 36: 609–662. doi:10.1080/10408440600845619.

Clayden, M.G., Lescord, G.L., Kidd, K.A., Wang, X., Muir, D.C.G., and O'Driscoll, N.J. 2017. Using sulfur stable isotopes to assess mercury bioaccumulation and biomagnification in temperate lake food webs. Environ. Toxicol. Chem. 36: 661–670. doi:10.1002/etc.3615.

Compeau, G.C., and Bartha, R. 1985. Sulfate-reducing bacteria: principal methylators of mercury in anoxic estuarine sediment. Appl. Environ. Microbiol. 50: 498–502. doi:0099-2240/85/080498-05$02.00/0.

Cory, R.M., and McKnight, D.M. 2005. Fluorescence spectroscopy reveals ubiquitous presence of oxidized and reduced quinones in dissolved organic matter fluorescence spectroscopy reveals ubiquitous presence of oxidized and reduced quinones in dissolved organic matter. Environ. Sci. Technol. 39: 8142–8149. doi:10.1021/es0506962.

Curtis, P.J., and Schindler, D.W. 1997. The role of DOC in protecting freshwaters subjected to climatic warming and acidification from UV exposure. Biogeochemistry 36: 1–8. doi:10.1023/A:1005768527751.

Dang, F., and Wang, W.X. 2012. Why mercury concentration increases with fish size? Biokinetic explanation. Environ. Pollut. 163: 192–198. doi:10.1016/j.envpol.2011.12.026.

Daviglus, M.L., Stamler, J., Orencia, A.J., Dyer, A.R., Liu, K., Greenland, P., Walsh, M.K., Morris, D., and Shekelle, R.B. 1997. Fish consumption and the 30-year risk of fatal myocardial infarction. N. Engl. J. Med. 336: 1046–1053. doi:10.1056/NEJM199704103361502.

DeJong, R.A. 2017. Life history characteristics of Lake Whitefish (*Coregonus clupeaformis*), Cisco (Coregonus artedi), and Northern Pike (*Esox lucius*) in rivers of the Hudson Bay Lowlands. MSc thesis, University of Waterloo. Available at:

https://uwspace.uwaterloo.ca/bitstream/handle/10012/11891/DeJong_Rachel.pdf?sequence=5.

Demers, J.D., Driscoll, C.T., Fahey, T.J., and Yavitt, J.B. 2007. Mercury cycling in litter and soil in different forest types in the Adirondack region, New York, USA. Ecol. Appl. 17: 1341–1351. doi:10.1890/06-1697.1.

Depew, D.C., Burgess, N.M., Anderson, M.R., Baker, R., Bhavsar, S.P., Bodaly, R.A., Eckley, C.S., Evans, M.S., Gantner, N., Graydon, J.A., Jacobs, K., LeBlanc, J.E., St. Louis, V.L., Campbell, L.M., and Kidd, K. 2013. An overview of mercury concentrations in freshwater fish species: a national fish mercury dataset for Canada. Can. J. Fish. Aquat. Sci. 70: 436–451. doi:10.1139/cjfas-2012-0338.

Despault, T.M. 2016. Dissolved organic matter in subarctic streams and rivers : Direct and proxy measures of quantity, quality, and mercury. MSc thesis, University of Western Ontario. Available at: http://ir.lib.uwo.ca/cgi/viewcontent.cgi?article=5141&context=etd.

Diéguez, M.C., Queimaliños, C.P., Guevara, S.R., Marvin-DiPasquale, M., Cárdenas, C.S., and Arribére, M.A. 2013. Influence of dissolved organic matter character on mercury incorporation by planktonic organisms: an experimental study using oligotrophic water from Patagonian lakes. J. Environ. Sci. 25: 1980–91. doi: 10.1016/S1001-0742(12)60281-2

Dijkstra, J.A., Buckman, K.L., Ward, D., Evans, D.W., Dionne, M., and Chen, C.Y. 2013. Experimental and natural warming elevates mercury concentrations in estuarine fish. PLoS One. doi:10.1371/journal.pone.0058401.

Domingo, J.L., Bocio, A., Falcó, G., and Llobet, J.M. 2007. Benefits and risks of fish consumption Part I. A quantitative analysis of the intake of omega-3 fatty acids and chemical contaminants. Toxicology 230: 219–226. doi:10.1016/j.tox.2006.11.054.

Dormann, C.F., Elith, J., Bacher, S., Buchmann, C., Carl, G., Carré, G., Marquéz, J.R.G., Gruber, B., Lafourcade, B., Leitão, P.J., Münkemüller, T., McClean, C., Osborne, P.E., Reineking, B., Schröder, B., Skidmore, A.K., Zurell, D., and Lautenbach, S. 2013. Collinearity: A review of methods to deal with it and a simulation study evaluating their performance. Ecography. 36: 027–046. doi:10.1111/j.1600-0587.2012.07348.x.

Dutton, J., and Fisher, N.S. 2014. Modeling metal bioaccumulation and tissue distribution in killifish (*Fundulus heteroclitus*) in three contaminated estuaries. Environ. Toxicol. Chem. 33: 89–101. doi:10.1002/etc.2392.

Eagles-Smith, C.A., Herring, G., Johnson, B., and Graw, R. 2016. Conifer density within lake catchments predicts fish mercury concentrations in remote subalpine lakes. Environ. Pollut. 212: 279–289. doi:10.1016/j.envpol.2016.01.049.

Eckley, C.S., and Hintelmann, H. 2006. Determination of mercury methylation potentials in the water column of lakes across Canada. Sci. Total Environ. 368: 111–125. doi:10.1016/j.scitotenv.2005.09.042.

Edlund, M.B., Almendinger, J.E., Fang, X., Hobbs, J.M.R., VanderMeulen, D.D., Key, R.L., and Engstrom, D.R. 2017. Effects of climate change on lake thermal structure

and biotic response in northern wilderness lakes. Water. 9: 678. doi:10.3390/w9090678.

Eklöf, K., Fölster, J., Sonesten, L., Bishop, K., Eklof, K., Folster, J., Sonesten, L., and Bishop, K. 2012. Spatial and temporal variation of THg concentrations in run-off water from 19 boreal catchments, 2000-2010. Environ. Pollut. 164: 102–109. doi:10.1016/j.envpol.2012.01.024.

Eklöf, K., Lidskog, R., and Bishop, K. 2016. Managing Swedish forestry's impact on mercury in fish: Defining the impact and mitigation measures. Ambio 45: 163–174. doi:10.1007/s13280-015-0752-7.

Eklöf, K., Meili, M., Åkerblom, S., von Brömssen, C., Bishop, K., Eklof, K., Meili, M., Akerblom, S., von Bromssen, C., Bishop, K., Eklöf, K., Meili, M., Åkerblom, S., von Brömssen, C., and Bishop, K. 2013. Impact of stump harvest on run-off concentrations of total mercury and methylmercury. For. Ecol. Manage. 290: 83–94. doi:10.1016/j.foreco.2012.05.039.

Eklöf, K., Schelker, J., Sørensen, R., Meili, M., Laudon, H., Von Brömssen, C., Bishop, K., Eklof, K., Schelker, J., Sorensen, R., Meili, M., Laudon, H., von Bromssen, C., and Bishop, K. 2014. Impact of forestry on total and methyl-mercury in surface waters: Distinguishing effects of logging and site preparation. Environ. Sci. Technol. 48: 4690–4698. doi:10.1021/es404879p.

Eldøy, S.H., Davidsen, J.G., Thorstad, E.B., Whoriskey, F., Aarestrup, K., Næsje, T.F., Rønning, L., Sjursen, A.D., Rikardsen, A.H., and Arnekleiv, J.V. 2015. Marine migration and habitat use of anadromous brown trout (*Salmo trutta*). Can. J. Fish. Aquat. Sci. 72: 1366–1378. doi:10.1139/cjfas-2014-0560.

Ellis, L.E., and Jones, N.E. 2013. Longitudinal trends in regulated rivers: a review and synthesis within the context of the serial discontinuity concept. Environ. Rev. 21: 136–148. doi:10.1139/er-2012-0064.

Elser, J.J., Andersen, T., Baron, J.S., Bergstrom, A.-K., Jansson, M., Kyle, M., Nydick, K.R., Steger, L., and Hessen, D.O. 2009. Shifts in lake N:P stoichiometry and nutrient limitation driven by atmospheric nitrogen deposition. Science. 326: 835–837. doi:10.1126/science.1176199.

Emmerton, C.A., Cooke, C.A., Wentworth, G.R., Graydon, J.A., Ryjkov, A., and Dastoor, A. 2018. Total mercury and methylmercury in lake water of Canada's oil sands region. Environ. Sci. Technol. 52: 10946–10955. doi:10.1021/acs.est.8b01680.

Enrico, M., Roux, G. Le, Marusczak, N., Heimbürger, L.-E., Claustres, A., Fu, X., Sun, R., and Sonke, J.E. 2016. Atmospheric mercury transfer to peat bogs dominated by gaseous elemental mercury dry deposition. Environ. Sci. Technol. 50: 2405–2412. doi:10.1021/acs.est.5b06058.

Fagan, K.A., Koops, M.A., Arts, M.T., and Power, M. 2011. Assessing the utility of C:N ratios for predicting lipid content in fishes. Can. J. Fish. Aquat. Sci. 68: 374–385. doi:10.1139/F10-119.

Fang, T., Aronson, K.J., and Campbell, L.M. 2012. Freshwater fish-consumption relations with total hair mercury and selenium among women in Eastern China. Arch. Environ. Contam. Toxicol. 62: 323–332. doi:10.1007/s00244-011-9689-4.

Le Faucheur, S., Campbell, P.G.C., Fortin, C., and Slaveykova, V.I. 2014. Interactions between mercury and phytoplankton: Speciation, bioavailability, and internal handling. Environ. Toxicol. Chem. 33: 1211–1224. doi:10.1002/etc.2424.

Findlay, D.L., Kasian, S.E.., Stainton, M.P., Beaty, K., and Lyng, M. 2001. Climatic influences on algal populations of boreal forest lakes in the Experimental Lakes Area. Limnol. Oceanogr. 46: 1784–1793. doi: 10.4319/lo.2001.46.7.1784.

Fox, J., Weisberg, S., Adler, D., Bates, D., Baud-Bovy, G., Ellison, S., Firth, D., Friendly, M., Gorjanc, G., Graves, S., Heiberger, R., Laboissiere, R., Monette, G., Murdoch, D., Nilsson, H., Ogle, D., Ripley, B., Venables, W., Winsemius, D., Zeileis, A., and R-Core 2017. Package 'car', Companion to Applied Regression, v.2.1-5. Comprehensive R Archive Network (CRAN). Available at: https://cran.r-project.org/web/packages/car/car.pdf

France, R., Culbert, H., and Peters, R. 1996. Decreased carbon and nutrient input to boreal lakes from particulate organic matter following riparian clear-cutting. Environ. Manage. 20: 579–583. doi:10.1007/BF01474657.

French, T.D., Houben, A.J., Desforges, J.W., Kimpe, L.E., Kokelj, S. V, Poulain, A.J., Smol, J.P., Wang, X., and Blais, J.M. 2014. Dissolved organic carbon thresholds affect mercury bioaccumulation in Arctic lakes. Environ. Sci. Technol. 48: 3162–3168. doi: 10.1021/es403849d.

Fry, B. 2006. Stable Isotope Ecology. Springer-Verlag, New York, New York. doi:10.1007/0-387-33745-8.

Gabriel, M.C., Howard, N., and Osborne, T.Z. 2014. Fish mercury and surface water sulfate relationships in the Everglades Protection Area. Environ. Manage. 53: 583–593. doi:10.1007/s00267-013-0224-4.

Gandhi, N., Tang, R.W.K., Bhavsar, S.P., and Arhonditsis, G.B. 2014. Fish mercury levels appear to be increasing lately: A report from 40 years of monitoring in the province of Ontario, Canada. Environ. Sci. Technol. 48: 5404–5414. doi:10.1021/es403651x.

Gantner, N., Muir, D.C., Power, M., Iqaluk, D., Reist, J.D., Babaluk, J.A., Meili, M., Borg, H., Hammar, J., Michaud, W., Dempson, B., and Solomon, K.R. 2010. Mercury concentrations in landlocked arctic char (*Salvelinus alpinus*) from the Canadian arctic. Part II: Influence of lake biotic and abiotic characteristics on geographic trends in 27 populations. Environ. Toxicol. Chem. 29: 633–643. doi:10.1002/etc.96.

Gates, A., Hanning, R.M., Gates, M., and Tsuji, L.J.S. 2016. The food and nutrient intakes of First Nations youth living in northern Ontario, Canada: Evaluation of a harvest sharing program. J. Hunger Environ. Nutr. 11: 491-508. doi:10.1080/19320248.2016.1157552.

Gergel, S.E., Turner, M.G., and Kratz, T.K. 2010. Dissolved organic carbon as an indicator of the scale of watershed influence on lakes and rivers. Ecol. Appl. 9: 1377–1390. doi: 10.1890/1051-0761(1999)009[1377:DOCAAI]2.0.CO;2.

Gilmour, C.C., Podar, M., Bullock, A.L., Graham, A.M., Brown, S.D., Somenahally, A.C., Johs, A., Hurt, R.A., Bailey, K.L., and Elias, D.A. 2013. Mercury methylation by novel microorganisms from new environments. Environ. Sci. Technol. 47: 11810–11820. doi:10.1021/es403075t.

Girault, L., Lemaire, P., Boudou, A., and Dufourc, E.J. 1995. Inorganic mercury interactions with lipid components of biological membranes: 31P-NMR study of Hg(II) binding to headgroups of micellar phospholipids. Pages 95–98 *in* Mercury as a Global Pollutant. Springer Netherlands, Dordrecht. doi:10.1007/978-94-011-0153-0_11.

Glooschenko, W.A., Roulet, N.T., Barrie, L.A., Schiff, H.I., and McAdie, H.G. 1994. The Northern Wetlands Study (NOWES): An overview. J. Geophys. Res. 99: 1423. doi:10.1029/93JD02184.

Gorham, E. 1991. Northern peatlands: Role in the carbon cycle and probable responses to climatic warming. Ecol. Appl. 1: 182–195. doi:10.2307/1941811.

Graham, A.M., Aiken, G.R., and Gilmour, C.C. 2013. Effect of dissolved organic matter source and character on microbial Hg methylation in Hg − S − DOM solutions. Environ. Sci. Technol. 47: 5746–5754. doi: 10.1021/es400414a.

Graydon, J.A., St Louis, V.L., Hintelmann, H., Lindberg, S.E., Sandilands, K.A., Rudd, J.W.M., Kelly, C.A., Tate, M.T., Krabbenhoft, D.P., and Lehnherr, I. 2009. Investigation of uptake and retention of atmospheric Hg(II) by boreal forest plants using stable Hg isotopes. Environ. Sci. Technol. 43: 4960–4966. doi:10.1021/es900357s.

Grueber, C.E., Nakagawa, S., Laws, R.J., and Jamieson, I.G. 2011. Multimodel inference in ecology and evolution: Challenges and solutions. J. Evol. Biol. 24: 699–711. doi:10.1111/j.1420-9101.2010.02210.x.

Gugger, P.F. 2012. Redundancy analysis tutorial: Landscape genetics. Available at: https://popgen.nescent.org/2018-03-27_RDA_GEA.html.

Haitzer, M., Aiden, G., and Ryan, J.N. 2003. Binding of mercury (II) to aquatic humic substances : Influence of pH and source of humic substances. Environ. Sci. Technol. 37: 2436–2441.

Haitzer, M., Aiken, G.R., and Ryan, J.N. 2002. Binding of mercury(II) to dissolved organic matter: The role of the mercury-to-DOM concentration ratio. Environ. Sci. Technol. 36: 3564–3570. doi:10.1021/es025699i.

Hall, B.D., Bodaly, R.A., Fudge, R.J.P., Rudd, J.W.M., and Rosenberg, D.M. 1997. Food as the dominant pathway of methylmercury uptake by fish. Water Air Soil Pollut. 100: 13–24. doi:10.1023/A:1018071406537.

Hall, B.D., Cherewyk, K.A., Paterson, M.J., and Bodaly, R.A. 2009. Changes in methyl mercury concentrations in zooplankton from four experimental reservoirs with

differing amounts of carbon in the flooded catchments. Can. J. Fish. Aquat. Sci. 66: 1910–1919. doi:10.1139/F09-123.

Hamelin, S., Amyot, M., Barkay, T., Wang, Y., and Planas, D. 2011. Methanogens: Principal methylators of mercury in lake periphyton. Environ. Sci. Technol. 45: 7693–7700. doi:10.1021/es2010072.

Hammerschmidt, C.R., Fitzgerald, W.F., Balcom, P.H., and Visscher, P.T. 2008. Organic matter and sulfide inhibit methylmercury production in sediments of New York / New Jersey Harbor. Mar. Chem. 109: 165–182. doi:10.1016/J.MARCHEM.2008.01.007.

Hanson, P.C., Hamilton, D.P., Stanley, E.H., Preston, N., Langman, O.C., and Kara, E.L. 2011. Fate of allochthonous dissolved organic carbon in lakes: A quantitative approach. PLoS One 6: e21884. doi:10.1371/journal.pone.0021884.

Hare, F.K., and Ritchie, J.C. 1972. The boreal bioclimates. Geogr. Rev. 62: 333. doi:10.2307/213287.

Harris, H.H., Pickering, I.J., George, G.N., Harris, H.H., Pickering, I.J., and Georget, G.N. 2003. The chemical form of mercury in fish. Science. 301: 28–29. doi: 10.1126/science.1085941.

Harris, R.C., Rudd, J.W.M., Amyot, M., Babiarz, C.L., Beaty, K.G., Blanchfield, P.J., Bodaly, R.A., Branfireun, B.A., Gilmour, C.C., Graydon, J.A., Heyes, A., Hintelmann, H., Hurley, J.P., Kelly, C.A., Krabbenhoft, D.P., Lindberg, S.E., Mason, R.P., Paterson, M.J., Podemski, C.L., Robinson, A., Sandilands, K.A., Southworth, G.R., St Louis, V.L., and Tate, M.T. 2007. Whole-ecosystem study shows rapid fish-mercury response to changes in mercury deposition. Proc. Natl. Acad. Sci. USA. 104: 16586–91. doi:10.1073/pnas.0704186104.

Hassanin, M., Kerek, E., Chiu, M., Anikovskiy, M., and Prenner, E.J. 2016. Binding affinity of inorganic mercury and cadmium to biomimetic erythrocyte membranes. J. Phys. Chem. B 120: 12872–12882. doi:10.1021/acs.jpcb.6b10366.

Hastie, T., and Efron, B. 2013. lars: Least Angle Regression, Lasso and Forward Stagewise. Comprehensive R Archive Network (CRAN). Available at: https://cran.r-project.org/web/packages/lars/index.html [2017 Sep. 3].

Hastie, T., Tibshirani, R., and Friedman, J. 2009. The elements of statistical learning. Bayesian Forecast. Dyn. Model. 1: 1–694. doi:10.1007/b94608.

Havelková, M., Dušek, L., Némethová, D., Poleszczuk, G., and Svobodová, Z. 2008. Comparison of mercury distribution between liver and muscle - A biomonitoring of fish from lightly and heavily contaminated localities. Sensors 8: 4095–4109. doi:10.3390/s8074095.

Haynes, K.M., Kane, E.S., Potvin, L., Lilleskov, E.A., Kolka, R.K., and Mitchell, C.P.J. 2016. Mobility and transport of mercury and methylmercury in peat as a function of changes in water table regime and plant functional groups. Global Biogeochem. Cycles 31: 233–244. doi:10.1002/2016GB005471.

Health Canada 2014. Canadian Guidelines for Chemical Contaminants and Toxins in Fish and Fish Products. Standards and Methods Manual. Available at: http://www.inspection.gc.ca/food/fish-and-seafood/manuals/standards-and-methods/eng/1348608971859/1348609209602?chap=7#s20c7.

Hebiri, M., and Lederer, J. 2013. How correlations influence lasso prediction. IEEE Trans. Inf. Theory 59: 1846–1854. doi:10.1109/TIT.2012.2227680.

Heerschap, M.J. 2018. Ecology and food quality of fishes in coastal rivers of the Far North of Ontario. MSc thesis, Laurentian University. Available at: https://zone.biblio.laurentian.ca/bitstream/10219/2893/3/Heerschap-Thesis-Final-Draft-09Feb2018.pdf.

Helms, J.R., Stubbins, A., Ritchie, J.D., Minor, E.C., Kieber, D.J., and Mopper, K. 2008. Absorption spectral slopes and slope ratios as indicators of molecular weight, source, and photobleaching of chromophoric dissolved organic matter. Limnol. Oceanogr. 53: 955–969. doi:10.4319/lo.2008.53.3.0955.

Herrero Ortega, S., Catalán, N., Björn, E., Gröntoft, H., Hilmarsson, T.G., Bertilsson, S., Wu, P., Bishop, K., Levanoni, O., and Bravo, A.G. 2017. High methylmercury formation in ponds fueled by fresh humic and algal derived organic matter. Limnol. Oceanogr. doi:10.1002/lno.10722.

Herzsprung, P., Osterloh, K., von Tumpling, W., Harir, M., Hertkorn, N., Schmitt-Kopplin, P., Meissner, R., Bernsdorf, S., and Friese, K. 2017. Differences in DOM of rewetted and natural peatlands - Results from high-field FT-ICR-MS and bulk optical parameters. Sci. Total Environ. 15: 770–781. doi:10.1016/j.scitotenv.2017.02.054.

Hsu-Kim, H., Kucharzyk, K.H., Zhang, T., and Deshusses, M.A. 2013. Mechanisms regulating mercury bioavailability for methylating microorganisms in the aquatic environment: A critical review. Environ. Sci. Technol. 47: 2441–2456. doi:10.1021/es304370g.

Hudson, N., Baker, A., and Reynolds, D. 2007. Fluorescence analysis of dissolved organic matter in natural, waste and polluted waters—a review. River Res. Appl. 23: 631–649. doi:10.1002/rra.1005.

Huser, B.J., Futter, M.N., Wang, R., and Fölster, J. 2018. Persistent and widespread long-term phosphorus declines in Boreal lakes in Sweden. Sci. Total Environ. 613–614: 240–249. doi:10.1016/J.SCITOTENV.2017.09.067.

Hylander, L.D., Meili, M., Oliveira, L.J., dé Castro Silva, E., Guimaraes, J.R., Araujo, D.M., Stachiw, R., Barros, A.J., Silva, G.D., Brazií, B., and Hylander, L. 2000. Relationship of mercury with aluminum, iron and manganese oxy-hydroxides in sediments from the Alto Pantanal, Brazil. Sci Total Environ. 9: 97-107. doi:10.1016/S0048-9697(00)00544-1

Jaffé, R., McKnight, D., Maie, N., Cory, R., McDowell, W.H., and Campbell, J.L. 2008. Spatial and temporal variations in DOM composition in ecosystems: The importance of long-term monitoring of optical properties. J. Geophys. Res. Biogeosciences 113: 1–15. doi:10.1029/2008JG000683.

Jaglal, S.B., Haroun, V.A., Salbach, N.M., Hawker, G., Voth, J., Lou, W., Kontos, P., Cameron, J.E., Cockerill, R., and Bereket, T. 2013. Increasing access to chronic disease self-management programs in rural and remote communities using telehealth. Telemed. E-Health. 19: 467–473. doi:10.1089/tmj.2012.0197.

James, G., Witten, D., Hastie, T., and Tibshirani, R. 2013. An Introduction to Statistical Learning. Edited By: G. Casella, S. Fienberg, and I. Olkin. Springer, New York. doi:10.1007/978-1-4614-7138-7. Available at: https://www-bcf.usc.edu/~gareth/ISL/ISLR%20First%20Printing.pdf.

Jardine, T.D., McGeachy, S.A., Paton, C.M., Savoie, M., and Cunjak, R.A. 2003. Stable isotopes in aquatic systems: Sample preparation, analysis, and interpretation. Can. Manuscr. Rep. Fish. Aquat. Sci. 2656: 39 p.

Jeremiason, J.D., Engstrom, D.R., Swain, E.B., Nater, E.A., Johnson, B.M., Almendinger, J.E., Monson, B.A., and Kolka, R.K. 2006. Sulfate addition increases methylmercury production in an experimental wetland. Environ. Sci. Technol. 40: 3800–3806. doi:10.1021/es0524144.

Jeremiason, J.D., Reiser, T.K., Weitz, R.A., Berndt, M.E., and Aiken, G.R. 2016. Aeshnid dragonfly larvae as bioindicators of methylmercury contamination in aquatic systems impacted by elevated sulfate loading. Ecotoxicology 25: 456–468. doi:10.1007/s10646-015-1603-9.

Johnson, C.E., Driscoll, C.T., Siccama, T.G., and Likens, G.E. 2000. Element fluxes and landscape position in a northern hardwood forest watershed ecosystem. Ecosystems 3: 159–184. doi:10.1007/s100210000017.

Johnson, N.W., Mitchell, C.P.J., Engstrom, D.R., Bailey, L.T., Coleman Wasik, J.K., and Berndt, M.E. 2016. Methylmercury production in a chronically sulfate-impacted sub-boreal wetland. Environ. Sci. Process. Impacts 18: 725–734. doi:10.1039/C6EM00138F.

Johnsson, C., Schütz, A., and Sällsten, G. 2005. Impact of consumption of freshwater fish on mercury levels in hair, blood, urine, and alveolar air. J. Toxicol. Environ. Health Part A. 68: 129–140. doi:10.1080/15287390590885992.

Jones, J., Cunsolo, A., and Harper, S.L. 2018. Who is research serving? A systematic realist review of circumpolar environment-related Indigenous health literature. PLoS one. doi:10.1371/journal.pone.0196090.

Jørgensen, C., Enberg, K., and Mangel, M. 2016. Modelling and interpreting fish bioenergetics: A role for behaviour, life-history traits and survival trade-offs. J. Fish Biol. 88: 389–402. doi:10.1111/jfb.12834.

Kahilainen, K.K., Thomas, S.M., Keva, O., Hayden, B., Knudsen, R., Eloranta, A.P., Tuohiluoto, K., Amundsen, P.A., Malinen, T., and Järvinen, A. 2016. Seasonal dietary shift to zooplankton influences stable isotope ratios and total mercury concentrations in Arctic charr (*Salvelinus alpinus* (L.)). Hydrobiologia 783: 47–63. doi:10.1007/s10750-016-2685-y.

Kainz, M., and Mazumder, A. 2005. Effect of algal and bacterial diet on methyl mercury concentrations in zooplankton. Environ. Sci. Technol. 39: 1666–1672. doi:10.1021/es049119o.

Karimi, R., Chen, C.Y., and Folt, C.L. 2016. Comparing nearshore benthic and pelagic prey as mercury sources to lake fish: The importance of prey quality and mercury content. Sci. Total Environ. 565: 211–221. doi:10.1016/j.scitotenv.2016.04.162.

Karimi, R., Chen, C.Y., Pickhardt, P.C., Fisher, N.S., and Folt, C.L. 2007. Stoichiometric controls of mercury dilution by growth. Proc. Natl. Acad. Sci. USA. 104: 7477–7482. doi:10.1073/pnas.0611261104.

Kaufman, S.D., Johnston, T.A., Leggett, W.C., Moles, M.D., Casselman, J.M., and Schulte-Hostedde, A.I. 2007. Relationships between body condition indices and proximate composition in adult walleyes. Trans. Am. Fish. Soc. 136: 1566–1576. doi:10.1577/T06-262.1.

Keller, W. 2007. Implications of climate warming for Boreal Shield lakes: a review and synthesis. Environ. Rev. 15: 99–112. doi:10.1139/A07-002.

Kelly, C.A. Rudd, J.W.M., and Holoka, M.H. 2003. Effect of pH on mercury uptake by an aquatic bacterium: implications for Hg cycling. Environ. Sci. Technol. 37: 2941–2946. doi:10.1021/es026366o.

Kerek, E., Hassanin, M., Zhang, W., and Prenner, E.J. 2017. Preferential binding of inorganic mercury to specific lipid classes and its competition with cadmium. Biochim. Biophys. Acta - Biomembr. 1859: 1211–1221. doi:10.1016/j.bbamem.2017.03.022.

Kinghorn, A., Solomon, P., and Chan, H. 2007. Temporal and spatial trends of mercury in fish collected in the English–Wabigoon river system in Ontario, Canada. Sci. Total Environ. 372: 615–623. doi:10.1016/j.scitotenv.2006.10.049.

Kipanyula, M.J., Maina, K.W., and Maulilio Kipanyula, C.J. 2016. Morphological and adaptational changes associated with fish migration from fresh to marine water bodies. Int. J. Fish. Aquat. Stud. 4: 125–129.

Kirk, J.L., Muir, D.C.G., Gleason, A., Wang, X., Lawson, G., Frank, R.A., Lehnherr, I., and Wrona, F. 2014. Atmospheric deposition of mercury and methylmercury to landscapes and waterbodies of the Athabasca oil sands region. Environ. Sci. Technol. 48: 7374–7383. doi:10.1021/es500986r.

Klapstein, S.J., and O'Driscoll, N.J. 2018. Methylmercury biogeochemistry in freshwater ecosystems: A review focusing on DOM and photodemethylation. Bull. Environ. Contam. Toxicol. 100: 14–25. doi:10.1007/s00128-017-2236-x.

Klapstein, S.J., Ziegler, S.E., and O'Driscoll, N.J. 2017. Methylmercury photodemethylation is inhibited in lakes with high dissolved organic matter. Environ. Pollut. 232: 392–401. doi:10.1016/J.ENVPOL.2017.09.049.

Kratz, T.K., Webster, K.E., Bowser, C.J., Magnuson, J.J., and Benson, B.J. 1997. The influence of landscape position on lakes in northern Wisconsin. Freshw. Biol. 37: 209–217. doi:10.1046/j.1365-2427.1997.00149.x.

Kraus, A. 2011. Factors controlling the temporal variability of mercury in runoff from seven catchments in northern and southern Sweden. Swedish University of Agricultural Sciences, Uppsala, Sweden. Available at: https://stud.epsilon.slu.se/3180/3/Kraus_a_110826.pdf

Kreutzweiser, D., Beall, F., Webster, K., Thompson, D., and Creed, I. 2013. Impacts and prognosis of natural resource development on aquatic biodiversity in Canada's boreal zone 1. Environ. Rev. 21: 227–259. doi:10.1139/er-2013-0044.

Kucharzyk, K.H., Deshusses, M.A., Porter, K.A., and Hsu-Kim, H. 2015. Relative contributions of mercury bioavailability and microbial growth rate on net methylmercury production by anaerobic mixed cultures. Environ. Sci. Process. Impacts 17: 1568–77. doi:10.1039/c5em00174a.

Landry, J., and Rochefort, L. 2012. The drainage of peatlands: impacts and rewetting techniques. Université Laval, Québec, Canada. Available at: http://www.gret-perg.ulaval.ca/uploads/tx_centrerecherche/Drainage_guide_Web_02.pdf.

Larose, C., Prestat, E., Cecillon, S., Berger, S., Malandain, C., Lyon, D., Ferrari, C., Schneider, D., Dommergue, A., and Vogel, T.M. 2013. Interactions between snow chemistry, mercury inputs and microbial population dynamics in an Arctic snowpack. PLoS One 8: e79972. doi:10.1371/journal.pone.0079972.

Lasorsa, B., and Allen-Gil, S. 1995. The methylmercury to total mercury ratio in selected marine, freshwater, and terrestrial organisms. Water Air Soil Pollut. 80: 905–913. doi:10.1007/BF01189743.

Latif, M.A., Bodaly, R.A., Johnston, T.A., and Fudge, R.J.P. 2001. Effects of environmental and maternally derived methylmercury on the embryonic and larval stages of walleye (*Stizostedion vitreum*). Environ. Pollut. 111: 139–148. doi:10.1016/S0269-7491(99)00330-9.

Lavoie, R.A., Jardine, T.D., Chumchal, M.M., Kidd, K.A. and Campbell, L.M. 2013. Biomagnification of mercury in aquatic food webs: A worldwide meta-analysis. Environ. Sci. Technol. 47: 13385–13394. doi:10.1021/es403103t.

Lehnherr, I. 2014. Methylmercury biogeochemistry: A review with special reference to Arctic aquatic ecosystems. Environ. Rev. 243: 1–70. doi:10.1139/er-2013-0059.

Lehnherr, I., and St. Louis, V.L. 2009. Importance of ultraviolet radiation in the photodemethylation of methylmercury in freshwater ecosystems. Environ. Sci. Technol. 43: 5692–5698. doi:10.1021/es9002923.

Lehnherr, I., St. Louis, V.L., and Kirk, J.L. 2012. Methylmercury cycling in high Arctic wetland ponds: Controls on sedimentary production. Environ. Sci. Technol. 46: 10523–10531. doi:10.1021/es300577e.

Lenth, R., and Love, J. 2017. Package "lsmeans", Least-Squares Means v.2.27-2. Comprehensive R Archive Network (CRAN). Available at: https://cran.r-project.org/web/packages/lsmeans/lsmeans.pdf.

Lescord, G.L., Emilson, E., Johnston, T., Branfireun, B., and Gunn, J. 2018a. The optical properties of dissolved organic matter and their relation to mercury concentrations

in water and biota across a remote freshwater drainage basin. Environ. Sci. Technol. 52: 3344−3353. doi:10.1021/acs.est.7b05348.

Lescord, G.L., Johnston, T.A., Branfireun, B.A., and Gunn, J.M. 2018b. Percent methylmercury in the muscle tissue of freshwater fish varies with body size, age, and among species. Environ. Toxicol. Chem. 37: 2682–2691. doi:10.1002/etc.4233.

Lescord, G.L., Kidd, K.A., Kirk, J.L., O'Driscoll, N.J., Wang, X., and Muir, D.C.G. 2015. Factors affecting biotic mercury concentrations and biomagnification through lake food webs in the Canadian high Arctic. Sci. Total Environ. 509–510: 195–205. doi:10.1016/j.scitotenv.2014.04.133.

Liang, P., Feng, X., You, Q., Gao, X., Xu, J., Wong, M., Christie, P., and Wu, S.-C. 2017. The effects of aquaculture on mercury distribution, changing speciation, and bioaccumulation in a reservoir ecosystem. Environ. Sci. Pollut. Res. 24: 25923–25932. doi:10.1007/s11356-017-0189-6.

Loring, P.A., Duffy, L.K., and Murray, M.S. 2010. A risk-benefit analysis of wild fish consumption for various species in Alaska reveals shortcomings in data and monitoring needs. Sci. Total Environ. 408: 4532–4541. doi:10.1016/j.scitotenv.2010.07.013.

St. Louis, V.L., Rudd, J.W.M., Kelly, C.A., Beaty, K.G., Bloom, N.S., and Flett, R.J. 1994. Importance of wetlands as sources of methyl mercury to boreal forest ecosystems. Can. J. Fish. Aquat. Sci. 51: 1065–1076. doi:10.1139/f94-106.

Luek, J.L., Thompson, K.E., Larsen, R.K., Heyes, A., and Gonsior, M. 2017. Sulfate reduction in sediments produces high levels of chromophoric dissolved organic matter. Sci. Rep. 7: 1–8. doi:10.1038/s41598-017-09223-z.

Luyssaert, S., Schulze, E.-D., Borner, A., Knohl, A., Hessenmoller, D., Law, B.E., Ciais, P., and Grace, J. 2008. Old-growth forests as global carbon sinks. Nature 455: 213–216

MacLeod, J., Keller, W., and Paterson, A.M. 2018. Crustacean zooplankton in lakes of the far north of Ontario, Canada. Polar Biol. 41: 1257–1267. doi:10.1007/s00300-018-2282-9.

MacLeod, J., Keller, W.B., Paterson, A.M., Dyer, R.D., and Gunn, J.M. 2017. Scale and watershed features determine lake chemistry patterns across physiographic regions in the far north of Ontario, Canada. J. Limnol. 76: 211–220. doi:10.4081/jlimnol.2016.1553.

Magee, M.R., and Wu, C.H. 2017. Response of water temperatures and stratification to changing climate in three lakes with different morphometry. Hydrol. Earth Syst. Sci 21: 6253–6274. doi:10.5194/hess-21-6253-2017.

Mahaffey, K.R., Sunderland, E.M., Chan, H.M., Choi, A.L., Grandjean, P., Mariën, K., Oken, E., Sakamoto, M., Schoeny, R., Weihe, P., Yan, C.H., and Yasutake, A. 2011. Balancing the benefits of n-3 polyunsaturated fatty acids and the risks of methylmercury exposure from fish consumption. Nutr. Rev. 69: 493–508. doi:10.1111/j.1753-4887.2011.00415.x.

Mann, E., Ziegler, S., Mallory, M., and O'Driscoll, N. 2014. Mercury photochemistry in snow and implications for Arctic ecosystems. Environ. Rev. 22: 331–345. doi:10.1139/er-2014-0006.

Mann, S. 2017. Methods for preparing calcified structures for age interpretation used in the Fisheries Ageing Lab, Northwest Biodiversity and Monitoring Section. Ontario Ministry of Natural Resources and Forestry.

Marien, K., and Patrick, G.M. 2001. Exposure analysis of five fish-consuming populations for overexposure to methylmercury. J. Expo. Sci. Environ. Epidemiol. 11: 193–206. doi:10.1038/sj.jea.7500160.

Marquina-Márquez, A., Virchez, J., and Ruiz-Callado, R. 2016. Postcolonial healing landscapes and mental health in a remote Indigenous community in subarctic Ontario, Canada. Polar Geogr. 39: 20-39. doi:10.1080/1088937X.2016.1155673.

Martin, S.L., and Soranno, P.A. 2006. Lake landscape position: Relationships to hydrologic connectivity and landscape features. Limnol. Oceanogr. 51: 801–814. doi:10.4319/lo.2006.51.2.0801.

Mason, R.P., Laporte, J.M., and Andres, S. 2000. Factors controlling the bioaccumulation of mercury, methylmercury, arsenic, selenium, and cadmium by freshwater invertebrates and fish. Arch. Environ. Contam. Toxicol. 38: 283–297. doi:10.1007/s002449910038.

Maurer, F., Christl, I., Hoffmann, M., and Kretzschmar, R. 2012. Reduction and reoxidation of humic acid: Influence on speciation of cadmium and silver. Environ. Sci. Technol. 46: 8808–8816. doi:10.1021/es301520s.

Mazerolle, M.J. 2017. Model Selection and Multimodel Inference Based on AIC. Comprehensive R Archive Network (CRAN). Available at: https://cran.r-project.org/web/packages/AICcmodavg/AICcmodavg.pdf.

Megaritis, A.G., Murphy, B.N., Racherla, P.N., Adams, P.J., and Pandis, S.N. 2014. Impact of climate change on mercury concentrations and deposition in the eastern United States. Sci. Total Environ. 487: 299–312. doi:10.1016/j.scitotenv.2014.03.084.

Mieiro, C.L., Pacheco, M., Pereira, M.E., and Duarte, A.C. 2009. Mercury distribution in key tissues of fish (*Liza aurata*) inhabiting a contaminated estuary—implications for human and ecosystem health risk assessment. J. Environ. Monit. 11: 1004–1012. doi:10.1039/b821253h.

Mitchell, C.P.J., Branfireun, B.A., and Kolka, R.K. 2008. Total mercury and methylmercury dynamics in upland-peatland watersheds during snowmelt. Biogeochemistry 90: 225–241. doi:10.1007/s10533-008-9246-z.

MNDM 2018. Ring of Fire; Exploration and Development. Available at: https://www.mndm.gov.on.ca/en/ring-fire-secretariat/exploration-and-development.

Moniruzzaman, M., Lee, J.-H., Lee, J.-H., Won, S., Damusaru, J.H., and Bai, S.C. 2017. Interactive effect of dietary vitamin E and inorganic mercury on growth performance and bioaccumulation of mercury in juvenile olive flounder,

Paralichthys olivaceus treated with mercuric chloride. Anim. Nutr. 3: 276–283. doi:10.1016/j.aninu.2017.07.001.

Moore, C.W., Cosby, B.J., Galloway, J.N., and Castro, M.S. 2009. Relationship between pH and stream water total mercury concentrations in Shenandoah National Park. Water Air Soil Pollut. 201: 233–238. doi:10.1007/s11270-008-9940-4.

Murphy, K.R., Stedmon, C.A., Graeber, D., and Bro, R. 2013. Fluorescence spectroscopy and multi-way techniques. PARAFAC. Anal. Methods 5: 6557. doi:10.1039/c3ay41160e.

Murphy, K.R., Stedmon, C.A., Wenig, P., and Bro, R. 2014. OpenFluor– an online spectral library of auto-fluorescence by organic compounds in the environment. Anal. Methods 6: 658–661. doi:10.1039/C3AY41935E.

Natcher, D., Shirley, S., Rodon, T., and Southcott, C. 2016. Constraints to wildlife harvesting among aboriginal communities in Alaska and Canada. Food Secur. 8: 1153–1167. doi:10.1007/s12571-016-0619-1.

National Research Council (NRC) Canada 2012. DORM-4: Fish protein certified reference material for trace metals. Available at: https://www.nrc-cnrc.gc.ca/eng/solutions/advisory/crm/certificates/dorm_4.html [2018 Mar. 29].

Natural Resources Canada 2017. The Atlas of Canada - Toporama. Available at: http://atlas.gc.ca/toporama/en/index.html.

Nimptsch, J., Woelfl, S., Kronvang, B., Giesecke, R., González, H.E., Caputo, L., Gelbrecht, J., von Tuempling, W., and Graeber, D. 2014. Does filter type and pore size influence spectroscopic analysis of freshwater chromophoric DOM composition? Limnologica 48: 57–64. doi:10.1016/j.limno.2014.06.003.

O'Driscoll, N.J., and Evans, R.D. 2000. Analysis of methyl mercury binding to freshwater humic and fulvic acids by gel permeation chromatography / hydride generation. Environ. Sci. Technol. 34: 4039–4043. doi: 10.1021/es0009626

Ohno, T. 2002. Fluorescence inner-filtering correction for determining the humification index of dissolved organic matter. Environ. Sci. Technol. 36: 742–746. doi:10.1021/es0155276.

Økelsrud, A., Lydersen, E., and Fjeld, E. 2016. Biomagnification of mercury and selenium in two lakes in southern Norway. Sci. Total Environ. 566–567: 596–607. doi:10.1016/j.scitotenv.2016.05.109.

Oksanen, J., Blanchet, F.G., Friendly, M., Kindt, R., Legendre, P., Mcglinn, D., Minchin, P.R., O 'hara, R.B., Simpson, G.L., Solymos, P., Henry, M., Stevens, H., Szoecs, E., Wagner, H., and Oksanen, M.J. 2017. Community Ecology R Package. Comprehensive R Archive Network (CRAN). Available at: https://cran.r-project.org/web/packages/vegan/vegan.pdf.

Olefeldt, D., Persson, A., and Turetsky, M.R. 2014. Influence of the permafrost boundary on dissolved organic matter characteristics in rivers within the Boreal and Taiga plains of western Canada. Environ. Res. Lett. 9: 1–9. doi:10.1088/1748-9326/9/3/035005.

OMNRF. 2017. Watershed flow assessment tool (OFAT). Available at: https://www.ontario.ca/page/watershed-flow-assessment-tool.

OMOECC. 1983. Handbook of Analytical Methods for Environmental Sampling : Ontario Ministry of the Environment : Free Download & Streaming : Internet Archive. Ontario Ministry of the Environment and Climate Change. Toronto, Ontario. doi:PIBS 4748.

Orlova, J., and Branfireun, B.A. 2014. Surface water and groundwater contributions to streamflow in the James Bay surface water and groundwater contributions to streamflow in the James Bay Lowland, Canada. Arctic Antarc. Alp. Res. 46: 236–250. doi: 10.1657/1938-4246-46.1.236

Pachauri, R.K., Meyer, L., Hallegatte France, S., Bank, W., Hegerl, G., Brinkman, S., van Kesteren, L., Leprince-Ringuet, N., and van Boxmeer, F. 2014. Climate Change 2014; Synthesis Report. IPCC. Gian-Kasper Plattner, Geneva Switzerland. Available at: http://www.ipcc.ch.

Pacyna, E.G., Pacyna, J.M., Sundseth, K., Munthe, J., Kindbom, K., Wilson, S., Steenhuisen, F., and Maxson, P. 2010. Global emission of mercury to the atmosphere from anthropogenic sources in 2005 and projections to 2020. Atmos. Environ. 44: 2487–2499. doi:10.1016/j.atmosenv.2009.06.009.

Pacyna, J.M., Travnikov, O., Simone, F. De, Hedgecock, I.M., Sundseth, K., Pacyna, E.G., Steenhuisen, F., Pirrone, N., Munthe, J., and Kindbom, K. 2016. Current and future levels of mercury atmospheric pollution on a global scale. Atmos. Chem. Phys. 16: 12495–12511. doi:10.5194/acp-16-12495-2016.

Palmer-Young, E., Amy, D., Burgin, J., and Groffman, P.M. 2008. How does NO_3^- reduction in lake sediments respond to NO_3- amendment? Available at: https://www.caryinstitute.org/sites/default/files/public/reprints/Palmer_Young_2008_REU.pdf.

Paranjape, A.R., and Hall, B.D. 2017. Recent advances in the study of mercury methylation in aquatic systems. Facets 2: 85–119. doi:10.1139/facets-2016-0027.

Parks, J.M., Johs, A., Podar, M., Bridou, R., Hurt, R.A., Smith, S.D., Tomanicek, S.J., Qian, Y., Brown, S.D., Brandt, C.C., Palumbo, A. V, Smith, J.C., Wall, J.D., Elias, D.A., and Liang, L. 2013. Supplement: The genetic basis for bacterial mercury methylation. Science 1332. doi:10.1126/science.1230667

Parlanti, E., Worz, K., Geoffroy, L., and Lamotte, M. 2000. Dissolved organic matter fuorescence spectroscopy as a tool to estimate biological activity in a coastal zone submitted to anthropogenic inputs. Org. Geochem. 31: 1765–1781. doi:10.1016/S0146-6380(00)00124-8

Peng, X., Liu, F., and Wang, W.X. 2016. Organ-specific accumulation, transportation, and elimination of methylmercury and inorganic mercury in a low Hg accumulating fish. Environ. Toxicol. Chem. 35: 2074–2083. doi:10.1002/etc.3363

Peterson, B.J., and Fry, B. 1987. Stable isotopes in ecosystem studies. Annu. Rev. Ecol. Syst. 18: 293–320. doi:10.1146/annurev.ecolsys.18.1.293

Pickhardt, P.C., Folt, C.L., Chen, C.Y., Klaue, B., and Blum, J.D. 2002. Algal blooms reduce the uptake of toxic methylmercury in freshwater food webs. Proc. Natl. Acad. Sci. USA 99: 4419–4423. doi: 10.1073/pnas.072531099

Pickhardt, P.C., Stepanova, M., and Fisher, N.S. 2006. Contrasting uptake routes and tissue distributions of inorganic and methylmercury in mosquitofish (*Gambusia affinis*) and redear sunfish (*Lepomis microlophus*). Environ. Toxicol. Chem. 25: 2132. doi:10.1897/05-595R.1.

Plourde, Y., Lucotte, M., and Pichet, P. 1997. Contribution of suspended particulate matter and zooplankton to MeHg contamination of the food chain in midnorthern Quebec (Canada). Can. J. Fish. Aquat. Sci. 54: 821–831. doi:10.1139/f96-340.

Pohlert, T. 2016. Calculate Pairwise Multiple Comparisons of Mean Rank Sums. Comprehensive R Archive Network (CRAN). Available at: https://cran.r-project.org/web/packages/PMCMR/PMCMR.pdf.

Pollman, C.D., and Axelrad, D.M. 2014. Mercury bioaccumulation factors and spurious correlations. Sci. Total Environ. 496: vi–xii. doi:10.1016/j.scitotenv.2014.07.050.

Poręba, R., Skoczyńska, A., Gać, P., Turczyn, B., and Wojakowska, A. 2012. Left ventricular diastolic function in workers occupationally exposed to mercury vapour without clinical presentation of cardiac involvement. Toxicol. Appl. Pharmacol. 263: 368–373. doi:10.1016/j.taap.2012.07.012.

Porvari, P., Verta, M., Munthe, J., and Haapanen, M. 2003. Forestry practices increase mercury and methyl mercury output from boreal forest catchments. Environ. Sci. Technol. 37: 2389–2393. doi:10.1021/es0340174.

Post, D.M. 2002. Using stable isotopes to estimate trophic position: Models, methods, and assumptions. Ecology 83: 703–718. doi: 10.1890/0012-9658(2002)083[0703:USITET]2.0.CO;2

Poste, A.E., Braaten, H.F.V., de Wit, H.A., Sørensen, K., Larssen, T.T., Sorensen, K., and Larssen, T.T. 2015. Effects of photodemethylation on the methylmercury budget of boreal Norwegian lakes. Environ. Toxicol. Chem. 34: 1213–1223. doi:10.1002/etc.2923

Powers, S.M., Labou, S.G., Baulch, H.M., Hunt, R.J., Lottig, N.R., Hampton, S.E., and Stanley, E.H. 2017. Ice duration drives winter nitrate accumulation in north temperate lakes. Limnol. Oceanogr. Lett. 2: 177–186. doi:10.6073/pasta/75bf5bffd90cac6d29ed2aa8e8554c0c

Qian, Y., Yin, X., Lin, H., Rao, B., Brooks, S.C., Liang, L., and Gu, B. 2014. Why dissolved organic matter enhances photodegradation of methylmercury. Environ. Sci. Technol. Lett. 1: 426–431. doi:10.1021/ez500254z

R Core Team 2017. R: The R Project for Statistical Computing. Available at: https://www.r-project.org/

Ravichandran, M. 2004. Interactions between mercury and dissolved organic matter - A review. Chemosphere 55: 319–331. doi:10.1016/j.chemosphere.2003.11.011

Rea, A.W., Keeler, G.J., and Scherbatskoy, T. 1996. The deposition of mercury in throughfall and litterfall in the Lake Champlain watershed: A short-term study. Atmos. Environ. 30: 3257–3263. doi:10.1016/1352-2310(96)00087-8

Reiche, M., Hädrich, A., Lischeid, G., and Küsel, K. 2009. Impact of manipulated drought and heavy rainfall events on peat mineralization processes and source-sink functions of an acidic fen. J. Geophys. Res. 114: 2021. doi:10.1029/2008JG000853

Ribeiro, D.O.C.A., Belger, L., Pelletier, É., and Rouleau, C. 2002. Histopathological evidence of inorganic mercury and methyl mercury toxicity in the Arctic charr (*Salvelinus alpinus*). Environ. Res. 90: 217–225. doi:10.1016/S0013-9351(02)00025-7

Rice, K.M., Walker, E.M., Wu, M., Gillette, C., and Blough, E.R. 2014. Environmental mercury and its toxic effects. J. Prev. Med. Public Health 47: 74–83. doi:10.3961/jpmph.2014.47.2.74

Riget, F., Jeppesen, E., Landkildehus, F., and Lauridsen, T. 2000. Landlocked Arctic charr (*Salvelinus alpinus*) population structure and lake morphometry in Greenland–is there a connection? Polar Biol. 23: 550–558. doi:10.1007/s003000000120

Ritson, J.P., Bell, M., Graham, N.J.D., Templeton, M.R., Brazier, R.E., Verhoef, A., Freeman, C., and Clark, J.M. 2014. Simulated climate change impact on summer dissolved organic carbon release from peat and surface vegetation: Implications for drinking water treatment. Water Res. 67: 66–76. doi:10.1016/j.watres.2014.09.015

Sandheinrich, M.B., and Drevnick, P.E. 2016. Relationship among mercury concentration, growth rate, and condition of northern pike: A tautology resolved? Environ. Toxicol. Chem. 35: 2910–2915. doi:10.1002/etc.3521

SAS Institute Inc 2013. SAS, Version 9.4. Available at: https://www.sas.com/en_us/home.html.

Schaefer, J.K., Kronberg, R.-M., Morel, F.M.M., and Skyllberg, U. 2014. Detection of a key Hg methylation gene, hgcA , in wetland soils. Environ. Microbiol. Rep. 6: 441-447. doi:10.1111/1758-2229.12136

Schartup, A.T., Balcom, P.H., Soerensen, A.L., Gosnell, K.J., Calder, R.S.D., Mason, R.P., and Sunderland, E.M. 2015a. Freshwater discharges drive high levels of methylmercury in Arctic marine biota. Proc. Natl. Acad. Sci. USA 112: 11789–11794. doi:10.1073/pnas.1505541112

Schartup, A.T., Ndu, U., Balcom, P.H., Mason, R.P., and Sunderland, E.M. 2015b. Contrasting effects of marine and terrestrially derived dissolved organic matter on mercury speciation and bioavailability in seawater. Environ. Sci. Technol. 49: 5965–5972. doi:10.1021/es506274x

Schelker, J., Burns, D.A., Weiler, M., and Laudon, H. 2011. Hydrological mobilization of mercury and dissolved organic carbon in a snow-dominated, forested watershed: Conceptualization and modeling. J. Geophys. Res. Biogeosciences 116: 1–17. doi:10.1029/2010JG001330.

Scudder, B.C., Chasar, L.C., Wentz, D.A., Brigham, M.E., Moran, P.W., and Krabbenhoft, D.P. 2010. Mercury in fish, bed sediment, and water from streams across the United States, 1998-2005. National Water-Quality Assessment Program, Toxic Substances Hydrology Program. U.S. Geological Survey. Scientific Investigations Report: 2009-5109. 74 p.

Seabert, T.A., Pal, S., Pinet, B.M., Haman, F., Robidoux, M.A., Imbeault, P., Kruemmel, E.M., Kimpe, L.E., and Blais, J.M. 2014. Elevated contaminants contrasted with potential benefits of omega-3 fatty acids in wild food consumers of two remote First Nations communities in northern Ontario, Canada. PLoS One 9: e90351. doi:10.1371/journal.pone.0090351

Selvendiran, P., Driscoll, C.T., Montesdeoca, M.R., and Bushey, J.T. 2008. Inputs, storage, and transport of total and methyl mercury in two temperate forest wetlands. J. Geophys. Res. 113. doi:10.1029/2008JG000739

Shvidenko, A., and Apps, M. 2006. The International Boreal Forest Research Association: Understanding boreal forests and forestry in a changing world. Mitig. Adapt. Strateg. Glob. Chang. 11: 5–32. doi:10.1007/s11027-006-0986-6

Sigg, C. 2014. Non-Negative and Sparse PCA. Comprehensive R Archive Network (CRAN). Available at: https://cran.r-project.org/web/packages/nsprcomp/index.html [2017 Sep. 3]

Skinner, K., Hanning, R., Desjardins, E., and Tsuji, L. 2013. Giving voice to food insecurity in a remote indigenous community. BMC Public Health 13:427. doi: 10.1186/1471-2458-13-427

Skyllberg, U., Westin, M.B.B., Meili, M., Björn, E., and Bjorn, E. 2009. Elevated concentrations of methyl mercury in streams after forest clear-cut: A consequence of mobilization from soil or new methylation? Environ. Sci. Technol. 43: 8535–8541. doi:10.1021/es900996z

Smith, T.A., and Kraft, C.E. 2005. Stream fish assemblages in relation to landscape position and local habitat variables. Trans. Am. Fish. Soc. 134: 430–440. doi:10.1577/T03-051.1.

Stefansson, E.S., Heyes, A., and Rowe, C.L. 2013. Accumulation of dietary methylmercury and effects on growth and survival in two estuarine forage fish*: Cyprinodon variegatus* and *Menidia beryllina*. Environ. Toxicol. Chem. 32: 848–856. doi:10.1002/etc.2130.

Steffen, A., Douglas, T., Amyot, M., Ariya, P., Aspmo, K., Berg, T., Bottenheim, J., Brooks, S., Cobbett, F., Dastoor, A., Dommergue, A., Ebinghaus, R., Ferrari, C., Gardfeldt, K., Goodsite, M.E., Lean, D., Poulain, A.J., Scherz, C., Skov, H., Sommar, J., and Temme, C. 2008. A synthesis of atmospheric mercury depletion event chemistry linking atmosphere, snow and water. Atmos. Chem. Phys. 8: 1445–1482. doi:10.5194/acpd-7-10837-2007.

Stewart, R.B., Wheaton, E., and Spittlehouse, D.L. 1998. Climate change: implications for the Boreal forest. In: Emerging Air Issues for the 21st Century: The Need for Multidisciplinary Mangement, Proceedings of a Speciality Conference, Sep. 22-24,

1997, Calgary, AB, Legge, A.H. and L.L. Jones (eds.), Air and Waste Management Assoc., Pittsburg, PA, pp 86-101. Available at: https://www.for.gov.bc.ca/hre/pubs/pubs/1124.htm

Strandberg, U., Bhavsar, S.P., Parmar, T.P., and Arts, M.T. 2018. Spatial and length-dependent variation of the risks and benefits of consuming Walleye (*Sander vitreus*). Environ. Int. 112: 251–260. doi:10.1016/j.envint.2017.12.029

Sumner, A.W. 2016. The effects of climate on the bioaccumulation of mercury in two large- bodied fish species in northern Ontario lakes. MSc thesis, Laurentian University. Available at: https://zone.biblio.laurentian.ca/bitstream/10219/2629/1/Sumner-MSc-Thesis-29Jun2016.pdf.

Szkokan-Emilson, E.J., Kielstra, B., Watmough, S., and Gunn, J. 2013. Drought-induced release of metals from peatlands in watersheds recovering from historical metal and sulphur deposition. Biogeochemistry 116: 131–145. doi:10.1007/s10533-013-9919-0.

Tang, R.W.K., Johnston, T.A., Gunn, J.M., and Bhavsar, S.P. 2013. Temporal changes in mercury concentrations of large-bodied fishes in the boreal shield ecoregion of northern Ontario, Canada. Sci. Total Environ. 444: 409–16. doi:10.1016/j.scitotenv.2012.11.109

Tareq, S.M., Maruo, M., and Ohta, K. 2013. Characteristics and role of groundwater dissolved organic matter on arsenic mobilization and poisoning in Bangladesh. Phys. Chem. Earth 58–60: 77–84. doi:10.1016/j.pce.2013.04.014

Thera, J.C. 2017. Among-lake variability in methylmercury and amino acids in aquatic invertebrates from Kejimkujik National Park. PhD thesis, University of New Brunswick. Available at: https://unbscholar.lib.unb.ca/islandora/object/unbscholar%3A9101

Thomas, S.M., Melles, S.J., and Bhavsar, S.P. 2018. Broad-scale mercury bioaccumulation patterns in two freshwater sport fishes: testing the role of growth dilution in a warming climate. PrePrint. bioRxiv: 280107. Cold Spring Harbor Laboratory. doi:10.1101/280107

Tibshirani, R., Tibshirani, R., Taylor, J., Loftus, J., and Reid, S. 2017. Package selectiveInference. Comprehensive R Archive Network (CRAN). Available at: https://cran.r-project.org/web/packages/selectiveInference/index.html

Todorova, S.G., Driscoll, C.T., Matthews, D.A., Effler, S.W., Hines, M.E., and Henry, E.A. 2009. Evidence for regulation of monomethyl mercury by nitrate in a seasonally stratified, eutrophic lake. Environ. Sci. Technol. 43: 6572–6578. doi:10.1021/es900887b

Tremblay, A., Lucotte, M., and Rowan, D. 1995. Different factors related to mercury concentration in sediments and zooplankton of 73 Canadian Lakes. Water Air Soil Pollut. 80: 961–970. doi:10.1007/BF01189750

Tremblay, A., Lucotte, M., and Schetagne, R. 1998. Total mercury and methylmercury accumulation in zooplankton of hydroelectric reservoirs in northern Quebec (Canada). Sci. Total Environ. 213: 307–315. doi:10.1016/S0048-9697(98)00107-7

Trudel, M., and Rasmussen, J.B. 1997. Modeling the elimination of mercury by fish. Environ. Sci. Technol. 31: 1716–1722. doi:10.1021/es960609t

Trudel, M., and Rasmussen, J.B. 2006. Bioenergetics and mercury dynamics in fish: a modelling perspective. Can. J. Fish. Aquat. Sci. 63: 1890–1902. doi:10.1139/f06-081

Tsui, M.T.K., and Finlay, J.C. 2011. Influence of dissolved organic carbon on methylmercury bioavailability across Minnesota stream ecosystems. Environ. Sci. Technol. 45: 5981–5987. doi:10.1021/es200332f

Tye, A.M., and Lapworth, D.J. 2016. Characterising changes in fluorescence properties of dissolved organic matter and links to N cycling in agricultural floodplains. Agric. Ecosyst. Environ. 221: 245–257. doi:10.1016/j.agee.2016.01.033

Ullrich, S.M., Tanton, T.W., and Svetlana, A. 2001. Mercury in the aquatic environment : A review of factors affecting methylation. Crit. Rev. Environ. Sci. Technol. 31: 241–293. doi:10.1080/20016491089226

USEPA and FDA 2017. Advice About Eating Fish: What Pregnant Women & Parents Should Know. United States Environmental Protection Agency. Available at: https://www.fda.gov/Food/FoodborneIllnessContaminants/Metals/ucm393070.htm

Urquizo, N., Bastedo, J., Brydges, T., and Shear, H. 2000. Ecological assessment of the Boreal Shield ecozone. Available at: http://publications.gc.ca/collections/collection_2014/ec/En40-600-2000-eng.pdf

USEPA 2012. The Economic Benefits of Protecting Healthy Watersheds. United States Environmental Protection Agency. Available at: www.epa.gov/healthywatersheds

Valois, A., Keller, W.B., and Ramcharan, C. 2010. Abiotic and biotic processes in lakes recovering from acidification: the relative roles of metal toxicity and fish predation as barriers to zooplankton re-establishment. Freshw. Biol. 55: 2585–2597. doi:10.1111/j.1365-2427.2010.02488.x

Vannote, R.L., Minshall, G.W., Cummins, K.W., Sedell, J.R., and Cushing, C.E. 1980. The river continuum concept. Can. J. Fish. Aquat. Sci. 37: 130–137. doi:10.1139/f80-017

Vidon, P., Carleton, W., and Mitchell, M.J. 2014. Mercury proxies and mercury dynamics in a forested watershed of the US Northeast. Environ. Monit. Assess. 186: 7475–7488. doi:10.1007/s10661-014-3941-0

Wallschlager, D., Desai, M.V.M., and Wilken, R.-D. 1996. The role of humic substances in the aqueous mobilization of mercury from contaminated floodplain soils. Water Air Soil Pollut. 90: 507–520. doi: 10.1007/BF00282665

Walters, D.M., Raikow, D.F., Hammerschmidt, C.R., Mehling, M.G., Kovach, A., and Oris, J.T. 2015. Methylmercury bioaccumulation in stream food webs declines with

increasing primary production. Environ. Sci. Technol. 49: 7762–7769. doi:10.1021/acs.est.5b00911

Wang, R., and Wang, W.-X. 2018. Diet-specific trophic transfer of mercury in tilapia (*Oreochromis niloticus*): Biodynamic perspective. Environ. Pollut. 234: 288–296. doi:10.1016/j.envpol.2017.11.071

Wang, R., and Wang, W.X. 2010. Importance of speciation in understanding mercury bioaccumulation in tilapia controlled by salinity and dissolved organic matter. Environ. Sci. Technol. 44: 7964–7969. doi:10.1021/es1011274

Wang, R., and Wang, W.X. 2012. Contrasting mercury accumulation patterns in tilapia (*Oreochromis niloticus*) and implications on somatic growth dilution. Aquat. Toxicol. 114–115: 23–30. doi:10.1016/j.aquatox.2012.02.014

Wang, R., Wong, M.-H., and Wang, W.-X. 2010. Mercury exposure in the freshwater tilapia *Oreochromis niloticus*. Environ. Pollut. 158: 2694–2701. doi:10.1016/j.envpol.2010.04.019

Wang, W.X., and Wong, R.S.K. 2003. Bioaccumulation kinetics and exposure pathways of inorganic mercury and methylmercury in a marine fish, the sweetlips *Plectorhinchus gibbosus*. Mar. Ecol. Prog. Ser. 261: 257–268. doi:10.3354/meps261257

Waples, J.S., Nagy, K.L., Aiken, G.R., and Ryan, J.N. 2005. Dissolution of cinnabar (HgS) in the presence of natural organic matter. Geochim. Cosmochim. Acta 69: 1575–1588. doi:10.1016/j.gca.2004.09.029

Wasik, J.K.C., Engstrom, D.R., Mitchell, C.P.J., Swain, E.B., Monson, B.A., Balogh, S.J., Jeremiason, J.D., Branfireun, B.A., Kolka, R.K., and Almendinger, J.E. 2015. The effects of hydrologic fluctuation and sulfate regeneration on mercury cycling in an experimental peatland. J. Geophys. Res. 120: 1697–1715. doi:10.1002/2015JG002993

Watras, C.J., Morrison, K.A., and Back, R.C. 1996. Mass balance studies of mercury and methyl mercury in small temperate / boreal lakes of the northern hemisphere. *In*: Baeyens W., Ebinghaus R., Vasiliev O. (eds) Global and Regional Mercury Cycles: Sources, Fluxes and Mass Balances. NATO ASI Series (Series 2: Environment), vol 21. Springer, Dordrecht

Watras, C.J., Morrison, K.A., Kent, A., Price, N., Regnell, O., Eckley, C., Hintelmann, H., and Hubacher, T. 2005. Sources of methylmercury to a wetland-dominated lake in northern Wisconsin. Environ. Sci. Technol. 39: 4747–4758. doi:10.1021/es040561g.

Webster, K.L., Beall, F.D., Creed, I.F., and Kreutzweiser, D.P. 2015. Impacts and prognosis of natural resource development on water and wetlands in Canada's boreal zone. Environ. Rev. 23: 78–131. doi:10.1139/er-2014-0063.

Weishaar, J., Aiken, G., Bergamaschi, B., Fram, M., Fujii, R., and Mopper, K. 2003. Evaluation of specific ultra-violet absorbance as an indicator of the chemical content of dissolved organic carbon. Environ. Sci. Technol. 37: 4702–4708. doi:10.1021/es030360x.

Wellen, C., Shatilla, N.J., and Carey, S.K. 2018. The influence of mining on hydrology and solute transport in the Elk Valley, British Columbia, Canada. Environ. Res. Lett. 13: 074012. doi:10.1088/1748-9326/aaca9d

Wells, J., Roberts, D., Lee, P., Cheng, R., and Darveau, M. 2010. A forest of blue: Canada's boreal forest: The world's waterkeeper. PEW Environmental Group. Seattle, WA. Available at: www.pewenvironment.org

Wickham, H., and Chang, W. 2016. Create Elegant Data Visualisations Using the Grammar of Graphics. Comprehensive R Archive Network (CRAN). Available at: https://cran.r-project.org/web/packages/ggplot2/ggplot2.pdf.

Wieder, K., Vitt, D.H., and Benscoter, B.W. 2006. Peatlands and the boreal forest. in Boreal Peatland Ecosystems. *In*: Wieder, R.K. and Vitt, D.H. Boreal Peatland Ecosystems. Springer, New York, pp. 1 – 8. doi:10.1007/978-3-540-31913-9_1

Wilson, H.F., and Xenopoulos, M.A. 2009. Effects of agricultural land use on the composition of fluvial dissolved organic matter. Nat. Geosci. 2: 37–41. doi:10.1038/ngeo391.

de Wit, H.A., Granhus, A., Lindholm, M., Kainz, M.J., Lin, Y., Braaten, H.F.V., and Blaszczak, J. 2014. Forest harvest effects on mercury in streams and biota in Norwegian boreal catchments. For. Ecol. Manage. 324: 52–63. doi:10.1016/j.foreco.2014.03.044

Wolf, M., Kappler, A., Jiang, J., and Meckenstock, R.U. 2009. Effects of humic substances and quinones at low concentrations on ferrihydrite reduction by *Geobacter metallireducens*. Environ. Sci. Technol. 43: 5679–5685. doi:10.1021/es803647r

Wu, P., Bishop, K., von Brömssen, C., Eklöf, K., Futter, M., Hultberg, H., Martin, J., and Åkerblom, S. 2018. Does forest harvest increase the mercury concentrations in fish? Evidence from Swedish lakes. Sci. Total Environ. 622–623: 1353–1362. doi:10.1016/J.SCITOTENV.2017.12.075

Yin, Y., Allen, H.E., and Huang, C.P. 1997. Kinetics of mercury(II) adsorption and desorption on soil. Environ. Sci. Technol. 31: 496–503. doi:10.1021/ES9603214

Young-Robertson, J.M., Robert Bolton, W., Bhatt, U.S., Cristóbal, J., and Thoman, R. 2016. Deciduous trees are a large and overlooked sink for snowmelt water in the boreal forest. Nature 6: 29504. doi:10.1038/srep29504

Zhang, L., Campbell, L.M., and Johnson, T.B. 2012. Seasonal variation in mercury and food web biomagnification in Lake Ontario, Canada. Environ. Pollut. 161: 178–184. doi:10.1016/j.envpol.2011.10.023.

Zhang, L., Wang, S.X., Wang, L., and Hao, J.M. 2013. Atmospheric mercury concentration and chemical speciation at a rural site in Beijing, China: implications of mercury emission sources. Atmos. Chem. Phys. 13: 10505–10516. doi:10.5194/acp-13-10505-2013.

Zhang, L., and Wang, W.X. 2006. Significance of subcellular metal distribution in prey in influencing the trophic transfer of metals in a marine fish. Limnol. Oceanogr. 51: 2008–2017. doi: 10.4319/lo.2006.51.5.2008

Zhu, H., Yan, B.-X., Zhang, F.-S., Lu, Y.-Z., and Wang, L.-X. 2010. Effects of particle-sizes, pH and organic matter on adsorption and desorption of mercury to sediments in the Songhua River. Huan Jing Ke Xue 31: 2315–2320.

Supplementary Information

SI information for Chapter 2

Table SI- 1: A list of all physical and chemical parameters considered in this study and their associated abbreviations, units, and method detection limits (MDLs). The percent (%) of data above the MDL for a given parameter is also presented.

Parameter	Abbreviations	Units	MDL	% above MDL
Chemical parameters				
Methyl mercury	[MeHg]	ng/L	0.0006	100
Total mercury	[THg]	ng/L	0.05	100
Dissolved organic carbon	DOC	mg/L	0.17	100
Dissolved inorganic carbon	DIC	mg/L	0.12	100
Sulfate	SO_4^{2-}	mg/L	0.36	36
Total Nitrogen	TN	mg/L	0.02103	96
Ammonia + Ammonium	NH_3+NH_4	µg/L	4.15	70
Nitrate + Nitrite	NO_2+NO_3	µg/L	2.62	89
Total Phosphorus	TP	mg/L	0.00018	100
True Colour	Colour	TCU	1	96
Alkalinity	Alk	mg/L CaCO3	---	---
Conductivity	Cond	uS/cm	0.91	100
pH	---	---	---	---
Aluminum[2]	Al	mg/L	0.0005	100
Arsenic[2]	As	mg/L	0.0005	51
Calcium[2]	Ca	mg/L	0.00006	100
Chloride[2]	Cl	µg/L	10	72
Copper[2]	Cu	µg/L	0.2	53
Iron[2]	Fe	mg/L	0.01	100
Magnesium[2]	Mg	mg/L	0.01	100
Manganese[2]	Mn	µg/L	0.05	100
Potassium[2]	K	mg/L	0.02	100
Selenium[2]	Se	mg/L	0.0005	4
Silicon[2]	Si	mg/L	0.03	96
Sodium[2]	Na	mg/L	0.01	100
Titanium[2]	Ti	µg/L	0.5	53
Physical attributes[1]				
Latitude	Lat.	DD	---	---
Longitude	Long.	DD	---	---
Dissolved Oxygen	D.O.	%	---	---
Surface temperature	Temp	^{0}C	---	---
River order	---	---	---	---
Secchi depth	---	m	---	---
Elevation	---	m	---	---
Max depth	---	m	---	---
Surface area	SA	ha	---	---
Drainage area	DA	km2	---	---
Wetlands area	Wetlands	km2	---	---
Mean basin slope	Slope	%	---	---

[1]Calculated using the Ontario Flow Assessment Tool (OFAT) or NRCAN toporama; [2]Total, unfiltered concentrations.

Table SI- 2: Physical characteristics of 27 river sites sampled for this study. Data are grouped as main-stem Attawapiskat River sites, Attawapiskat River tributaries, and Muketei River tributaries.

Waterbody	Elevation (m)	Long (DD)	Lat (DD)	Surface Temp.	Surface D.O.	Drainage Area(km^2)	Wetlands Area (km^2)	Slope (%)
River mouth	10	-82.27	52.97	ND	ND	49630.5	28528.3	2.1
Naysh rapids	46	-83.51	52.89	ND	ND	45572.4	25301.9	2.2
Victor	59	-83.91	52.87	19.6	5.6	43374.7	23501.2	2.3
Streatfield convergence	146	-85.94	52.65	18.7	5.8	1004.9	878.3	1.2
Missisa convergence	93	-85.44	53.09	20.6	8.0	40062.9	20970.3	2.3
Muketei convergence	100	-85.26	53.13	ND	ND	3929.5	3429.6	1.3
Canada Lake	158	-86.03	52.47	ND	ND	27262.5	10196.8	2.8
Pym island	175	-86.35	52.16	ND	ND	26859.5	9885.6	2.8
Windsor Lake	231	-87.36	52.19	ND	ND	21707.0	6878.9	3.0
Beteau Lake	210	-87.12	52.07	ND	ND	1107.5	231.6	2.8
Attawapiskat River tributary1	122	-85.44	53.09	20.6	8.0	1599.0	1416.9	1.2
Attawapiskat River tributary2	145	-85.94	52.70	17.9	6.1	18.6	17.5	1.1
Attawapiskat River tributary3	152	-85.89	52.72	16.9	7.3	109.3	92.2	1.0
Attawapiskat River tributary4	166	-86.18	52.38	17.9	6.1	1004.8	878.3	1.2
Coomer Creek	168	-86.32	52.71	16.9	7.3	208.7	187.6	1.5
Gleason Creek	126	-85.85	52.95	19.3	8.1	488.7	443.2	1.2
Highbank Creek	175	-86.17	52.40	22.6	7.4	42.9	24.6	1.3
McFaulds Creek	147	-85.92	52.80	20.7	6.6	109.2	92.1	1.0
Koper Creek1	155	-86.22	52.90	22.6	7.4	213.3	193.0	1.3
Koper Creek2	160	-86.19	52.80	18.1	7.0	177.7	148.9	1.2
Muketei River	167	-86.36	52.68	17.0	8.0	295.5	280.1	1.7
Muketei River tributary1	102	-85.30	53.14	19.6	5.6	54.8	47.1	1.4
Muketei River tributary2	165	-86.34	52.70	17.6	7.4	6.8	6.5	1.5
Muketei River tributary3	124	-85.83	53.12	17.9	7.1	1.7	1.6	1.2
Muketei River tributary4	113	-85.49	53.20	25.5	7.6	48.3	39.0	1.2
Muketei River tributary5	108	-85.43	53.20	16.8	6.9	11.6	7.4	0.9
Muketei River tributary6	171	-86.34	52.64	16.8	6.9	239.0	188.8	1.2

Table SI- 3: Chemical characteristics of 27 river sites sampled for this study. All water samples were taken at a depth of 1 m. All water chemistry analysis was performed the Ontario MOECC. See Table SI-1 for definitions of abbreviations.

Waterbody	[MeHg] (ng/L UF)	[THg] (ng/L UF)	DOC (mg/L)	Colour (TCU)	Fe (mg/L)	NO_2+NO_3 (µg/L)	NH_3+NH_4 (µg/L)	TN (mg/L)
River mouth	ND	ND	ND	ND	ND	ND	ND	ND
Naysh rapids	ND	ND	ND	ND	ND	ND	ND	ND
Victor	ND	ND	20.1	82	0.26	2.00	62.0	0.47
Streatfeild con.	0.024	5.85	21.8	220	0.59	26.00	0.3	0.39
Missisa con.	ND	ND	13.5	85	ND	2.00	20.0	0.03
Muketei con.	ND	ND	ND	76	ND	6.00	18.0	0.41
Canada Lake	ND	ND	ND	ND	ND	ND	ND	ND
Pym island	ND	ND	11.9	63	0.10	2.00	20.0	0.37
Windsor Lake	ND	ND	ND	ND	ND	ND	ND	ND
Beteau Lake	ND	ND	13.7	94	ND	24.00	10.0	0.47
A. River trib 1	0.040	5.97	23.8	246	0.72	28.00	8.0	0.43
A. River trib 2	0.022	3.99	22.6	202	0.69	30.00	0.5	0.35
A. River trib 3	0.030	6.62	29.1	282	0.90	30.00	0.1	0.41
A. River trib 4	0.040	2.14	22.6	185	0.50	20.00	0.8	0.43
Coomer Creek	0.038	2.99	19.7	156	0.43	12.00	0.4	0.37
Gleason Creek	0.037	3.55	24.2	183	0.61	24.00	12.0	0.41
Highbank Creek	0.041	2.73	20.3	151	0.50	22.00	0.0	0.43
McFaulds Creek	0.036	1.82	23.1	186	0.47	22.00	1.2	0.37
Koper Creek1	0.015	7.35	21.6	191	0.59	24.00	1.1	0.40
Koper Creek2	0.029	5.16	21.6	185	0.51	24.00	1.2	0.41
Muketei River	0.041	2.83	21.3	154	0.46	16.00	0.9	0.34
Muketei trib 1	0.089	2.26	25.4	241	0.51	30.00	0.4	0.39
Muketei trib 2	0.018	1.54	14.4	74	0.21	6.00	0.5	0.29
Muketei trib 3	0.039	4.11	22.5	182	0.54	24.00	18.0	0.50
Muketei trib 4	0.056	3.69	23.8	226	0.62	30.00	8.0	0.47
Muketei trib 5	0.044	3.22	18.3	149	0.28	16.00	14.0	0.36
Muketei trib 6	0.040	4.69	21.6	202	0.73	24.00	1.7	0.37

Table SI-3-continued: **Chemical characteristics of 27 river sites sampled for this study. See Table SI-1 for definitions of abbreviations.**

Waterbody	TP (mg/L)	Sulfate (mg/L)	pH	Alk. (mg/L)	Al (µg/L)	Cond. (uS/cm)	Ca (mg/L)	Cl (µg/L)	Cu (µg/L)	DIC (me/L)
River mouth	ND	ND	ND	ND	ND	ND	ND	ND	ND	ND
Naysh rapids	ND	ND	ND	ND	ND	ND	ND	ND	ND	ND
Victor	0.014	9.450	7.87	60.4	53.1	227.0	21.2	21700.0	1.30	14.30
Streatfeild con.	0.021	0.170	7.19	30.3	112.0	60.8	11.4	170.0	0.30	6.72
Missisa con.	ND	0.150	7.80	55.3	ND	108.0	14.6	440.0	ND	ND
Muketei con.	ND	ND	7.78	43.4	ND	91.2	14.4	ND	ND	ND
Canada Lake	ND	ND	ND	ND	ND	ND	ND	ND	ND	ND
Pym island	0.010	0.700	7.76	44.7	33.7	91.6	15.0	250.0	0.40	10.20
Windsor Lake	ND	ND	ND	ND	ND	ND	ND	ND	ND	ND
Beteau Lake	0.014	0.450	7.71	36.7	ND	80.4	12.4	140.0	ND	7.66
A. River trib 1	0.025	0.040	7.48	36.1	128.0	74.7	14.1	130.0	0.40	7.66
A. River trib 2	0.010	0.110	7.09	19.2	33.6	41.0	8.2	23.0	0.09	5.36
A. River trib 3	0.022	0.160	6.98	23.5	163.0	50.3	10.3	120.0	0.30	5.58
A. River trib 4	0.009	0.150	7.17	30.3	49.7	61.7	11.6	28.0	0.08	6.66
Coomer Creek	0.013	0.030	7.21	29.3	82.6	60.3	10.6	16.0	0.09	6.88
Gleason Creek	0.016	0.060	7.34	33.6	60.9	67.8	11.8	180.0	0.01	7.40
Highbank Creek	0.022	0.150	7.43	34.7	77.8	71.8	12.3	150.0	0.30	7.84
McFaulds Creek	0.011	0.020	6.92	20.2	40.5	43.5	8.3	35.0	0.04	5.26
Koper Creek1	0.018	0.080	7.14	29.7	98.4	61.8	11.0	150.0	0.05	7.20
Koper Creek2	0.018	0.140	7.00	28.3	61.0	59.2	10.6	140.0	0.04	7.70
Muketei River	0.008	0.160	7.38	40.0	34.8	80.8	14.2	260.0	0.07	9.40
Muketei trib 1	0.014	0.180	6.81	17.2	75.3	39.8	7.6	360.0	0.00	4.86
Muketei trib 2	0.003	0.160	7.32	48.6	5.3	96.9	16.9	36.0	0.05	12.20
Muketei trib 3	0.015	0.100	7.23	41.6	54.5	67.3	11.3	450.0	0.10	7.58
Muketei trib 4	0.020	0.150	7.27	35.3	98.6	75.4	12.5	840.0	0.02	8.20
Muketei trib 5	0.014	0.400	7.49	27.7	47.4	63.3	9.6	1200.0	0.30	6.00
Muketei trib 6	0.011	0.070	7.05	27.4	60.5	56.2	10.5	120.0	0.04	7.00

Table SI-3-continued: Chemical characteristics of 27 river sites sampled for this study. See Table SI-1 for definitions of abbreviations.

Waterbody	Mg (mg/L)	Mn (µg/L)	K (mg/L)	Se (µg/L)	Si (mg/L)	Na (mg/L)	St (µg/L)	Ti (µg/L)	Zn (µg/L)
River mouth	ND	ND	ND	ND	ND	ND	ND	ND	ND
Naysh rapids	ND	ND	ND	ND	ND	ND	ND	ND	ND
Victor	6.09	12.90	0.68	0.300	1.52	12.90	95.30	2.20	1.50
Streatfeild con.	1.95	30.90	0.10	0.182	1.08	0.47	20.40	3.70	2.30
Missisa con.	3.15	ND	0.38	ND	1.64	0.82	ND	ND	ND
Muketei con.	2.82	ND	0.40	ND	ND	0.69	ND	ND	ND
Canada Lake	ND	ND	ND	ND	ND	ND	ND	ND	ND
Pym island	2.94	8.10	0.45	0.200	1.44	0.61	17.10	1.00	0.30
Windsor Lake	ND	ND	ND	ND	ND	ND	ND	ND	ND
Beteau Lake	2.42	ND	0.46	ND	1.26	0.57	ND	ND	ND
A. River trib 1	2.17	48.90	0.10	0.184	1.06	0.52	22.60	3.80	2.10
A. River trib 2	1.06	16.20	0.03	0.066	0.84	0.25	14.00	0.60	2.80
A. River trib 3	1.41	58.90	0.10	0.134	0.96	0.32	15.80	4.60	3.10
A. River trib 4	1.78	43.00	0.18	0.151	1.08	0.47	21.30	1.10	1.90
Coomer Creek	1.75	33.20	0.06	0.130	1.18	0.59	26.70	2.40	1.60
Gleason Creek	2.06	45.00	0.08	0.182	1.34	0.56	22.50	1.70	1.90
Highbank Creek	2.20	39.20	0.16	0.071	1.12	0.66	26.80	2.30	1.30
McFaulds Creek	1.19	15.60	0.05	0.003	0.94	0.41	15.70	0.80	2.70
Koper Creek1	1.92	59.70	0.09	0.173	1.24	0.63	27.00	3.00	2.20
Koper Creek2	1.99	50.90	0.12	0.141	1.32	0.61	25.50	1.80	2.50
Muketei River	2.18	32.60	0.06	0.145	1.44	0.50	23.00	0.80	1.50
Muketei trib 1	1.07	14.70	0.09	0.129	0.50	0.76	16.30	2.10	1.70
Muketei trib 2	2.44	22.00	0.04	0.216	1.56	0.43	22.70	0.05	0.90
Muketei trib 3	1.84	38.50	0.10	0.179	1.18	0.87	19.20	1.50	1.70
Muketei trib 4	2.13	28.80	0.10	0.111	1.18	1.65	18.60	3.50	1.60
Muketei trib 5	1.54	12.00	0.14	0.010	0.60	1.95	18.40	1.50	0.90
Muketei trib 6	1.57	29.00	0.06	0.053	1.30	0.48	21.00	1.70	2.60

Table SI- 4: Physical characteristics of 11 Lowland lakes sampled for this study. ^Deep water samples also taken; data available upon request. See Table SI-1 for definitions of abbreviations.

Waterbody	Elevation (m)	Longitude (DD)	Latitude (DD)	Lake Area (ha)	Max Depth (m)	Drainage Area (km^2)	Wetlands Area (km^2)	Mean Slope (%)	Secchi Depth	Surface Temp.	Surface D.O.
Fishtrap	174	-86.41	52.35	2030	1.3	144.3	103.4	1.3	1.0	18.0	9.1
Goods	194	-86.74	52.53	742	3.7	129.3	101.5	1.5	1.6	17.6	8.7
Highbank	178	-86.18	52.32	1450	1.8	84.7	57.5	1.4	1.1	18.2	8.2
Kapiskau	157	-85.30	52.18	180	1.6	675.0	566.0	1.3	0.9	17.5	8.2
Kitchie	178	-86.52	52.43	2300	ND	683.1	584.4	1.4	ND	ND	ND
Koper	170	-86.25	52.72	44	3.8	ND	ND	ND	1.5	ND	ND
McFaulds	157	-86.07	52.77	957.5	3.2	33.6	22.6	0.9	ND	ND	ND
Missisa	168	-85.20	52.31	19212	7.0	576.1	292.2	0.9	0.5	16.5	9.7
Napken	158	-85.33	51.88	1570	3.4	580.2	463.2	1.5	1.0	18.2	8.4
Quantz^	169	-85.38	51.16	727	10.4	79.3	49.1	1.7	1.2	18.6	8.8
Streatfeild	180	-85.90	52.14	2090	2.1	179.9	141.0	1.1	0.5	17.9	8.8
Wabimeig	151	-85.59	51.50	5062	1.9	592.9	479.3	1.3	0.6	18.1	9.3

Table SI- 5: Chemical characteristics of 11 Lowland lakes sampled for this study. All water samples were taken at a depth of 1 m. All water chemistry analysis was performed the Ontario MOECC. ^Deep water samples also taken; data available upon request. See Table SI-1 for definitions of abbreviations.

Waterbody	[MeHg] (ng/L UF)	[THg] (ng/L UF)	DOC (mg/L)	Colour (TCU)	Fe (mg/L)	NO_2+NO_3 (µg/L)	NH_3+NH_4 (µg/L)	TN (mg/L)
Fishtrap	0.017	1.95	13.6	53	0.14	4.00	1.9	0.45
Goods	0.032	2.73	17.7	105	0.17	4.00	0.3	0.37
Highbank	0.001	1.60	14.8	74	0.20	1.10	10.0	0.49
Kapiskau	0.024	2.51	21.1	168	0.61	14.00	16.0	0.41
Kitchie	ND	ND	18.5	81	0.12	2.00	28.0	0.49
Koper	ND	ND	10.9	84	0.06	2.00	24.0	0.38
McFaulds	ND	ND	ND	ND	ND	ND	ND	ND
Missisa	0.000	2.24	10.5	38	0.23	6.00	0.2	0.56
Napken	0.035	2.36	18.4	127	0.23	10.00	18.0	0.39
Quantz^	0.028	1.81	16.4	114	0.15	10.00	32.0	0.35
Streatfeild	0.000	2.94	13.5	87	0.35	0.30	0.7	0.35
Wabimeig	0.001	2.81	17.2	97	0.20	8.00	0.9	0.43

Table SI-5 –continued: Chemical characteristics of 11 Lowland lakes sampled for this study. See Table SI-1 for definitions of abbreviations.

Waterbody	TP (mg/L)	Sulfate (mg/L)	pH	Alk. (mg/L)	Al (µg/L)	Cond. (uS/cm)	Ca (mg/L)	Cl (µg/L)	Cu (µg/L)	DIC (me/L)
Fishtrap	0.020	0.130	7.57	26.7	29.2	56.7	8.6	260.0	0.03	5.84
Goods	0.010	0.160	7.43	22.8	32.1	48.0	8.6	110.0	0.01	4.60
Highbank	0.023	0.060	7.62	31.2	33.0	66.9	10.3	260.0	0.30	7.02
Kapiskau	0.014	0.040	7.57	43.5	36.4	88.6	15.4	390.0	0.03	10.30
Kitchie	0.016	0.050	7.50	25.9	30.8	57.0	9.8	150.0	0.60	6.14
Koper	0.012	0.050	6.71	6.0	29.0	17.8	2.7	190.0	2.70	1.46
McFaulds	ND	ND	ND	ND	ND	ND	ND	ND	ND	ND
Missisa	0.042	0.040	7.97	57.2	52.7	113.0	18.1	260.0	20.20	14.10
Napken	0.017	0.050	7.61	33.8	31.4	69.9	12.0	150.0	0.30	7.82
Quantz^	0.020	0.040	7.59	30.6	25.4	63.2	10.2	130.0	0.30	6.96
Streatfeild	0.034	0.030	7.41	21.8	148.0	46.5	7.6	180.0	0.50	4.64
Wabimeig	0.019	0.060	7.44	19.6	68.8	43.2	7.5	190.0	0.40	4.18

Table SI-5 –continued: Chemical characteristics of 11 Lowland lakes sampled for this study. See Table SI-1 for definitions of abbreviations.

Waterbody	Mg (mg/L)	Mn (µg/L)	K (mg/L)	Se (µg/L)	Si (mg/L)	Na (mg/L)	St (µg/L)	Ti (µg/L)	Zn (µg/L)
Fishtrap	1.55	22.90	0.17	0.208	0.40	0.54	15.40	1.10	1.20
Goods	1.27	24.30	0.11	0.106	0.96	0.32	13.90	1.00	1.40
Highbank	2.08	20.90	0.21	0.241	0.70	0.69	25.70	1.40	1.60
Kapiskau	2.32	29.30	0.12	0.120	1.36	0.82	29.00	1.40	1.30
Kitchie	1.65	33.50	0.14	0.100	0.40	0.47	16.80	0.70	1.20
Koper	0.43	5.50	0.15	0.100	0.06	0.35	6.50	0.20	1.50
McFaulds	ND	ND	ND	ND	ND	ND	ND	ND	ND
Missisa	2.95	35.80	0.19	0.064	0.40	0.78	18.90	2.90	1.30
Napken	1.99	14.90	0.13	0.023	0.86	0.74	19.70	1.00	1.30
Quantz^	2.01	7.40	0.19	0.150	0.36	0.49	17.00	0.70	1.60
Streatfeild	1.33	24.10	0.16	0.170	0.36	0.48	16.10	8.20	2.80
Wabimeig	1.27	29.00	0.14	0.194	0.12	0.49	11.10	2.70	1.70

Table SI- 6: Physical characteristics of 20 Shield lakes sampled for this study. ^Deep water samples also taken; data available upon request. See Table SI-1 for definitions of abbreviations.

Waterbody	Elevation (m)	Long (DD)	Lat (DD)	Lake Area (ha)	Max Depth (m)	Drainage Area (km^2)	Wetlands Area (km^2)	Slope (%)	Secchi Depth	Surface Temp.	Surface D.O.
Attawapiskat^	242	-87.90	52.30	28100	23.5	21361.1	6834.9	3.0	1.9	19.3	8.1
Badesdawa^	330	-89.71	51.78	3113	14.6	9054.8	2781.1	3.2	1.5	18.5	8.1
Carpenter^	381	-90.76	51.19	779	19.0	39.9	8.8	3.5	2.4	19.0	8.2
Kabania	244	-88.41	52.19	7681.4	22.0	18827.8	6467.1	3.0	1.6	ND	ND
Kapkichi^	361	-90.40	51.46	1277	13.1	826.9	199.9	3.6	2.2	19.5	8.0
Lang^	384	-91.51	51.58	1001	21.1	189.7	50.4	3.1	2.7	18.4	8.2
Margaree	341	-89.52	51.79	199	3.0	5.3	0.3	2.9	3.0	18.6	8.7
Menako^	351	-90.21	52.08	7161	17.7	452.5	173.9	2.8	1.9	18.0	8.5
Monmonawson	345	-89.48	51.71	676	3.0	87.4	29.3	3.1	1.6	18.9	9.0
Ozhiski^	272	-88.57	51.95	6362	19.0	11723.4	3804.9	3.1	1.9	19.9	8.2
Pickle^	354	-90.23	51.45	1112	19.2	91.6	19.2	4.0	3.1	18.5	8.5
Richter	258	-87.88	52.09	480	3.2	119.0	23.4	2.7	2.0	18.7	8.4
Stark	267	-87.69	51.88	393	3.0	170.3	64.9	2.4	1.8	19.1	8.5
Tarp	356	-90.11	51.57	1161	3.1	62.6	23.3	2.2	1.0	ND	ND
Totogan	311	-89.20	52.06	2775.9	7.0	351.0	143.5	2.2	2.0	ND	ND
Trading	283	-88.96	51.82	465	4.5	828.6	322.2	3.0	2.4	18.1	8.1
Unnamed	382	-90.68	51.43	491	1.4	154.1	41.2	3.2	1.4	18.4	8.5
Wigwascence	297	-89.41	52.45	1525.3	4.0	1960.7	670.4	2.7	1.7	ND	ND
Williams^	372	-90.78	51.82	4132	13.0	376.7	80.2	3.4	2.6	18.1	8.2
Wright^	383	-90.95	51.33	1257	13.0	142.7	25.9	2.8	2.1	18.7	8.3

Table SI- 7: Chemical characteristics of 20 Shield lakes sampled for this study. All water samples were taken at a depth of 1 m. All water chemistry analysis was performed the Ontario MOECC. ^Deep water samples also taken; data available upon request. See Table SI-1 for definitions of abbreviations.

Waterbody	[MeHg] (ng/L UF)	[THg] (ng/L UF)	DOC (mg/L)	Colour (TCU)	Fe (mg/L)	NO_2+NO_3 (µg/L)	NH_3+NH_4 (µg/L)	TN (mg/L)
Attawapiskat^	0.023	1.96	13.4	70	0.09	14.00	26.0	0.36
Badesdawa^	0.003	2.28	16.0	90	0.14	18.00	16.0	0.40
Carpenter^	0.017	1.25	10.7	46	0.07	4.00	8.0	0.31
Kabania	ND	ND	ND	ND	ND	ND	ND	ND
Kapkichi^	0.024	1.44	12.6	60	0.08	6.00	40.0	0.35
Lang^	0.001	1.27	12.9	58	0.04	6.00	14.0	0.36
Margaree	0.007	0.32	5.4	12	0.03	8.00	22.0	0.30
Menako^	0.028	1.53	13.7	65	0.10	6.00	26.0	0.35
Monmonawson	0.009	1.19	13.0	41	0.10	0.40	22.0	0.50
Ozhiski^	0.043	1.95	15.1	83	0.10	16.00	24.0	0.39
Pickle^	0.005	0.51	8.4	25	0.05	1.10	12.0	0.28
Richter	0.002	1.48	13.7	66	0.08	6.00	22.0	0.40
Stark	0.026	1.46	15.0	75	0.11	1.10	0.9	0.42
Tarp	0.006	1.90	14.3	69	0.11	6.00	20.0	0.50
Totogan	ND	ND	ND	ND	ND	ND	ND	ND
Trading	0.041	1.59	15.5	83	0.14	16.00	10.0	0.39
Unnamed	0.025	1.78	16.2	80	0.08	4.00	26.0	0.46
Wigwascence	ND	ND	ND	ND	ND	ND	ND	ND
Williams^	0.020	1.50	9.7	37	0.06	8.00	22.0	0.32
Wright^	0.005	0.83	11.5	44	0.07	4.00	16.0	0.34

Table SI-7-continued: Chemical characteristics of 20 Shield lakes sampled for this study. See Table SI-1 for definitions of abbreviations.

Waterbody	TP (mg/L)	Sulfate (mg/L)	pH	Alk. (mg/L)	Al (µg/L)	Cond. (uS/cm)	Ca (mg/L)	Cl (µg/L)	Cu (µg/L)	DIC (me/L)
Attawapiskat^	0.013	0.400	7.72	41.7	30.3	87.4	13.4	120.0	0.30	10.10
Badesdawa^	0.011	0.450	7.54	219.0	26.3	70.8	11.6	30.0	0.30	8.12
Carpenter^	0.008	0.550	7.64	33.5	8.1	70.8	10.9	120.0	0.07	8.10
Kabania	ND	ND	ND	ND	ND	ND	ND	ND	ND	ND
Kapkichi^	0.020	0.550	7.71	195.0	9.0	80.8	13.1	120.0	0.08	9.44
Lang^	0.008	0.700	7.51	23.9	15.4	53.3	8.0	110.0	0.30	0.28
Margaree	0.009	0.110	8.25	105.0	1.6	200.0	31.9	150.0	0.04	26.30
Menako^	0.013	0.070	7.41	213.0	11.8	60.0	9.8	47.0	0.09	6.76
Monmonawson	0.012	0.020	7.54	23.5	19.5	49.5	7.9	29.0	0.04	4.98
Ozhiski^	0.013	0.500	7.68	40.3	24.7	82.2	12.3	25.0	0.30	9.26
Pickle^	0.010	0.900	7.95	54.9	3.6	114.0	18.2	420.0	0.60	12.60
Richter	0.013	0.160	7.58	29.5	19.4	62.8	9.6	26.0	0.09	7.14
Stark	0.010	0.070	7.76	40.9	20.1	85.9	13.8	120.0	0.30	9.28
Tarp	0.023	0.030	7.23	108.0	25.9	34.7	5.4	42.0	0.02	3.48
Totogan	ND	ND	ND	ND	ND	ND	ND	ND	ND	ND
Trading	0.008	0.090	7.82	50.3	16.9	101.0	16.0	19.0	0.07	11.80
Unnamed	0.011	0.130	7.62	44.4	31.0	63.8	10.5	25.0	0.05	6.46
Wigwascence	ND	ND	ND	ND	ND	ND	ND	ND	ND	ND
Williams^	0.013	0.650	7.59	32.9	10.0	66.5	9.9	150.0	0.90	7.70
Wright^	0.012	0.750	7.62	30.6	8.6	65.7	9.8	150.0	0.02	7.26

Table SI-7-continued: Chemical characteristics of 20 Shield lakes sampled for this study. See Table SI-1 for definitions of abbreviations.

Waterbody	Mg (mg/L)	Mn (µg/L)	K (mg/L)	Se (µg/L)	Si (mg/L)	Na (mg/L)	St (µg/L)	Ti (µg/L)	Zn (µg/L)
Attawapiskat^	2.67	12.80	0.39	0.197	1.36	0.51	15.80	0.80	0.10
Badesdawa^	2.31	20.50	0.25	0.056	1.32	0.40	12.40	0.80	1.50
Carpenter^	1.80	21.80	0.42	0.051	1.16	0.43	11.40	0.11	0.80
Kabania	ND	ND	ND	ND	ND	ND	ND	ND	ND
Kapkichi^	2.34	22.90	0.35	0.026	1.24	0.46	13.30	0.04	1.10
Lang^	1.67	9.60	0.36	0.197	1.20	0.48	10.70	0.03	0.80
Margaree	6.37	23.50	0.86	0.207	2.66	0.89	28.80	0.08	1.00
Menako^	1.84	15.90	0.27	0.244	1.14	0.34	10.00	0.15	1.20
Monmonawson	1.69	20.10	0.17	0.095	0.64	0.29	2.10	0.09	0.90
Ozhiski^	2.52	18.20	0.28	0.027	1.36	0.44	15.10	0.70	0.70
Pickle^	3.02	17.80	0.52	0.209	1.48	0.66	18.40	0.11	0.20
Richter	2.02	12.80	0.39	0.115	0.28	0.34	11.10	0.13	0.10
Stark	2.71	11.90	0.19	0.087	1.26	0.37	16.10	0.02	1.00
Tarp	1.19	24.10	0.15	0.072	0.46	0.24	6.90	0.24	1.00
Totogan	ND	ND	ND	ND	ND	ND	ND	ND	ND
Trading	3.42	18.30	0.20	0.134	1.68	0.41	16.50	0.06	1.30
Unnamed	1.99	13.60	0.24	0.096	0.96	0.36	12.10	0.12	1.30
Wigwascence	ND	ND	ND	ND	ND	ND	ND	ND	ND
Williams^	1.97	15.70	0.54	0.136	0.68	0.38	11.90	0.04	0.80
Wright^	1.82	23.60	0.32	0.171	1.16	0.41	11.30	0.19	1.00

Additional details on the Attawapiskat Drainage Basin (ADB): To date, the ADB has experienced relatively minimal anthropogenic disturbance. It is sparsely populated (total resident population ~ 2500 people) with only one First Nations community (Neskantaga) and one municipality (Pickle Lake) on the shield, and one First Nations community on the lowlands near James Bay (Attawapiskat). There is no commercial forest harvesting in the ADB, no water regulation structures along the entire drainage basin. There is only one all-season road, crossing the middle of the shield portion. The south-central shield region near Pickle Lake was once an active gold mining area (1928-1995; peaked pre-1970), but the only current mining activity in the ADB is the DeBeers Victor diamond mine in the lowlands, 100 km west of the James Bay coast. Study lakes were selected, in part, based on availability of historic aquatic survey information; most lakes contained both walleye and northern pike as apex predators, but a few unexpectedly contained only northern pike.

Aging of fish: Ages of large-bodied fishes were determined by counting growth annuli on bony structures. Whitefish otoliths were mounted in epoxy, and transverse thin sections were cut through the nucleus, mounted on glass slides, polished with fine-grit sandpaper, and viewed under a microscope with reflected light. Sucker fin rays were also mounted in epoxy, and thin tranverse sections were cut from the proximal end, and mounted, polished and read as for whitefish otoliths. Walleye otoliths were prepared by the crack-and-burn technique, and burned cross-sections were viewed under a dissecting scope using reflected light. Pike cleithra were cleaned of all flesh and dried, then examined whole under a dissecting scope using reflected light.

Additional water sampling: In lakes sampled in 2015 with maximum depths greater than 4 m (n = 11), water samples were also taken at 1 m above bottom near the deepest point in the lake using a Van Dorn water sampler, and analyzed for Hg and chemistry. These data are available on request. Further AIC modeling was performed with these samples (see below).

Baseline corrections of isotopes:
Baseline-corrections were done within-site by subtracting $\delta^{13}C$ or $\delta^{15}N$ values measured in clams from a given lake or river site from that of the fish (n = 21 sites with baseline clam data). In an additional eight sites where clams were not found, but stable isotope data were available for other invertebrate taxa, we first estimated clam $\delta^{13}C$ and $\delta^{15}N$ based on values from these other invertebrates (from amphipods in seven lakes, and from crayfish in one lake) using the following linear relationships developed across ADB sites where both taxa were present:

(1) Clam $\delta^{13}C = -10.394943 + 0.788606 \times$ Amphipod $\delta^{13}C$, (n = 15 sites)
(2) Clam $\delta^{13}C = -10.002771 + 0.808212 \times$ Crayfish $\delta^{13}C$, (n = 11 sites)
(3) Clam $\delta^{15}N = 1.790228 + 0.850963 \times$ Amphipod $\delta^{15}N$, (n = 15 sites)
(4) Clam $\delta^{15}N = -1.750317 + 0.934888 \times$ Crayfish $\delta^{15}N$, (n = 11 sites)

Converting [THg] between analytical methods: Conversion of wet-weight [THg] determinations ($[THg]_w$, measured via CVF-AAS) to dry-weight [THg] values ($[THg]_D$, as measured via TDA-AAS) was carried out with the following species-specific linear

equations generated from fish samples from across northern Ontario that were analyzed with both methods (T.A. Johnston, unpubl. data, Ontario Ministry of Natural Resources and Forestry):

(1) Lake Whitefish (n = 104):
$[THg]_D = -0.017641 + (4.119734 \times [THg]_W)$

(2) Northern Pike (n = 189):
$[THg]_D = -0.071315 + (4.4371164 \times [THg]_W)$

(3) White sucker (n = 302):
$[THg]_D = -0.020080 + (4.689174 \times [THg]_W)$

(4) Walleye (n = 863):
$[THg]_D = -0.378613 + (4.970530 \times [THg]_W)$

Table SI- 8: Mean ± SD whole body [MeHg] (ppm dry; n = number of composite samples) of various invertebrate taxa from all sites sampled in this study. ^Zooplankton were not collected on river sites

Site	Region	Amphipods	Mayflies	Caddisflies	Zooplankton^
Beteau Lake	River	0.029±0.000 (1)	0.024±0.000 (1)	0.076±0.000 (1)	ND
Missisa con.	River	ND	0.024±0.000 (1)	ND	ND
Muketei con.	River	ND	0.052±0.000 (1)	ND	ND
Naysh Rapids	River	ND	0.063±0.000 (1)	ND	ND
Streatfeild con.	River	ND	0.049±0.012 (2)	ND	ND
Victor	River	ND	0.051±0.037 (2)	ND	ND
Fishtrap	Lowland	0.021±0.004 (3)	ND	0.024±0.022 (3)	0.021±0.001 (1)
Goods	Lowland	0.010±0.004 (2)	0.023±0.018 (2)	0.047±0.001 (1)	0.029±0.006 (4)
Highbank	Lowland	0.006±0.005 (3)	0.007±0.009 (2)	0.026±0.011 (2)	0.018±0.003 (3)
Kapiskau	Lowland	0.024±0.016 (4)	0.024±0.011 (5)	0.022±0.007 (2)	0.004±0.001 (2)
Napken	Lowland	0.052±0.045 (3)	ND	0.030±0.020 (2)	0.005±0.001 (3)
Quantz	Lowland	0.041±0.001 (1)	0.028±0.009 (3)	0.022±0.006 (3)	0.005±0.001 (1)
Carpenter	Shield	0.030±0.001 (1)	0.024±0.006 (2)	0.017±0.008 (2)	0.030±0.008 (3)
Kapkichi	Shield	0.053±0.016 (3)	0.025±0.010 (3)	0.019±0.001 (1)	0.032±0.001 (1)
Lang	Shield	0.013±0.001 (1)	ND	ND	0.030±0.002 (4)
Menako	Shield	0.022±0.001 (2)	0.023±0.001 (1)	0.049±0.007 (3)	ND
Ozhiski	Shield	ND	0.028±0.001 (1)	0.018±0.005 (4)	0.030±0.002 (3)
Pickle	Shield	0.029±0.001 (2)	ND	ND	ND
Richter	Shield	ND	ND	0.022±0.006 (2)	0.050±0.001 (3)
Tarp	Shield	0.018±0.006 (2)	ND	0.033±0.001 (1)	0.016±0.001 (2)
Trading	Shield	ND	0.013±0.001 (1)	0.069±0.001 (1)	ND
Williams	Shield	0.032±0.001 (1)	0.107±0.001 (1)	ND	0.018±0.008 (3)

Table SI- 9: Mean ± SD predicted muscle [THg] at 500 g (ppm dry; n = number of individual fish) for large-bodied fish species sampled in this study.

Site	Region	Year of collection	Walleye	Northern Pike	White Sucker	Lake whitefish
Beteau Lake	River	2014	1.09±0.17 (21)	0.86±0.26 (19)	0.18±0.07 (8)	0.69±0.02 (3)
Canada Lake	River	2016	1.67±0.18 (28)	ND	ND	ND
Missisa con.	River	2011, 2013	1.63±0.22 (33)	0.73±0.12 (21)	0.44±0.02 (15)	ND
Muketei con.	River	2013	1.45±0.25 (24)	0.67±0.20 (11)	0.43±0.06 (7)	ND
Pym Island	River	2013	1.11±0.25 (20)	0.59±0.12 (21)	0.29±0.08 (10)	1.32±0.06 (5)
River mouth	River	2009, 2013-2015	2.11±0.28 (11)	1.04±0.12 (24)	ND	0.66±0.03 (51)
Streatfeild con.	River	2013	1.56±0.17 (20)	0.60±0.19 (8)	0.35±0.04 (4)	ND
Windsor Lake	River	2016	1.80±0.16 (28)	0.87±0.10 (24)	0.56±0.04 (16)	0.51±0.05 (14)
Victor	River	2015	1.49±0.17 (21)	0.93±0.14 (23)	0.23±0.05 (17)	0.52±0.05 (13)
Fishtrap	Lowland	2013	0.66±0.10 (39)	0.71±0.14 (24)	0.21±0.03 (21)	0.20±0.03 (11)
Goods	Lowland	2014	1.58±0.13 (22)	0.73±0.09 (19)	0.15±0.05 (19)	0.39±0.02 (14)
Highbank	Lowland	2014	0.41±0.11 (22)	0.68±0.16 (21)	0.11±0.03 (19)	0.12±0.01 (21)
Kapiskau	Lowland	2015	0.94±0.13 (18)	0.77±0.06 (16)	0.32±0.04 (17)	ND
Kitchie	Lowland	2013	ND	0.33±0.09 (16)	0.14±0.02 (19)	ND
Koper	Lowland	2013	ND	0.88±0.07 (10)	ND	ND
McFaulds	Lowland	2012	ND	0.32±0.07 (20)	0.13±0.07 (13)	ND
Missisa	Lowland	2014	1.63±0.26 (21)	0.69±0.07 (22)	0.16±0.03 (19)	0.29±0.03 (12)
Napken	Lowland	2015	1.87±0.13 (20)	1.09±0.27 (11)	0.27±0.04 (14)	ND
Quantz	Lowland	2011, 2015	1.61±0.16 (21)	0.62±0.13 (20)	0.25±0.04 (10)	ND
Streatfeild	Lowland	2014, 2015	0.93±0.09 (22)	0.52±0.06 (20)	0.13±0.04 (22)	ND
Wabimeig	Lowland	2015	1.56±0.09 (20)	0.85±0.11 (13)	0.23±0.02 (18)	ND
Attawapiskat	Shield	2014	1.29±0.14 (23)	0.70±0.32 (16)	0.29±0.03 (26)	0.25±0.02 (17)
Badesdawa	Shield	2009	2.19±0.22 (15)	1.46±0.14 (15)	0.33±0.11 (10)	0.13±0.04 (7)
Carpenter	Shield	2014	1.49±0.14 (21)	0.76±0.16 (11)	0.25±0.06 (14)	0.85±0.04 (15)
Kabania	Shield	2015	2.42±0.52 (5)	ND	ND	ND
Kapkichi	Shield	2014	1.35±0.15 (23)	0.88±0.13 (13)	0.42±0.05 (12)	0.44±0.02 (21)
Lang	Shield	2012, 2015	1.90±0.26 (19)	1.16±0.15 (22)	0.32±0.06 (19)	0.27±0.05 (10)
Menako	Shield	2012	1.22±0.20 (20)	0.34±0.25 (20)	0.29±0.05 (19)	0.19±0.01 (15)
Monmon.	Shield	2015	ND	0.38±0.08 (20)	0.13±0.01 (20)	ND
Ozhiski	Shield	2014	1.92±0.14 (22)	1.32±0.23 (21)	0.28±0.03 (14)	0.48±0.07 (9)
Pickle	Shield	2009	1.04±0.13 (10)	0.62±0.13 (15)	0.23±0.04 (9)	0.40±0.06 (15)
Richter	Shield	2014	1.42±0.14 (21)	0.54±0.16 (20)	0.27±0.03 (20)	0.13±0.02 (10)
Tarp	Shield	2015	0.33±0.11 (20)	0.52±0.07 (16)	0.16±0.01 (4)	ND
Totogan	Shield	2012	0.76±0.08 (20)	0.58±0.17 (10)	ND	ND
Trading	Shield	2015	2.24±0.19 (21)	1.54±0.15 (16)	0.35±0.11 (11)	ND
Wigwascence	Shield	2012	0.93±0.12 (19)	0.42±0.12 (20)	0.30±0.04 (20)	ND
Williams	Shield	2015	1.00±0.12 (20)	0.82±0.13 (20)	0.09±0.04 (19)	ND
Wright	Shield	2012	1.23±0.14 (20)	0.46±0.14 (20)	0.19±0.03 (19)	0.21±0.02 (20)

Table SI- 10: QAQC results for various analytical procedures. Blank concentrations ([ ]), relative percent differences (RPD), and percent recovery (%Rec) are presented as mean ± standard deviation (SD), pooled across all sample runs for each analysis. THg and MeHg in biota data from this study, as well as the QAQC data presented below, were part of larger datasets. Note: DMA = direct mercury analyzer, MDL = method detection limit, CRM = certified reference materials, NA = not applicable. Table adapted from Lescord et al. (2018a).

QA/QC measure		[THg] Water	[MeHg] Water	[THg] Biota	[MeHg] Biota
MDL	*ng/g or L*	0.05[2]	0.0006[3]	2.50[4]	0.12[5]
Daily standards	*n*	21	14	-----	97
	%Rec	101.2±8.6	100.0±7.6	-----	98.8±9.2
Method Blanks	*n*	14	8	77	95
	ng/g	0.002±0.002	0.009±0.006	0.09±0.08	6.6±35.1
Initial precision replicates (IPRs)	*n*	15	8	-----	76
	%Rec	95.2±4.6	97.3±3.1	-----	98.5±11.3
Operating precision replicates (OPRs)	*n*	22	9	-----	135
	%Rec	93.8±3.8	100.8±7.7	-----	99.8±8.3
Certified reference material (CRMs)[1]	*n*	-----	-----	67	50
	%RPD	-----	-----	1.2±4.6	-4.7±10.7
Digestion duplicates	*n*	6	8	-----	77
	%RPD	3.0±28.3	1.8±8.2	-----	-3.7±29.1
Analytical duplicates	*n*	-----	-----	61	79
	%RPD	-----	-----	0.48±6.6	10.6±23.8
Sample spikes	*n*	17	16	32	-----
	%Rec	104.4±26.5	116.6±19.8	97.0±4.7	-----
Analytical Method:		Tekran© 2700 THg System, EPA 245.7	Tekran 2600 MeHg System, EPA 1630	Milestone DMA-80, EPA 7473	Tekran 2600 MeHg System, EPA 1630

[1]DORM-4, NRC 2015 (http://www.nrc-cnrc.gc.ca/eng/solutions/advisory/crm/certificates/dorm_4.html), [2]Calculated assuming a sample volume of 0.025 L, [3]Calculated assuming a sample volume of 0.040 L, [4]Calculated assuming a sample dry weight of 0.02g, [5]Calculated assuming a sample dry weight of 0.05g.

Table SI- 11: Quality assurance and control results for stable carbon (C) and nitrogen (N) isotope analysis. Data are based on a larger data set including samples from multiple projects analyzed simultaneously (see Lescord et al. 2018b).

QA/QC measure	$\delta^{13}C$ (‰)	$\delta^{15}N$ (‰)
Certified reference material (CRMs)[1,2]	948 <0.01±0.01	953 0.2±7.5
Analytical duplicates	263 <0.01±0.06	263 <0.01±0.18
Analytical Method:	Continuous Flow-Isotope Ratio Mass Spectrometry (CF-IRMS)	

Table SI- 12: Mean ± SD C and N stable isotope ratios for foot muscle of clams (Unionidae) sampled in this study.

Site	Region	n	$\delta^{13}C$ (‰)	$\delta^{15}N$ (‰)	Comments
Canada Lake	River	0	ND	ND	
Missisa con.	River	18	-31.83±0.12	4.83±0.04	
River Mouth	River	0	ND	ND	
Muketei con.	River	19	-32.84±0.07	4.16±0.07	
Pym Island	River	10	-32.32±0.10	4.72±0.08	
Streatfeild con.	River	--	-32.75	4.25	Estimated from crayfish
Beteau Lake	River	3	-32.66±0.32	5.19±0.22	
Windsor Lake	River	0	ND	ND	
Victor	River	30	-32.27±0.04	4.46±0.06	
Fishtrap	Lowland	10	-29.50±0.12	2.72±0.13	
Goods	Lowland	10	-31.12±0.06	4.09±0.09	
Highbank	Lowland	--	-30.7	3.69	Estimated from amphipod
Kapiskau	Lowland	10	-33.80±0.08	5.52±0.08	
Kitchie	Lowland	0	ND	ND	
Koper	Lowland	0	ND	ND	
McFaulds	Lowland	0	ND	ND	
Missisa	Lowland	--	-29.64	3.14	Estimated from amphipod
Napken	Lowland	12	-32.38±0.12	4.30±0.06	
Quantz	Lowland	30	-32.29±0.14	3.55±0.06	
Streatfeild	Lowland	--	-34.31	3.19	Estimated from amphipod
Wabimeig	Lowland	0	ND	ND	
Attawapiskat	Shield	--	-33.19	4.29	Estimated from amphipod
Badesdawa	Shield	0	ND	ND	
Carpenter	Shield	10	-31.51±0.08	4.97±0.14	
Kabania	Shield	0	ND	ND	
Kapkichi	Shield	10	-31.73±0.06	4.77±0.10	
Lang	Shield	20	-31.71±0.08	3.47±0.09	
Menako	Shield	--	-32.56	4.1	Estimated from amphipod
Monmonawson	Shield	5	-23.32±0.24	2.25±0.05	
Ozhiski	Shield	1	-32.66±0.00	5.90±0.00	
Pickle	Shield	--	-30.54	4.77	Estimated from amphipod
Richter	Shield	19	-30.49±0.04	5.34±0.05	
Tarp	Shield	--	-27.49	4.25	Estimated from amphipod
Totogan	Shield	10	-32.03±0.06	3.86±0.05	
Trading	Shield	10	-33.41±0.07	4.76±0.08	
Wigwascence	Shield	3	-33.13±0.20	5.40±0.18	
Williams	Shield	4	-29.03±0.21	4.52±0.08	
Wright	Shield	10	-30.42±0.05	3.70±0.10	

Table SI- 13: Mean ± SD whole body $\delta^{13}C$ (n = number of composite samples) for invertebrate taxa examined in this study.

Site	Region	Amphipod	Caddisflies	Mayflies	Zooplankton
Beteau Lake	River	-27.92 (1)	-28.58(1)	-31.42(1)	---
Canada Lake	River	---	---	---	---
Missisa con.	River	---	-29.82(1)	-30.20±2.59 (2)	---
Muketei con.	River	---	-29.40(1)	-28.59(1)	---
Naysh rapids	River	---	---	---	---
Pym island	River	---	---	---	---
River mouth	River	---	---	---	---
Streatfeild con.	River	---	---	---	---
Windsor Lake	River	-25.19 (1)	-22.87 (1)	-27.59±0.74 (3)	---
Victor	River	---	---	---	---
Fishtrap	Lowland	-27.27±2.71 (3)	-25.95±1.86 (3)	---	-26.16 (1)
Goods	Lowland	-23.98±1.49 (2)	-24.14 (1)	-24.97±1.85 (2)	-31.70±0.16 (4)
Highbank	Lowland	-25.75±1.43 (3)	-26.32±5.15 (2)	-23.80±1.44 (2)	-26.78±0.18 (3)
Kapiskau	Lowland	-30.31±0.57 (4)	-29.39±0.06 (2)	-32.38±1.57 (5)	-32.84±0.03 (2)
Kitchie	Lowland	---	---	---	---
Koper	Lowland	---	---	---	---
McFaulds	Lowland	---	---	---	---
Missisa	Lowland	-24.41 (1)	---	-23.89 (1)	-23.31±0.49 (4)
Napken	Lowland	-28.63±0.35 (3)	-28.45±1.82 (2)	---	-35.51±0.20 (3)
Quantz	Lowland	-29.00 (1)	-29.12±0.74 (3)	-27.11±1.95 (3)	-31.55 (1)
Streatfeild	Lowland	---	---	---	---
Wabimeig	Lowland	---	---	---	---
Attawapiskat	Shield	-28.90 (1)	-28.86±0.24 (3)	-30.63±1.91 (4)	---
Badesdawa	Shield	---	---	---	---
Carpenter	Shield	-26.73 (1)	-25.11±2.26 (2)	-26.35±1.51 (2)	-31.21±0.14 (3)
Kabania	Shield	---	---	---	---
Kapkichi	Shield	-27.24±0.22 (3)	-27.20 (1)	-26.71±2.01 (3)	-32.86 (1)
Lang	Shield	-23.70 (1)	---	---	-31.76±3.67 (4)
Margaree	Shield	---	---	---	---
Menako	Shield	-28.11±0.18 (2)	-31.16±1.32 (3)	-29.29 (1)	-33.38±0.06 (3)
Monmon.	Shield	---	---	---	---
Ozhiski	Shield	---	-28.32±0.32 (4)	-29.42 (1)	-33.03±0.52 (3)
Pickle	Shield	-26.34±2.65 (2)	---	---	-30.82±0.11 (3)
Richter	Shield	---	-27.23±0.64 (2)	---	-31.48±0.26 (3)
Tarp	Shield	-21.68±3.14 (2)	-24.35 (1)	---	-25.83±0.64 (2)
Totogan	Shield	---	---	---	---
Trading	Shield	---	-37.43 (1)	-29.69 (1)	-34.20±0.22 (3)
Wigwascence	Shield	---	---	---	---
Williams	Shield	-24.35 (1)	---	-21.57 (1)	-32.49±0.36 (3)
Wright	Shield	-27.92 (1)	-28.58 (1)	-31.42 (1)	-26.16 (1)

Table SI- 14: Mean ± SD whole body $\delta^{15}N$ (n = number of composite samples) for invertebrate taxa examined in this study.

Site	Region	Amphipod	Caddisflies	Mayflies	Zooplankton
Beteau Lake	River	3.51 (1)	3.98 (1)	3.37 (1)	---
Canada Lake	River	---	---	---	---
Missisa con.	River	---	4.66 (1)	3.27±0.18 (2)	---
Muketei con.	River	---	2.97 (1)	4.19 (1)	---
Pym Island	River	---	---	---	---
River mouth	River	---	---	---	---
Streatfeild con.	River	---	---	---	---
Windsor Lake	River	---	---	3.84±0.09 (2)	---
Victor	River	3.54 (1)	1.85 (1)	3.47±0.34 (3)	---
Fishtrap	Lowland	---	---	---	2.51 (1)
Goods	Lowland	0.89±0.81 (3)	1.47±1.33 (3)		4.44±0.13 (4)
Highbank	Lowland	1.83±0.32 (2)	3.13 (1)	2.11±0.21 (2)	1.95±0.00 (3)
Kapiskau	Lowland	2.23±0.66 (3)	2.50±0.57 (2)	2.32±0.25 (2)	4.78±0.16 (2)
Kitchie	Lowland	4.18±0.57 (4)	4.44±0.38 (2)	3.75±0.83 (5)	---
Koper	Lowland	---	---	---	---
McFaulds	Lowland	---	---	---	---
Missisa	Lowland	---	---	---	1.59±0.20 (4)
Napken	Lowland	1.59 (1)	---	1.98 (1)	3.64±0.11 (3)
Quantz	Lowland	3.57±1.19 (3)	3.71±1.01 (2)	---	3.24 (1)
Streatfeild	Lowland	3.61 (1)	3.43±0.54 (3)	2.87±0.22 (3)	---
Wabimeig	Lowland	---	---	---	---
Attawapiskat	Shield	---	---	---	---
Badesdawa	Shield	2.94 (1)	3.27±0.73 (3)	3.27±0.46 (4)	---
Carpenter	Shield	---	---	---	5.45±0.28 (3)
Kabania	Shield	3.16 (1)	3.70±0.36 (2)	2.85±0.56 (2)	---
Kapkichi	Shield	---	---	---	5.35 (1)
Lang	Shield	4.33±0.38 (3)	2.93 (1)	3.46±0.34 (3)	5.70±0.70 (4)
Menako	Shield	1.86 (1)	---	---	---
Monmon.	Shield	---	---	---	4.72±0.01 (3)
Ozhiski	Shield	2.72±0.33 (2)	4.21±0.39 (3)	2.80 (1)	---
Pickle	Shield	---	---	---	7.18±0.11 (3)
Richter	Shield	---	4.01±1.93 (4)	4.34 (1)	4.73±0.08 (3)
Tarp	Shield	3.31±0.85 (2)		---	3.67±0.09 (3)
Totogan	Shield	---	4.55±1.10 (2)	---	4.28±0.09 (2)
Trading	Shield	2.89±1.11 (2)	4.95 (1)	---	---
Wigwascence	Shield	---	---	---	5.53±0.25 (3)
Williams	Shield	---	4.06 (1)	3.80 (1)	---
Wright	Shield	---	---	---	4.49±0.41 (3)

Table SI- 15: Mean ± SD body condition (residual $\log_e$ mass; n = number of individual fish) of large-bodied fish species examined in this study..

Site	Region	Walleye	Northern Pike	White Sucker	Lake Whitefish
Beteau Lake	River	0.05±0.02 (21)	0.08±0.04 (20)	0.07±0.03 (18)	0.04±0.03 (3)
Canada Lake	River	-0.02±0.01 (82)	---	-0.03±0.02 (16)	---
Missisa con.	River	-0.04±0.02 (33)	0.03±0.02 (21)	-0.08±0.02 (15)	---
Muketei con.	River	-0.03±0.02 (24)	0.10±0.03 (11)	-0.10±0.05 (7)	---
Naysh rapids	River	---	---	---	---
Pym island	River	0.01±0.02 (20)	0.04±0.02 (21)	<0.01±0.01 (11)	-0.27±0.06 (5)
River mouth	River	0.03±0.03 (11)	0.08±0.03 (24)	---	-0.02±0.02 (88)
Streatfeild con.	River	<0.01±0.02 (20)	0.14±0.03 (8)	-0.07±0.02 (4)	---
Windsor Lake	River	-0.01±0.02 (39)	0.08±0.02 (39)	-0.02±0.03 (16)	-0.11±0.02 (31)
Victor	River	-0.02±0.02 (23)	-0.01±0.04 (22)	-0.04±0.01 (17)	-0.12±0.04 (14)
Fishtrap	Lowland	0.01±0.01 (40)	-0.05±0.04 (26)	-0.02±0.02 (21)	-0.07±0.02 (11)
Goods	Lowland	0.02±0.02 (22)	0.01±0.03 (19)	0.06±0.01 (20)	0.05±0.02 (14)
Highbank	Lowland	0.03±0.02 (21)	-0.19±0.05 (21)	0.08±0.02 (20)	0.22±0.04 (21)
Kapiskau	Lowland	-0.02±0.04 (18)	0.05±0.03 (16)	0.06±0.02 (16)	---
Kitchie	Lowland	---	0.03±0.02 (16)	-0.01±0.01 (40)	---
Koper	Lowland	---	-0.02±0.02 (10)	---	---
McFaulds	Lowland	---	0.02±0.01 (45)	-0.03±0.02 (18)	---
Missisa	Lowland	-0.07±0.02 (21)	-0.06±0.03 (22)	-0.10±0.03 (20)	-0.15±0.03 (12)
Napken	Lowland	0.05±0.01 (20)	0.01±0.04 (11)	<0.01±0.01 (14)	---
Quantz	Lowland	0.07±0.02 (23)	-0.02±0.02 (20)	0.08±0.02 (20)	---
Streatfeild	Lowland	-0.05±0.02 (23)	-0.08±0.02 (20)	0.03±0.02 (20)	---
Wabimeig	Lowland	-0.02±0.02 (51)	0.00±0.03 (13)	-0.12±0.05 (18)	---
Attawapiskat	Shield	0.05±0.03 (34)	0.05±0.02 (32)	0.03±0.02 (31)	0.01±0.05 (17)
Badesdawa	Shield	0.04±0.02 (21)	-0.10±0.03 (17)	0.07±0.02 (16)	0.11±0.02 (7)
Carpenter	Shield	-0.03±0.02 (21)	-0.08±0.04 (11)	-0.02±0.01 (14)	0.09±0.03 (16)
Kabania	Shield	0.07±0.05 (6)	---	---	---
Kapkichi	Shield	0.02±0.02 (23)	-0.07±0.03 (13)	-0.05±0.03 (12)	0.03±0.02 (21)
Lang	Shield	-0.04±0.00 (14)	-0.01±0.02 (29)	-0.03±0.01 (58)	-0.09±0.04 (10)
Margaree	Shield	---	---	---	---
Menako	Shield	<0.01±0.01 (21)	0.01±0.02 (20)	-0.04±0.02 (20)	0.03±0.02 (15)
Monmon.	Shield	---	-0.01±0.03 (20)	-0.05±0.02 (21)	---
Ozhiski	Shield	-0.02±0.03 (23)	<0.01±0.02 (20)	0.06±0.02 (15)	0.14±0.04 (9)
Pickle	Shield	0.27±0.02 (10)	0.08±0.03 (20)	-0.04±0.02 (20)	-0.10±0.01 (20)
Richter	Shield	-0.02±0.01 (21)	-0.07±0.04 (20)	0.03±0.01 (20)	0.09±0.02 (10)
Tarp	Shield	0.04±0.02 (20)	-0.09±0.06 (16)	0.10±0.06 (4)	---
Totogan	Shield	0.04±0.00 (12)	0.03±0.02 (46)	0.02±0.01 (92)	0.21±0.03 (11)
Trading	Shield	0.05±0.02 (21)	-0.08±0.03 (16)	0.01±0.02 (11)	---
Wigwascence	Shield	0.04±0.01 (20)	-0.03±0.02 (20)	0.03±0.02 (20)	---
Williams	Shield	0.02±0.02 (20)	-0.03±0.03 (20)	-0.02±0.03 (19)	---
Wright	Shield	-0.02±0.02 (20)	0.06±0.03 (20)	0.03±0.01 (20)	<0.01±0.02 (20)

Table SI- 16: Mean ± SD lifetime growth rate at 1000 g (g / year; n = number of individual fish) for large-bodied fish species examined in this study.

Site	Region	Walleye	Northern Pike	White Sucker	Lake Whitefish
Beteau Lake	River	102.53±4.65 (21)	146.93±10.50 (20)	144.09±8.18 (18)	109.78±11.39 (3)
Canada Lake	River	80.28±2.18 (82)	---	136.23±4.86 (16)	---
Missisa outlet	River	89.02±4.35 (33)	152.35±7.33 (21)	150.97±3.80 (15)	---
Muketei outlet	River	85.71±3.78 (24)	215.92±16.37 (11)	199.43±1.83 (7)	---
Naysh rapids	River	---	---	---	---
Pym island	River	98.36±3.62 (20)	179.88±11.77 (21)	128.50±6.34 (11)	89.71±7.35 (5)
River mouth	River	86.87±11.03 (11)	236.73±17.06 (24)	---	134.53±2.82 (88)
Streatfeild outlet	River	69.69±3.78 (20)	235.06±24.38 (8)	113.42±6.99 (4)	---
Windsor Lake	River	90.21±3.51 (39)	236.17±13.67 (39)	118.51±3.31 (16)	111.46±4.14 (31)
Victor	River	---	---	---	---
Fishtrap	Lowland	89.98±3.49 (40)	127.08±10.10 (26)	176.82±14.39 (21)	146.74±9.96 (11)
Goods	Lowland	68.87±2.10 (22)	146.75±7.68 (19)	123.08±7.00 (20)	103.76±3.42 (14)
Highbank	Lowland	125.90±6.79 (21)	163.55±7.95 (21)	165.51±9.86 (20)	218.70±8.45 (21)
Kapiskau	Lowland	91.48±6.01 (18)	161.46±8.33 (16)	118.03±4.66 (16)	---
Kitchie	Lowland	---	161.50±6.50 (16)	0.00±0.00 (40)	---
Koper	Lowland	---	88.73±6.35 (10)	---	---
McFaulds	Lowland	---	258.09±7.16 (45)	63.86±4.28 (18)	---
Missisa	Lowland	47.66±2.68 (21)	175.72±8.07 (22)	88.57±5.51 (20)	121.42±3.44 (12)
Napken	Lowland	49.58±1.87 (20)	199.58±18.30 (11)	115.16±8.11 (14)	---
Quantz	Lowland	74.81±4.30 (23)	219.71±9.45 (20)	134.89±5.53 (20)	---
Streatfeild	Lowland	69.06±2.84 (23)	137.12±6.83 (20)	100.21±6.81 (20)	---
Wabimeig	Lowland	29.25±1.98 (51)	148.50±6.59 (13)	120.76±3.88 (18)	---
Attawapiskat	Shield	89.38±4.11 (34)	154.54±6.62 (32)	119.12±3.40 (31)	91.79±5.83 (17)
Badesdawa	Shield	87.60±4.37 (21)	151.56±6.47 (17)	132.31±7.78 (16)	147.53±9.99 (7)
Carpenter	Shield	85.11±4.49 (21)	211.89±20.37 (11)	106.42±4.48 (14)	144.04±7.55 (16)
Kabania	Shield	73.12±5.08 (6)	---	---	---
Kapkichi	Shield	91.98±3.90 (23)	178.86±11.86 (13)	120.05±9.07 (12)	89.34±3.08 (21)
Lang	Shield	73.78±3.16 (14)	184.78±11.31 (29)	121.43±4.48 (58)	59.23±6.39 (10)
Margaree	Shield	---	---	---	---
Menako	Shield	66.64±3.86 (21)	176.14±9.28 (20)	118.41±6.70 (20)	105.26±7.59 (15)
Monmon.	Shield	---	241.42±15.16 (20)	143.97±2.03 (21)	0.00±0.00 (0)
Ozhiski	Shield	76.68±2.98 (23)	179.06±9.33 (20)	135.29±6.28 (15)	76.65±10.88 (9)
Pickle	Shield	165.09±9.64 (10)	278.88±18.92 (20)	92.17±4.03 (20)	85.51±4.12 (20)
Richter	Shield	68.07±3.27 (21)	178.25±8.33 (20)	124.81±6.54 (20)	144.26±8.63 (10)
Tarp	Shield	38.48±3.50 (20)	220.59±16.78 (16)	269.14±3.73 (4)	---
Totogan	Shield	64.71±1.06 (12)	184.12±6.25 (46)	111.64±2.83 (92)	155.53±7.93 (11)
Trading	Shield	77.87±4.87 (21)	201.87±8.79 (16)	117.79±10.37 (11)	---
Wigwascence	Shield	77.26±4.25 (20)	164.28±9.03 (20)	120.71±5.07 (20)	---
Williams	Shield	68.40±3.22 (20)	246.93±10.93 (20)	128.43±4.18 (19)	---
Wright	Shield	84.69±4.12 (20)	256.90±18.37 (20)	131.69±6.49 (20)	139.79±10.40 (20)

Table SI- 17: Mean ± SD muscle $\delta^{13}C_{cor}$ at 500 g (n = number of individual fish sampled) for large-bodied fish species examined in this study.

Site	Region	Walleye	Northern Pike	White Sucker	Lake Whitefish
Beteau Lake	River	4.89±0.41 (10)	5.79±0.24 (10)	4.34±0.25 (10)	8.23±0.32 (3)
Canada Lake	River	---	---	---	---
Missisa outlet	River	3.82±0.45 (10)	3.13±0.25 (10)	2.23±0.39 (10)	---
Muketei outlet	River	4.81±0.13 (10)	4.11±0.17 (11)	2.67±0.61 (7)	---
Naysh rapids	River	---	---	---	---
Pym island	River	4.81±0.32 (15)	4.51±0.19 (20)	3.45±0.61 (11)	7.72±0.25 (5)
River mouth	River	---	---	---	---
Streatfeild outlet	River	4.22±0.15 (10)	4.53±0.24 (8)	4.72±0.62 (4)	---
Windsor Lake	River	4.54±0.08 (26)	3.81±0.19 (12)	3.24±0.34 (10)	9.92±0.54 (20)
Victor	River				
Fishtrap	Lowland	6.50±0.09 (11)	6.73±0.08 (10)	5.35±0.58 (11)	4.38±0.81 (11)
Goods	Lowland	2.76±0.24 (10)	2.95±0.23 (10)	3.19±0.35 (10)	1.66±0.23 (10)
Highbank	Lowland	5.28±0.19 (10)	5.46±0.10 (10)	4.69±0.26 (10)	5.26±0.17 (10)
Kapiskau	Lowland	3.09±0.09 (10)	3.08±0.10 (10)	-0.36±0.43 (10)	---
Kitchie	Lowland	---	---	---	---
Koper	Lowland	---	---	---	---
McFaulds	Lowland	---	---	---	---
Missisa	Lowland	6.99±0.10 (10)	6.40±0.17 (10)	5.96±0.24 (10)	6.00±0.15 (12)
Napken	Lowland	2.80±0.14 (10)	3.06±0.18 (10)	2.08±0.53 (10)	---
Quantz	Lowland	3.18±0.12 (12)	2.99±0.09 (10)	2.29±0.40 (10)	---
Streatfeild	Lowland	6.57±0.07 (13)	5.01±0.30 (10)	5.05±0.13 (10)	---
Wabimeig	Lowland	---	---	---	---
Attawapiskat	Shield	4.00±0.14 (32)	4.77±0.14 (24)	4.81±0.35 (19)	5.38±0.35 (15)
Badesdawa	Shield	---	---	---	---
Carpenter	Shield	3.88±0.21 (11)	4.49±0.11 (11)	2.75±0.31 (10)	-0.46±0.69 (9)
Kabania	Shield	---	---	---	---
Kapkichi	Shield	2.59±0.10 (14)	3.40±0.16 (10)	2.90±0.46 (10)	1.59±0.13 (12)
Lang	Shield	4.07±0.18 (9)	5.52±0.11 (12)	5.03±0.44 (10)	4.74±0.64 (10)
Margaree	Shield	---	---	---	---
Menako	Shield	4.73±0.10 (10)	5.85±0.13 (10)	5.49±0.31 (10)	5.54±0.29 (10)
Monmon.	Shield	---	---	---	---
Ozhiski	Shield	3.45±0.18 (13)	3.82±0.19 (10)	4.36±0.40 (10)	3.57±0.59 (9)
Pickle	Shield	2.92±0.19 (10)	1.96±0.26 (10)	4.19±0.56 (10)	1.89±0.36 (10)
Richter	Shield	2.78±0.17 (10)	3.50±0.18 (9)	4.49±0.52 (9)	-3.69±0.30 (10)
Tarp	Shield	3.73±0.17 (10)	3.37±0.12 (10)	2.87±0.22 (4)	---
Totogan	Shield	3.38±0.31 (12)	4.39±0.26 (10)	---	---
Trading	Shield	3.50±0.17 (11)	4.02±0.10 (10)	2.26±0.40 (10)	---
Wigwascence	Shield	5.12±0.15 (10)	5.79±0.10 (10)	5.62±0.32 (10)	---
Williams	Shield	3.41±0.23 (10)	2.30±0.36 (10)	2.19±0.48 (10)	---
Wright	Shield	4.76±0.34 (10)	3.37±0.30 (10)	2.90±0.60 (10)	2.33±0.68 (10)

Table SI- 18: Mean ± SD muscle $\delta^{15}N_{cor}$ at 500 g (n = number of individual fish sampled) for large-bodied fish species examined in this study.

Site	Region	Walleye	Northern Pike	White Sucker	Lake Whitefish
Beteau Lake	River	5.24±0.17 (10)	4.87±0.22 (10)	2.65±0.27 (10)	3.23±0.10 (3)
Canada Lake	River	---	---	---	---
Missisa outlet	River	5.52±0.09 (10)	4.80±0.17 (10)	2.82±0.14 (10)	---
Muketei outlet	River	6.45±0.07 (10)	5.74±0.09 (11)	2.62±0.16 (7)	---
Naysh rapids	River	---	---	---	---
Pym island	River	5.47±0.19 (15)	4.66±0.16 (20)	2.01±0.21 (11)	5.29±0.21 (5)
River mouth	River	---	---	---	---
Streatfeild outlet	River	6.20±0.17 (10)	5.02±0.15 (8)	2.71±0.09 (4)	---
Windsor Lake	River	6.14±0.08 (26)	5.27±0.04 (12)	2.95±0.12 (10)	5.44±0.15 (20)
Victor	River	---	---	---	---
Fishtrap	Lowland	6.79±0.11 (11)	5.54±0.05 (10)	2.94±0.18 (11)	4.58±0.10 (11)
Goods	Lowland	6.82±0.15 (10)	6.19±0.18 (10)	2.88±0.17 (10)	4.12±0.14 (10)
Highbank	Lowland	6.04±0.10 (10)	5.45±0.08 (10)	1.82±0.12 (10)	2.84±0.05 (10)
Kapiskau	Lowland	5.45±0.08 (10)	5.03±0.07 (10)	2.05±0.15 (10)	---
Kitchie	Lowland	---	---	---	---
Koper	Lowland	---	---	---	---
McFaulds	Lowland	---	---	---	---
Missisa	Lowland	6.61±0.09 (10)	6.10±0.06 (10)	3.02±0.10 (10)	4.26±0.13 (12)
Napken	Lowland	6.71±0.07 (10)	6.79±0.12 (10)	3.84±0.19 (10)	---
Quantz	Lowland	7.40±0.17 (12)	6.90±0.19 (10)	4.38±0.12 (10)	---
Streatfeild	Lowland	6.50±0.07 (13)	6.37±0.11 (10)	2.71±0.08 (10)	---
Wabimeig	Lowland	---	---	---	---
Attawapiskat	Shield	6.72±0.12 (32)	6.39±0.11 (24)	4.47±0.24 (19)	4.92±0.26 (15)
Badesdawa	Shield	---	---	---	---
Carpenter	Shield	6.43±0.13 (11)	5.80±0.15 (11)	4.37±0.19 (10)	5.21±0.10 (9)
Kabania	Shield	---	---	---	---
Kapkichi	Shield	6.61±0.11 (14)	6.43±0.07 (10)	4.11±0.32 (10)	4.24±0.07 (12)
Lang	Shield	6.05±0.10 (9)	6.01±0.11 (12)	3.29±0.12 (10)	4.85±0.16 (10)
Margaree	Shield	---	---	---	---
Menako	Shield	6.24±0.17 (10)	5.90±0.16 (10)	3.35±0.24 (10)	3.79±0.10 (10)
Monmon.	Shield	---	---	---	---
Ozhiski	Shield	5.51±0.11 (13)	5.26±0.13 (10)	4.11±0.28 (10)	4.30±0.15 (9)
Pickle	Shield	6.28±0.14 (10)	6.33±0.09 (10)	3.20±0.21 (10)	5.94±0.30 (10)
Richter	Shield	6.99±0.11 (10)	6.01±0.14 (9)	1.91±0.20 (9)	5.87±0.18 (10)
Tarp	Shield	6.13±0.12 (10)	5.41±0.13 (10)	3.15±0.12 (4)	---
Totogan	Shield	7.02±0.07 (12)	6.86±0.17 (10)	---	---
Trading	Shield	6.16±0.10 (11)	6.47±0.18 (10)	3.31±0.09 (10)	---
Wigwascence	Shield	5.42±0.14 (10)	5.22±0.08 (10)	2.49±0.14 (10)	---
Williams	Shield	5.85±0.09 (10)	5.46±0.25 (10)	3.22±0.16 (10)	---
Wright	Shield	6.97±0.15 (10)	6.73±0.14 (10)	4.06±0.12 (10)	4.89±0.30 (10)

Table SI- 19: Loadings from Principal Components Analysis (PCA) of water chemistry and drainage basin characteristics using data from all lake and river sites examined in this study.

Parameter	PC1	PC2	PC3	PC4	PC5	PC6
DOC	0.302	-0.117	0.069	-0.034	0.012	-0.102
Sulfate	-0.195	-0.059	-0.121	-0.219	-0.419	0.117
TN	0.096	0.098	-0.088	0.200	0.380	-0.409
TP	0.119	0.039	-0.384	0.414	-0.088	-0.139
NH_3+NH_4	-0.203	0.009	-0.082	-0.028	-0.026	-0.482
NO_2+NO_3	0.254	-0.202	0.060	-0.115	-0.196	-0.155
Colour	0.300	-0.145	0.010	-0.045	-0.086	-0.052
pH	-0.283	-0.068	-0.159	0.130	0.129	-0.080
Conductivity	-0.174	-0.423	-0.016	0.028	0.119	0.078
Alkalinity	-0.119	-0.086	0.121	0.002	-0.094	-0.349
Al	00.250	-0.035	-0.190	0.291	-0.146	0.000
As	0.250	-0.146	0.051	0.019	-0.199	-0.219
Ca	-0.094	-0.470	0.064	0.052	0.117	0.115
Cl	0.058	-0.115	-0.552	-0.321	0.129	0.016
Cu	-0.096	-0.031	-0.327	0.216	-0.418	0.137
Fe	0.295	-0.152	0.024	0.038	-0.053	0.033
Mg	-0.179	-0.387	0.033	0.132	0.113	-0.044
Mn	0.203	-0.156	0.050	0.293	-0.018	0.062
K	-0.267	0.030	-0.110	0.015	-0.291	-0.021
Se	-0.012	-0.045	-0.062	0.379	-0.016	0.371
Na	0.082	-0.157	-0.511	-0.321	0.148	-0.064
D.O.	-0.208	0.133	-0.130	0.319	0.232	-0.071
DIC	-0.120	-0.435	0.087	0.017	0.129	0.046
Wetlands	-0.062	-0.174	0.065	0.119	-0.311	-0.383
Slope	-0.285	-0.002	0.103	-0.029	-0.172	-0.120
Eigen-Value	9.51	3.73	2.10	1.93	1.71	1.49
Proportion of Variance	0.38	0.15	0.08	0.08	0.07	0.06

Table SI- 20: Loadings from Principal Components Analysis (PCA) of water chemistry and drainage basin characteristics using data from all lakes examined in this study.

Parameter	PC1	PC2	PC3	PC4	PC5	PC6
DOC	0.212	0.258	0.205	-0.088	-0.039	0.059
Sulfate	-0.256	-0.073	-0.131	0.154	-0.274	0.222
TN	0.176	-0.035	0.169	-0.252	0.304	0.034
TP	0.190	0.040	-0.186	0.231	0.027	-0.489
NH_3+NH_4	-0.142	0.028	0.263	0.052	-0.082	-0.476
NO_2+NO_3	-0.065	0.285	0.285	0.137	-0.060	0.126
Colour	0.179	0.317	0.108	0.009	-0.137	-0.014
pH	-0.242	0.140	-0.151	-0.232	0.259	-0.014
Conductivity	-0.233	0.268	-0.124	-0.151	0.093	-0.028
Alkalinity	-0.096	0.052	0.203	0.053	-0.358	-0.406
Al	0.230	0.033	-0.115	0.230	0.092	-0.126
As	0.106	0.318	0.147	0.191	-0.108	0.196
Ca	-0.198	0.303	-0.119	-0.180	0.046	-0.040
Cl	0.032	0.146	-0.476	0.010	-0.091	0.093
Cu	-0.075	0.007	-0.249	0.306	0.088	-0.168
Fe	0.203	0.286	-0.117	0.009	-0.184	-0.002
Mg	-0.228	0.248	-0.009	-0.165	0.213	-0.114
Mn	0.141	0.069	-0.142	-0.044	-0.316	0.296
K	-0.277	-0.125	-0.118	0.147	-0.058	-0.012
Se	0.025	-0.053	-0.278	0.233	0.181	-0.044
Na	0.040	0.298	-0.292	0.059	-0.092	-0.027
D.O.	0.213	-0.175	-0.090	-0.050	0.241	0.066
DIC	-0.187	0.281	-0.080	-0.156	0.102	-0.122
Wetlands	-0.096	0.191	0.215	0.347	0.295	0.204
Slope	-0.300	-0.098	0.099	-0.039	-0.080	-0.007
Surface Area	-0.087	0.099	0.117	0.413	0.377	0.104
Max. Depth	-0.252	-0.012	0.055	0.320	-0.147	0.114
Secchi Depth	-0.303	-0.114	-0.031	-0.067	-0.095	0.133
Eigen-Value	8.9	5.3	3.2	2.7	1.5	1.2
Proportion of Variance	0.32	0.19	0.11	0.10	0.05	0.04

Table SI- 21: Among-region (i.e., Shield lakes vs. Lowland lakes vs. river sites) comparisons of physico-chemical parameters.

Parameter	Kruskal Wallis p-value	Post-Hoc comparison p-values		
		Shield vs. Lowland	Shield vs. River	Lowland vs. River
Al	<0.001	<0.001	<0.001	0.030
Alk	0.042	0.036	0.340	0.535
As	<0.001	0.167	<0.001	0.015
Ca	0.098	0.999	0.570	0.110
Cl	0.003	0.003	0.011	0.936
Colour	<0.001	0.002	<0.001	0.013
Cond.	0.330	0.590	0.999	0.510
Cu	0.237	0.620	0.999	0.290
D.O.	<0.001	0.038	<0.001	<0.001
DIC	0.043	0.043	0.372	0.736
DOC	<0.001	0.181	<0.001	<0.001
D. area	0.388	0.830	0.999	0.530
Fe	<0.001	0.047	<0.001	<0.001
K	<0.001	<0.001	<0.001	0.999
Max depth	0.022	0.022	NA	NA
Mg	0.163	0.170	0.999	0.610
Mn	0.198	0.999	0.330	0.430
Na	<0.001	0.999	<0.001	0.012
NH_3/NH_4	0.004	0.163	0.002	0.845
NO2+NO3	0.002	0.207	0.064	0.001
pH	0.045	0.999	0.042	0.397
Se	0.811	0.999	0.999	0.999
Secchi	<0.001	<0.001	NA	NA
Slope	<0.001	<0.001	<0.001	0.999
Sulfate	<0.001	<0.001	0.010	0.015
S. Area	0.757	0.757	NA	NA
TN	0.059	0.999	0.120	0.150
TP	0.007	0.004	0.290	0.193
Wetlands	0.223	0.999	0.280	0.920

Table SI- 22: Linear relationships between various physicochemical measurements in surface water of lakes and river sites and system elevation across the ADB. Significant results are bolded. *Sample sizes differed among models because not all chemical measurements were taken at all sites.

Parameter	Equation	n*	p-value	r2
Lake and River sites				
$MeHg_{surface}$	**y = <0.001x + 0.046**	**44**	**<0.001**	**0.228**
$THg_{surface}$	**y = -0.011x + 4.969**	**44**	**<0.001**	**0.378**
Ca	y = -0.002x + 11.562	48	0.603	-0.015
D.O.	y = 0.004x + 6.893	27	0.202	0.001
DOC	**y = -0.035x + 24.771**	**49**	**<0.001**	**0.445**
Mean Slope	**y = 0.007x + 0.597**	**27**	**<0.001**	**0.563**
Na	**y = -0.001x + 0.867**	**47**	**0.001**	**0.187**
NO2NO3	**y = -0.051x + 23.651**	**27**	**<0.001**	**0.218**
pH	**y = 0.001x + 7.171**	**49**	**0.003**	**0.155**
Sulfate	**y = 0.001x -0.069**	**27**	**<0.001**	**0.264**
TN	y = 0.028x + 384.092	49	0.815	-0.020
TP	**y = -0.018x + 18.614**	**27**	**0.046**	**0.065**
Lakes only				
$MeHg_{surface}$	y = <0.001x + 0.0197	24	0.667	0.008
$THg_{surface}$	**y = -0.005x + 3.158**	**24**	**<0.001**	**0.462**
$MeHg_{deep}$	y = <0.001x + 0.0216	8	0.787	0.009
THg_{deep}	y = -0.005x + 3.077	8	0.065	0.255
Ca	y = 0.005x + 9.181	49	0.533	-0.024
D.O.	y = -0.002x + 8.917	27	0.112	0.061
DOC	**y = -0.019x + 19.468**	**47**	**0.001**	**0.312**
Mean Slope	**y = 0.009x + 0.057**	**27**	**<0.001**	**0.753**
Na	**y = -0.007x + 0.649**	**48**	**0.016**	**0.180**
NO2NO3	y = -0.003x + 7.363	27	0.794	-0.037
pH	y = 0.001x + 7.373	43	0.178	0.034
Sulfate	**y = 0.002x -2.717**	**24**	**<0.001**	**0.367**
TN	y = -0.152x + 439.240	56	0.296	0.005
TP	**y = -0.030x + 22.604**	**26**	**0.021**	**0.164**

Table SI- 23: Within-group and among-region comparisons in [Hg] (i.e., Shield lakes vs. Lowland lakes vs. river sites) in water, invertebrates, fish, as well as TMSs and TMIs). *Zooplankton were sampled in lakes only

Model	Kruskal Wallis p-value	Post-Hoc comparisons		
		Shield-Lowland	Shield-River	Lowland-River
Water [THg] (Surface)	<0.001	0.002	<0.001	0.023
Water [MeHg] (Surface)	<0.001	0.999	0004	0.008
Water [THg] (Deep, lakes only)	0.527	---	---	---
Water [MeHg] (Deep, lakes only)	0.633	---	---	---
Invertebrate [MeHg], amphipods	0.464	0.999	0.999	0.970
Invertebrate [MeHg], caddisflies	0.063	0.999	0.063	0.129
Invertebrate [MeHg], mayflies	0.238	0.450	0.999	0.430
Invertebrate [MeHg], zooplankton*	0.032	0.032	---	---
Fish [THg] @ 500g, white sucker	0.011	0.152	0.194	0.005
Fish [THg] @ 500g, lake whitefish	0.024	0.928	0.039	0.015
Fish [THg] @ 500g, northern pike	0.811	0.999	0.999	0.999
Fish [THg] @ 500g, walleye	0.499	0.999	0.999	0.760
TMSs	0.710	0.999	0.999	0.999
TMIs	0.968	0.999	0.999	0.999

Table SI-23-continued: Post hoc comparisons for [THg] in fish (standardized to 500g) using convers test

	White sucker	Whitefish	Northern pike
Whitefish	0.056	---	<0.001
Northern pike	<0.001	<0.001	---
Walleye	<0.001	<0.001	<0.001

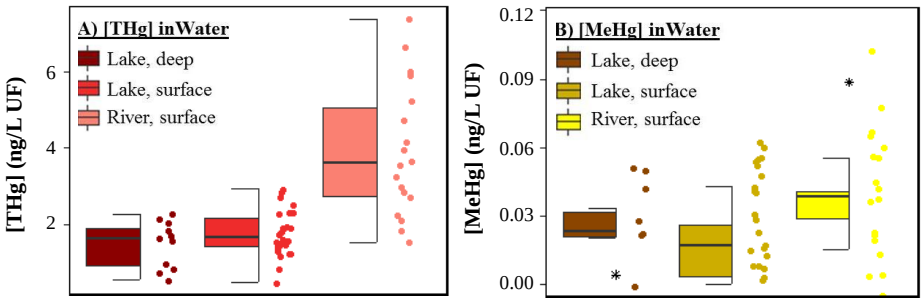

Figure SI- 1: Mercury concentrations in water from lakes and river sites at differing depths across the Attawapiskat Drainage Basin. Each data point represented 1 measure/lake or river site. Note that all river sites were sampled as a surface grab. Lakes that were >4m in maximum depth were samples both at the surface and deep points (1m off bottom at the deepest accessible part). Lakes that were <4m in maximum depth were only samples at the surface.

Table SI- 24: Within-group and among-region comparisons in ecological end-points (i.e., Shield lakes vs. Lowland lakes vs. river sites) in invertebrates and fish. Fish isotope values and body condition were standardized to 500g round weight; LGR was standardized to 1kg round weight. *Zooplankton were sampled in lakes only. Note: cond. = condition; LGR = lifetime growth rate.

Model	Kruskal Wallis p-value	Post-Hoc comparisons		
		Shield-Lowland	Shield-River	Lowland-River
Invertebrate $\delta^{15}N$, amphipods	0.558	0.999	0.999	0.940
Invertebrate $\delta^{15}N$, caddisflies	0.249	0.400	0.690	0.999
Invertebrate $\delta^{15}N$, mayflies	0.054	0.377	0.602	0.041
Invertebrate $\delta^{15}N$, zooplankton*	0.006	0.003	---	---
Fish $\delta^{15}N_{cor}$ @ 500g, white sucker	0.006	0.065	0.002	0.541
Fish $\delta^{15}N_{cor}$ @ 500g, lake whitefish	0.231	0.400	0.999	0.480
Fish $\delta^{15}N_{cor}$ @ 500g, northern pike	0.010	0.999	0.008	0.014
Fish $\delta^{15}N_{cor}$ @ 500g, walleye	0.128	0.730	0.740	0.130
Invertebrate $\delta^{13}C$, amphipods	0.591	0.999	0.999	0.999
Invertebrate $\delta^{13}C$, caddisflies	0.560	0.999	0.999	0.930
Invertebrate $\delta^{13}C$, mayflies	0.219	0.999	0.790	0.290
Invertebrate $\delta^{13}C$, zooplankton*	0.380	0.400	---	---
Fish $\delta^{13}C_{cor}$, white sucker	0.766	0.999	0.999	0.999
Fish $\delta^{13}C_{cor}$, lake whitefish	0.027	0.999	0.012	0.094
Fish $\delta^{13}C_{cor}$, northern pike	0.923	0.999	0.999	0.999
Fish $\delta^{13}C_{cor}$, walleye	0.189	0.999	0.230	0.999
Fish LGR, white sucker	0.300	0.999	0.520	0.540
Fish LGR, lake whitefish	0.121	0.130	0.999	0.740
Fish LGR, northern pike	0.042	0.053	0.999	0.133
Fish LGR, walleye	0.187	0.999	0.290	0.360
Fish cond., white sucker	0.116	0.999	0.380	0.130
Fish cond., lake whitefish	0.430	0.999	0.730	0.900
Fish cond., northern pike	0.001	0.999	<0.001	0.002
Fish cond., walleye	0.362	0.999	0.440	0.999

Table SI- 25: Regression statistics for food web metric calculations including trophic magnification slopes (TMSs) and intercepts (TMIs) within lakes or river sites. Note: Amp = amphipods, Cad = caddisflies, May = mayflies, Stone = stoneflies, WS = white suckers, NP = northern pike, Wall = walleye, Shiner, = shiners.

Waterbody	Type	TMS	TMI	p-value	r2	Taxa included (n):
Attawapiskat	Lake	0.211	-2.133	<0.001	0.817	Amp (2), Cad (5), May (6), NP (20), Shiner (8), Wall (24), WS (23)
Beteau	River Site	0.225	-2.251	<0.001	0.714	Amp (1), Cad (1), May (1), NP (10), Stone (1), Wall (10), WS (8)
Carpenter	Lake	0.233	-2.362	<0.001	0.885	Amp (1), Cad (2), May (2), NP (11), Shiner (3), Wall (11), WS (10)
Fishtrap	Lake	0.215	-1.939	<0.001	0.869	Amp (3), Cad (3), NP (12), Shiner (7), Wall (12), WS (11)
Goods	Lake	0.229	-2.229	<0.001	0.873	Amp (2), Cad (1), May (2), NP (10), Shiner (8), Wall (10), WS (10)
Highbank	Lake	0.292	-2.682	<0.001	0.823	Amp (3), Cad (2), May (2), NP (11), Shiner (5), Wall (10), WS (10)
Kapkichi	Lake	0.213	-2.246	<0.001	0.866	Amp (3), Cad (1), May (3), NP (10), Shiner (2), Wall (16), WS (10)
Lang	Lake	0.282	-2.455	<0.001	0.723	Amp (1), NP (15), Shiner (4), Stone (1), Wall (10), WS (11)
Missisa	Lake	0.261	-2.324	<0.001	0.760	Amp (1), May (1), NP (10), Shiner (6), Wall (13), WS (11)
Missisa outflow	River Site	0.245	-2.313	<0.001	0.855	Cad (1), May (1), NP (10), Stone (2), Wall (10), WS (10)
Muketei outflow	River Site	0.248	-2.372	<0.001	0.833	May (1), NP (11), Stone (2), Wall (10), WS (7), Amp (3)
Napken	Lake	0.221	-2.220	<0.001	0.887	Amp (3), Cad (2), NP (10), Shiner (2), Wall (10), WS (10)
Ozhiski	Lake	0.244	-2.572	<0.001	0.809	Cad (4), May (1), NP (10), Shiner (5), Wall (12), WS (9)
Richter	River Site	0.164	-1.829	<0.001	0.655	Cad (2), NP (10), Wall (10), WS (10)
Streatfeild	Lake	0.227	-2.220	<0.001	0.722	Amp (2), Cad (1), NP (10), Shiner (1), Wall (14), WS (13)
Streatfeild outflow	River Site	0.231	-2.147	<0.001	0.849	May (2), NP (8), Wall (10), WS (4)
Trading	Lake	0.265	-2.594	<0.001	0.808	Cad (1), May (1), NP (10), Shiner (2), Wall (12), WS (14)
Victor	Lake	0.218	-2.024	<0.001	0.896	May (2), NP (12), Stone (3), Wall (15), WS (10)
Williams	Lake	0.158	-1.626	<0.001	0.529	Amp (1), May (1), NP (10), Shiner (4), Wall (13), WS (11)

Table SI- 26: Linear models included (i.e., with delta AICc <4) in model averaging to determine important predictors of aqueous [THg] in the surface waters of lakes only. The intercept value was 0.220. VIF vales were all <10 and no models were excluded due to multicollinearity.

Model # and Metrics			Standardized Coefficients									
	R^2	*Wt.*	*Slope*	*Ca*	*Na*	*pH*	*DOC*	SO_4	*TP*	*TN*	NO_2+NO_3	*DO*
517	0.67	0.82	---	---	---	---	0.245	---	0.167	---	---	---
41	0.66	0.18	-0.246	---	---	---	---	---	---	---	0.152	---
		VIF:	8.4	10.2	4.1	9.8	6.5	5.3	3.8	2.7	2.0	3.1
		Mean±SE (full):	-0.05±0.10	---	---	---	0.20±0.10	---	0.14±0.07	---	0.03±0.06	---
		p-value (full):	0.641	---	---	---	0.051	---	0.071	---	0.652	---
		Mean±SE (cond.):	-0.25±0.04	---	---	---	0.24±0.04	---	0.17±0.04	---	0.15±0.04	---
		p-value (cond.):	<0.001	---	---	---	<0.001	---	<0.001	---	0.001	---
		Importance:	0.18	---	---	---	0.82	---	0.82	---	0.18	---
		N:	1	---	---	---	1	---	1	---	1	---

Table SI- 27: Linear models included (i.e., with delta AICc <4) in model averaging to determine important predictors of aqueous [MeHg] in the surface waters of lakes only. The intercept value was -2.157. VIF vales were all <10 and no models were excluded due to multicollinearity.

Model # and Metrics				Standardized Coefficients				
	R^2	*Wt.*		*Slope*	*Ca*	*Na*	*pH*	*DOC*
513	*0.48*	*0.20*		---	---	---	---	---
545	*0.53*	*0.15*		---	---	---	---	---
517	*0.53*	*0.14*		---	---	---	---	*0.367*
514	*0.52*	*0.12*		---	*0.334*	---	---	---
641	*0.51*	*0.11*		---	---	---	---	---
577	*0.50*	*0.07*		---	---	---	*0.225*	---
529	*0.49*	*0.07*		---	---	*0.232*	---	---
521	*0.49*	*0.06*		*-0.196*	---	---	---	---
515	*0.48*	*0.05*		---	---	---	---	---
769	*0.48*	*0.05*		---	---	---	---	---
		VIF:		8.4	10.2	4.1	9.8	6.5
		Mean±SE (full):		-0.01±0.09	0.04±0.14	0.02±0.10	0.02±0.09	0.05±0.16
		p-value (full):		0.911	0.783	0.880	0.866	0.748
		Mean±SE (cond.):		-0.20±0.35	0.33±0.26	0.23±0.30	0.23±0.26	0.37±0.25
		p-value (cond.):		0.594	0.221	0.47	0.419	0.174
		Importance:		0.06	0.12	0.06	0.07	0.14
		N:		1	1	1	1	1

Table SI-27 continued.

Model # and Metrics			Standardized Coefficients				
	R^2	Wt.	SO_4	TP	TN	NO_2+NO_3	DO
513	*0.48*	*0.20*	---	*-1.197*	---	---	---
545	*0.53*	*0.15*	---	*-1.130*	---	*0.375*	---
517	*0.53*	*0.14*	---	*-1.165*	---	---	---
514	*0.52*	*0.12*	---	*-1.236*	---	---	---
641	*0.51*	*0.11*	*-0.338*	*-1.326*	---	---	---
577	*0.50*	*0.07*	---	*-1.225*	---	---	---
529	*0.49*	*0.07*	---	*-1.315*	---	---	---
521	*0.49*	*0.06*	---	*-1.326*	---	---	---
515	*0.48*	*0.05*	---	*-1.123*	---	---	*-0.132*
769	*0.48*	*0.05*	---	*-1.198*	*0.002*	---	---
VIF:			5.3	3.8	2.7	2.0	3.1
Mean±SE (full):			-0.04±0.14	-1.21±0.28	0.0002±0.06	0.06±0.17	-0.01±0.08
p-value (full):			0.800	<0.001	0.999	0.744	0.934
Mean±SE (cond.):			-0.34±0.28	-1.21±0.28	0. 0002±0.29	0.38±0.26	-0.13±0.32
p-value (cond.):			0.25	<0.001	0.996	0.169	0.698
Importance:			0.11	1	0.05	0.15	0.05
N:			1	10	1	1	1

Table SI- 28: Linear models included (i.e., with delta AICc <4) in model averaging to determine important predictors of aqueous [THg] in surface waters of lakes and river sites. The intercept value was 0.359. VIF vales were all <10 and no models were excluded due to multicollinearity.

Model # and Metrics			Standardized Coefficients									
	R^2	Wt.	Slope	Ca	Na	pH	DOC	SO_4^{2-}	TP	TN	NO_2+NO_3	DO
517	0.73	0.61	---	---	---	---	0.379	---	0.155	---	---	---
41	0.72	0.39	-0.226	---	---	---	---	---	---	---	0.250	---
VIF:			5.5	2.0	1.7	8.5	9.8	3.5	2.1	1.9	7.4	4.5
Mean±SE (full):			-0.09±0.11	---	---	---	0.23±0.19	---	0.10±0.08	---	0.10±0.13	---
p-value (full):			0.445	---	---	---	0.214	---	0.246	---	0.442	---
Mean±SE (cond.):			-0.23±0.05	---	---	---	0.38±0.04	---	0.16±0.04	---	0.25±0.05	---
p-value (cond.):			<0.001	---	---	---	<0.001	---	<0.001	---	<0.001	---
Importance:			0.39	---	---	---	0.61	---	0.61	---	0.39	---
N:			1	---	---	---	1	---	1	---	1	---

Table SI- 29: Linear models included (i.e., with delta AICc <4) in model averaging to determine important predictors of aqueous [MeHg] in surface waters of lakes and river sites. The intercept value was -1.864. VIF vales were all <10 and no models were excluded due to multicollinearity.

Model # and Metrics			Standardized Coefficients									
	R^2	*Wt.*	*Slope*	*Ca*	*Na*	*pH*	*DOC*	SO_4	*TP*	*TN*	NO_2+NO_3	*DO*
545	0.56	0.65	---	---	---	---	---	---	-0.825	---	0.811	---
517	0.55	0.35	---	---	---	---	0.793	---	-0.819	---	---	---
		VIF:	5.5	2.0	1.7	8.5	9.8	3.5	2.1	1.9	7.4	4.5
		Mean±SE (full):	---	---	---	---	0.28±0.39	---	-0.82±0.16	---	0.52±0.41	---
		p-value (full):	---	---	---	---	0.474	---	<0.001	---	0.199	---
		Mean±SE (cond.):	---	---	---	---	0.79±0.16	---	-0.82±0.16	---	0.81±0.16	---
		p-value (cond.):	---	---	---	---	<0.001	---	<0.001	---	<0.001	---
		Importance:	---	---	---	---	0.35	---	1	---	0.65	---
		N:	---	---	---	---	1	---	2	---	1	---

Table SI- 30: Linear models included (i.e., with delta AICc <4) in model averaging to determine important predictors of caddisfly [MeHg]. The intercept value was -1.559. Note that due to high VIF values, DOC was excluded from the global model and no models including both SO_4 and DOC (Pearson's r = 0.622) were considered.

Model			Standardized Coefficients								
	R^2	*Wt.*	*Slope*	*Ca*	*Na*	*pH*	*DOC*	SO_4	*TP*	*TN*	NO_2+NO_3
131	*0.55*	*0.18*	---	---	---	*-0.186*	*NA*	---	---	---	---
3	*0.35*	*0.14*	---	---	---	---	*NA*	---	---	---	---
1281	*0.53*	*0.13*	---	---	---	---	*NA*	*-0.233*	*-0.192*	---	---
4	*0.50*	*0.09*	---	*-0.191*	---	---	*NA*	---	---	---	---
289	0.49	0.08	---	---	-0.185	---	*NA*	-0.249	---	---	---
67	0.49	0.08	---	---	---	---	*NA*	---	---	---	-0.183
257	0.27	0.06	---	---	---	---	*NA*	-0.189	---	---	---
259	0.47	0.06	---	---	---	---	*NA*	-0.136	---	---	---
1	0.00	0.05	---	---	---	---	*NA*	---	---	---	---
11	0.43	0.04	---	---	---	---	*NA*	---	---	---	---
35	0.42	0.03	---	---	-0.097	---	*NA*	---	---	---	---
19	0.41	0.03	-0.096	---	---	---	*NA*	---	---	---	---
1027	0.40	0.03	---	---	---	---	*NA*	---	-0.08359	---	---
		VIF:	73.6	19.2	6.6	4.9	*NA*	71.8	3.0	*2.9*	13.6
		Mean±SE (full):	0.00±0.02	-0.02±0.06	-0.02±0.06	-0.03±0.08	*NA*	-0.07±0.11	-0.03±0.07	---	-0.01±0.06
		p-value (full):	0.904	0.799	0.768	0.682	*NA*	0.544	0.721	---	0.816
		Mean±SE (cond.):	-0.10±0.09	-0.19±0.11	-0.16±0.10	-0.19±0.09	*NA*	-0.21±0.10	-0.17±0.09	---	-0.18±0.11
		p-value (cond.):	0.355	0.128	0.136	0.059	*NA*	0.049	0.094	---	0.147
		Importance:	0.03	0.09	0.12	0.18	*NA*	0.34	0.15	---	0.08
		N:	1	1	2	1	*NA*	4	2	---	1

Table SI-30 continued.

Model	R^2	*Wt.*	Standardized Coefficients *DO*	$\delta^{13}C$	$\delta^{15}N$
131	*0.55*	*0.18*	---	*-0.299*	---
3	*0.35*	*0.14*	---	*-0.216*	---
1281	*0.53*	*0.13*	---	---	---
4	*0.50*	*0.09*	---	*-0.343*	---
289	0.49	0.08	---	---	---
67	0.49	0.08	---	-0.338	---
257	0.27	0.06	---	---	---
259	0.47	0.06	---	-0.175	---
1	0.00	0.05	---	---	---
11	0.43	0.04	0.109	-0.249	---
35	0.42	0.03	---	-0.212	---
19	0.41	0.03	---	-0.238	---
1027	0.40	0.03	---	-0.192	---
		VIF:	9.0	43.3	11.6
		Mean±SE (full):	0.01±0.03	-0.18±0.15	---
		p-value (full):	0.888	0.260	---
		Mean±SE (cond.):	0.11±0.09	-0.27±0.11	---
		p-value (cond.):	0.297	0.029	---
		Importance:	0.04	0.68	---
		N:	1	9	---

Table SI- 31: Linear models included (i.e., with delta AICc <4) in model averaging to determine important predictors of amphipod [MeHg]. The intercept value was -1.644. Note that due to high VIF values, no models including both SO_4 and drainage basin slope (Pearson r = 0.898), SO_4 and DOC (r = -0.690), slope and DOC (r = -0.642), slope and TN (r = -0.802), or TP and TN (r = 0.843) were considered.

Model			Standardized Coefficients								
	R^2	*Wt.*	*Slope*	*Ca*	*Na*	*pH*	*DOC*	SO_4	*TP*	*TN*	NO_2+NO_3
34	0.63	0.25	---	---	---	---	---	---	---	---	0.303
1026	0.63	0.23	---	---	---	---	---	---	---	-0.301	---
514	0.63	0.23	---	---	---	---	---	---	---	0.322	---
1153	0.57	0.09	---	---	---	---	---	0.282		-0.329	---
3	0.41	0.07	0.371	---	---	---	---	---	---		---
1027	0.53	0.05	0.279	---	---	---	---	---	---	-0.224	---
161	0.53	0.05	---	---	---	---	---	0.343	---	---	0.308
2	0.36	0.04	---	---	---	---	---	---	---	---	---
		VIF:	129.5	14.9	10.3	29.5	60.0	39.8	32.6	29.6	3.0
		Mean±SE (full):	0.09±0.15	---	---	---	---	0.07±0.15	---	-0.11±0.16	0.04±0.11
		p-value (full):	0.566	---	---	---	---	0.622	---	0.501	0.718
		Mean±SE (cond.):	0.30±0.11	---	---	---	---	0.32±0.12	---	-0.30±0.12	0.30±0.12
		p-value (cond.):	0.014	---	---	---	---	0.013	---	0.022	0.025
		Importance:	0.29	---	---	---	---	0.23	---	0.37	0.14
		N:	2	---	---	---	---	1	---	3	2

Table SI-31 continued.

Model	Standardized Coefficients				
	R^2	*Wt.*	*DO*	$\delta^{13}C$	$\delta^{15}N$
34	0.63	0.25	---	-0.389	---
1026	0.63	0.23	---	-0.313	---
514	0.63	0.23	---	-0.470	---
1153	0.57	0.09	---	---	---
3	0.41	0.07	---	---	0.371
1027	0.53	0.05	---	---	0.279
161	0.53	0.05	---	---	---
2	0.36	0.04	---	-0.349	---
		VIF:	11.8	7.1	24.3
		Mean±SE (full):	---	-0.29±0.20	0.04±0.12
		p-value (full):	---	0.165	0.742
		Mean±SE (cond.):	---	-0.39±0.13	0.33±0.14
		p-value (cond.):	---	0.006	0.028
		Importance:	---	0.74	0.12
		N:	---	4	2

Table SI- 32: Linear models included (i.e., with delta AICc <4) in model averaging to determine important predictors of mayfly [MeHg]. The intercept value was -1.621. Note that due to high VIF values, DOC was excluded from all models and no models including both Mean slope and SO_4 (Pearson's r = 0.793) were considered.

Model			Standardized Coefficients								
	R^2	*Wt.*	*Slope*	*Ca*	*Na*	*pH*	*DOC*	SO_4	*TP*	*TN*	NO_2+NO_3
513	0.61	0.29	---	---	---	---	*NA*	---	---	*-0.556*	---
577	0.71	0.24	---	---	---	---	*NA*	---	---	*-0.534*	*0.226*
515	0.68	0.11	---	---	---	---	*NA*	---	---	*-0.496*	---
385	0.65	0.06	---	---	---	*-0.390*	*NA*	*0.456*	---	---	---
769	0.65	0.06	---	---	---	---	*NA*	*0.156*	---	*-0.469*	---
641	0.65	0.06	---	---	---	*-0.141*	*NA*	---	---	*-0.498*	---
1537	0.64	0.05	---	---	---	---	*NA*	---	*0.188*	*-0.708*	---
545	0.63	0.05	---	---	0.150	---	*NA*	---	---	-0.671	---
521	0.63	0.05	---	---	---	---	*NA*	---	---	-0.526	---
529	0.63	0.04	-0.122	---	---	---	*NA*	---	---	-0.639	---
		VIF:	17.4	8.9	6.1	13.5	*NA*	5.8	4.0	*8.9*	10.8
		Mean±SE (full):	-0.01±0.05	---	0.01±0.05	-0.03±0.11	*NA*	0.04±0.12	0.01±0.07	*-0.52±0.20*	0.05±0.11
		p-value (full):	0.917	---	0.909	0.774	*NA*	0.771	0.895	*0.017*	0.647
		Mean±SE (cond.):	-0.12±0.19	---	0.15±0.21	-0.27±0.19	*NA*	0.31±0.21	0.19±0.23	*-0.55±0.16*	0.23±0.12
		p-value (cond.):	0.566	---	0.532	0.186	*NA*	0.172	0.472	*0.002*	0.099
		Importance:	0.04	---	0.05	0.12	*NA*	0.12	0.05	*0.94*	0.24
		N:	1	---	1	2	*NA*	2	1	*9*	1

Table SI-32 continued.

Model	Standardized Coefficients				
	R^2	*Wt.*	*DO*	$\delta^{13}C$	$\delta^{15}N$
513	0.61	0.29	---	---	---
577	0.71	0.24	---	---	---
515	0.68	0.11	*-0.192*	---	---
385	0.65	0.06	---	---	---
769	0.65	0.06	---	---	---
641	0.65	0.06	---	---	---
1537	0.64	0.05	---	---	---
545	0.63	0.05	---	---	---
521	0.63	0.05	---	---	0.098
529	0.63	0.04	---	---	---
		VIF:	6.5	7.2	9.1
		Mean±SE (full):	-0.02±0.07	---	0.01±0.04
		p-value (full):	0.787	---	0.913
		Mean±SE (cond.):	-0.19±0.13	---	0.10±0.14
		p-value (cond.):	0.209	---	0.548
		Importance:	0.11	---	0.04
		N:	1	---	1

Table SI- 33: Linear models included (i.e., with delta AICc <4) in model averaging to determine important predictors of zooplankton [MeHg]. The intercept value was -1.843. Note that due to high VIF values, no models including both SO_4 and slope (Pearson's r = 0.824), or DOC and slope (r = 0.581) were considered.

Model			Standardized Coefficients								
	R^2	Δ	*Slope*	*Ca*	*Na*	*pH*	*DOC*	SO_4	*TP*	*TN*	NO_2+NO_3
19	0.76	0.74	---	---	-0.662	---	---	---	---	---	---
17	0.66	0.26	---	---	-0.749	---	---	---	---	---	---
		VIF:	65.2	12.4	7.0	13.3	29.0	14.0	6.0	*11.7*	4.8
		Mean±SE (full):	---	---	-0.68±0.14	---	---	---	---	---	---
		p-value (full):	---	---	5.87E-06	---	---	---	---	---	---
		Mean±SE (cond.):	---	---	-0.68±0.14	---	---	---	---	---	---
		p-value (cond.):	---	---	<0.001	---	---	---	---	---	---
		Importance:	---	---	1	---	---	---	---	---	---
		N:	---	---	2	---	---	---	---	---	---

Table SI-33 continued.

Model			Standardized Coefficients		
	R^2	Δ	*DO*	$\delta^{13}C$	$\delta^{15}N$
19	0.76	0.74	-0.306	---	---
17	0.66	0.26	---	---	---
		VIF:	10.3	11.6	18.2
		Mean±SE (full):	-0.23±0.17	---	---
		p-value (full):	0.211	---	---
		Mean±SE (cond.):	-0.31±0.13	---	---
		p-value (cond.):	0.032	---	---
		Importance:	0.74	---	---
		N:	1	---	---

Table SI- 34: Linear models included (i.e., with delta AICc <4) in model averaging to determine important predictors of [THg] in white sucker. The intercept value was 0.6595. Note that due to high VIF values, no models including both SO_4 and slope (Pearson's r = 0.828), TN and slope (r = -0.696), or pH and Ca (r = 0.876) were considered.

Model			Standardized Coefficients							
	R^2	Δ	*Slope*	*Ca*	*Na*	*pH*	*DOC*	SO_4	*TP*	*TN*
13	0.46	0.29	0.289	---	---	---	**0.258**	---	---	---
33	0.29	0.12	---	---	---	---	---	---	---	---
41	0.39	0.09	0.125	---	---	---	---	---	---	---
4129	0.39	0.08	---	---	---	---	---	---	---	---
545	0.38	0.08	---	---	---	---	---	---	**-0.121**	---
1057	0.37	0.06	---	---	---	---	---	---	---	---
4101	0.36	0.06	---	---	---	---	**0.152**	---	---	---
4097	0.22	0.05	---	---	---	---	---	---	---	---
514	0.34	0.05	---	0.147	---	---	---	---	-0.186	---
289	0.34	0.04	---	---	---	---	---	---	---	-0.087
513	0.20	0.04	---	---	---	---	---	---	-0.170	---
35	0.33	0.04	---	---	---	---	---	---	---	---
		VIF:	50.1	18.9	5.2	19.7	14.5	7.1	5.7	*7.9*
		Mean±SE (full):	0.09±0.14	0.01±0.03	---	---	0.08±0.13	---	-0.02±0.07	*<0.01±0.02*
		p-value (full):	0.500	0.854	---	---	0.518	---	0.718	*0.882*
		Mean±SE (cond.):	0.25±0.11	0.15±0.08	---	---	0.24±0.09	---	-0.15±0.09	*-0.09±0.08*
		p-value (cond.):	0.032	0.096	---	---	0.019	---	0.109	*0.322*
		Importance:	0.38	0.04	---	---	0.35	---	0.16	*0.04*
		N:	2	1	---	---	2	---	3	*1*

Table SI-34 continued.

Model	R^2	Δ	Standardized Coefficients					
			TN	*NO_2+NO_3*	*DO*	*$\delta^{13}C$*	*$\delta^{15}N$*	*Condition*
13	0.46	0.29	---	---	---	---	---	---
33	0.29	0.12	---	0.206	---	---	---	---
41	0.39	0.09	---	0.191	---	---	---	---
4129	0.39	0.08	---	0.167	---	---	0.126	---
545	0.38	0.08	---	0.171	---	---	---	---
1057	0.37	0.06	---	0.234	---	---	---	-0.111
4101	0.36	0.06	---	---	---	---	0.216	---
4097	0.22	0.05	---	---	---	---	0.178	---
514	0.34	0.05	---	---	---	---	---	---
289	0.34	0.04	-0.087	0.211	---	---	---	---
513	0.20	0.04	---	---	---	---	---	---
35	0.33	0.04	---	0.178	-0.085	---	---	---
		VIF:	*7.9*	4.1	11.2	2.8	3.6	3.6
		Mean±SE (full):	*<0.01±0.02*	0.10±0.11	<0.01±0.02	---	0.03±0.08	-0.01±0.03
		p-value (full):	*0.882*	0.390	0.893	---	0.681	0.842
		Mean±SE (cond.):	*-0.09±0.08*	0.19±0.08	-0.08±0.09	---	0.17±0.09	-0.11±0.08
		p-value (cond.):	*0.322*	0.033	0.363	---	0.086	0.212
		Importance:	*0.04*	0.52	0.04	---	0.19	0.06
		N:	*1*	7	1	---	3	1

Table SI- 35: Linear models included (i.e., delta AICc <4) in model averaging to determine important predictors of [THg] in northern pike. The intercept value was -0.1240. Note that due to high VIF values, no models including both SO_4 and slope (Pearson's r = 0.828), TN and slope (r = -0.697), or pH and Ca (r = 0.876) were considered.

Model			Standardized Coefficients						
	R^2	Δ	*Slope*	*Ca*	*Na*	*pH*	*DOC*	*SO_4*	*TP*
33	*0.33*	*0.23*	---	---	---	---	---	---	---
97	*0.43*	*0.20*	---	---	---	---	---	---	---
545	*0.36*	*0.07*	---	---	---	*0.06181*	---	---	---
1057	*0.36*	*0.07*	---	---	---	---	---	*0.05703*	---
35	*0.35*	*0.06*	---	---	---	---	---	---	---
41	*0.34*	*0.05*	*0.03852*	---	---	---	---	---	---
4129	*0.34*	*0.05*	---	---	---	---	---	---	*-0.0351*
2081	*0.33*	*0.05*	---	---	---	---	---	---	---
49	0.33	0.05	---	---	0.01958	---	---	---	---
289	0.33	0.05	---	---	---	---	---	---	---
161	0.33	0.05	---	---	---	---	---	---	---
34	0.33	0.04	---	0.01162	---	---	---	---	---
37	0.33	0.04	---	---	---	---	-0.01137	---	---
		VIF:	42.5	36.6	5.7	50.0	17.3	27.5	7.7
		Mean±SE (full):	<0.01±0.02	<0.01±0.02	<0.01±0.01	<0.01±0.02	<0.01±0.02	<0.01±0.02	<0.01±0.02
		p-value (full):	0.915	0.975	0.956	0.861	0.977	0.872	0.925
		Mean±SE (cond.):	0.04±0.07	0.01±0.07	0.02±0.07	0.06±0.07	-0.01±0.08	0.06±0.07	-0.04±0.07
		p-value (cond.):	0.599	0.882	0.790	0.396	0.892	0.433	0.645
		Importance:	0.05	0.04	0.05	0.07	0.04	0.07	0.05
		N:	1	1	1	1	1	1	1

Table SI-35 continued.

Model	R^2	Δ	Standardized Coefficients					
			TN	*NO_2+NO_3*	*DO*	*$\delta^{13}C$*	*$\delta^{15}N$*	*Condition*
33	*0.33*	*0.23*	---	*0.1821*	---	---	---	---
97	*0.43*	*0.20*	---	*0.2123*	---	---	---	*-0.1076*
545	*0.36*	*0.07*	---	*0.1709*	---	---	---	---
1057	*0.36*	*0.07*	---	*0.1912*	---	---	---	---
35	*0.35*	*0.06*	---	*0.1647*	*-0.05255*	---	---	---
41	*0.34*	*0.05*	---	*0.1776*	---	---	---	---
4129	*0.34*	*0.05*	---	*0.1719*	---	---	---	---
2081	*0.33*	*0.05*	*0.02397*	*0.1807*	---	---	---	---
49	0.33	0.05	---	0.1816	---	---	---	---
289	0.33	0.05	---	0.1802	---	---	-0.01947	---
161	0.33	0.05	---	0.1783	---	-0.01941	---	---
34	0.33	0.04	---	0.1781	---	---	---	---
37	0.33	0.04	---	0.1875	---	---	---	---
		VIF:	*12.5*	8.0	9.1	4.5	4.0	11.1
		Mean±SE (full):	<0.01±0.02	0.19±0.07	<0.01±0.02	<0.01±0.02	<0.01±0.02	-0.02±0.05
		p-value (full):	*0.946*	0.013	0.889	0.957	0.957	0.689
		Mean±SE (cond.):	*0.02±0.07*	0.19±0.07	-0.05±0.07	-0.02±0.07	-0.02±0.07	-0.11±0.06
		p-value (cond.):	*0.744*	0.013	0.492	0.795	0.792	0.127
		Importance:	*0.05*	1	0.06	0.05	0.05	0.2
		N:	*1*	13	1	1	1	1

Table SI- 36: Linear models included (i.e., with delta AICc <4) in model averaging to determine important predictors of walleye. The intercept value was 0.0984. Note that due to high VIF values, no models including both SO_4 and slope (Pearson's r = 0.828), TN and slope (r = -0.697), or pH and Ca (r = 0.876) were considered.

Model			Standardized Coefficients							
	R^2	Δ	*Slope*	*Ca*	*Na*	*pH*	*DOC*	SO_4	*TP*	*TN*
33	*0.27*	*0.18*	---	---	---	---	---	---	---	---
4129	*0.36*	*0.10*	---	---	---	---	---	---	---	---
49	*0.35*	*0.10*	---	---	*-0.104*	---	---	---	---	---
289	*0.34*	*0.08*	---	---	---	---	---	---	---	*-0.093*
41	*0.32*	*0.06*	*0.082*	---	---	---	---	---	---	---
2081	*0.32*	*0.06*	---	---	---	---	---	---	---	---
161	*0.31*	*0.06*	---	---	---	---	---	*0.077*	---	---
2049	*0.17*	*0.05*	---	---	---	---	---	---	---	---
37	*0.30*	*0.05*	---	---	---	---	*-0.075*	---	---	---
1	*0.00*	*0.04*	---	---	---	---	---	---	---	---
35	*0.29*	*0.04*	---	---	---	---	---	---	---	---
545	*0.28*	*0.04*	---	---	---	---	---	---	*-0.042*	---
97	*0.28*	*0.04*	---	---	---	*0.033*	---	---	---	---
1057	*0.27*	*0.03*	---	---	---	---	---	---	---	---
34	0.27	0.03	---	0.012	---	---	---	---	---	---
3073	0.26	0.03	---	---	---	---	---	---	---	---
18	0.26	0.03	---	0.186	-0.201	---	---	---	---	---
		VIF:	31.9	16.7	5.0	27.0	23.4	8.4	5.4	*8.9*
		Mean±SE (full):	0.01±0.03	0.01±0.04	-0.02±0.05	<0.01±0.02	<0.01±0.03	<0.01±0.03	<0.01±0.02	*-0.01±0.03*
		p-value (full):	0.861	0.889	0.774	0.948	0.892	0.872	0.934	*0.835*
		Mean±SE (cond.):	0.08±0.08	0.09±0.13	-0.13±0.09	0.03±0.08	-0.07±0.09	0.08±0.08	-0.04±0.08	*-0.09±0.08*
		p-value (cond.):	0.335	0.492	0.195	0.711	0.442	0.370	0.640	*0.266*
		Importance:	0.06	0.06	0.12	0.04	0.05	0.06	0.04	*0.08*
		N:	1	2	2	1	1	1	1	*1*

Table 36 continued.

Model	R^2	Δ	Standardized Coefficients				
			NO_2+NO_3	*DO*	$\delta^{13}C$	$\delta^{15}N$	*Condition*
33	*0.27*	*0.18*	*0.190*	---	---	---	---
4129	*0.36*	*0.10*	*0.224*	---	---	*0.112*	---
49	*0.35*	*0.10*	*0.193*	---	---	---	---
289	*0.34*	*0.08*	*0.196*	---	---	---	---
41	*0.32*	*0.06*	*0.180*	---	---	---	---
2081	*0.32*	*0.06*	*0.155*	---	*-0.084*	---	---
161	*0.31*	*0.06*	*0.202*	---	---	---	---
2049	*0.17*	*0.05*	---	---	*-0.149*	---	---
37	*0.30*	*0.05*	*0.226*	---	---	---	---
1	*0.00*	*0.04*	---	---	---	---	---
35	*0.29*	*0.04*	*0.207*	*0.049*	---	---	---
545	*0.28*	*0.04*	*0.178*	---	---	---	---
97	*0.28*	*0.04*	*0.184*	---	---	---	---
1057	*0.27*	*0.03*	*0.189*	---	---	---	*-0.017*
34	0.27	0.03	0.186	---	---	---	---
3073	0.26	0.03	---	---	-0.207	---	-0.128
18	0.26	0.03	---	---	---	---	---
VIF:			4.3	6.5	6.3	2.8	3.9
Mean±SE (full):			0.16±0.10	<0.01±0.02	-0.02±0.06	0.01±0.04	<0.01±0.03
p-value (full):			0.125	0.924	0.759	0.796	0.891
Mean±SE (cond.):			0.19±0.08	0.05±0.08	-0.13±0.10	0.11±0.08	-0.07±0.10
p-value (cond.):			0.029	0.591	0.198	0.194	0.522
Importance:			0.85	0.04	0.14	0.1	0.06
N:			13	1	3	1	2

Table SI- 37: Linear models included (i.e., with delta AICc <4) in model averaging to determine important predictors of TMIs. The intercept value was -2.245. Note that due to high VIF values, no models including both SO_4 and slope (Pearson's r = 0.831) or pH and Ca (r = 0.961) were considered.

Model			Standardized Coefficients				
	R^2	Δ	*Slope*	*Ca*	*Na*	*pH*	*DOC*
1	0	0.23	---	---	---	---	---
5	0.11	0.10	---	---	---	---	-0.194
2	0.09	0.09	---	-0.181	---	---	---
17	0.09	0.09	---	---	-0.180	---	---
65	0.06	0.07	---	---	---	-0.151	---
257	0.06	0.07	---	---	---	---	---
3	0.03	0.05	---	---	---	---	---
33	0.02	0.05	---	---	---	---	---
129	0.02	0.05	---	---	---	---	---
259	0.26	0.05	---	---	---	---	---
9	0.00	0.05	0.035	---	---	---	---
513	0.00	0.04	---	---	---	---	---
69	0.24	0.04	---	---	---	-0.229	-0.262
6	0.23	0.04	---	-0.208	---	---	-0.220
		VIF:	15.3	141.7	12.1	285.6	25.9
		Mean±SE (full):	<0.01±0.04	-0.02±0.08	-0.02±0.07	-0.02±0.08	-0.04±0.11
		p-value (full):	0.969	0.794	0.832	0.813	0.739
		Mean±SE (cond.):	0.03±0.17	-0.19±0.16	-0.18±0.16	-0.18±0.17	-0.22±0.16
		p-value (cond.):	0.854	0.297	0.321	0.339	0.239
		Importance:	0.04	0.12	0.09	0.11	0.17
		N:	1	2	1	2	3

Table SI- 37 continued.

Model	R^2	Δ	Standardized Coefficients SO_4	TP	TN	NO_2+NO_3	DO
1	0	0.23	---	---	---	---	---
5	0.11	0.10	---	---	---	---	---
2	0.09	0.09	---	---	---	---	---
17	0.09	0.09	---	---	---	---	---
65	0.06	0.07	---	---	---	---	---
257	0.06	0.07	---	---	-0.146	---	---
3	0.03	0.05	---	---	---	---	0.095
33	0.02	0.05	---	---	---	-0.090	---
129	0.02	0.05	0.074	---	---	---	---
259	0.26	0.05	---	---	-0.386	---	0.356
9	0.00	0.05	---	---	---	---	---
513	0.00	0.04	---	-0.009	---	---	---
69	0.24	0.04	---	---	---	---	---
6	0.23	0.04	---	---	---	---	---
		VIF:	12.9	4.4	13.7	*82.6*	8.2
		Mean±SE (full):	<0.01±0.04	<0.01±0.04	*-0.03±0.11*	<0.01±0.04	0.02±0.10
		p-value (full):	0.935	0.992	*0.804*	0.922	0.834
		Mean±SE (cond.):	0.07±0.17	-0.01±0.17	*-0.24±0.22*	-0.09±0.17	0.22±0.23
		p-value (cond.):	0.694	0.964	*0.308*	0.635	0.385
		Importance:	0.05	0.04	*0.11*	0.05	0.1
		N:	1	1	*2*	1	2

Table SI- 38: Linear models included (i.e., with delta AICc <4) in model averaging to determine important predictors of TMSs. The intercept value was 0.2296. Note that due to high VIF values, no models including both SO_4 and slope (Pearson's r = 0.831) or pH and Ca (r = 0.961) were considered.

Model			Standardized Coefficients				
	R^2	Δ	*Slope*	*Ca*	*Na*	*pH*	*DOC*
1	0.00	0.18	---	---	---	---	---
17	0.20	0.17	---	---	0.035	---	---
257	0.17	0.13	---	---	---	---	---
9	0.07	0.06	-0.020	---	---	---	---
2	0.05	0.05	---	0.017	---	---	---
65	0.05	0.05	---	---	---	0.017	---
5	0.05	0.05	---	---	---	---	0.017
129	0.03	0.04	---	---	---	---	---
513	0.02	0.04	---	---	---	---	---
3	0.01	0.04	---	---	---	---	---
33	0.00	0.04	---	---	---	---	---
259	0.25	0.03	---	---	---	---	---
21	0.24	0.03	---	---	0.034	---	0.015
529	0.24	0.03	---	---	0.046	---	---
273	0.22	0.03	---	---	0.024	---	---
19	0.22	0.03	---	---	0.040	---	---
261	0.21	0.03	---	---	---	---	0.016
		VIF:	82.6	141.7	12.1	---	---
		Mean±SE (full):	<0.01±0.01	<0.01±0.01	0.01±0.02	<0.01±0.01	<0.01±0.01
		p-value (full):	0.880	0.897	0.63	0.899	0.856
		Mean±SE (cond.):	-0.02±0.02	0.02±0.02	0.04±0.02	0.02±0.02	0.02±0.02
		p-value (cond.):	0.409	0.476	0.156	0.485	0.502
		Importance:	0.05	0.05	0.28	0.05	0.1
		N:	1	1	5	1	3

Table SI-38 continued.

Model	R^2	Δ	Standardized Coefficients				
			SO_4	*TP*	*TN*	*NO2+NO3*	*DO*
1	0.00	0.18	---	---	---	---	---
17	0.20	0.17	---	---	---	---	---
257	0.17	0.13	---	---	0.032	---	---
9	0.07	0.06	---	---	---	---	---
2	0.05	0.05	---	---	---	---	---
65	0.05	0.05	---	---	---	---	---
5	0.05	0.05	---	---	---	---	---
129	0.03	0.04	-0.014	---	---	---	---
513	0.02	0.04	---	0.012	---	---	---
3	0.01	0.04	---	---	---	---	0.006
33	0.00	0.04	---	---	---	-0.003	---
259	0.25	0.03	---	---	0.052	---	0.029
21	0.24	0.03	---	---	---	---	---
529	0.24	0.03	---	-0.018	---	---	---
273	0.22	0.03	---	---	0.015	---	---
19	0.22	0.03	---	---	---	---	0.011
261	0.21	0.03	---	---	0.032	---	---
		VIF:	13.7	8.2		4.4	12.9
		Mean±SE (full):	<0.01±0.01	<0.01±0.01	*0.01±0.02*	<0.01±0.00	<0.01±0.01
		p-value (full):	0.92	0.995	*0.703*	0.983	0.918
		Mean±SE (cond.):	-0.01±0.02	0.00±0.03	*0.03±0.02*	0.00±0.02	-0.01±0.03
		p-value (cond.):	0.577	0.981	*0.225*	0.906	0.725
		Importance:	0.04	0.07	*0.21*	0.03	0.1
		N:	1	2	*4*	1	3

Table SI- 39: Physicochemical predictors of [THg] and [MeHg] in water from lakes and river sites across the ADB. Results shown are the ranges of model strength (i.e., r^2 and weight) and the full averaged coefficients of each predictor across all linear models with a ΔAIC_c value <4, for each subset of data (i.e., group: surface or deep water from lakes and/or river sites). Models included in each group are listed in the SI file. Statistically significant predictors ($p < 0.05$ based on constrained coefficients) are bolded and reddened (see SI file for exact p-values).

Group (n)	**Model metrics** r^2	*Weight*	**Equation** (standardized full coefficients)
Surface, all sites (43)	0.55-0.56	0.35-0.65	[MeHg] = **(0.28*DOC)** + **(-0.82*TP)** + **(0.52*NO_2/NO_3)** -1.864
	0.72-0.73	0.39-0.61	[THg] **= (-0.09*Slope)** + **(0.23*DOC)** + **(0.10*TP)** + **(0.10*NO_2/NO_3)** + 0.359
Surface, river only (18)	0.03-0.35	0.03-0.23	[MeHg] = (<0.001*Slope) - (0.01*Ca) + (0.10*Na) + (<0.01*pH) + (0.04*DOC) + (<0.01*SO_4) + (0.01*TN) + (0.01*NO_2/NO_3) + (<0.01*D.O.)
	0.48-0.51	0.06-0.33	[THg] = (<0.001*Slope) + (<0.001*Ca) - (<0.001*Na) + (<0.001*pH) + (<0.001*DOC) + (<0.001*SO_4) + **(0.27*TP)** + (<0.001*TN) + (0.01*NO_2/NO_3) + (<0.001*D.O.)
Surface, lakes only (25)	0.48-0.53	0.05-0.20	[MeHg] = (-0.20*Slope) + (0.33*Ca) + (0.23*Na) + (0.23*pH) + (0.37*DOC) - (0.34*SO_4) **– (1.21*TP)** + (0. 0002*TN) + (0.38*NO_2/NO_3) - (0.13*D.O.) - 2.157
	0.66-0.70	0.18-0.82	[THg] **= (-0.05*Slope)** + **(0.20*DOC)** + **(0.14*TP)** + **(0.03*NO_2/NO_3)** + 0.220
Deep, lakes* only (13)	0.21-0.54	0.12-0.35	[MeHg] = (0.16*Slope) + (0.15*Ca) + (0.04*Na) **- (0.10*SO_4)**
	0.77-0.87	0.39-0.61	[THg] = **(0.37*DOC) - (0.08*D.O.)**

*In the deep water models, TN removed due to a high VIF value and strong correlations (Pearson r >0.8) with numerous parameters

SI information for Chapter 3

Table SI- 40: Physical and chemical characteristics of 20 river sites sampled for this study. Dissolved organic carbon (DOC) and iron concentrations, as well as pH were measured in surficial waters by the Ontario MOECC. Stream orders were determined using the MOECC CABIN database. Water temperature (Temp) and dissolved oxygen (DO) were measured in field at time of water collection. Secchi depths were not taken on river sites. *Sites only have DOM and biotic data

Site Name	Long (DD)	Lat (DD)	Stream order	Secchi depth (m)	Max depth (m)	Temp (°C)	DO (mg/L)	pH	Iron (mg/L)	DOC (mg/L)
Attawapiskat River tributary1	-85.44	53.09	Fifth	N/A	N/A	19.6	5.6	7.48	0.72	23.8
Attawapiskat River tributary2	-85.94	52.70	First	N/A	N/A	20.6	8.0	7.09	0.69	22.6
Attawapiskat River tributary3	-85.89	52.72	Second	N/A	N/A	19.3	8.1	6.98	0.90	29.1
Attawapiskat River tributary4	-86.18	52.38	First	N/A	N/A	17.9	6.1	7.17	0.50	22.6
Coomer Creek	-86.32	52.71	Third	N/A	N/A	16.9	7.3	7.21	0.43	19.7
Gleason Creek	-85.85	52.95	Third	N/A	N/A	20.7	6.6	7.34	0.61	24.2
Highbank Creek	-86.17	52.40	Third	N/A	N/A	17.3	7.5	7.43	0.50	20.3
Koper Creek1	-86.22	52.90	Third	N/A	N/A	22.6	7.4	7.14	0.59	21.6
Koper Creek2	-86.18	52.80	Third	N/A	N/A	18.1	7.0	7.00	0.51	21.6
McFaulds Creek	-85.92	52.80	Second	N/A	N/A	16.6	8.4	6.92	0.47	23.1
Muketei River	-86.36	52.68	Third	N/A	N/A	17.0	8.0	7.38	0.46	21.3
Muketei River tributary1	-85.30	53.14	First	N/A	N/A	16.3	5.6	6.81	0.51	25.4
Muketei River tributary2	-86.34	52.70	First	N/A	N/A	17.6	7.4	7.32	0.21	14.4
Muketei River tributary3	-85.83	53.12	Third	N/A	N/A	17.9	7.1	7.23	0.54	22.5
Muketei River tributary4	-85.49	53.20	Third	N/A	N/A	25.5	7.6	7.27	0.62	23.8
Muketei River tributary5	-85.43	53.20	First	N/A	N/A	16.8	6.9	7.49	0.28	18.3
Muketei River tributary6	-86.34	52.64	Second	N/A	N/A	20.8	7.0	7.05	0.73	21.6
Streatfield River	-85.94	52.65	Third	N/A	N/A	18.7	5.8	7.19	0.59	21.8
Victor Mine*	-83.91	52.87	Sixth	N/A	N/A	19.6	5.6	7.87	0.26	20.1
Missisa Outflow*	-85.44	53.09	Sixth	N/A	N/A	20.6	8.0	7.48	0.72	23.8

Table SI- 41:Physical and chemical characteristics of 9 Lowland lakes sampled for this study. Dissolved organic carbon (DOC) and iron concentrations were measured by the Ontario MOECC and averaged between surface (1m from surface) and deep water samples (1m off bottom). Lake size and depth were obtained from the Ontario Ministry of Natural Resources and Forestry (MNRF). Surface water temperatures (Temp), dissolved oxygen levels (DO), and Secchi depths were measured in field at time of water collection. Secchi depths are means of two or more readings by different personnel.

Waterbody	Long (DD)	Lat (DD)	Lake area (ha)	Secchi depth (m)	Maximum depth (m)	Temp (°C)	DO (mg/L)	pH	Iron (mg/L)	DOC (mg/L)
Fishtrap	-86.41	52.35	2030	1.0	1.3	18.0	9.1	7.57	0.14	13.6
Goods	-86.74	52.53	742	1.6	3.7	17.6	8.7	7.43	0.17	17.7
Highbank	-86.18	52.32	1450	1.1	1.8	18.2	8.2	7.62	0.20	14.8
Kapiskau*	-85.30	52.18	180	0.9	1.6	17.5	8.2	7.57	0.61	21.1
Missisa	-85.20	52.31	19212	0.5	7.0	16.5	9.7	7.97	0.23	10.5
Napken*	-85.33	51.88	1570	1.0	3.4	18.2	8.4	7.61	0.23	18.4
Quantz*	-85.38	51.16	727	1.2	10.4	18.6	8.8	7.58	0.16	16.4
Streatfeild	-85.90	52.14	2090	0.5	2.1	17.9	8.8	7.41	0.35	13.5
Wabimeig*	-85.59	51.50	5062	0.6	1.9	18.1	9.3	7.44	0.20	17.2

*Outside of the Attawapiskat Watershed, part of the Albany system.

Table SI- 42: Physical and chemical characteristics of 18 Shield lakes sampled for this study. Dissolved organic carbon (DOC) and iron concentrations were measured by the Ontario MOECC and averaged between surface (1m from surface) and deep water samples (1m off bottom). Lake size and depth were obtained from the Ontario Ministry of Natural Resources and Forestry (MNRF). Surface water temperatures (Temp), dissolved oxygen levels (DO), and Secchi depths were measured in field at time of water collection. Secchi depths are means of two or more readings by different personnel. ^Removed as an outlier for PCA, LASSO, and RDA analyses (as per Cooks distance).

Waterbody	Long (DD)	Lat (DD)	Lake area (ha)	Secchi depth (m)	Maximum depth (m)	Temp (°C)	DO (mg/L)	pH	Iron (mg/L)	DOC (mg/L)
Asselin	-88.01	51.98	269	1.7	3.0	19.0	9.0	7.61	0.06	13.0
Attawapiskat	-87.90	52.30	28100	1.9	23.5	19.3	8.1	7.72	0.09	13.4
Badesdawa	-89.71	51.78	3113	1.5	14.6	18.5	8.1	7.55	0.16	16.0
Carpenter	-90.76	51.19	779	2.4	19.0	19.0	8.2	7.39	0.24	10.7
Kapkichi	-90.40	51.46	1277	2.2	13.1	19.5	8.0	7.67	0.20	12.6
Lang	-91.51	51.58	1001	2.7	21.1	18.4	8.2	7.22	0.10	12.9
Margaree^	-89.52	51.79	199	3.0	3.0	18.6	8.7	8.25	0.03	5.4
Menako	-90.21	52.08	7161	1.9	17.7	18.0	8.5	7.36	0.11	13.7
Monmonawson	-89.48	51.71	676	1.6	3.0	18.9	9.0	7.54	0.10	13.0
Ozhiski	-88.57	51.95	6362	1.9	19.0	19.9	8.2	7.51	0.15	15.1
Pickle	-90.23	51.45	1112	3.1	19.2	18.5	8.5	7.66	0.24	8.4
Richter	-87.88	52.09	480	2.0	3.2	18.7	8.4	7.58	0.08	13.7
Stark	-87.69	51.88	393	1.8	3.0	19.1	8.5	7.76	0.11	15.0
Tarp	-90.11	51.57	1161	1.0	3.1	ND	ND	7.23	0.11	14.3
Trading	-88.96	51.82	465	2.4	4.5	18.1	8.1	7.82	0.14	15.5
Unnamed	-90.68	51.43	491	1.4	1.4	18.4	8.5	7.62	0.08	16.2
Williams	-90.78	51.82	4132	2.6	13.0	18.1	8.2	7.60	0.06	9.7
Wright	-90.95	51.33	1257	2.1	13.0	18.7	8.3	7.61	0.07	11.5

Table SI- 43: QA/QC results for various analytical procedures. Blank concentrations ([ ]), relative percent differences (RPD), and percent recovery are presented as mean ± standard deviation (SD), pooled across all sample runs for each analysis. THg and MeHg in biota data from this study, as well as the QAQC data presented below, were part of larger datasets. Note: DMA = direct mercury analyzer, MDL = method detection limit, CRM = certified reference materials, NA = not applicable.

QA/QC measure		[THg] Water	[MeHg] Water	[THg] Biota	[MeHg] Biota
MDL	*ng/g or L*	0.05[2]	0.0006[3]	2.50[4]	0.12[5]
Daily standards	*n*	21	14	-----	97
	%Rec	101.2±8.6	100.0±7.6	-----	98.8±9.2
Method Blanks	*n*	14	8	77	95
	ng/g	0.002±0.002	0.009±0.006	0.09±0.08	6.6±35.1
Initial precision replicates (IPRs)	*n*	15	8	-----	76
	%Rec	95.2±4.6	97.3±3.1	-----	98.5±11.3
Operating precision replicates (OPRs)	*n*	22	9	-----	135
	%Rec	93.8±3.8	100.8±7.7	-----	99.8±8.3
Certified reference material (CRMs)[1]	*n*	-----	-----	67	50
	%RPD	-----	-----	1.2±4.6	-4.7±10.7
Digestion duplicates	*n*	6	8	-----	77
	%RPD	103.0±28.3	-1.8±8.2	-----	-3.7±29.1
Analytical duplicates	*n*	-----	-----	61	79
	%RPD	-----	-----	0.48±6.6	10.6±23.8
Sample spikes	*n*	17	16	32	-----
	%Rec	104.4±26.5	116.6±19.8	97.0±4.7	-----
Analytical Method:		Tekran© 2700 THg System, EPA245.7	Tekran 2600 MeHg System, EPA 1630	Milestone DMA-80, EPA 7473	Tekran 2600 MeHg System, EPA 1630

[1]DORM-4, NRC 2015 (http://www.nrc-cnrc.gc.ca/eng/solutions/advisory/crm/certificates/dorm_4.html), [2]Calculated assuming a sample volume of 0.025 L, [3]Calculated assuming a sample volume of 0.040 L, [4]Calculated assuming a sample dry weight of 0.02g, [5]Calculated assuming a sample dry weight of 0.05g

Section SI-3.1: Further analytical and QA/QC procedures for Chapter 3

THg and MeHg in Water: For THg analysis of water samples, 25.0±0.01g of unfiltered water was weighed into clean glass vials and spiked with 125 µL of BrCl. After sitting overnight (or a minimum of 8 hours) in an ultra-clean fume-hood, 60µL of SnCl2 and 30µL of HA was added to each sample. Samples were analyzed using cold vapour atomic fluorescence spectroscopy (CVAFS) on a Tekran© 2700 THg System. Final instrument readings (reported in parts-per-thousand, PPT) were divided by 0.025 L (the volume of 25 g of water) to obtain results in ng/L. None of the resulting [THg] data were below the MDL (0.05 ng/L). Once calculated, these [THg] were blanks-corrected by subtracting the average method blank concentration (0.002±0.002 ng/L) from each result. Similar to method blanks, instrument calibration blanks and reagent blank concentrations were consistent and low, averaging 0.005±0.001 and 0.004±0.003 ng/L, respectively. A duplicate, spiked sample, and method blank were run every 10 samples. After building a calibration curve but prior to sample measurement, initial precision replicates (IPRs) were run to ensure accurate instrument readings. Similarly, operating precision replicates (OPRs) were run every 20 samples to ensure ongoing analytical accuracy. Average recoveries of all QA/QC measures are presented in Table SI-2.

For analysis of [MeHg] in water, 40.0±0.01g of unfiltered water was weighed into clean glass vials and spiked with 180 µL of APDC (ammonium pyrrolidinedithiocarbamate), 30 µL of ascorbic acid, and 225 µL of buffer solution. Samples were volatilized using 30 µL of sodium tetraethylborate (NaBet4) and analyzed using CVAFS on a Tekran© 2600 MeHg System paired with a gas chromatograph (GC). Final instrument readings (reported in parts-per-thousand, PPT) were divided by 0.040 L (the volume of 40 g of water) to obtain results in ng/L. None of the resulting [MeHg] data were below the MDL (0.0006 ng/L). Once calculated, these [MeHg] were blank-corrected by subtracting the average method blank concentration (0.009±0.006 ng/L) from each result. The same QA/QC procedure described for THg analysis above were also implemented during MeHg measurement, the recoveries of which are presented in Table SI-2. Field/travel blanks were also collected and analyzed for both THg and MeHg (n = 5, all values <MRLs).

THg in biota: Total [Hg] in fish was measured using a Milestone DMA-80 as per EPA method 7473 (EPA 2007). Briefly, for each fish approximately 30-75 mg of dried and ground muscle tissue was measured into a nickel sample boat and placed on the DMA auto-sampler. Approximately 10% of samples were duplicated, and blanks and certified reference material (DORM-4, NRC 2015) were analyzed every 10 samples (see QA/QC results in Table SI-2).

MeHg in biota: To analyze invertebrates and forage fish for [MeHg], a KOH digestion was used (Bloom & Fitzgerald 1988): approximately 50-100 mg of dried and ground biotic tissue was weighed into digestion tubes. 10.0 mL of 25% KOH (in methanol) solution was added and the tubes were placed on a hot block. The temperature was slowly raised to approximately 105 ˚C over the first hour and allowed to gently boil for an additional 3 hours. Once cooled, sample volumes were brought to 50.0 mL and digests were frozen until analysis. All digests were warmed to room temperature and gently shaken just prior to preparation for analysis. Once warmed, approximately 30-50 µL of sample digest was added to approximately 30 g of distilled water and 225 µL of buffer solution in an auto-sampler tube. Samples were volatilized using 30 µL of NaBet4

and tightly sealed until analyzed using the same CVAFS-GC set up as for water samples. All results were blank-corrected by subtracting the mean method blank concentrations measured in a given batch.

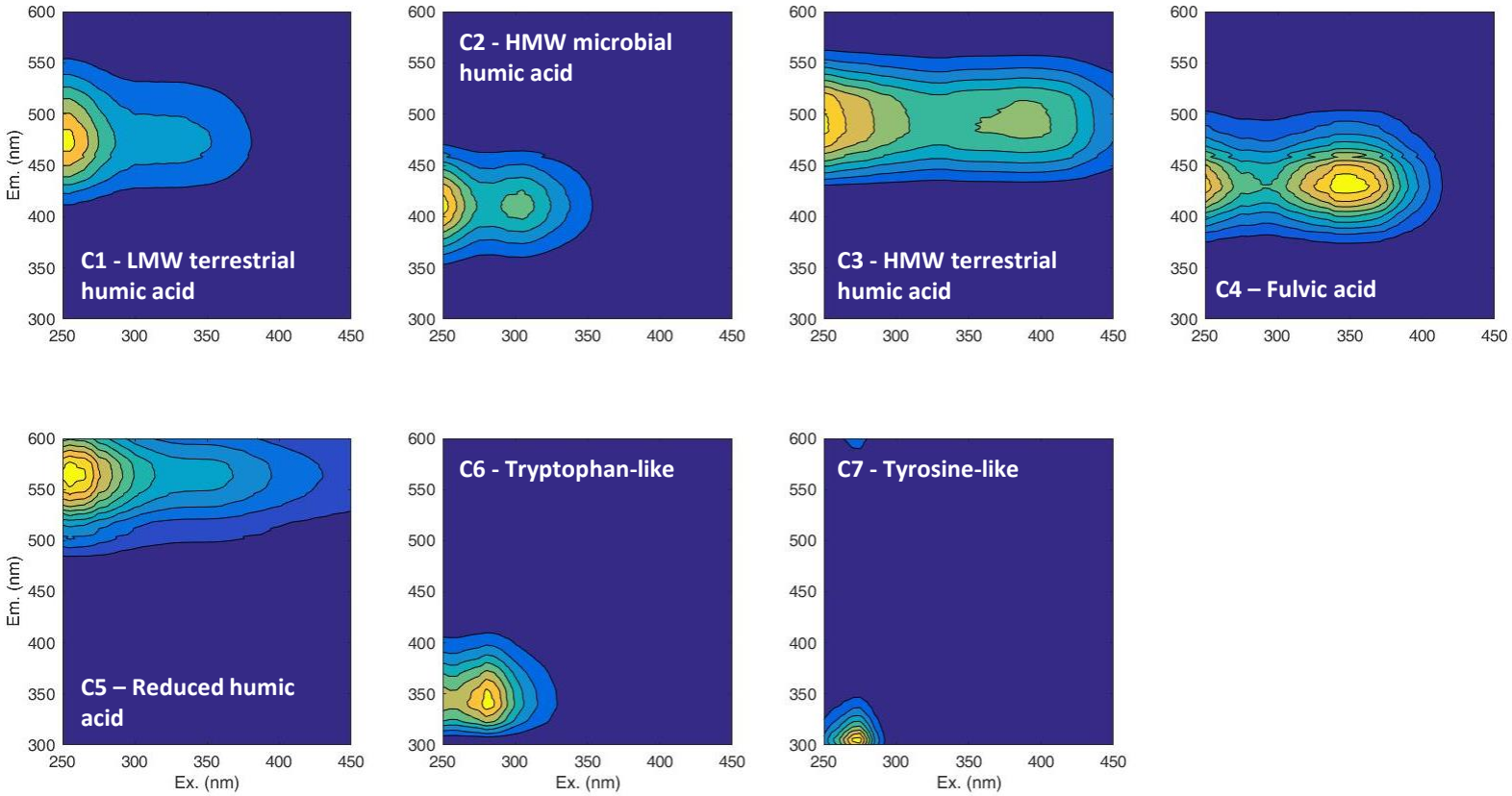

Figure SI- 2: Emission and excitation matrices (EEMs) of the 7 components detected in the PARAFAC model. Component were identified using OpenFluor and have been labeled with their associated DOM traits.

Table SI- 44:Mean, median, and inter-quartile range (IQR) values of DOM indices, PARAFAC components, and mercury concentrations in water (ng/L unfiltered) and biota (µg/g dry weight) by region. Values for DOM quality and mercury in water were calculated by averaging 1 samples/system within a region; data for biotic mercury concentrations were calculated by averaging system means within a region. *Indicates a significant difference in a given parameter across regions; see SI section for significance levels and pairwise comparisons. ^n represents the number of systems means, not the number of individual fish within a species/group.

Parameter	Shield Lakes				Lowland Lakes				River sites			
	Mean ± SD	*Median*	*IQR*	*n*	*Mean ± SD*	*Median*	*IQR*	*n*	*Mean ± SD*	*Median*	*IQR*	*n*
[DOC] (mg/L)*	13.2±2.2	13.4	2.4	18	15.9±3.2	16.4	4.1	9	22.2±3.0	22.2	2.3	20
mHIX*	0.88±0.06	0.89	0.07	18	0.87±0.10	0.89	0.04	9	0.95±0.03	0.96	0.03	20
FI*	1.72±0.13	1.74	0.17	18	1.69±0.18	1.63	0.10	9	1.59±0.06	1.60	0.05	20
β:α*	0.44±0.05	0.43	0.06	18	0.42±0.06	0.42	0.05	9	0.34±0.02	0.33	0.02	20
SUVA*	3.31±0.31	3.39	0.38	18	3.36±0.46	3.51	0.54	9	4.19±0.47	4.25	0.48	20
SAC*	22.8±3.6	24.1	4.6	18	24.0±3.9	25.1	4.9	9	33.6±4.3	34.4	4.3	20
E2:E3	5.14±0.50	4.90	0.55	18	4.86±0.46	4.85	0.54	9	4.30±0.19	4.22	0.24	20
C1 proportion*	0.41±0.04	0.41	0.05	18	0.38±0.04	0.39	0.02	9	0.32±0.07	0.34	0.02	20
C2 proportion*	0.35±0.04	0.35	0.05	18	0.33±0.03	0.33	0.03	9	0.26±0.06	0.27	0.02	20
C3 proportion*	0.04±0.02	0.04	0.02	18	0.06±0.03	0.06	0.03	9	0.11±0.03	0.12	0.02	20
C4 proportion*	0.04±0.02	0.04	0.03	18	0.05±0.02	0.04	0.03	9	0.09±0.02	0.09	0.01	20
C5 proportion*	0.11±0.02	0.11	0.03	18	0.12±0.03	0.12	0.02	9	0.15±0.04	0.16	0.01	20
C6 proportion*	0.03±0.02	0.02	0.01	18	0.03±0.02	0.02	0.03	9	<0.01±<0.01	0.00	0.00	20
C7 proportion	0.03±0.04	0.02	0.04	18	0.05±0.05	0.04	0.09	9	0.03±0.03	0.02	0.03	20
Surface water [THg]*	1.49±0.43	1.48	0.52	18	2.33±0.47	2.36	0.78	9	3.92±1.70	3.62	2.29	18
Surface water [MeHg]*	0.017±0.013	0.020	0.020	18	0.015±0.015	0.020	0.028	9	0.038±0.016	0.040	0.012	18
Zooplankton[MeHg]	0.043±0.071	0.019	0.021	10^	0.015±0.500	0.010	0.022	9^	ND	ND	ND	0^
Caddisflies[MeHg]	0.032±0.018	0.026	0.018	8^	0.026±0.010	0.023	0.005	8^	0.084	0.084	<0.001	1^
Amphipods[MeHg]	0.027±0.014	0.029	0.014	8^	0.021±0.017	0.019	0.022	9^	ND	ND	ND	0^
Mayflies[MeHg]	0.018±0.011	0.026	0.014	5^	0.037±0.030	0.024	0.007	8^	0.042±0.016	0.051	0.014	3^
Shiners[THg][1]	0.26±1.69	0.23	0.15	8^	0.26±1.69	0.30	0.20	6^	ND	ND	ND	0^
W. Sucker[THg][2]	0.31±1.48	0.29	0.18	11^	0.24±1.33	0.23	0.07	9^	0.42±1.24	0.41	0.10	4^
N. Pike[THg][3]	1.27±1.54	1.35	0.91	10^	1.11±1.15	1.07	0.22	8^	0.98±1.10	0.97	0.12	4^
Walleye[THg][4]	1.12±1.81	1.35	0.52	8^	1.16±1.58	1.05	0.97	9^	1.32±0.50	1.63	0.29	4^

[1]standardized to 74.3 mm total length; [2]standardized to 374.5 mm total length; [3]standardized to 547.6 mm total length; [4]standardized to 385.9 mm total length.

Table SI- 45: Results from Kruskal Wallis and Conover post-hoc tests (Pohlert 2016) comparing DOM indices and DOC concentrations in surface waters across river sites and lakes listed in Table 5. Note: KW = Kruskal Wallis. *Indicates a significant result.

[DOC] (KW p < 0.001*)			
Conover pos-hoc test	Shield lakes	Lowland lakes	River sites
Shield lakes	---	0.046	< 0.001*
Lowland lakes	0.046	---	< 0.001*
River sites	< 0.001*	< 0.001*	---
mHIX (KW p < 0.001*)			
Conover pos-hoc test	Shield lakes	Lowland lakes	River sites
Shield lakes	---	0.999	< 0.001*
Lowland lakes	0.999	---	< 0.001*
River sites	< 0.001*	< 0.001*	---
FI (KW p = 0.001)			
Conover pos-hoc test	Shield lakes	Lowland lakes	River sites
Shield lakes	---	0.245	0.004*
Lowland lakes	0.245	---	0.309
River sites	0.004*	0.309	---
β:α (KW p < 0.001*)			
Conover pos-hoc test	Shield lakes	Lowland lakes	River sites
Shield lakes	---	0.980	< 0.001*
Lowland lakes	0.980	---	< 0.001*
River sites	< 0.001*	< 0.001*	---
SAC (KW p < 0.001*)			
Conover pos-hoc test	Shield lakes	Lowland lakes	River sites
Shield lakes	---	0.999	< 0.001*
Lowland lakes	0.999	---	< 0.001*
River sites	< 0.001*	< 0.001*	---
SUVA (KW p < 0.001*)			
Conover pos-hoc test	Shield lakes	Lowland lakes	River sites
Shield lakes	---	0.999	< 0.001*
Lowland lakes	0.999	---	< 0.001*
River sites	< 0.001*	< 0.001*	---

Table SI-45 *continued*: Results from Kruskal Wallis and Conover post-hoc tests (Pohlert 2016) comparing PARAFAC components in surface waters across river sites and lakes listed in Table 5.Note: KW = Kruskal Wallis. *Indicates a significant result.

C1 (KW p < 0.001*)			
Conover pos-hoc test	Shield lakes	Lowland lakes	River sites
Shield lakes	---	0.303	< 0.001*
Lowland lakes	0.303	---	0.012*
River sites	< 0.001*	0.012*	---
C2 (KW p < 0.001*)			
Conover pos-hoc test	Shield lakes	Lowland lakes	River sites
Shield lakes	---	0.150	< 0.001*
Lowland lakes	0.150	---	< 0.001*
River sites	< 0.001*	< 0.001*	---
C3 (KW p < 0.001*)			
Conover pos-hoc test	Shield lakes	Lowland lakes	River sites
Shield lakes	---	0.230	< 0.001*
Lowland lakes	0.230	---	< 0.001*
River sites	< 0.001*	< 0.001*	---
C4 (KW p < 0.001*)			
Conover pos-hoc test	Shield lakes	Lowland lakes	River sites
Shield lakes	---	0.500	< 0.001*
Lowland lakes	0.500	---	< 0.001*
River sites	< 0.001*	< 0.001*	---
C5 (KW p < 0.001*)			
Conover pos-hoc test	Shield lakes	Lowland lakes	River sites
Shield lakes	---	0.440	< 0.001*
Lowland lakes	0.440	---	< 0.001*
River sites	< 0.001*	< 0.001*	---
C6 (KW p < 0.001*)			
Conover pos-hoc test	Shield lakes	Lowland lakes	River sites
Shield lakes	---	0.930	< 0.001*
Lowland lakes	0.930	---	< 0.001*
River sites	< 0.001*	< 0.001*	---
C7 (KW p = 0.381)			
Conover pos-hoc test	Shield lakes	Lowland lakes	River sites
Shield lakes	---	0.520	0.999
Lowland lakes	0.520	---	0.940
River sites	0.999	0.940	---

Table SI- 46: Rotated loadings of each DOM quality parameter and [DOC] on the first 3 principal components (PCs) resulting from a PCA run using all DOM data across the ADB (n = 44, 1 outliers removed).^all PARAFAC proportion data were logit transformed

Parameter:	PC1	PC2	PC3	PC4
FI	-0.220	-0.084	-0.484	0.697
SAC	0.288	0.059	-0.348	-0.233
mHIX	0.253	-0.416	0.096	0.018
β:α	-0.299	0.145	-0.062	-0.181
SUVA	0.291	-0.008	-0.252	-0.276
E2:E3	-0.194	-0.214	0.639	0.223
C1^	-0.244	-0.420	-0.079	-0.202
C2^	-0.290	-0.234	-0.123	-0.128
C3^	0.314	-0.034	0.105	0.159
C4^	0.303	-0.078	0.082	0.309
C5^	0.298	-0.021	0.286	-0.151
C6^	-0.283	0.207	0.058	-0.250
C7^	-0.045	0.675	0.170	0.150
[DOC]	0.297	0.113	-0.084	0.122
Eigen Value:	9.74	1.91	1.15	9.74
Variance explained (%):	69.5	13.7	8.2	69.5

Table SI-46b: Rotated loadings of each DOM quality parameter and [DOC] on the first 3 principal components (PCs) resulting from a PCA run using all DOM data across lakes within the ADB (n = 26, river sites excluded).^all PARAFAC proportion data were logit transformed

Parameter:	PC1	PC2	PC3	PC4
FI	-0.249	0.173	-0.172	0.721
SAC	0.223	0.071	-0.528	-0.157
mHIX	0.278	0.356	0.125	-0.043
β:α	-0.310	-0.159	-0.170	-0.162
SUVA	0.274	0.135	-0.377	-0.242
E2:E3	0.005	0.063	0.661	-0.029
C1^	-0.181	0.494	0.072	-0.160
C2^	-0.264	0.363	-0.133	-0.085
C3^	0.357	-0.026	0.065	0.129
C4^	0.342	0.024	0.040	0.302
C5^	0.333	-0.065	0.175	-0.300
C6^	-0.289	-0.248	0.005	-0.310
C7^	-0.074	-0.553	-0.020	0.072
[DOC]	0.306	-0.206	-0.096	0.190
Eigen Value:	5.48	3.28	2.91	1.68
Variance explained (%):	53.6	19.2	15.1	5.1

Table SI-46c: Rotated loadings of each DOM quality parameter and [DOC] on the first 3 principal components (PCs) resulting from a PCA run using all DOM data across river sites within the ADB (n = 18, all lakes excluded).^all PARAFAC proportion data were logit transformed

Parameter:	PC1	PC2	PC3	PC4
FI	-0.120	-0.147	0.507	-0.072
SAC	0.322	0.127	-0.318	-0.301
mHIX	0.211	-0.447	-0.102	0.060
β:α	-0.376	0.093	-0.086	-0.065
SUVA	0.274	0.096	-0.309	-0.530
E2:E3	-0.235	-0.176	0.198	-0.561
C1^	-0.084	-0.460	-0.349	0.082
C2^	-0.295	-0.317	-0.178	0.108
C3^	0.371	-0.094	0.252	-0.027
C4^	0.245	-0.222	0.471	-0.239
C5^	0.308	0.138	-0.106	-0.018
C6^	-0.256	0.265	-0.079	-0.174
C7^	-0.070	0.500	0.172	0.103
[DOC]	0.329	0.061	0.053	0.427
Eigen Value:	4.88	3.67	2.27	2.18
Variance explained (%):	42.5	24.0	9.2	8.5

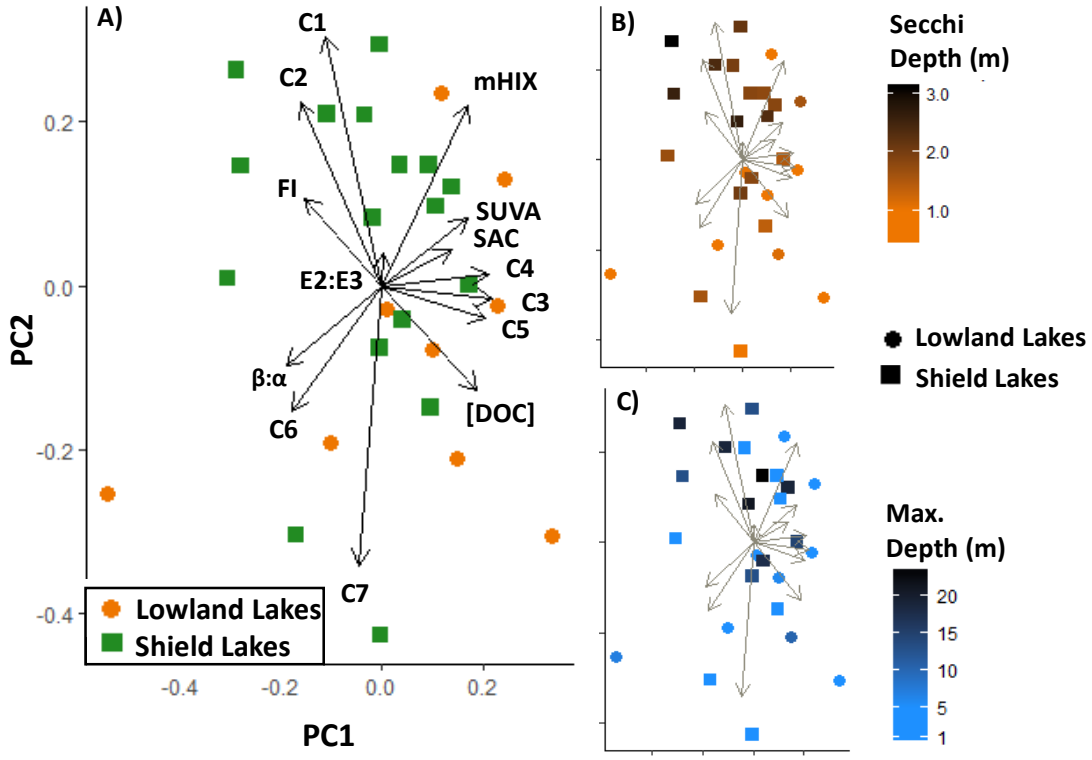

Figure SI- 3: A) Scatter plot of first two principal components (PC1, PC2) of a PCA on all DOM indices, PARAFAC components and [DOC] measured in Shield lakes (green squares, n = 17) and Lowland lakes (orange circles, n = 9) from across the ADB. PC1 and PC2 explained 53.6 and 19.2% of the variability in these data, respectively. Vectors show the influence of the various measures of DOM composition and [DOC] across the watershed. B) The same scatter plot as in A but with sites colour-coded by Secchi depth (darker colour indicates deeper Secchi reading). C) The same scatter plot as in A but with sites colour-coded by maximum depth (darker colour indicates greater depth).

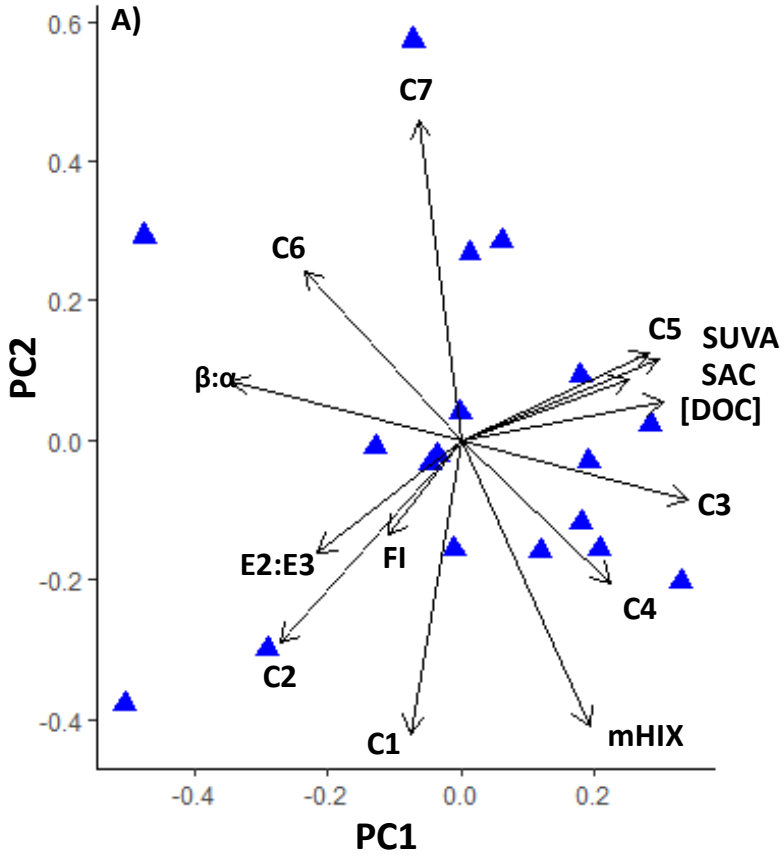

Figure SI- 4: Scatter plot of first two principal components (PC1, PC2) of a PCA on all DOM indices, PARAFAC components and [DOC] measured in river sites (n = 18) from across the ADB. PC1 and PC2 explained 42.5 and 24.0% of the variability in these data, respectively. Vectors show the influence of the various measures of DOM composition and [DOC] across the watershed.

Table SI- 47: Pearson correlations between Hg concentrations, DOM indices, PARAFAC components, and [DOC] across 18 river sites, 17 Shield lakes, and 9 Lowland lakes. ^all proportion data were logit transformed.*p<0.05.

	THg	MeHg	FI	SAC	mHIX	β:α	SUVA	E2:E3
THg	---	0.222	-0.295	0.765*	0.431*	-0.659*	0.735*	-0.621*
MeHg	0.222	---	-0.357*	0.422*	0.531*	-0.449*	0.463*	-0.166
FI	-0.295	-0.357*	---	-0.498*	-0.524*	0.594*	-0.550*	0.184
SAC	0.765*	0.422*	-0.498*	---	0.623*	-0.780*	0.979*	-0.822*
mHIX	0.431*	0.531*	-0.524*	0.623*	---	-0.845*	0.695*	-0.240
β:α	-0.659*	-0.449*	0.594*	-0.780*	-0.845*	---	-0.795*	0.448*
SUVA	0.735*	0.463*	-0.550*	0.979*	0.695*	-0.795*	---	-0.708*
E2:E3	-0.621*	-0.166	0.184	-0.822*	-0.240	0.448*	-0.708*	---
C1^	-0.661*	-0.465*	0.559*	-0.680*	-0.282	0.580*	-0.648*	0.548*
C2^	-0.747*	-0.464*	0.678*	-0.781*	-0.522*	0.830*	-0.759*	0.538*
C3^	0.728*	0.549*	-0.670*	0.813*	0.810*	-0.922*	0.835*	-0.493*
C4^	0.712*	0.559*	-0.579*	0.773*	0.820*	-0.898*	0.806*	-0.450*
C5^	0.610*	0.525*	-0.825*	0.728*	0.775*	-0.876*	0.770*	-0.368*
C6^	-0.607*	-0.456*	0.490*	-0.768*	-0.867*	0.916*	-0.784*	0.478*
C7^	0.016	-0.099	-0.069	-0.124	-0.605*	0.276	-0.191	-0.044
[DOC]	0.792*	0.498*	-0.569*	0.848*	0.634*	-0.829*	0.809*	-0.663*

Table SI-47 continued: Pearson correlations between Hg concentrations, DOM indices, PARAFAC components, and [DOC] across 18 river sites, 17 Shield lakes, and 9 Lowland lakes. ^all proportion data were logit transformed.*p<0.05.

	C1*	C2*	C3*	C4*	C5*	C6*	C7*	[DOC]
THg	-0.661*	-0.747*	0.728*	0.712*	0.610*	-0.607*	0.016	0.792*
MeHg	-0.465*	-0.464*	0.549*	0.559*	0.525*	-0.456*	-0.099	0.498*
FI	0.559*	0.678*	-0.670*	-0.579*	-0.825*	0.490*	-0.069	-0.569*
SAC	-0.680*	-0.781*	0.813*	0.773*	0.728*	-0.768*	-0.124	0.848*
mHIX	-0.282	-0.522*	0.810*	0.820*	0.775*	-0.867*	-0.605*	0.634*
β:α	0.580*	0.830*	-0.922*	-0.898*	-0.876*	0.916*	0.276	-0.829*
SUVA	-0.648*	-0.759*	0.835*	0.806*	0.770*	-0.784*	-0.191	0.809*
E2:E3	0.548*	0.538*	-0.493*	-0.450*	-0.368*	0.478*	-0.044	-0.663*
C1^	---	0.879*	-0.762*	-0.723*	-0.710*	0.484*	-0.428*	-0.790*
C2^	0.879*	---	-0.885*	-0.827*	-0.871*	0.706*	-0.193	-0.890*
C3^	-0.762*	-0.885*	---	0.984*	0.942*	-0.873*	-0.168	0.892*
C4^	-0.723*	-0.827*	0.984*	---	0.887*	-0.877*	-0.210	0.842*
C5^	-0.710*	-0.871*	0.942*	0.887*	---	-0.753*	-0.137	0.825*
C6^	0.484*	0.706*	-0.873*	-0.877*	-0.753*	---	0.323*	-0.765*
C7^	-0.428*	-0.193	-0.168	-0.210	-0.137	0.323*	---	-0.020
[DOC]	-0.790*	-0.890*	0.892*	0.842*	0.825*	-0.765*	-0.020	---

Table SI- 48: Pearson correlations between Hg concentrations, DOM indices, PARAFAC components, and [DOC] across 17 Shield lakes and 9 Lowland lakes. All proportion data were logit transformed.*p<0.05.

	THg	MeHg	FI	SAC	mHIX	β:α	SUVA	E2:E3
THg	---	-0.163	-0.075	0.429*	0.131	-0.269	0.346	-0.355
MeHg	-0.163	---	-0.177	0.046	0.381	-0.169	0.213	0.283
FI	-0.075	-0.177	---	-0.273	-0.415*	0.506*	-0.426*	-0.222
SAC	0.429*	0.046	-0.273	---	0.395*	-0.353	0.943*	-0.704*
mHIX	0.131	0.381	-0.415*	0.395*	---	-0.806*	0.617*	0.261
β:α	-0.269	-0.169	0.506*	-0.353	-0.806*	---	-0.502*	-0.215
SUVA	0.346	0.213	-0.426*	0.943*	0.617*	-0.502*	---	-0.438*
E2:E3	-0.355	0.283	-0.222	-0.704*	0.261	-0.215	-0.438*	---
C1^	-0.473*	-0.258	0.440*	-0.265	0.099	0.147	-0.251	0.139
C2^	-0.466*	-0.200	0.675*	-0.219	-0.207	0.586*	-0.260	-0.077
C3^	0.529*	0.344	-0.625*	0.500*	0.734*	-0.816*	0.657*	0.109
C4^	0.537*	0.383	-0.469*	0.496*	0.746*	-0.795*	0.655*	0.100
C5^	0.290	0.327	-0.850*	0.378	0.688*	-0.767*	0.564*	0.239
C6^	-0.402*	-0.192	0.309	-0.520*	-0.815*	0.861*	-0.638*	-0.032
C7^	0.125	-0.094	-0.103	-0.191	-0.681*	0.366	-0.323	-0.111
[DOC]	0.676*	0.257	-0.529*	0.532*	0.430*	-0.564*	0.570*	-0.163

Table SI-48 continued: Pearson correlations between Hg concentrations, DOM indices, PARAFAC components, and [DOC] across 17 Shield lakes and 9 Lowland lakes. All proportion data were logit transformed.*p<0.05, **p<0.01, ^p<0.001.

	C1	C2	C3	C4	C5	C6	C7	[DOC]
THg	-0.473*	-0.466*	0.529*	0.537*	0.290	-0.402*	0.125	0.676*
MeHg	-0.258	-0.200	0.344	0.383	0.327	-0.192	-0.094	0.257
FI	0.440*	0.675*	-0.625*	-0.469*	-0.850*	0.309	-0.103	-0.529*
SAC	-0.265	-0.219	0.500*	0.496*	0.378	-0.520*	-0.191	0.532*
mHIX	0.099	-0.207	0.734*	0.746*	0.688*	-0.815*	-0.681*	0.430*
β:α	0.147	0.586*	-0.816*	-0.795*	-0.767*	0.861*	0.366	-0.564*
SUVA	-0.251	-0.260	0.657*	0.655*	0.564*	-0.638*	-0.323	0.570*
E2:E3	0.139	-0.077	0.109	0.100	0.239	-0.032	-0.111	-0.163
C1	---	0.776*	-0.544*	-0.499*	-0.480*	0.044	-0.606*	-0.735*
C2	0.776*	---	-0.737*	-0.642*	-0.763*	0.386	-0.404*	-0.747*
C3	-0.544*	-0.737*	---	0.976*	0.904*	-0.751*	-0.184	0.845*
C4	-0.499*	-0.642*	0.976*	---	0.808*	-0.777*	-0.233	0.797*
C5	-0.480*	-0.763*	0.904*	0.808*	---	-0.571*	-0.148	0.738*
C6	0.044	0.386	-0.751*	-0.777*	-0.571*	---	0.404*	-0.500*
C7	-0.606*	-0.404*	-0.184	-0.233	-0.148	0.404*	---	0.076
[DOC]	-0.735*	-0.747*	0.845*	0.797*	0.738*	-0.500*	0.076	---

Table SI- 49: Pearson correlations between Hg concentrations, DOM indices, PARAFAC components, and [DOC] across 18 river sites. All proportion data were logit transformed. *p<0.05, **p<0.01, ^p<0.001.

	MeHg	THg	FI	SAC	mHIX	β:α	SUVA	E2:E3
THg	1.000	-0.310	0.221	0.575*	-0.012	-0.524*	0.556*	-0.239
MeHg	-0.310	1.000	-0.515*	0.111	0.202	-0.115	-0.028	-0.536*
FI	0.221	-0.515*	1.000	-0.333	-0.058	0.010	-0.285	0.307
SAC	0.575*	0.111	-0.333	1.000	0.212	-0.670*	0.952*	-0.484*
mHIX	-0.012	0.202	-0.058	0.212	1.000	-0.561*	0.188	-0.058
β:α	-0.524*	-0.115	0.010	-0.670*	-0.561*	1.000	-0.540*	0.547*
SUVA	0.556*	-0.028	-0.285	0.952*	0.188	-0.540*	1.000	-0.201
E2:E3	-0.239	-0.536*	0.307	-0.484*	-0.058	0.547*	-0.201	1.000
C1	-0.196	0.147	0.152	-0.233	0.604*	0.033	-0.188	0.247
C2	-0.531*	0.110	0.274	-0.631*	0.136	0.562*	-0.558*	0.415
C3	0.418	0.029	-0.158	0.527*	0.595*	-0.845*	0.445	-0.366
C4	0.349	-0.279	0.088	0.247	0.557*	-0.598*	0.258	0.048
C5	0.409	0.072	-0.328	0.587*	0.204	-0.616*	0.505*	-0.464
C6	0.068	-0.411	0.162	-0.308	-0.750*	0.607*	-0.236	0.249
C7	0.020	0.013	-0.151	-0.002	-0.839*	0.310	-0.053	-0.208
[DOC]	0.427	0.342	-0.178	0.496*	0.343	-0.763*	0.298	-0.716*

Table SI-49 continued: Pearson correlations between Hg concentrations, DOM indices, PARAFAC components, and [DOC] across 18 river sites. All proportion data were logit transformed.*p<0.05, **p<0.01, ^p<0.001.

	C1*	C2*	C3*	C4*	C5*	C6*	C7*	[DOC]
THg	-0.196	-0.531*	0.418	0.349	0.409	0.068	0.020	0.427
MeHg	0.147	0.110	0.029	-0.279	0.072	-0.411	0.013	0.342
FI	0.152	0.274	-0.158	0.088	-0.328	0.162	-0.151	-0.178
SAC	-0.233	-0.631*	0.527*	0.247	0.587*	-0.308	-0.002	0.496*
mHIX	0.604*	0.136	0.595*	0.557*	0.204	-0.750*	-0.839*	0.343
β:α	0.033	0.562*	-0.845*	-0.598*	-0.616*	0.607*	0.310	-0.763*
SUVA	-0.188	-0.558*	0.445	0.258	0.505*	-0.236	-0.053	0.298
E2:E3	0.247	0.415	-0.366	0.048	-0.464	0.249	-0.208	-0.716*
C1	1.000	0.677*	-0.198	-0.037	-0.297	-0.186	-0.837*	-0.182
C2	0.677*	1.000	-0.589*	-0.326	-0.697*	0.144	-0.425	-0.648*
C3	-0.198	-0.589*	1.000	0.803*	0.681*	-0.639*	-0.279	0.663*
C4	-0.037	-0.326	0.803*	1.000	0.224	-0.590*	-0.390	0.299
C5	-0.297	-0.697*	0.681*	0.224	1.000	-0.132	-0.050	0.607*
C6	-0.186	0.144	-0.639*	-0.590*	-0.132	1.000	0.365	-0.502*
C7	-0.837*	-0.425	-0.279	-0.390	-0.050	0.365	1.000	0.025
[DOC]	-0.182	-0.648*	0.663*	0.299	0.607*	-0.502*	0.025	1.000

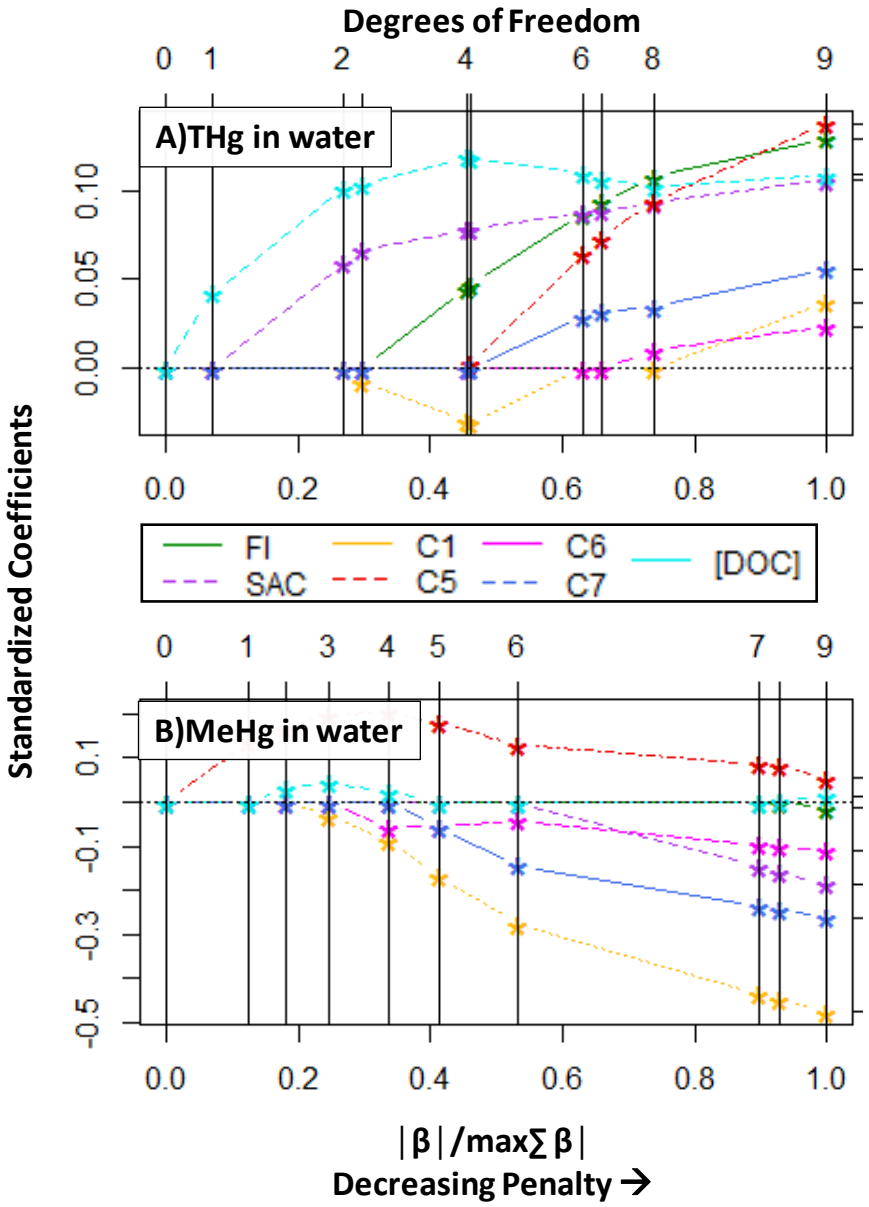

Figure SI- 5: LASSO path plots showing the standardized coefficients in relation to decreasing penalty parameter (lambda). Vertical lines represent the degrees of freedom of a given model after the addition or removal of one of the 7 explanatory parameters. The 2 panels show LASSO paths for[MeHg] and [THg] in surface waters using the 6 measures of DOM quality and [DOC] as explanatory variables. Final model coefficients were selected based on Marlow's Cp and are presented in the main manuscript.

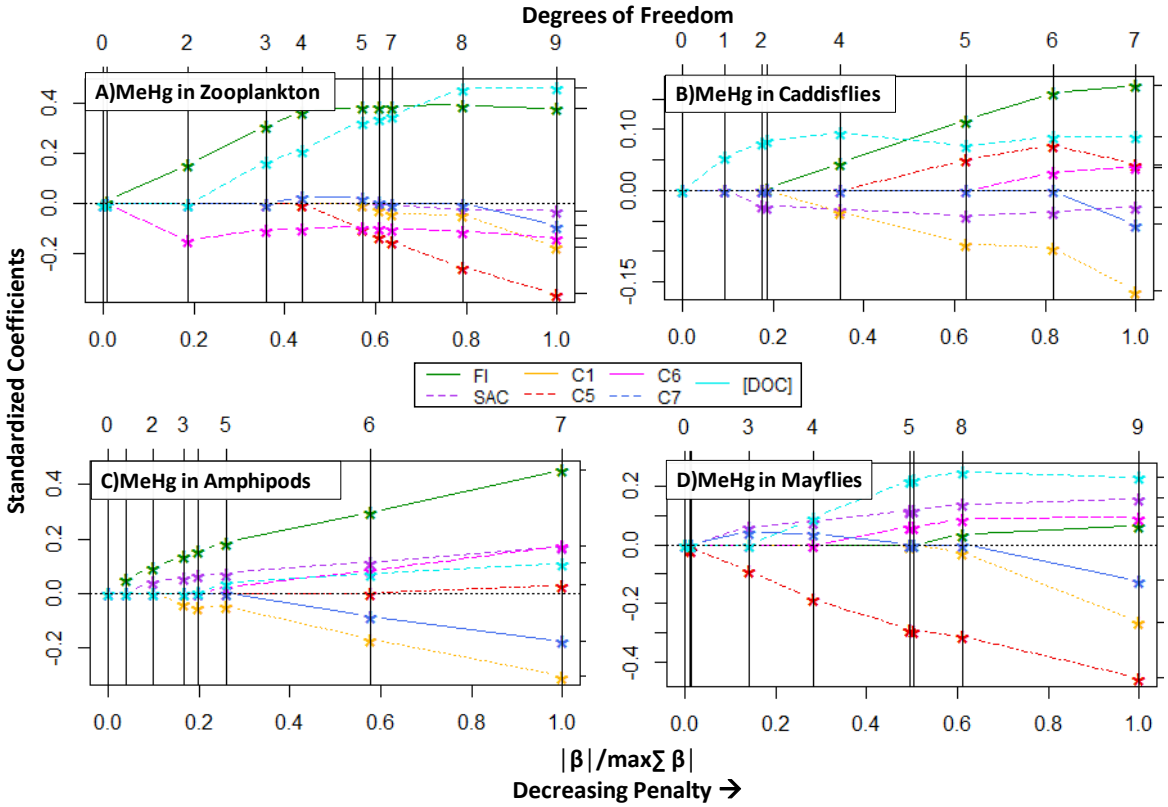

Figure SI- 6: LASSO path plots showing the standardized coefficients in relation to decreasing penalty parameter (lambda). Vertical lines represent the degrees of freedom of a given model after the addition or removal of one of the 7 explanatory parameters. The 4 panels show LASSO paths for[MeHg] in invertebrate groups (3 benthic invertebrate orders and bulk zooplankton) using the 6 measures of DOM quality and [DOC] as explanatory variables. Invertebrate [MeHg] are system means calculated from 1-5 replicates. Final model coefficients were selected based on Marlow's Cp and are presented in the main manuscript.

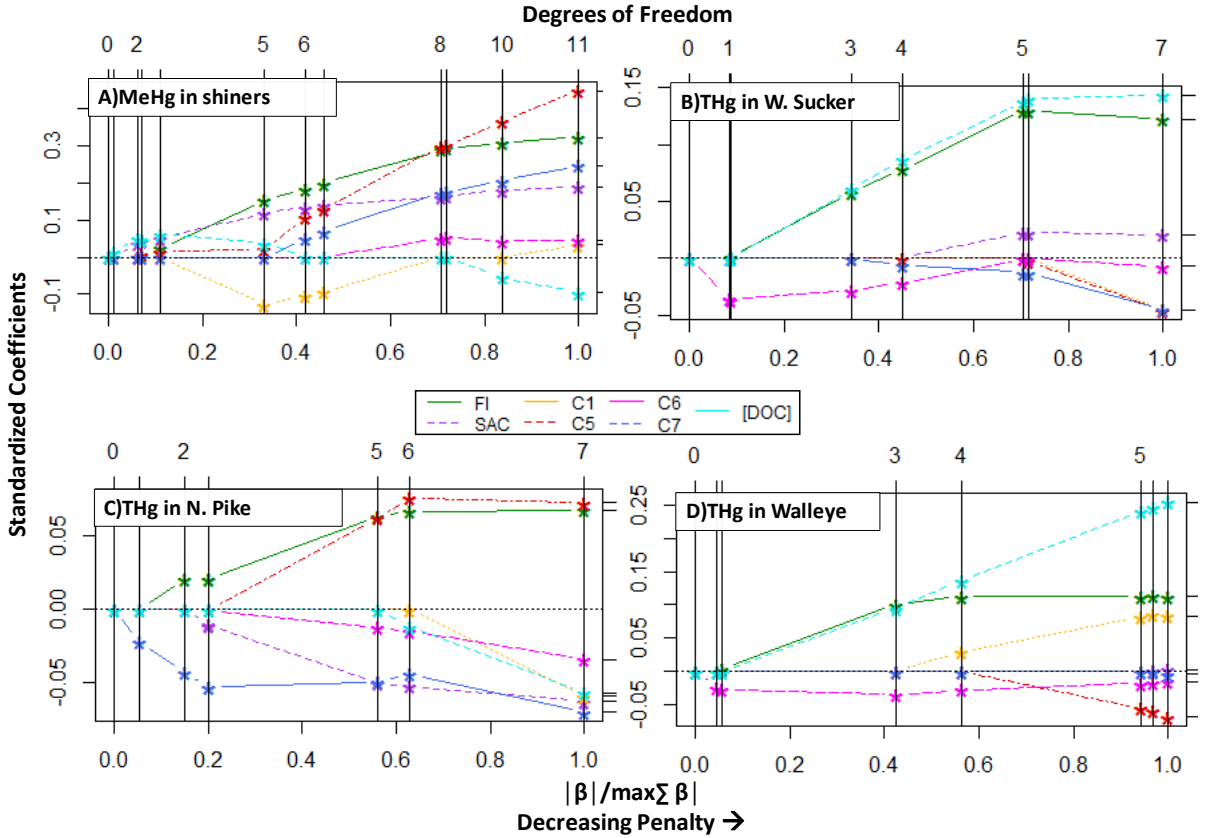

Figure SI- 7: LASSO path plots showing the standardize coefficients in relation to decreasing penalty parameter (lambda). Vertical lines represent the degrees of freedom of a given model after the addition or removal of one of the 7 explanatory parameters. The 4 panels show LASSO paths for [MeHg] in one forage fish (shiners) and [THg] in 3 large-bodied fish species (white sucker, northern pike, walleye) using the 6 measures of DOM quality and [DOC] as explanatory variables. Final model coefficients were selected based on Marlow's Cp and are presented in the main manuscript.

Table SI- 50: Variance partitioning results for water RDA and pRDAs. PARAFAC components were logit transformed and [Hg] were logged prior to scaling. *Total explainable variance is the total inertia for the full RDA model, i.e., rda(Hg ~ fi + sac + c1 + c5 + c6 + c7 + doc).

RDA parameters	Inertia	Proportion	ANOVA p-value
WATER (n = 44)			
Total explainable*	1.703	----	0.001
[DOC]	0.065	0.16	0.103
DOM quality	0.352	0.84	0.041
Quality + [DOC]	0.418	1.00	----
Fish (n = 18)			
Total explainable*	0.220	----	0.150
[DOC]	0.058	0.23	0.087
DOM quality	0.195	0.77	0.152
Quality + [DOC]	0.253	1.00	----

SI information for Chapter 4

Table SI- 51:General attributes of sample lakes and corresponding fish catch records. Note that region refers to Boreal Shield, Hudson Bay Lowlands. *Data from OMNRF (2017), https://www.ontario.ca/page/chemical-water-quality-lake-nipissing

Lake Name	Region	Latitude, Longitude (DD)	Year(s) sampled	Surface Area (ha)	Secchi Depth (m)	Max Depth (m)	Sample sizes of fish				
							Sculpin	*Shiner*	*Sucker*	*Pike*	*Walleye*
Attawapiskat	Shield	52.30, -87.90	2012, 2014	28,100	1.9	23.5	---	---	7	---	10
Fishtrap	Lowland	52.35, -86.41	2013, 2015	2,030	1.0	1.3	---	7	---	7	---
Lang	Shield	51.58, -91.51	2012, 2015	1,001	2.7	21.1	4	3	6	10	---
Missisa	Lowland	52.31, -85.20	2014, 2015	19,212	0.5	7.0	---	4	8	---	8
Monmon.	Shield	51.71, -89.48	2015	676	1.6	3.0	---	3	1	6	---
Nipissing	Shield	46.27, -79.80	2012, 2015	82,200*	2.2*	52.0*	---	---	5	2	8
Quantz	Lowland	51.16, -85.38	2011, 2015	727	1.2	10.4	---	1	---	---	9
Streatfield	Lowland	52.14, -85.90	2014, 2015	2,090	0.5	2.1	---	2	9	---	11
Trading	Shield	51.82, -88.96	2015	465	2.4	4.5	1	2	7	4	6
Williams	Shield	51.82, -90.78	2015	4,132	2.6	13.0	6	4	4	---	9
Total count:							**11**	**26**	**47**	**29**	**61**

Section SI-4.1 Fish aging methodology, Ontario Ministry of Natural Resources and Forestry:
Pike cleithra were cleaned of all flesh and dried, then examined whole under a dissecting scope using reflected light. Walleye otoliths were prepared by the crack-and-burn technique, and burned cross-sections were viewed under a dissecting scope using reflected light. Sucker fin rays were set in epoxy, and thin cross-sections were cut from the proximal end with a jeweller's saw. These sections were mounted on microscope slides, polished with fine-grit sandpaper, and viewed under a compound microscope using reflected light. Ages were not determined for sculpins or shiners.

Table SI- 52:Quality assurance and control results. Data for mercury values are based on a broader dataset (see Lescord et al. 2018). Data for isotopes are also based on a larger data set including samples from multiple projects analyzed simultaneously.

QA/QC measure		[THg] Biota	[MeHg] Biota	$\delta^{13}C$ (‰)	$\delta^{15}N$ (‰)
MDL	*ng/g or L*	2.50[3]	0.12[4]	NA	NA
Daily standards	*n*	-----	97	NA	NA
	%Rec	-----	98.8±9.2		
Method Blanks	*n*	77	95	NA	NA
	ng/g	0.09±0.08[3]	6.6±35.1[4]		
Initial precision replicates (IPRs)	*n*	-----	76	-----	-----
	%Rec	-----	98.5±11.3	-----	-----
Operating precision replicates (OPRs)	*n*	-----	135	-----	-----
	%Rec	-----	99.8±8.3	-----	-----
Certified reference material (CRMs)[1,2]	*n*	67	50	948	953
	%RPD	1.2±4.6	-4.7±10.7	<0.01±0.01	0.2±7.5
Digestion duplicates	*n*	-----	77	-----	-----
	%RPD	-----	-3.7±29.1	-----	-----
Analytical duplicates	*n*	61	79	263	263
	%RPD	0.48±6.6	10.6±23.8	<0.01±0.06	<0.01±0.18
Sample spikes	*n*	32	-----	-----	-----
	%Rec	97.0±4.7	-----	-----	-----
Analytical Method:		Milestone DMA-80, EPA 7473	Tekran 2600 MeHg System, EPA 1630	Continuous Flow-Isotope Ratio Mass Spectrometry (CF-IRMS)	Continuous Flow-Isotope Ratio Mass Spectrometry (CF-IRMS)

[1]DORM-4, NRC 2015 (http://www.nrc-cnrc.gc.ca/eng/solutions/advisory/crm/certificates/dorm_4.html); [2]working standards calibrated against and traceable to IAEA primary standards (CH6, CH7, N1, and N2) by the Stable Isotopes in Nature Laboratory at the University of New Brunswick; [3]Calculated assuming a sample dry weight of 0.02 g; [4]Calculated assuming a sample dry weight of 0.05 g.

Figure SI- 8: An example of a fully homogenized sample of fish muscle tissue as a result of the ball milling technique used in this study.

Table SI- 53:Data for fish samples with percent of methylmercury (%MeHg) exceeding 100%.

Group	Size Class	TL	MeHg	THg	%MeHg
Pike	B (200-400)	405	0.649	0.601	108
Pike	C (400-600)	518	0.595	0.551	108
Pike	C (400-600)	452	0.620	0.569	109
Pike	C (400-600)	485	0.682	0.599	114
Pike	D (600-800)	762	7.834	6.410	122
Sculpin	E (0-60)	56	0.776	0.735	105
Shiner	H (80-91)	89	0.618	0.560	110
Sucker	B (200-400)	398	0.309	0.276	112
Sucker	C (400-600)	445	0.409	0.372	110
Sucker	C (400-600)	498	1.012	0.817	124
Walleye	B (200-400)	223	0.776	0.735	105
Walleye	B (200-400)	230	0.861	0.778	111
Walleye	B (200-400)	385	1.960	1.765	111
Walleye	B (200-400)	268	0.737	0.659	112
Walleye	C (400-600)	497	2.249	2.124	106
Walleye	C (400-600)	431	1.998	1.852	108
Walleye	C (400-600)	555	3.113	2.828	110

Table SI- 54: Paired-comparisons t-tests of differences in the percentage of total mercury as methylmercury (%MeHg) between various tissues in adult walleye and white sucker sampled from Lake Nipissing, Ontario, in spring 2015 (n = number of individual fish).

Tissue comparison	n	Trend	Mean Difference	t-statistic	p-value
Walleye					
Muscle vs Soma	5	M < S	8	-0.53	0.630
Muscle vs Liver	5	M > L	34	2.35	0.078
Soma vs Liver	**5**	**S > L**	**42**	**11.1**	**< 0.001**
White Sucker					
Muscle vs Soma	5	M > S	17	1.04	0.360
Muscle vs Liver	**5**	**M > L**	**55**	**4.36**	**0.012**
Soma vs Liver	**5**	**S > L**	**38**	**4.98**	**0.008**

Table SI- 55:Results of one-way ANOVA comparing the percentage of total mercury as methylmercury (%MeHg) between adult walleye (WALL) and white sucker (WS) sampled from Lake Nipissing, Ontario, in spring 2015. Five individuals of each species were sampled, and the test is repeated for each of three tissue types analyzed.

Tissue	Trend	Mean Difference	F	df_{error}	p-value
Muscle	WALL > WS	6	0.10	8	0.760
Soma	**WALL > WS**	**31**	**29.2**	**8**	**< 0.001**
Liver	**WALL > WS**	**26**	**21.2**	**8**	**0.002**

Table SI- 56: Results assessing the relationship between the percent of methylmercury (%MeHg) and fish weight within large-bodied fish species (white sucker, northern pike, and walleye) only (model: %MeHg = species + log-weight + species* log-weight+ site). Site was included as a random effect. The overall model conditional R^2= 0.322 and 0.283 with and without the interaction term, respectively.

Parameter	F-value	p-value
Including interaction term		
Intercept	**3585.2**	**<0.001**
Species	**5.0**	**0.001**
Weight	**28.1**	**<0.001**
Species* Weight	**2.5**	**0.044**
Excluding interaction term		
Intercept	**5756.7**	**<0.001**
Species	**5.5**	**<0.001**
Weight	**26.0**	**<0.001**

Table SI- 57: Results assessing the relationship between the percent of methylmercury (%MeHg) and fish age within large-bodied fish species (white sucker, northern pike, and walleye) only (model: %MeHg = species + log-age + species*log-age + site). Site was included as a random effect. The overall model conditional R^2adj = 0.311 and 0. 311 with and without the interaction term, respectively. Note: 1 was added to all ages to reduce the influence of age-0 (young of the year) fish.

Parameter	F-value	p-value
Including interaction term		
Intercept	4773.8	<0.001
Species	11.6	<0.001
Age	16.5	<0.001
Species*Age	5.4	0.006
Excluding interaction term		
Intercept	4417.7	<0.001
Species	10.7	<0.001
Age	15.3	<0.001

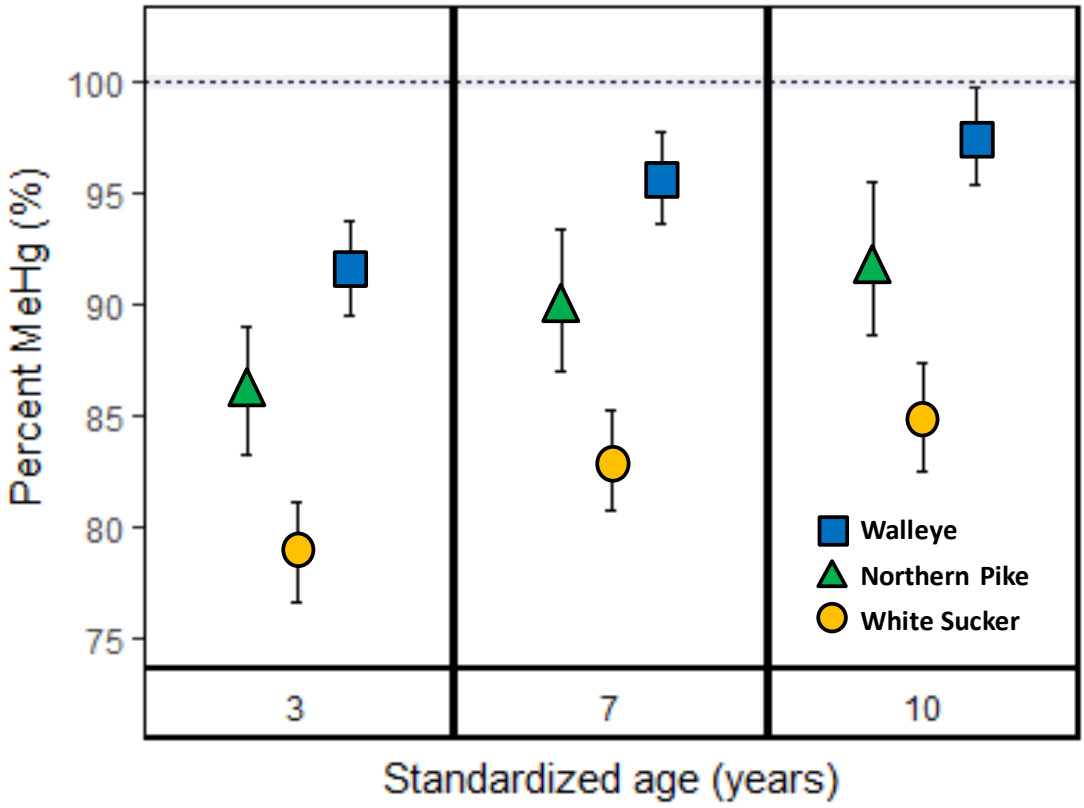

Figure SI- 9: Least-squared means (±SE) of %MeHg in fish muscle at standardized ages.

Table SI- 58: Tukey's post hoc testing on least squared mean estimates of the percent of methylmercury (%MeHg) in the 3 large-bodied species at specified levels of the co-variate, fish weight. p-values were corrected for multiple comparisons.

Standardized weight (g)	Species contrast	LS mean difference	SE	t-ratio	p-value
10	Pike - Sucker	-0.035	0.054	-0.649	0.794
	Pike - Walleye	**-0.220**	**0.061**	**-3.627**	**0.001**
	Sucker - Walleye	**-0.184**	**0.052**	**-3.577**	**0.002**
100	Pike - Sucker	0.023	0.035	0.659	0.788
	Pike - Walleye	**-0.117**	**0.035**	**-3.297**	**0.004**
	Sucker - Walleye	**-0.140**	**0.030**	**-4.615**	**<0.001**
500	Pike - Sucker	0.064	0.037	1.722	0.202
	Pike - Walleye	-0.045	0.036	-1.241	0.432
	Sucker - Walleye	**-0.109**	**0.030**	**-3.625**	**0.001**
1000	Pike - Sucker	0.082	0.042	1.93	0.136
	Pike - Walleye	-0.014	0.042	-0.338	0.939
	Sucker - Walleye	**-0.096**	**0.035**	**-2.763**	**0.019**

Table SI- 59: Results assessing the relationship between the percent of methylmercury (%MeHg) and weight in forage fish species (shiners and sculpins) only (model: %MeHg = species + log-weight + species* log-weight+ site). Site was included as a random effect. The overall model conditional R^2= 0.467 and 0.474 with and without the interaction term, respectively.

Parameter	F-value	p-value
Including interaction term		
Intercept	**417.10**	**<0.001**
Species	0.07	0.798
Weight	**7.24**	**0.014**
Species* Weight	<0.001	0.960
Excluding interaction term		
Intercept	**429.29**	**<0.001**
Species	0.07	0.795
Weight	**7.54**	**0.012**

Table SI- 60:Tukey's post hoc testing on least squared mean estimates of the percent of methylmercury (%MeHg) in sculpins and shiners at specified levels of the covariate, fish weight. P-values were corrected for multiple comparisons.

Standardized weight (g)	Species contrast	LS mean difference	SE	t-ratio	p-value
2	Sculpin-Shiner	-0.031	0.076	-0.408	0.687
4	Sculpin-Shiner	-0.028	0.076	-0.364	0.720
8	Sculpin-Shiner	-0.024	0.124	-0.194	0.848

Table SI- 61: ANCOVA results assessing the relationship between the percent of methylmercury (%MeHg) and fish weight across all fish species (model: %MeHg = species + log-weight + species* log-weight+ site). Site was included as a random effect. The overall model conditional R^2= 0.322 and 0.250 with and without the interaction term, respectively.

Parameter	F-value	p-value
Including interaction term		
Intercept	4773.77	<0.001
Species	11.56	<0.001
Weight	16.53	<0.001
Species* Weight	5.39	0.006
Excluding interaction term		
Intercept	4417.71	<0.001
Species	10.70	<0.001
Weight	15.30	<0.001

Table SI- 62: Tukey's post hoc testing on least squared mean estimates of the percent of methylmercury (%MeHg) in all fish species at 8 g body weight. p-values were corrected for multiple comparisons and degrees of freedom = 20.

Species contrast	LS mean difference	SE	t-ratio	p-value
Pike - Sculpin	-0.118	0.061	-1.922	0.311
Pike - Shiner	**-0.132**	**0.047**	**-2.785**	**0.048**
Pike - Sucker	0.038	0.035	1.071	0.821
Pike - Walleye	-0.084	0.034	-2.448	0.109
Sculpin - Shiner	-0.014	0.057	-0.251	0.999
Sculpin - Sucker	0.156	0.059	2.648	0.068
Sculpin - Walleye	0.034	0.059	0.571	0.979
Shiner - Sucker	**0.170**	**0.044**	**3.857**	**0.002**
Shiner - Walleye	0.048	0.044	1.082	0.816
Sucker - Walleye	**-0.122**	**0.029**	**-4.193**	**0.001**

Table SI- 63: Results from linear mixed effects models between the percent of methylmercury (%MeHg) in fish muscle and baseline-corrected carbon stable isotope signatures (δ13Cadj), including site as a random variable (model: %MeHg = $\delta^{13}C_{adj}$ + site). Conditional R^2 (R_{cond}^2) was estimated using the MuMIn package. Significance of each model was assessed with a Type 3 ANOVA through the car package.

Model	Model R_{cond}^2	Parameter	F- statistic	Df.res	p-value	Coef.
All fish	0.077	**Intercept**	**2070.71**	**7.82**	**<0.001**	**87.06**
		$\delta^{13}C_{adj}$	0.01	124.12	0.917	-0.10
Large-bodied fish	0.064	**Intercept**	**1985.20**	**7.71**	**<0.001**	**87.74**
		$\delta^{13}C_{adj}$	0.01	96.38	0.927	-0.11
White sucker	0.083	**Intercept**	**843.38**	**4.70**	**<0.001**	**80.49**
		$\delta^{13}C_{adj}$	2.71	33.41	0.109	-3.72
Northern pike	0.124	**Intercept**	**292.48**	**3.05**	**<0.001**	**82.74**
		$\delta^{13}C_{adj}$	1.35	20.24	0.260	2.90
Walleye	0.132	**Intercept**	**3871.72**	**5.76**	**<0.001**	**95.43**
		$\delta^{13}C_{adj}$	**5.54**	**37.64**	**0.024**	**-4.88**
Forage fish	0.041	**Intercept**	**692.28**	**5.35**	**<0.001**	**85.16**
		$\delta^{13}C_{adj}$	0.02	25.91	0.885	-0.254
Sculpin	0.274	**Intercept**	**278.09**	**1.27**	**0.019**	**86.45**
		$\delta^{13}C_{adj}$	1.82	5.31	0.232	-3.43
Shiner	0.250	**Intercept**	**244.82**	**4.76**	**<0.001**	**88.90**
		$\delta^{13}C_{adj}$	0.78	14.11	0.393	2.82

Table SI- 64: Results from linear mixed effects models between the percent of methylmercury (%MeHg) in fish muscle and carbon-to-nitrogen ratios (C:N), including site as a random variable (model: %MeHg = C:N + site). Conditional R^2 (R_{cond}^2) was estimated using the MuMIn package. Significance of each model was assessed with a Type 3 ANOVA through the car package.

Model	Model R_{cond}^2	Parameter	F- statistic	Df.res	p-value	Coef.
All fish	0.058	**Intercept**	**46.12**	**119.10**	**<0.001**	**120.26**
		C:N	3.54	122.01	0.062	-10.07
Large-bodied fish	0.094	**Intercept**	**22.83**	**90.03**	**<0.001**	**130.61**
		C:N	2.47	91.49	0.119	-13.31
White sucker	0.002	**Intercept**	**5.30**	**24.75**	**0.030**	**92.17**
		C:N	0.06	24.77	0.801	-3.08
Northern pike	0.170	Intercept	0.89	9.04	0.371	245.66
		C:N	0.38	9.04	0.551	-50.06
Walleye	0.019	**Intercept**	**5.31**	**26.24**	**0.029**	**87.28**
		C:N	0.03	26.58	0.863	2.10
Forage fish	0.132	**Intercept**	**10.70**	**21.42**	**0.004**	**127.80**
		C:N	1.19	22.27	0.286	-11.92
Sculpin	0.871	**Intercept**	**39.22**	**4.59**	**0.002**	**326.77**
		C:N	**21.28**	**4.54**	**0.007**	**-70.97**
Shiner	0.151	**Intercept**	**5.77**	**7.97**	**0.043**	**116.65**
		C:N	0.40	8.46	0.542	-8.40

Table SI- 65: Results from linear mixed effects models between the percent of methylmercury (%MeHg) in fish muscle and the percent of nitrogen (%N), including site as a random variable (model: %MeHg = %N + site). Conditional R^2 (R_{cond}^2) was estimated using the MuMIn package. Significance of each model was assessed with a Type 3 ANOVA through the car package.

Model	Model R_{cond}^2	Parameter	F-statistic	Df.res	p-value	Coef.
All fish	0.109	**Intercept**	**7.42**	**131.79**	**0.007**	**45.97**
		%N	**5.99**	**132.00**	**0.016**	**2.91**
Large-bodied	0.209	Intercept	0.49	101.66	0.487	15.43
		%N	**10.79**	**101.23**	**0.001**	**5.02**
White sucker	0.086	Intercept	0.26	31.41	0.611	19.45
		%N	2.74	31.39	0.108	4.42
Northern pike	0.249	Intercept	0.88	21.55	0.358	-59.77
		%N	**4.79**	**21.33**	**0.040**	**9.99**
Walleye	0.010	**Intercept**	**13.19**	**26.12**	**0.001**	**101.84**
		%N	0.08	26.61	0.779	-0.54
Forage fish	0.061	**Intercept**	**4.61**	**27.77**	**0.041**	**87.81**
		%N	0.004	27.71	0.952	-0.19
Sculpin	0.858	**Intercept**	**12.90**	**4.15**	**0.022**	**21.94**
		%N	**32.98**	**4.07**	**0.004**	**1.35**
Shiner	0.225	**Intercept**	**5.82**	**17.05**	**0.027**	**122.03**
		%N	0.50	16.76	0.489	-2.78

Table SI- 66: Results from linear mixed effects models between the percent of methylmercury (%MeHg) in fish muscle and baseline-corrected stable nitrogen isotope values ($\delta^{15}N_{adj}$) including site as a random variable (model: %MeHg = $\delta^{15}N_{adj}$ + site). Conditional R^2 (R_{cond}^2) was estimated using the MuMIn package. Significance of each model was assessed with a Type 3 ANOVA through the car package.

Model	Model R_{cond}^2	Parameter	F- statistic	Df.res	p-value	Coef.
All fish	0.080	**Intercept**	**2066.64**	**7.82**	**<0.001**	**87.06**
		$\delta^{15}N_{adj}$	0.43	124.12	0.515	0.26
Large-bodied fish	0.067	**Intercept**	**1977.67**	**7.66**	**<0.001**	**87.70**
		$\delta^{15}N_{adj}$	0.20	95.03	0.658	0.18
White sucker	0.067	**Intercept**	**461.95**	**8.65**	**<0.001**	**86.54**
		$\delta^{15}N_{adj}$	2.10	16.98	0.165	3.99
Northern pike	0.036	**Intercept**	**393.69**	**2.39**	**0.001**	**84.73**
		$\delta^{15}N_{adj}$	0.36	19.96	0.556	-0.33
Walleye	0.023	**Intercept**	**1279.94**	**6.35**	**<0.001**	**95.80**
		$\delta^{15}N_{adj}$	0.73	11.75	0.411	-1.65
Forage fish	0.574	**Intercept**	**280.16**	**6.64**	**<0.001**	**91.25**
		$\delta^{15}N_{adj}$	**4.95**	**27.31**	**0.034**	**8.93**
Sculpin	0.600	**Intercept**	**141.60**	**1.62**	**0.014**	**88.72**
		$\delta^{15}N_{adj}$	1.78	5.67	0.233	6.55
Shiner	0.613	**Intercept**	**155.86**	**4.52**	**<0.001**	**91.44**
		$\delta^{15}N_{adj}$	2.04	10.21	0.183	10.60